

Lineage diversification and differentiation in mouse ureter development

Von der Naturwissenschaftlichen Fakultät der
Gottfried Wilhelm Leibniz Universität Hannover

zur Erlangung des Grades
Doktor der Naturwissenschaften (Dr. rer. nat.)

genehmigte Dissertation

von

Tobias Eberhard Bohnenpoll, M. Sc.
geboren am 10.06.1986 in Hildesheim

2017

Referent: Prof. Dr. rer. nat. Andreas Kispert

Korreferent: PD Dr. med. Roland Schmitt

Korreferentin: Prof. Dr. rer. nat. Monika Hassel

Tag der Promotion: 26.07.2017

MHH

Medizinische Hochschule
Hannover



Angefertigt am
Institut für Molekularbiologie
der Medizinischen Hochschule Hannover
unter der Betreuung von
Prof. Dr. rer. nat. Andreas Kispert

Erklärung zur kumulativen Dissertation von Tobias Bohnenpoll (geboren am 10.06.1986 in Hildesheim)

Diese kumulative Dissertation basiert auf folgenden veröffentlichten Fachartikeln und bisher unveröffentlichten Manuskripten:

1. Tobias Bohnenpoll, Eva Bettenhausen, Anna-Carina Weiss, Anna B. Foik, Mark-Oliver Trowe, Patrick Blank, Rannar Airik and Andreas Kispert. “Tbx18 expression demarcates multipotent precursor populations in the developing urogenital system but is exclusively required within the ureteric mesenchymal lineage to suppress a renal stromal fate”. *Developmental Biology* 2013, August 380(1), 25-36.
2. Tobias Bohnenpoll, Sarah Feraric, Marvin Nattkemper, Anna-Carina Weiss, Carsten Rudat, Max Meuser, Mark-Oliver Trowe and Andreas Kispert. “Diversification of cell lineages in ureter development”. *Journal of the American Society of Nephrology* 2016, December, ePub ahead of print
3. Tobias Bohnenpoll, Anna B. Wittern, Tamrat M. Mamo, Anna-Carina Weiss, Karin Schuster-Gossler, Carsten Rudat, Marc-Jens Kleppa, Mark-Oliver Trowe and Andreas Kispert. “A SHH-FOXF1-BMP4 signaling axis regulating growth and differentiation of epithelial and mesenchymal tissues in ureter development”. Manuscript under revision at *PLOS Genetics*.
4. Tobias Bohnenpoll, Anna-Carina Weiss, Maurice Labuhn and Andreas Kispert. “Retinoic acid signaling maintains epithelial and mesenchymal progenitors in the developing mouse ureter”. Manuscript in preparation.
5. Asaf Vivante, Nina Mann, Hagith Yonath, Anna-Carina Weiss, Maike Getwan, Michael Kaminski, Tobias Bohnenpoll, Catherine Teyssier, Jing Chen, Shirlee Shril, Amelie T. van der Ven, Hadas Ityel, Johanna Magdalena Schmidt, Eugen Widmeier, Stuart B. Bauer, Simone Sanna-Cherchi, Ali G. Gharavi, Weining Lu, Daniella Magen, Rachel Shukrun, Richard P. Lifton, Velibor Tasic, Horia C. Stanescu, Vincent Cavaillès, Robert Kleta, Yair Anikster, Benjamin Dekel, Andreas Kispert, Soeren S. Lienkamp and Friedhelm Hildebrandt. “A dominant mutation in nuclear receptor interacting protein 1

causes urinary tract malformations via dysregulation of retinoic acid signaling”. *Journal of the American Society of Nephrology* 2017, April, ePub ahead of print

In **Artikel 1** habe ich die Abbildungen (Abb.) 1, Abb. 4 F, Abb. 5 A – C, Abb. 6 A und C, Abb. S1 und Abb. S6 experimentell und graphisch erstellt sowie zum inhaltlichen Konzept des Projekts beigetragen. Andreas Kispert hat das Projekt geplant und finanziert sowie das Manuskript geschrieben.

In **Artikel 2** habe ich einen Großteil der Abb. experimentell und graphisch erstellt (mit Ausnahme von Abb. 3 B und C, Abb. 4 A, Abb. S1 und Abb. S4). Das inhaltliche Konzept des Projekts wurde von Andreas Kispert und mir gemeinsam erarbeitet. Das Manuskript wurde von Andreas Kispert und mir gemeinsam geschrieben. Andreas Kispert finanzierte das Projekt.

In **Artikel 3** habe ich einen Großteil der Abb. experimentell und graphisch erstellt (mit Ausnahme von Abb. 4 A – D, Teilen von Abb. 5, Abb. 6 C und Abb. S3). Das inhaltliche Konzept des Projekts wurde von Andreas Kispert und mir gemeinsam erarbeitet. Das Manuskript wurde von Andreas Kispert und mir gemeinsam geschrieben. Andreas Kispert finanzierte das Projekt.

In **Artikel 4** habe ich einen Großteil der Abb. experimentell und graphisch erstellt (mit Ausnahme von Abb. 1 und Abb. S1). Das inhaltliche Konzept des Projekts wurde von Andreas Kispert und mir gemeinsam erarbeitet. Das Manuskript wurde von Andreas Kispert und mir gemeinsam geschrieben. Andreas Kispert finanzierte das Projekt.

Zu **Artikel 5** habe ich einen kleinen experimentellen Beitrag geleistet (Abb. 4 B). Der Großteil der Arbeiten wurde von der Arbeitsgruppe um Friedhelm Hildebrandt und weiteren Kooperationspartnern durchgeführt.

Summary

The ureters are integral components of the urinary system that serve the transport of urine from the renal pelvis to the bladder. They are composed of an inner epithelial lining with layers of basal, intermediate, and superficial cells, and an outer mesenchymal coat with peristaltically active smooth muscle cells and surrounding fibrocytes of the tunica adventitia and the lamina propria. How these cell types arise in embryonic development from two multipotent progenitor populations in the intermediate mesoderm, the epithelial ureteric bud and its surrounding mesenchyme, has remained poorly understood.

In an attempt to delineate sub-pools of progenitor cells in the anlage of the urogenital system, comparative expression analysis was used to demarcate the expression domain of the T-Box transcription factor gene *Tbx18* with respect to known markers. It was shown that *Tbx18* was not only expressed in mesenchymal progenitors of the ureter but was also transiently expressed in the adrenogonadal primordium. Genetic fate mapping and lineage tracing approaches revealed that cells from these expression domains significantly contributed to the mesenchymal wall of the ureter and to the renal stroma as well as to cells of the gonads and adrenal glands. *Tbx18* was functionally required only in the ureteric mesenchymal lineage to restrict a renal stromal fate and to allow smooth muscle differentiation by rendering cells competent for inductive signals from the ureteric epithelium.

Using cell type specific markers and genetic lineage tracing experiments the time course of differentiation, and the lineage relations and restrictions of the mesenchymal and epithelial cell types of the ureter were further defined. An early subdivision of the ureteric mesenchyme separated adventitial fibrocytes from smooth muscle and lamina propria progenitors. While adventitial fibrocytes started to differentiate at embryonic day (E) 13.5, smooth muscle progenitors diversified into subepithelial fibrocytes of the lamina propria and differentiated smooth muscle cells from E16.5 onwards. The uncommitted epithelium of the distal ureteric bud gave rise to intermediate cells at E14.5 and began to stratify. Intermediate cells subsequently differentiated into superficial and basal cells at E15.5 and E16.5, respectively, to form the three layered urothelium at E18.5. In homeostasis, intermediate cells continued to give rise to basal cells and superficial cells, whereas basal cells were terminally differentiated.

Growth and differentiation of the epithelial and mesenchymal components of the ureter need to be precisely coordinated within and between the two tissue compartments. Previous work implied paracrine sonic hedgehog (SHH) signaling from the ureteric epithelium in the control of proliferation and differentiation of the mesenchyme. Here, a combination of genetic loss- and

gain-of-function approaches was employed to study the cellular and molecular mechanisms that underlie SHH function in the developing ureter in more depth. Genetic deletion or activation of the SHH signal transducer *smoothed* in the ureteric mesenchyme confirmed the involvement of the pathway in mesenchymal growth and differentiation and revealed its requirement for mesenchymal survival and urothelial differentiation. The forkhead transcription factor gene *Foxf1* was identified as a target of SHH signaling in the ureteric mesenchyme and misexpression of a dominant negative allele recapitulated the proliferation and differentiation defects observed under hedgehog loss-of-function conditions. Genetic and pharmacological rescue experiments uncovered a SHH-FOXF1-BMP4 regulatory module that couples growth and differentiation of the mesenchymal and epithelial tissues in the ureter.

Expression analysis of components and target genes of retinoic acid (RA) signaling indicated that this pathway was specifically active in the mesenchymal and epithelial progenitor populations of the ureter. In order to address a potential function of RA, pharmacological loss- and gain-of-function experiments in ureter explant cultures were performed. Inhibition of RA signaling prior to the onset of differentiation resulted in an expansion of smooth muscle cells at the expense of lamina propria cells in the mesenchymal wall of the ureter and an expansion of superficial cells at the expense of intermediate cells in the urothelium, while activation experiments gave complementary results. A depletion of the mesenchymal and epithelial progenitor pools by precocious differentiation was identified as the cellular cause for the observed phenotypes. Potential effector genes of the pathway were identified that may explain a function of RA in the maintenance of ureteric progenitors. A human genetics research group identified a kindred with an autosomal dominant form of congenital anomalies of the kidney and the urinary tract. Heterozygous truncating mutation in the *NRIP1* gene were identified as a cause for the disease. Biochemical analysis revealed that NRIP1 protein negatively regulates RA mediated transcriptional activity by a physical interaction with RA receptors. I contributed to the analysis and was able to show that developmental *Nrip1* expression in the mouse nephric duct and ureteric bud was strongly RA dependent.

Taken together, this thesis provided novel insight into the multipotent progenitor populations and into the temporal and spatial profile of lineage diversification and differentiation in the developing ureter. A SHH-FOXF1-BMP4 signaling axis was identified as a crucial regulatory module that coordinates growth and differentiation of the epithelial and mesenchymal tissue compartments of the ureter while RA signaling was implicated in the maintenance of ureteric progenitor cells.

Keywords: ureter development, lineage tracing, hedgehog signaling, retinoic acid signaling

Zusammenfassung

Die Ureteren sind wichtige Komponenten des Harnsystems und dienen dem Transport von Urin aus dem Nierenbecken zur Harnblase. Sie bestehen aus einer inneren epithelialen Auskleidung mit Schichten von Basal-, Intermediär- und Superfizialzellen und einem äußeren mesenchymalen Mantel mit peristaltisch aktiven Glattmuskelzellen und sie umgebenden Fibrozyten der Tunica adventitia und der Lamina propria. Wie diese Zelltypen im Verlaufe der Embryonalentwicklung aus zwei multipotenten Vorläuferpopulationen, der epithelialen Ureterknospe und dem sie umgebenden Mesenchym, entstehen, ist nur unzureichend verstanden.

In einem Versuch, unterschiedliche Gruppen von Vorläuferzellen in der Anlage des Urogenitalsystems darzustellen, wurden vergleichende Expressionsstudien durchgeführt, um die Expressionsdomänen des T-Box Transkriptionsfaktors *Tbx18* von bekannten Markern abzugrenzen. Es konnte gezeigt werden, dass *Tbx18* nicht nur in den mesenchymalen Vorläufern des Ureters, sondern auch vorübergehend in der adrenogonadalen Organanlage exprimiert war. Genetische Schicksalkartierungs- und Zellverfolgungsexperimente konnten zeigen, dass Zellen dieser Expressionsdomänen einen signifikanten Beitrag zur mesenchymalen Wand des Ureters und zum Interstitium der Niere sowie zu Geweben der Gonade und der Nebenniere leisteten. Die Funktion von *Tbx18* war auf die Abstammungslinie des Uretermesenchyms beschränkt, um den zellulären Beitrag zum renalen Interstitium einzuschränken und Zellen empfänglich für induktive Signale aus dem Ureterepithel zu machen.

Um den zeitlichen Verlauf der Differenzierung und die Abstammungsverhältnisse der mesenchymalen und epithelialen Zelltypen des Ureters genauer zu beschreiben, wurden Zelltyp-spezifische Marker und Zellverfolgungsstudien eingesetzt. Eine frühe Unterteilung des Uretermesenchyms in adventitiale Fibrozyten und Vorläuferzellen der glatten Muskulatur und der Lamina propria konnte beobachtet werden. Während adventitiale Fibrozyten bereits am Embryonaltag (E) 13.5 differenzierten, spaltete sich die glattmuskuläre Vorläuferpopulation am E16.5 weiter in differenzierte Glattmuskelzellen und Fibrozyten der Lamina propria auf. Die epithelialen Zellen der distalen Ureterknospe entwickelten sich am E14.5 zunächst zu Intermediärzellen und begannen zu stratifizieren. Diese differenzierten am E15.5 und E16.5 jeweils in Superfizial- und Basalzellen, um am E18.5 das dreischichtige Urothel hervorzubringen. In der Gewebehomöostase waren Intermediärzellen weiterhin Vorläufer von Basal- und Superfizialzellen, wohingegen Basalzellen einen terminal differenzierten Zustand einnahmen.

Das Wachstum und die Differenzierung der epithelialen und mesenchymalen Bestandteile des Ureters müssen im Verlaufe der Organentwicklung räumlich und zeitlich präzise koordiniert werden. Vorherige Studien konnten zeigen, dass Sonic Hedgehog (SHH) Signale aus dem Ureterepithel die Proliferation und Differenzierung des Uretermesenchyms steuern. In dieser Arbeit wurde eine Kombination aus genetischen Funktionsverlust- und Funktionsgewinnexperimenten genutzt, um den SHH Signalweg in der Ureterentwicklung genauer zu untersuchen. Der genetische Verlust oder die Aktivierung des SHH Signalvermittlers Smoothed im Uretermesenchym bestätigten die Notwendigkeit des Signalwegs für das Wachstum und die Differenzierung des Mesenchyms und konnten bisher unbekannte Funktionen für das mesenchymale Überleben und die urotheliale Differenzierung aufdecken. Der Forkhead Transkriptionsfaktor *Foxf1* wurde als ein Zielgen des SHH Signalwegs im Uretermesenchym identifiziert und die Misexpression eines dominant-negativen Allels konnte die Proliferations- und Differenzierungsdefekte des SHH Verlusts rekapitulieren. Genetische und pharmakologische Rettungsexperimente konnten die Funktion einer SHH-FOXF1-BMP4 Signalachse in der Kopplung des Wachstums und der Differenzierung der epithelialen und mesenchymalen Gewebe des Ureters entschlüsseln.

Expressionsstudien von Komponenten und Zielgenen des Retinsäure (RS) Signalwegs zeigten, dass dessen Aktivität auf die mesenchymalen und epithelialen Vorläuferpopulationen des Ureters beschränkt war. Um eine mögliche Funktion von RS zu adressieren, wurden pharmakologische Funktionsverlust- und Funktionsgewinnstudien in Gewebekulturen des Ureters durchgeführt. Eine Hemmung des Signalwegs vor dem Einsetzen der Differenzierung führte zu einer Ausweitung des glattmuskulären Kompartiments zu Lasten der Lamina propria in der Ureterwand und zu einer Vermehrung von Superfizialzellen zu Lasten von Intermediärzellen des Urothels. Eine Aktivierung des Signalwegs hatte den gegenteiligen Effekt. Ein Schwund der mesenchymalen und epithelialen Vorläuferpopulationen durch eine verfrühte zelluläre Differenzierung wurde als Ursache für die beobachteten Phänotypen erkannt. Zudem wurden potentielle Zielgene des Signalwegs identifiziert, welche eine Funktion von RS in der Aufrechterhaltung der Vorläuferzellen erklären könnten. Die Beschreibung einer Familie mit einer autosomal-dominanten Form von angeborenen Fehlbildungen der Niere und des Harnleiters durch eine humangenetische Forschergruppe lieferte weitere Anregungen zur Studie des RS Signalwegs in der Entwicklung des Harnsystems. Eine heterozygote Mutation des *NRIP1* Gens wurde von ihnen als ursächlich für die Erkrankung erkannt. Ihre biochemischen Studien legten nahe, dass NRIP1 die transkriptionelle Aktivität von RS durch eine direkte physikalische Interaktion mit RS Rezeptoren beeinträchtigt. Ich konnte zu dieser Studie beitragen und zeigen, dass die

Zusammenfassung

Nrip1 Expression im Nephrischen Gang und der Ureterknospe der Maus abhängig von RS Aktivität reguliert wird.

Insgesamt konnte die vorliegende Arbeit neue Einsichten in die multipotenten Vorläufergewebe und in das zeitliche und räumliche Profil der Diversifizierung und Differenzierung der Zelltypen des Ureters liefern. Eine SHH-FOXF1-BMP4 Signalkaskade wurde als wichtiges regulatorisches Modul identifiziert, welches das Wachstum und die Differenzierung der mesenchymalen und epithelialen Bestandteile des Ureters in der Organentwicklung koordiniert. Zudem konnte eine Funktion des RS Signalwegs mit der Aufrechterhaltung der Vorläuferpopulation des Ureters in Zusammenhang gebracht werden.

Schlagworte: Ureterentwicklung, genetische Abstammungsverfolgung, Hedgehog Signalweg, Retinsäure Signalweg

Table of contents

Erklärung zur kumulativen Dissertation	II
Summary	IV
Zusammenfassung	VI
Introduction	1
Aims of the thesis	12
Part 1 - Tbx18 lineage in urogenital development	14
"Tbx18 expression demarcates multipotent precursor populations in the developing urogenital system but is exclusively required within the ureteric mesenchymal lineage to suppress a renal stromal fate"	
Part 2 - Lineage diversification in the ureter	34
"Diversification of cell lineages in mouse ureter development"	
Part 3 - SHH signaling in ureter development	55
"A SHH-FOXF1-BMP4 regulatory axis regulating growth and differentiation of epithelial and mesenchymal tissues in ureter development"	
Part 4 - RA signaling in ureter development	98
"Retinoic acid signaling maintains epithelial and mesenchymal progenitors in the developing mouse ureter"	
Part 5 - A dominant mutation in NRIP1 causes CAKUT	146
"A dominant mutation in nuclear receptor interacting protein 1 causes urinary tract malformations via dysregulation of retinoic acid signaling"	
Concluding remarks	160
References	168
Appendix	175
Acknowledgements	182

Curriculum vitae	183
List of publications.....	184

Introduction

Structure and function of the ureter

The ureters are paired muscular ducts that connect the renal pelvis to the urinary bladder to facilitate an efficient drainage of the urine which is produced in the kidneys. They are positioned in the retroperitoneal space where they are attached to fibrous and adipose connective tissue. The upper aspects of the ureters emanate from the sinus of the kidneys in a funnel-shaped form and pass through the abdomen into the pelvic region where they integrate into the urinary bladder.¹

The ureteric wall is composed of two tissue compartments, an inner epithelial lining and an outer mesenchymal coat. The luminal lining of the ureter is formed by a specialized transitional epithelium, the urothelium, which is highly distensible yet provides efficient sealing towards the hypertonic urine. The urothelium is stratified into three to four cell layers and is comprised of at least three distinct cell types: the superficial, intermediate and basal cells (Figure 1).² The ureteric lumen is sealed by one layer of large squamous superficial cells which covers the whole surface of the longitudinally folded urothelium. Underneath a population of small cuboidal intermediate cells is located which only represent a minor fraction of the urothelium. The major cell type of the urothelium are small cuboidal or column-shaped basal cells which are organized in two to three cell layers at the urothelial base and tightly adhere to the mesenchymal coat of the ureter.^{1,2} The ureteric mesenchyme is organized into three histologically distinct compartments: the lamina propria, the tunica muscularis and the tunica adventitia (Figure 1).¹ The lamina propria is a loose connective tissue, comprised of fibrocytes and fibroelastic material, which connects urothelial basal cells to the smooth muscle coat of the tunica muscularis. Ureteric smooth muscle cells are elongated and organized in bundles with circular or longitudinal arrangement which are separated by collagen fibers.³ Individual smooth muscle cells are interconnected via gap junctions and form a functional syncytium.⁴ The tunica muscularis is thin-walled in the proximal, funnel-shaped aspect of the ureter and thickens as the ureter proceeds antegrade towards the urinary bladder. A surrounding sheet of connective tissue, rich in collagen fibers and interspersed with circularly arranged fibrocytes, forms the tunica adventitia which is covered by adipose tissue and anchored in the extraperitoneal cavity.¹ The abdominal aspect of the ureter is supplied with blood from the renal and ovarian or testicular arteries whereas the pelvic aspect is vascularized from vesical and rectal vessels. The vasculature of the ureter is longitudinally arranged in the tunica adventitia from where it branches and supplies

Introduction

the tunica muscularis with capillaries. These capillaries form plexi in the lamina propria from where the urothelial cell types are supplied.¹ The innervation of the ureter runs in close association with the ureteric vasculature and forms plexi in the inner and outer connective tissue compartments whereas free nerve endings are not observed in the smooth muscle layer or urothelium.⁵

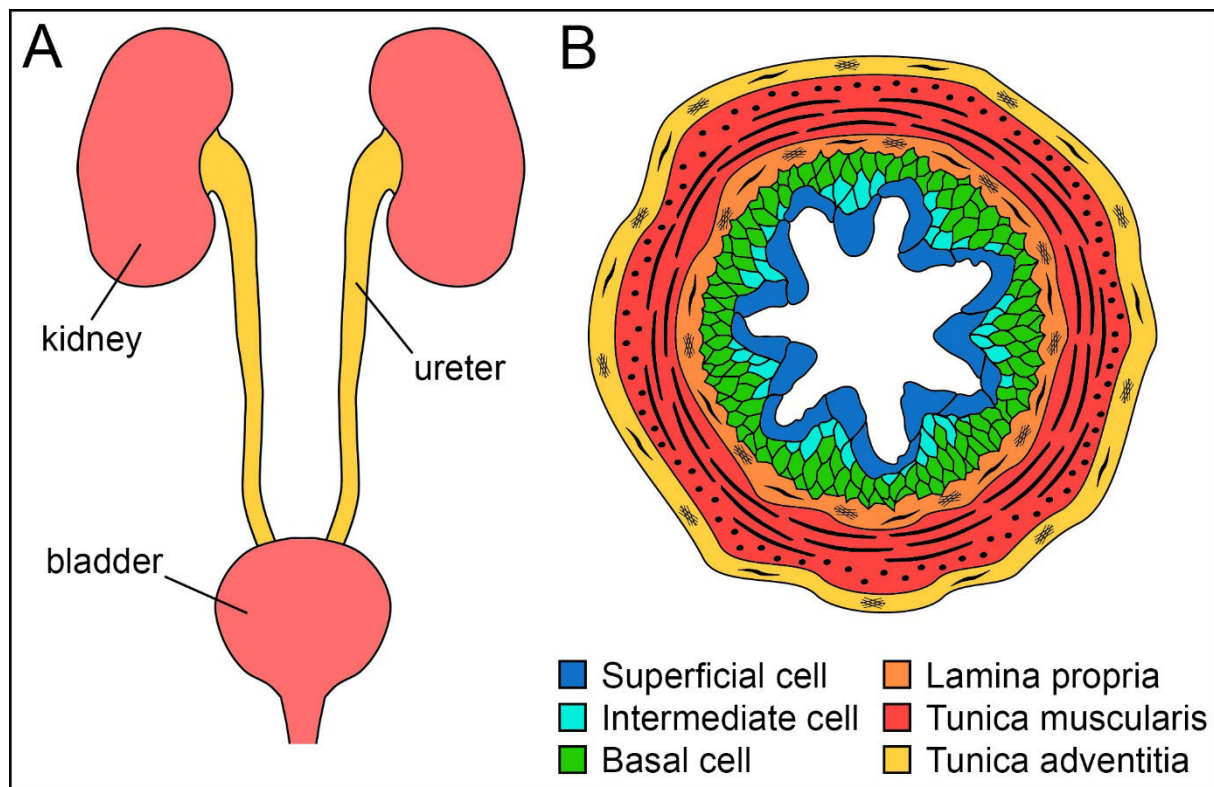


Figure 1: Schematic illustration of ureter morphology and histology.

(A) The ureters are paired tubular organs that connect the kidneys with the urinary bladder to actively drain urine. (B) Schematic representation of a transvers section of the proximal ureter. Urothelial cell types and mesenchymal tissue compartments are illustrated. Urothelial cell shapes were adapted from Hicks, 1965.²

The urine that is collected in the renal pelvis is not merely drained passively through the ureter but actively propelled towards the urinary bladder via coordinated peristaltic contractions of the smooth muscle layer.⁶ These peristaltic contractions are myogenic in nature and originate from atypical smooth muscle cells at the pelvicalyceal junction which show electrical autorhythmicity and propagate action potentials to the electrically quiescent typical smooth muscle cells.⁶⁻⁸ The pelvicalyceal origin of rhythmicity and the long refractory period of ureteric smooth muscle cells assure a proximodistal directionality of contractions which prevents urine reflux and kidney damage.⁹

The structural and functional integrity of the ureteric tissues and the patency of the ureteric junctions to the renal pelvis and the urinary bladder are essential for efficient urine drainage and maintenance of kidney function. Functional or physical obstruction of the urinary tract results in dilatation of the ureter (hydroureter) and the renal pelvis (hydronephrosis) due to increased hydrostatic pressure and culminates in the destruction of the renal parenchyma. Congenital ureter anomalies represent a prominent subgroup of congenital anomalies of the kidney and urinary tract (CAKUT) which are among the most common human birth defects, affecting approximately 1:500 live births and are the leading cause of end-stage renal disease in infants.^{10, 11} CAKUT comprises a broad spectrum of phenotypes including hydro- and megaureter, ureteropelvic junction obstruction, vesicoureteral reflux and hydronephrosis as well as renal agenesis, renal hypoplasia, duplex kidneys and multicystic kidneys. All of these malformations originate from defects in the development of the kidney and the urinary tract which disturb normal morphogenesis or cellular differentiation programs.^{12, 13} The study of normal and pathological kidney and ureter development is thus pivotal to understand the etiology of these common human birth defects.

Development of the mouse ureter

The development of the ureters is closely associated and coordinated with the development of the kidneys and the lower urinary tract, i.e. the bladder and urethra, and involves tissues of different germ layers. Whereas the kidneys and the ureters derive from the intermediate mesoderm, the lower urinary tract originates from endodermal tissues.¹⁴ In the mouse, kidney development is initiated with the emergence of the nephric duct at embryonic day (E) 8.5 via an epithelial-mesenchymal transition in the intermediate mesoderm of each body side.¹⁵ The nephric ducts extend caudally until they reach and fuse with the cloaca, the endodermal precursor of the lower urinary tract, at E9.5. This fusion process and additional tissue remodeling are crucial steps for the integration of the ureters into the urinary bladder which is essential for efficient urine drainage.^{16, 17} During its caudal elongation the nephric duct induces two generations of transient kidney structures in the adjacent intermediate mesoderm, the pro- and the mesonephros, which degenerate in higher vertebrates and only constitute ontogenetic relicts.¹⁸ Definitive kidney (metanephros) development starts at E10.5 with the evagination of the ureteric bud from the nephric duct epithelium at the approximate level of the hind limb buds. The ureteric bud subsequently elongates and invades a specialized mesenchymal population, the metanephric mesenchyme, which harbors all progenitors for nephrons and the renal stroma.¹⁹ Whereas the

proximal portion of the ureteric bud initiates nephrogenesis in the metanephric mesenchyme and undergoes serial events of dichotomous branching to establish the collecting duct system of the kidney, the distal, unbranched stalk of the ureteric bud merely elongates and interacts with the surrounding ureteric mesenchyme to form the ureter (Figure 2).

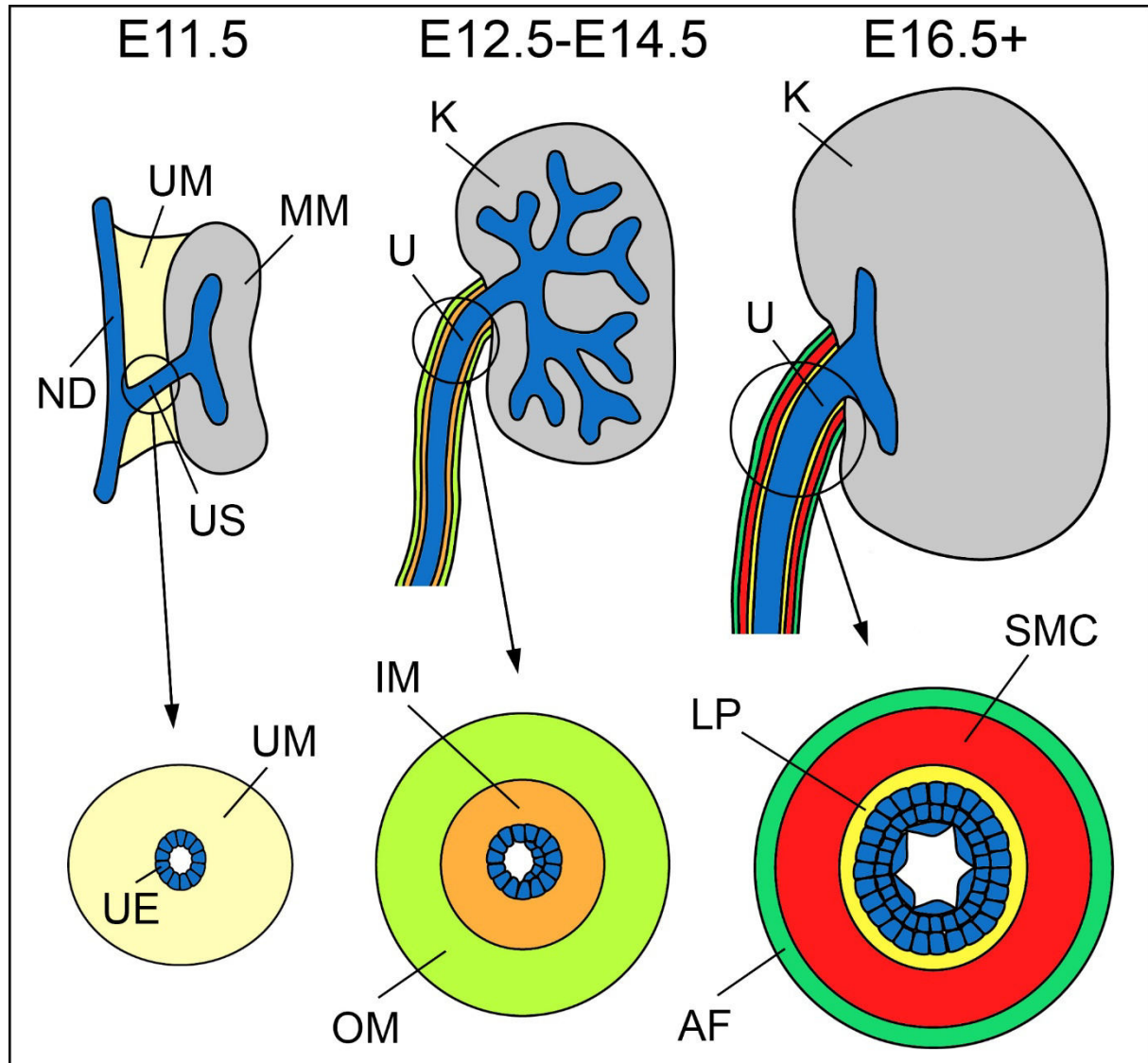


Figure 2: Schematic illustration of mouse ureter development.

The ureteric bud forms as an evagination of the nephric duct and its proximal end invades the metanephric mesenchyme to undergo serial branching events that form the collecting duct tree of the kidney. At E11.5 the distal, unbranched ureteric stalk epithelium is single-layered and surrounded by a homogenous mass of mesenchymal cells. Between E12.5 and E14.5 the ureteric mesenchyme is subdivided into two tissue compartments. The inner compartment is densely packed and harbors spherical cells whereas the outer compartment is loosely organized and interspersed with tangentially oriented fibrocytes. The ureteric epithelium which remains single-layered at E12.5 becomes double-layered at E14.5. From E16.5 onwards all three mesenchymal compartments, i.e. the lamina propria, tunica muscularis and tunica adventitia, are established. Urothelial stratification proceeds and the luminal surface is fully covered with differentiated superficial cells. Abbreviations: IM, inner mesenchyme; K, kidney; LP, lamina propria; MM, metanephric mesenchyme; ND, nephric duct; OM, outer mesenchyme; U, ureter; UE, ureteric epithelium; UM, ureteric mesenchyme; US, ureteric stalk. Adapted from Trowe et al., 2012.²⁰

At E11.5 the single layered ureteric epithelium is surrounded by a homogenous mass of mesenchymal cells which is cellular and molecular distinct from the metanephric mesenchyme.²¹ This ureteric mesenchyme becomes radially subdivided at E12.5 into an inner compartment harboring densely packed spherical cells and an outer compartment interspersed with tangentially oriented fibrocytes.²⁰ While the ureteric epithelium is still single-layered at E12.5 stratification is initiated at E13.5 and the epithelium becomes double-layered by E14.5.²² With the onset of substantial urine production at E16.5 all mesenchymal compartments, i.e. the lamina propria, tunica muscularis and tunica adventitia are established and the ureter becomes peristaltically active and thus functional.^{20, 23} The now three-layered urothelium is sealed with one layer of superficial cells that covers the whole luminal surface and protects the underlying tissues from the hypertonic urine.²⁴ Differentiation of urothelial basal and intermediate cells has also been reported but the temporal and spatial profile of their emergence is not well characterized.^{22, 25} Thereafter the ureter continues to grow and terminally differentiates shortly after birth.

Molecular control of ureter development

Beside its important function in urine drainage and the clinical significance of congenital ureteral anomalies, the ureter represents a simple model system to study epithelial-mesenchymal interactions and the molecular control of growth, patterning and differentiation in the development of a tubular organ. The analysis of genetically modified mouse models has shed light on some key regulators of ureter development and helped to elucidate the causality of genetic mutations to CAKUT phenotypes in human patients, but still many open questions remain.^{13, 14}

Specification and diversification of ureteric cell lineages

The differentiated cell types of the urothelium and the mesenchymal wall of the ureter originate from multipotent precursor cells in the early metanephric field, the distal ureteric bud and its surrounding mesenchyme. While the distal aspect of the ureteric bud is designated to become the ureter, the proximal portion and the surrounding metanephric mesenchyme are fated to form the collecting duct tree and the nephrons of the kidney. Embryonic explant cultures of kidney rudiments and tissue separation experiments clearly indicated that these processes are independent from extrinsic cues and solely rely on reciprocal signals between the ureteric bud epithelium and its surrounding mesenchyme.^{26, 27} Interestingly, ureter development also proceeds

Introduction

in absence of kidneys, indicating that the early metanephric field is intrinsically segmented into a proximal and distal portion with different fates that do not intermingle.²⁸ Both the urothelium and the collecting duct epithelium are derived from the *Pax2*⁺ nephric duct lineage.¹⁵ However, an early molecular subdivision of the unbranched ureteric stalk and the branching proximal aspect of the ureteric bud has not been described. Instead, it is likely that distinct molecular properties of the ureteric and metanephric mesenchyme guide the fate of the distal and proximal ureteric bud, respectively. While the metanephric mesenchyme is defined by the expression of a set of transcriptional regulators including *Six2* or *Pax2* and *Eya1* that culminate in nephrogenesis or the activation of a GDNF/Ret signaling module that drives kidney branching morphogenesis, the ureteric mesenchyme is devoid of these factors.¹⁸ Molecular lineage tracing of descendants of *Osr1* expressing cells indicated that the intermediate mesoderm initially contributes to all cell types of the metanephros including ureteric smooth muscle cells but that an early lineage segregation occurs that separates the ureteric mesenchyme from nephron and renal stromal progenitors.²⁹ Indeed, the ureteric mesenchyme specifically expresses the T-box transcription factor gene *Tbx18* in a narrow band of cells in between the nephric duct and the metanephric mesenchyme as early as E10.5.²¹ Genetic lineage tracing experiments revealed that cells from this expression domain are designated to constitute all differentiated cell types of the mesenchymal wall of the ureter.²⁰ However, it is not known whether these cells also contribute to additional lineages of the excretory system. The early subdivision of the ureteric mesenchyme into an inner domain with densely packed spherical cells and an outer domain with tangentially oriented cells with a fibrocyte-like shape already indicates that further lineage restrictions take place. It has been postulated but not formerly shown that the inner compartment harbors smooth muscle precursors whereas the outer domain is fated to differentiate into adventitial fibrocytes.²⁰ Furthermore, it has been speculated that lamina propria cells arise from smooth muscle precursors by spatial inhibition of the smooth muscle gene program but clear evidence is still lacking.²³ Further lineage tracing studies using tissue specific approaches should be performed to delineate the origin of differentiated cell types and clarify the lineage relations in the developing urogenital system.

Growth and differentiation of the ureteric mesenchyme

With completion of the proximal-distal compartmentalization of the metanephric field, the ureteric stalk is surrounded by an initially uniform mesenchymal tissue. The knowledge of the molecular and cellular mechanisms that transform this homogenous ureteric mesenchyme in a

precise temporal and spatial fashion into a radial arrangement of fibrocytes and smooth muscle cells has remained scarce.¹⁴ However, emerging evidence suggests that epithelial signals like sonic hedgehog (SHH) and members of the WNT family guide the growth, patterning and differentiation of the ureteric mesenchyme.^{20, 23, 30}

In renal development *Shh* expression is confined to the ureteric epithelium and medullary collecting ducts from E11.5 to E18.5. Specific expression of the hedgehog receptor and target gene of the pathway, patched homolog 1 (*Ptch1*), in the adjacent ureteric mesenchyme and medullary stroma suggests that signaling occurs in a paracrine fashion.²³ Systemic loss of *Shh* or tissue specific ablation from the ureteric epithelium results in decreased mesenchymal proliferation and delayed smooth muscle differentiation that culminate in hydroureter development.^{23, 30} On the other hand conditional overactivation of the hedgehog signal transducer smoothed (SMO) in the ureteric mesenchyme leads to mesenchymal hyperplasia with an expanded smooth muscle layer.³⁰ In contrast, treatment of primary ureteric mesenchymal cells with SHH protein dose-dependently inhibits smooth muscle differentiation. Moreover *Ptch1* expression becomes restricted to the lamina propria, a tissue that is devoid of smooth muscle cells, from E16.5 on. These observations suggest that hedgehog signaling either dose- or context-dependently activates or inhibits differentiation to allow the development of the smooth muscle layer and the lamina propria.²³ The factors that mediate growth and differentiation downstream of hedgehog signaling remain poorly understood. The bone morphogenetic protein 4 (BMP4) signaling pathway is a likely mediator of hedgehog function in the ureteric mesenchyme. On the one hand, *Bmp4* expression resembles *Ptch1* expression in the ureteric mesenchyme and is completely lost in *Shh*-deficient ureters.²³ On the other hand, phosphorylation of SMAD1/5/8, a transcriptional mediator of canonical BMP4 signaling, is strongly increased after overactivation of SMO.³⁰ BMP4 signaling has multiple crucial functions in ureter development. First, BMP4 controls elongation of the ureter and prevents ectopic budding from the nephric duct.³¹ Second, it acts as a chemoattractant for ureteric mesenchymal cells and promotes their differentiation towards smooth muscle cells *in vitro*.³² In support of this observation, genetic ablation of *Bmp4* or antagonism of BMP4 signaling in the ureteric mesenchyme disrupts smooth muscle investment of the ureter and leads to hydroureter formation.^{30, 33} This function is at least partially mediated by the canonical branch of the signaling pathway, as genetic deletion of *Smad4*, a transcriptional mediator of canonical BMP4 signaling, results in decreased ureteric smooth muscle differentiation and ureteropelvic junction obstruction.^{34, 35} The transcription factor tea-shirt zinc finger homeobox 3 (TSHZ3) has been identified as a potential effector of BMP4

Introduction

signaling in the ureteric mesenchyme.³⁶ Loss of *Tshz3* results in hydronephrosis without anatomical obstruction due to impaired ureteric smooth muscle differentiation. Whereas *Ptch1* and *Bmp4* expression are unaltered in *Tshz3*-deficient ureters *Tshz3* expression is inducible by exogenous BMP4 indicating that it acts downstream of the SHH-BMP4 signaling axis.³⁶ Nevertheless, it is unlikely that BMP4 and TSHZ3 are the only downstream effectors of hedgehog signaling in the ureteric mesenchyme and that they can fully explain the growth and differentiation defects that underlie the hedgehog loss-of-function phenotype. Further transcriptional profiling and detailed cellular and molecular analyses of hedgehog signaling in the ureter should provide us with a better understanding of the regulatory modules that control growth and differentiation downstream of this important pathway.

The canonical WNT signaling pathway is the second described mediator of epithelial-mesenchymal interactions in the control of ureteric growth and differentiation programs.²⁰ The WNT ligand genes *Wnt7b* and *Wnt9b* are specifically expressed in the ureteric epithelium from E11.5 to E18.5 and E11.5 to E14.5, respectively. Expression of the WNT receptor gene *Fzd1* and the bona fide target gene of the signaling pathway *Axin2* in the adjacent ureteric mesenchyme suggests a paracrine or juxtacrine mode of action. Conditional inactivation of *Ctnnb1*, the unique intracellular mediator of canonical WNT signaling, in the ureteric mesenchyme results in a hypoplastic hydroureter and hydronephrosis formation with a complete loss of differentiated smooth muscle cells. Misexpression of a stabilized form of CTNNB1 in the ureteric mesenchyme results in an ectopic cluster of differentiated smooth muscle cells along the ureter indicating that this pathway is not only required but also sufficient to induce their differentiation. Differentiation defects in *Ctnnb1*-deficient ureters are preceded by a loss of mesenchymal compartmentalization and reduced mesenchymal proliferation at E12.5. Furthermore, the expression of fibrocyte markers which is usually restricted to the outer compartment of the ureteric mesenchyme is expanded towards the urothelium at E16.5. These observations suggest that canonical WNT signaling controls the patterning of the ureteric mesenchyme by specification of smooth muscle precursor cells in direct vicinity of the urothelium or by repression of an adventitial fibrocyte fate.²⁰ The transcriptional effectors of canonical WNT signaling in the ureteric mesenchyme remain poorly understood. On the one hand WNT signaling is required to maintain the expression of *Tbx18* from E12.5 on. *Tbx18* is a crucial transcriptional mediator of ureter development which is probably involved in the early specification of the ureteric mesenchyme and thus required for subsequent differentiation programs.²¹ *Tbx18* expression is initially confined to a small band of mesenchymal cells surrounding the ureteric stalk and separating the nephric duct from the metanephric mesenchyme. Expression is maintained in smooth muscle

precursors but subsequently downregulated with the progression of differentiation at E16.5. *Tbx18*-deficient mice develop severe shortened hydroureter that completely lack a smooth muscle coat.²¹ However, reconstitution of *Tbx18* expression in *Ctnnb1*-deficient mice is not able to rescue smooth muscle differentiation defects and hydroureter formation indicating that it only has a minor contribution to the phenotype.²⁰ Another transcription factor that acts downstream of WNT signaling and *Tbx18* is the SRY-box protein SOX9. Expression of *Sox9* is restricted to the undifferentiated ureteric mesenchyme from E11.5 to E13.5 and is absent in *Ctnnb1*- and *Tbx18*-deficient ureters.^{20, 21, 37} Embryos with conditional inactivation of *Sox9* in the ureteric mesenchyme develop hydroureteronephrosis due to impaired smooth muscle differentiation and decreased extracellular matrix deposition.³⁷ Moreover a recent study suggests that SOX9 is critically involved in the timing of ureteric smooth muscle differentiation.³⁸ Both SOX9 and TSHZ3 compete with serum response factor (SRF) for binding to the master regulator of smooth muscle genes myocardin (MYOCD) and are suggested to repress the myogenic program. In support of this hypothesis prolonged expression of *Sox9* after E14.5 does not interfere with *Myocd* expression but strongly delays the expression of structural smooth muscle genes.^{37, 38} Although the SHH and WNT pathways are already active in the undifferentiated ureteric mesenchyme at E11.5, it is unclear how these signaling activities are balanced to activate the MYOCD-driven smooth muscle gene program only at E14.5. It is plausible to assume that additional permissive and restrictive factors converge on the initiation of the smooth muscle differentiation to provide a functional ureter at the onset of substantial urine production. Further temporal characterization of signaling activities and expression patterns of transcriptional regulators in the ureter should provide us with new candidates involved in this complex regulatory network.

Growth and differentiation of the urothelium

In contrast to the proximal aspect of the ureteric bud that branches into the single layered epithelial system of the renal collecting duct tree, its distal portion remains unbranched and develops into a multilayered and watertight transitional epithelium, the urothelium. The molecular mechanisms which guide the elongation and stratification of the distal ureteric bud and the differentiation of specialized urothelial cell types that provide elasticity yet efficient sealing towards the hypertonic urine have remained poorly understood.

Genetic and pharmacological manipulation of BMP4 signaling in the early metanephric field indicated that this signaling pathway is critically involved in the segmentation of the ureteric

Introduction

bud by inhibition of branching morphogenesis and promotion of elongation of its distal portion.^{31, 39} The elongation of the urothelium is under further control of the fibroblast growth factor (FGF) signaling pathway which shows a mitogenic function on urothelial cells *in vitro* and *in vivo* and controls elongation and branching of the ureteric bud.^{40, 41}

In contrast to the ureter where the knowledge of the molecular regulators of urothelial stratification and differentiation has remained scarce, more insights have been gained in the developing and regenerating bladder urothelium. A specific function for FGF7 in the stratification of the bladder urothelium has been proposed based on the findings that the *Fgf7*-deficient urothelium is thinned and lacks the intermediate cell layer. Furthermore, FGF7 maintains intermediate cells *in vitro* and inhibits their differentiation into superficial cells.⁴² The lineage relations of urothelial cell types and the nature of urothelial stem and progenitor cells is controversially discussed. Genetic fate mapping experiments in the regenerating bladder urothelium suggested that intermediate and superficial cells arise in a linear sequence from *Shh* expressing basal cells.⁴³ This hypothesis has been recently challenged by Gandhi and coworkers.⁴⁴ On the one hand they showed that *Shh* is not specifically expressed in basal cells but also marks intermediate cells in development and adulthood. On the other hand they thoroughly characterized the temporal profile of urothelial stratification and differentiation in development using cell type specific markers. In the adult urothelium, basal cells are positive for the intermediate filament protein cytokeratin 5 (KRT5) and an isoform of the transcription factor P63 (Δ NP63), whereas intermediate cells are KRT⁻ Δ NP63⁺ and additionally express uroplakins (UPK), and superficial cells are KRT⁻ Δ NP63⁻ UPK⁺. In development, intermediate cells appear first at E13.5 and are succeeded by superficial cells at E14.5. Basal cells just appear from E16.5 on but expand subsequently to constitute the major cell type of the mature urothelium. Moreover, an additional transient cell population of P-cells was proposed in the undifferentiated urothelium at E11.5 that shares the molecular profile of intermediate cells but is furthermore positive for the endodermal marker FOXA2. The late appearance of basal cells already indicates that these cells are unlikely to be progenitors in the developing urothelium. Indeed, genetic lineage tracing studies confirmed that basal cells are a unipotent cell population and that P-cells or intermediate cells are progenitors in the developing and regenerating urothelium, respectively. The retinoic acid (RA) signaling pathway was shown to be critically involved in the specification of these progenitors in development and repair of the bladder urothelium.⁴⁴ First, RA signaling is active in P-cells during development and becomes upregulated in intermediate cells under injury conditions in the adult. Second, misexpression of a dominant negative allele of the RA receptor alpha gene *Rara* leads to a loss of intermediate and superficial cell differentiation in development and

impaired urothelial regeneration after injury.⁴⁴ Whether these findings can be transferred to the ureteric epithelium remains an open question. Given the distinct developmental origin of the ureter and the bladder from the intermediate mesoderm and the endoderm, respectively, it is possible that significant differences exist in the molecular control of their development.

In the ureter deletion of the *Brg1* gene, encoding a component of the SWI/SNF chromatin remodeling complex, leads to severe urothelial stratification and differentiation defects.²² Expression of Δ NP63 and the peroxisome proliferator activated receptor gamma (PPARG) are reduced in *Brg1*-deficient ureter. A loss of Δ NP63 results in a mono-layered urothelium which correlates with the stratification defects observed in *Brg1* mutant ureters whereas a loss of PPARG diminishes superficial cell differentiation. In support of this observation a function of PPARG signaling in urothelial differentiation has previously been reported *in vitro*.^{45, 46} Furthermore, *Shh* expression is decreased after loss of *Brg1*. SHH signaling has been reported to guide mesenchymal growth and differentiation in the ureter but it cannot be excluded that mesenchymal signals downstream of this pathway act back on the urothelium. In support of this notion, loss of *Tbx18* in the ureteric mesenchyme also affects terminal differentiation of the urothelium which suggests the presence of such paracrine signals.²¹ Interestingly, genetic ablation of *Bmp4* in the ureteric mesenchyme leads to reduced UPK expression.³⁹ Furthermore, loss of the bone morphogenetic protein receptor type 1a gene *Bmpr1a* from the bladder urothelium impairs urothelial proliferation and regeneration after bacterial infection which renders BMP4 signaling a likely candidate for a paracrine pathway that controls urothelial self-renewal and differentiation.⁴⁷

Despite the significant body of knowledge that has been gathered especially in the control of urothelial development and regeneration in the bladder the transferability of these findings to the developing ureter is unclear. Future studies should carefully address the temporal profile of differentiation and the lineage relations specifically in the developing ureter urothelium and reassess the involvement of the reported molecular mediators that control these processes in bladder development and repair.

Aims of the thesis

The differentiated cell types of the ureter derive from multipotent progenitor cells of the ureteric bud and its surrounding mesenchyme. How these precursor cells diversify and differentiate into their prospective lineages is poorly understood. This thesis shall address in different independent experimental efforts the temporal and spatial profile of cellular diversification and differentiation and shall give mechanistic insights into the molecular pathways that control ureter development.

1. The fate of TBX18⁺ cells in the urogenital ridge.

The mesenchymal progenitor cells of the ureter specifically express the T-Box transcription factor gene *Tbx18*. While TBX18⁺ cells give rise to all differentiated cell types of the mesenchymal coat of the ureter, it is unclear if these cells also contribute to other components of the urogenital system and if TBX18 is functionally required for their development. Careful expression, fate mapping and phenotype analyses shall be performed to address these open questions.

2. Lineage diversification and differentiation in ureter development.

Several studies already described cellular differentiation of mesenchymal and epithelial tissues in the ureter. However, a precise temporal and spatial characterization of the diverse differentiation programs is still lacking, as is the timing of lineage segregation in this organ. This thesis shall provide a framework for further functional studies of ureteric progenitors and their differentiation into the respective lineages. To achieve this goal, a quantitative description of the temporal and spatial profile of ureteric differentiation shall be performed using cell type specific markers. Moreover, tissue and cell type specific reporter assays shall be utilized to delineate lineage relations in the developing ureter and to characterize stem and progenitor cells in development and homeostasis.

3. The cellular and molecular function of SHH signaling in ureter development.

Previous work suggested a critical role for *Shh* in differentiation of the ureteric mesenchyme. However, the full entity of the cellular functions of these pathways as well as its downstream effector genes in the ureteric mesenchyme have remained elusive. For this reason, genetic and pharmacologic loss- and gain-of-function studies shall be performed to identify and characterize the cellular programs triggered by SHH signaling in the ureter. Furthermore, molecular

analyses shall identify and functionally characterize the molecular mediators of hedgehog signaling in the ureteric mesenchyme, and define their precise epistatic relation.

4. The cellular and molecular function of RA signaling in ureter development.

Recent work suggested a role for RA signaling in specifying the urothelium in the bladder. Whether a similar role exist in the ureter has remained enigmatic. Therefore, this thesis shall screen for expression and targets of RA signaling in ureter development. A functional involvement in ureter development shall be addressed by pharmacological loss- and gain-of-function experiments in explants of embryonic ureters of different developmental stages. Further assays shall address the cellular function of RA signaling as well as its molecular targets in this organ.

5. Characterization of the *Nrip1* gene as a target of RA signaling in ureter development.

A heterozygous truncating mutation in the *Nrip1* gene was identified in a kindred with an autosomal dominant form of CAKUT. Biochemical characterization of the protein revealed that NRIP1 negatively regulates RA signaling via direct physical interaction with the RA receptor. The expression of *Nrip1* in the developing ureters and kidneys shall be analyzed and a potential dependency on the RA signaling pathway shall be tested.

Together, these projects shall provide novel insight into the cellular and molecular programs that guide the development of the mesenchymal and epithelial tissue compartments of the mammalian ureter.

Part 1 - Tbx18 lineage in urogenital development

Tbx18 expression demarcates multipotent precursor populations in the developing urogenital system but is exclusively required within the ureteric mesenchymal lineage to suppress a renal stromal fate

Tobias Bohnenpoll^{1,*}, Eva Bettenhausen^{1,*}, Anna-Carina Weiss¹,
Anna B. Foik¹, Mark-Oliver Trowe¹, Patrick Blank¹, Rannar Airik¹
and Andreas Kispert^{1,§}

¹ Institut für Molekularbiologie, Medizinische Hochschule Hannover, 30627 Hannover, Germany

* Equal contribution

§ Author for correspondence:

Email: kispert.andreas@mh-hannover.de

Tel: +49511 5324017

Fax: +49511 5324283

Published in Developmental Biology (Dev Biol (2013), 380: 25-36)

Reprinted with permission (see Appendix).



Contents lists available at SciVerse ScienceDirect

Developmental Biology

journal homepage: www.elsevier.com/locate/developmentalbiology

Tbx18 expression demarcates multipotent precursor populations in the developing urogenital system but is exclusively required within the ureteric mesenchymal lineage to suppress a renal stromal fate



Tobias Bohnenpoll¹, Eva Bettenhausen¹, Anna-Carina Weiss, Anna B. Foik, Mark-Oliver Trowe, Patrick Blank, Rannar Airik, Andreas Kispert^{*}

Institut für Molekularbiologie, OE5250, Medizinische Hochschule Hannover, Carl-Neuberg-Str. 1, D-30625 Hannover, Germany

ARTICLE INFO

Article history:

Received 11 October 2012

Received in revised form

30 April 2013

Accepted 30 April 2013

Available online 15 May 2013

Keywords:

Tbx18

Cre

Lineage tracing

Ureter

Urogenital system

ABSTRACT

The mammalian urogenital system derives from multipotent progenitor cells of different germinal tissues. The contribution of individual sub-populations to specific components of the mature system, and the spatiotemporal restriction of the respective lineages have remained poorly characterized. Here, we use comparative expression analysis to delineate sub-regions within the developing urogenital system that express the T-box transcription factor gene *Tbx18*. We show that *Tbx18* is transiently expressed in the epithelial lining and the subjacent mesenchyme of the urogenital ridge. At the onset of metanephric development *Tbx18* expression occurs in a band of mesenchyme in between the metanephros and the Wolffian duct but is subsequently restricted to the mesenchyme surrounding the distal ureter stalk. Genetic lineage tracing reveals that former *Tbx18*⁺ cells of the urogenital ridge and the metanephric field contribute substantially to the adrenal glands and gonads, to the kidney stroma, the ureteric and the bladder mesenchyme. Loss of *Tbx18* does not affect differentiation of the adrenal gland, the gonad, the bladder and the kidney. However, ureter differentiation is severely disturbed as the mesenchymal lineage adopts a stromal rather than a ureteric smooth muscle fate. Dil labeling and tissue recombination experiments show that the restriction of *Tbx18* expression to the prospective ureteric mesenchyme does not reflect an active condensation process but is due to a specific loss of *Tbx18* expression in the mesenchyme out of range of signals from the ureteric epithelium. These cells either contribute to the renal stroma or undergo apoptosis aiding in severing the ureter from its surrounding tissues. We show that *Tbx18*-deficient cells do not respond to epithelial signals suggesting that *Tbx18* is required to prepattern the ureteric mesenchyme. Our study provides new insights into the molecular diversity of urogenital progenitor cells and helps to understand the specification of the ureteric mesenchymal sub-lineage.

© 2013 Elsevier Inc. All rights reserved.

Introduction

The urinary system is a multi-component entity consisting of the kidneys, the ureters, the bladder and the urethra that together control the water and ionic balance of the blood by excretion of excess water, solutes and waste products. The urinary system is structurally and functionally tightly associated with the adrenal glands, as well as with the genital system that consists of sexually dimorphic gonads, sex ducts and external genitalia.

A number of studies have begun to identify the progenitor populations, their interaction and the temporal specification of

sublineages for the different components of the urogenital system in the mouse. While the lower parts of the urogenital system including the bladder epithelium, the urethra, and the lower aspect of the vagina derive from an infolding of the endoderm, the cloaca, and its surrounding mesenchyme, most other components are thought to be derivatives of the intermediate mesoderm (Mugford et al., 2008; Wang et al., 2011). Expression of the transcriptional regulator gene *Osr1* is activated broadly within the intermediate mesoderm starting from embryonic day (E) 7.5, and is required for the development of adrenals, gonads, kidneys and sex ducts suggesting that *Osr1* marks the progenitors for all of these components at this stage (James et al., 2006; Wang et al., 2005). Within the urogenital ridge of E9.5-E10.5 embryos, the first sublineages emerge. *Osr1* expression becomes gradually excluded from the (coelomic) epithelium that lines the urogenital ridge and from the epithelial Wolffian duct to be restricted to the

^{*} Corresponding author. Fax: +49 511 5324283.

E-mail address: kispert.andreas@mh-hannover.de (A. Kispert).

¹ Equal contribution.

Part 1 - Tbx18 lineage in urogenital development

mesenchymal compartment of the intermediate mesoderm, and later at around E10.5, to the most posterior aspect from which all cell types of the metanephros will arise (Mugford et al., 2008). The Wolffian duct epithelium that expresses the transcription factor genes *Lhx1*, *Pax2* and *Gata3* (Grote et al., 2006; Pedersen et al., 2005) contributes exclusively to the vas deferens in the male, the epithelium of the ureter and the collecting duct system of the kidney (Saxen, 1987), whereas the epithelial lining of the ridge harbors a common pool of precursor cells for the gonads and the adrenal glands (Hatano et al., 1996). This adrenogonadal primordium that is marked by expression of the orphan nuclear receptor gene *Sf1* divides between E10-E11 into distinct progenitor populations for the adrenals and gonads (Ikeda et al., 1994; Keegan and Hammer, 2002; Luo et al., 1994). The *Sf1*⁺ cells eventually differentiate into the cortical cells of the adrenal gland, Sertoli and Leydig cells of the testis, and granulosa and theca cells of the ovary (Bingham et al., 2006). At E10.5, signals from the mesenchymal condensation at the posterior end of the intermediate mesoderm, the metanephric blastema, induce the formation of an epithelial diverticulum from the Wolffian duct, the ureteric bud. During further development the ureteric bud invades the metanephric blastema and initiates a program of branching morphogenesis to generate the collecting duct system of the mature kidney. The distal part merely elongates and differentiates into a highly specialized type of epithelium, the urothelium. With each branching event a portion of the metanephric mesenchyme adjacent to the branch tip, is induced by tip signals to condense and undergo a mesenchymal-epithelial transition and form a renal vesicle from which the nephron will mature (for a recent review see (Little and McMahon, 2012)). This cap or metanephrogenic mesenchyme is a self-renewing population of nephron progenitors that expresses the transcription factor genes *Six2* and *Uncx* (Boyle et al., 2008; Karner et al., 2011; Kobayashi et al., 2008; Neidhardt et al., 1997; Self et al., 2006). Nephron progenitors are surrounded by *Foxd1*⁺ mesenchymal cells that will give rise to the stromal cells of the renal capsule, cortex and medulla as well as to mesangial and vascular smooth muscle cells (Hatini et al., 1996; Humphreys et al., 2010; Levinson et al., 2005). Separation of the *Six2*⁺ nephron lineage from the *Foxd1*⁺ stromal lineage within the *Osr1*⁺ precursor pool is thought to occur between E10.5 and E11.5 (Mugford et al., 2008). Finally, *Flk1*⁺ cells within the metanephric mesenchyme may contribute to the renal vasculature system (Gao et al., 2005). While the developmental origin of most of the cell types of the mature kidney has been characterized to an appreciable level, much less is known about the specification of the mesenchymal progenitor pool of the smooth muscle and fibroblast coatings of the ureter and the bladder, and the temporal separation of this lineage from the *Six2*⁺ and *Foxd1*⁺ progenitors of the metanephros. Notably, it has been suggested that stromal cells of the kidney and the ureteric mesenchyme do not actually arise from the intermediate mesoderm but originate in the paraxial and/or tail-bud mesoderm (Brenner-Anantharam et al., 2007; Guillaume et al., 2009).

We have previously shown that the T-box transcription factor gene *Tbx18* marks the undifferentiated ureteric mesenchyme from E12.5 to E14.5. At E11.5, *Tbx18* is expressed in a narrow band of cells between the mesenchyme surrounding the Wolffian duct and the metanephros (Airik et al., 2006). Prior to metanephric development expression of *Tbx18* was also noted in the mesonephros (Kraus et al., 2001). In *Tbx18*^{-/-} mice, descendants of former *Tbx18*-positive cells (short: *Tbx18*⁺ descendants) do not differentiate into smooth muscle cells of the ureter but dislocalize to the kidney and differentiate into fibroblast-like cells. As a consequence, the renal pelvis becomes dramatically enlarged at the expense of the ureter, and hydronephrosis develops at birth (Airik et al., 2006). This suggested that the ureteric mesenchymal lineage is separated

early from other mesenchymal lineages of the renal system, and that separation is disturbed in *Tbx18*-deficient mice. Fate mapping efforts based on a cre knock-in in the *Tbx18* locus harbored on a BAC identified smooth muscle cells of the ureter and the bladder as derivatives of former *Tbx18*⁺ progenitor cells (Wang et al., 2009). However, it remained unclear whether the genomic region covered by the BAC contained all *Tbx18* control elements for specific urogenital expression. Further, we neither know when the ureteric lineage is specified nor do we know the mechanisms by which the ureteric mesenchyme becomes localized around the ureteric epithelium.

Here, we characterize the expression of *Tbx18* in the developing urogenital system. We describe the cell lineages to which *Tbx18*⁺ descendants contribute in the mature urogenital system, and analyze their *Tbx18*-dependency. We investigate the mechanisms that restrict *Tbx18* expression to the ureteric mesenchyme, and provide evidence for the role that *Tbx18* plays within this tissue.

Materials and methods

Mice

R26^{mTmG} (*Gt(ROSA)26Sor^{tm4}(ACTB-tTomato-EGFP)^{Luo}*) reporter mice (Muzumdar et al., 2007), *Tbx18^{lacZ}* (*Tbx18^{tm3Akis}*), *Tbx18^{GFP}* (*Tbx18^{tm2Akis}*) and *Tbx18^{cre}* (*Tbx18^{tm4}(cre)^{Akis}*) knock-in alleles (Bussen et al., 2004; Christoffels et al., 2006; Trowe et al., 2010) were all maintained on an NMRI outbred background. Embryos for gene expression analysis were derived from matings of NMRI wildtype mice. *Tbx18^{cre/+};R26^{mTmG/+}* mice were obtained from matings of *Tbx18^{cre/+}* males and *R26^{mTmG/mTmG}* females. *Tbx18^{cre/lacZ};R26^{mTmG/+}* mice were obtained from matings of *Tbx18^{cre/+};R26^{mTmG/mTmG}* males and *Tbx18^{lacZ/+}* females. *Tbx18^{GFP/+}* embryos were obtained from matings of *Tbx18^{GFP/+}* males with NMRI females. For timed pregnancies, vaginal plugs were checked in the morning after mating, noon was taken as embryonic day (E) 0.5. Embryos, whole urogenital systems and kidneys were dissected in PBS. For *in situ* hybridization and immunofluorescence analyses specimens were fixed in 4% paraformaldehyde (PFA) in PBS and stored in methanol at -20 °C. Genomic DNA prepared from yolk sacs or tail biopsies was used for genotyping by PCR.

Organ cultures

Explant cultures of embryonic kidneys or urogenital systems were performed as previously described (Airik et al., 2010). The culture medium was replaced every 24 h.

For labeling experiments with the fluorescent carbocyanine dye Dil, a tungsten wire was dipped into the Dil tissue labeling paste (Invitrogen) and excessive material was removed with a tissue towel. The tungsten wire was then clamped into a micromanipulator. Labeling of mesenchymal subpopulations within the metanephric field of E11.5 *Tbx18^{GFP/+}* kidney rudiments was performed under visual control. Kidney explants were documented before and after treatment and the perpendicular distance of labeled cells from the ureteric epithelium was measured using ImageJ software (Schneider et al., 2012). After two days of culture the distribution of Dil labeled cells was assessed and plotted against the distance.

For the detection of apoptotic tissue in the metanephric field E11.5 kidney rudiments (*Tbx18^{GFP/+}*) were explanted and cultured for 24 h. The medium was subsequently replaced with 1 ml of 2.5 μM LysoTracker red DND-99 (L-7528, Invitrogen) in PBS and the explant cultures were incubated for 30 min at 37 °C. Cultures were then rinsed in PBS and documented.

For tissue recombination experiments, E11.5 acceptor kidney rudiments (*Tbx18^{GFP/+}*) were explanted. E12.5 ureters (*Tbx18^{cre/+}*;

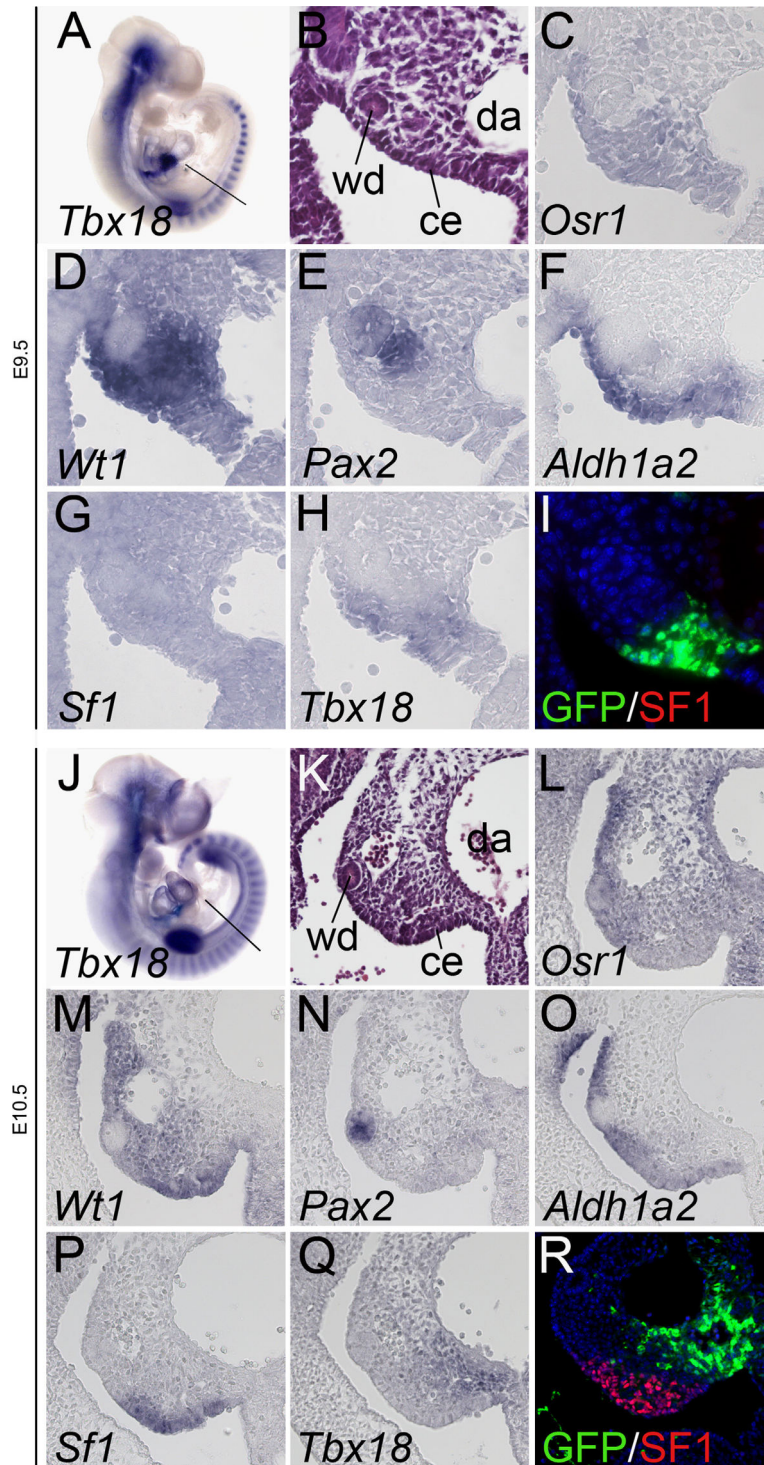


Fig. 1. *Tbx18* expression during early urogenital development: (A,J) *In situ* hybridization analysis of whole wildtype embryos for *Tbx18*; (B,D, K,L) Histological staining (HE) of transverse sections through the posterior trunk region on the planes indicated in (A,J) to describe anatomical landmarks. (C–H,L–Q) *In situ* hybridization analysis on adjacent sections to compare expression of *Tbx18* and markers of the intermediate mesoderm. (I,R) Co-immunofluorescence analysis for SF1 and GFP on adjacent sections of *Tbx18*^{GFP/+} embryos. Probes and stages are as indicated. ce: coelomic epithelium; da: dorsal aorta; wd: Wolffian duct.

Part 1 - Tbx18 lineage in urogenital development

28

T. Bohnenpoll et al. / *Developmental Biology* 380 (2013) 25–36

R26^{mTmG/+} were subsequently prepared and the ureteric epithelium was mechanically separated from the mesenchyme using forceps. The uncoated ureteric epithelium was transplanted into the *Tbx18*⁺ domain of the acceptor tissue distant to the endogenous ureteric epithelium. The recombined tissues were cultured for 3 days with daily documentation.

For bead implantation experiments, E11.5 acceptor kidney rudiments (*Tbx18^{GFP/+}*) were explanted. AffiGel Blue beads (153-7302, Bio-Rad) were rinsed in PBS and incubated with 50 µg/ml rmWNT9B (3669-WN, R&D Systems), 1.6 µg/ml rmSHH (PMC8034, Invitrogen), both or 1 mg/ml BSA for 4 hours at 4 °C. Beads were implanted into the GFP⁺ domain of the acceptor kidneys. Cultures were maintained for 2 days and GFP expression was documented daily.

Histological and histochemical analyses

Fixed embryos were dehydrated, paraffin embedded, and sectioned to 5 µm. For histological analyses sections were stained with haematoxylin and eosin. For the detection of antigens on these sections, the following primary antibodies and dilutions

were used: mouse anti-UPK1B (WH0007348M2-100UG, Sigma, 1:200), mouse anti-ACTA2 (F3777 and C6198, Sigma, 1:200), rabbit anti-CDH1 (kindly provided by R. Kemler, MPI for Immunobiology and Epigenetics, Freiburg, Germany, 1:200), rabbit anti-SF1 (TransGenic Inc., preparation of antibodies by Dr. Ken-Ichirou Morohashi, 1:200), rabbit anti-DDX4 (ab13840, Abcam, 1:50), rabbit anti-FOXD1 (kindly provided by A.P. McMahon, Harvard University, MA, USA, 1:2000), rabbit anti-SIX2 (kindly provided by A.P. McMahon, Harvard University, MA, USA, 1:1000), anti-SOX9 (AB5535, Millipore Chemicon, 1:200), rat anti-EMCN (kindly provided by D. Vestweber, MPI for Molecular Medicine, Münster, Germany, 1:10), mouse anti-GFP (11 814 460 001, Roche, 1:200), rabbit anti-GFP (sc-8334, Santa Cruz, 1:200). Fluorescent staining was performed using Alexa 488/555-conjugated secondary antibodies (A11034; A11008; 711-487-003; A21202; A21422; A21428, Invitrogen/Dianova; 1:500) or biotin-conjugated secondary antibodies (Dianova; 1:500) and the TSA Tetramethylrhodamine Amplification Kit (Perkin-Elmer).

Labeling with primary antibodies was performed at 4 °C overnight after antigen retrieval (Antigen Unmasking Solution, Vector Laboratories; 15 min, 100 °C), blocking of endogenous peroxidases with 3% H₂O₂/PBS for 10 min (required for TSA) and incubation in

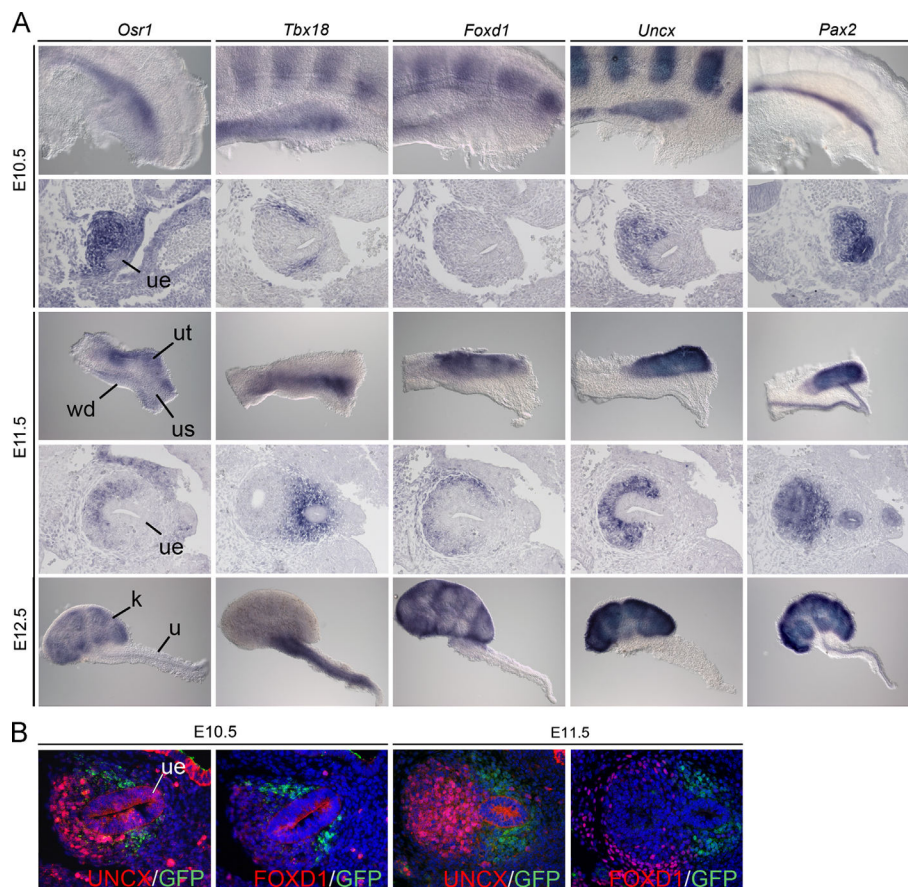


Fig. 2. *Tbx18* expression during early metanephric and ureter development. (A) *In situ* hybridization analysis of whole posterior trunk halves at E10.5 (first row), of transverse sections through the metanephric anlagen of the posterior trunk region at E10.5 (posterior is to the right, ventral to the bottom, second row), of whole E11.5 kidneys (third row), of transverse sections through the E11.5 metanephric kidney (fourth row) and of E12.5 kidneys with ureters (fifth row) to compare expression of *Tbx18* with an early pan-metanephric marker (*Osr1*), and with markers of the nephron lineage (*Uncx*, *Pax2*), of the collecting duct and ureter epithelium (*Pax2*) and of the stromal lineage (*Foxd1*) in wildtype embryos. and (B) Co-immunofluorescence analysis on sections through the metanephros at E10.5 and E11.5 with antibodies against GFP (visualizing TBX18 expression), FOXD1 and UNCX in *Tbx18^{GFP/+}* embryos. k: kidney; u: ureter; ue: ureteric epithelium; us: ureter stalk; wd: Wolffian duct.

blocking solutions provided with the kits. For monoclonal mouse antibodies an additional IgG blocking step was performed using the Mouse-on-Mouse Kit (Vector Laboratories). Sections were mounted with Mowiol (Roth) or IS mounting medium (Dianova).

Paraffin sections used for TUNEL assay were deparaffinized, rehydrated and then treated according to the protocol provided with the Apop Tag Fluorescence Apoptosis detection kit (S7111, Millipore).

In situ hybridization analysis

Whole-mount *in situ* hybridization was performed following a standard procedure with digoxigenin-labeled antisense riboprobes (Wilkinson and Nieto, 1993). Stained specimens were transferred in 80% glycerol prior to documentation. *In situ* hybridization on 10 μm paraffin sections was done essentially as described (Moorman et al., 2001). For each marker at least three independent specimens were analyzed.

Image analysis

Whole-mount specimens were photographed on Leica M420 with Fujix digital camera HC-300Z, sections on Leica DM5000 B with Leica digital camera DFC300 FX. All images were processed in Adobe Photoshop CS4.

Results

Tbx18 is expressed in a subregion of the urogenital ridge

Earlier work showed expression of *Tbx18* in the urogenital ridge but failed to delineate the precise subdomain (Kraus et al., 2001). We therefore performed comparative *in situ* hybridization analysis of expression of *Tbx18* and of markers of (subregions of) the urogenital ridge on transverse sections of E9.5 and E10.5 wildtype embryos (Fig. 1). At E9.5, the entire urogenital ridge was marked by expression of *Osr1* and *Wt1*; the Wolffian duct by expression of *Pax2*, the adjacent tubule-forming mesonephric mesenchyme by *Pax2*, and the epithelial (coelomic) lining of the ridge by *Aldh1a2*. *Sf1* was not expressed at this stage. *Tbx18* expression was never detected in the epithelial Wolffian duct and the *Pax2*⁺ mesonephric mesenchyme but was present in the more medially located mesenchyme close to the dorsal aorta, and overlapping with *Aldh1a2* expression in the coelomic epithelium (Fig. 1C H). At E10.5, the coelomic epithelium of the urogenital ridge was positive for *Sf1* and *Aldh1a2*, and the Wolffian duct for *Pax2* expression. *Osr1* was confined to the mesenchymal compartment of the intermediate mesoderm. *Tbx18* was found in a subregion of the *Osr1*⁺ mesenchyme in the medial aspect close to the hinge between the urogenital ridge and the dorsal mesenterium, complementary to *Wt1* that was expressed in the epithelium and the lateral mesenchyme. Expression of *Tbx18* was no longer detected

in the epithelial lining of the ridge that was positive for *Sf1* at this stage (Fig. 1K Q). Co-immunofluorescence analysis for GFP and SF1 (in *Tbx18*^{GFP/+} embryos) confirmed the expression domain of *Tbx18*

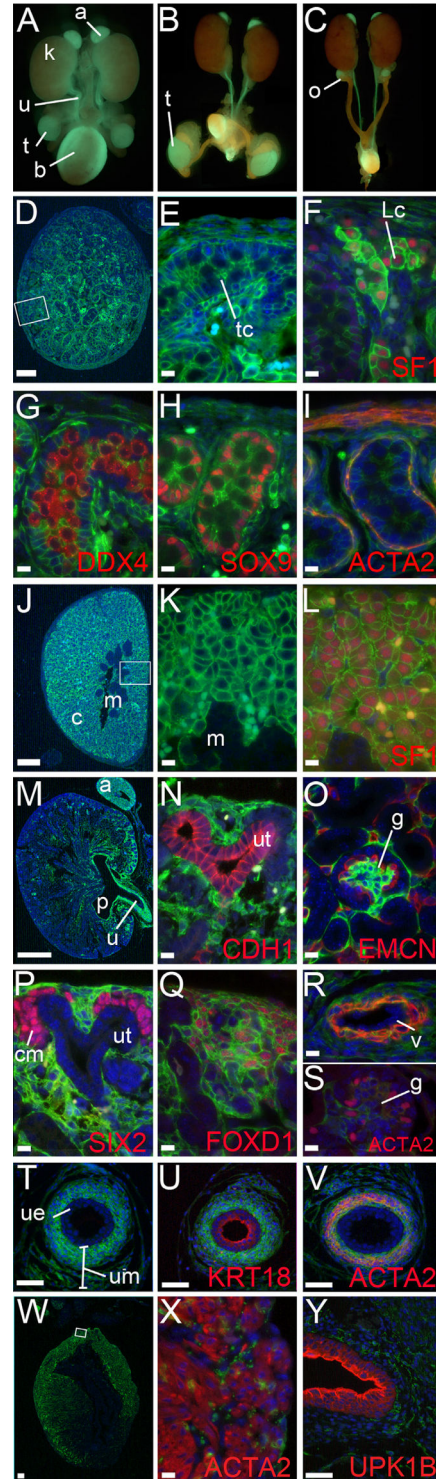


Fig. 3. Lineage analysis of *Tbx18*⁺ descendants in the urogenital system. (A–C) GFP/RFP epifluorescence analysis of urogenital systems from *Tbx18*^{Cre/+};*R26*^{mTmG/+} embryos at E18.5 (A) and at 3-weeks of age (B,C) of both male (A,B) and female sex (C). GFP (green) marks *Tbx18*⁺ cells and their descendants, RFP (red) marks all other cells in the urogenital system. (D–Y) Immunofluorescence analysis of expression of the lineage marker GFP and cell type markers on sections of E18.5 testis (D–I), adrenal gland (J–L), kidney (M–S), ureter (T–V) and bladder (W–Y). Boxed areas are magnified for co-expression analysis of GFP and cell type markers as indicated. Scale bars represent 100 μm (D,J), 500 μm (M,W), 50 μm (T–V,Y), 10 μm (E–I,K,L,N–S, X). a: adrenal gland; b: bladder; c: cortex; cm: cap mesenchyme; g: glomerulus; k: kidney; Lc: Leydig cell; m: medulla; p: pelvis; t: testis; tc: testis cord; u: ureter; ue: ureteric epithelium; um: ureteric mesenchyme; ut: ureter tip; v: vessel. (For interpretation of the references to color in this figure legend, the reader is referred to the web version of this article.)

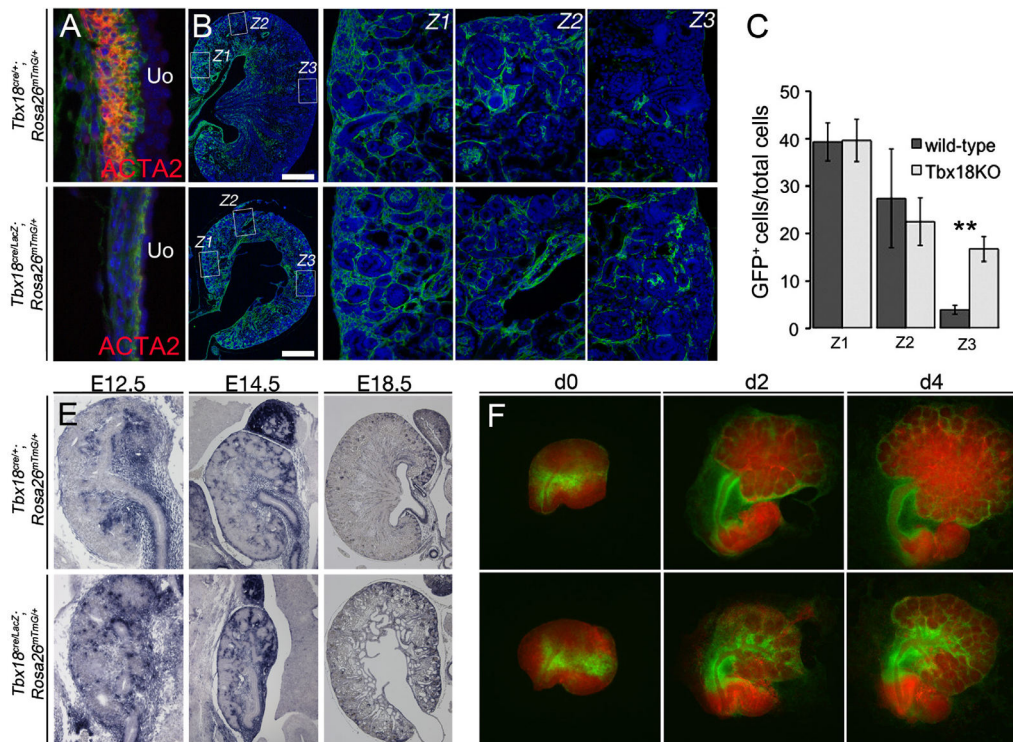


Fig. 4. Lineage analysis of *Tbx18*⁺ descendants in the metanephric/ureteric development. (A) Co-immunofluorescence analysis of expression of the lineage marker GFP and the marker of smooth muscle cells, ACTA2 on sagittal sections of the ureter at E18.5. (B) Co-immunofluorescence analysis of expression of the lineage marker GFP on sagittal sections of the kidney at E18.5. Z1–3 relate to three regions used to determine the contribution of GFP⁺ cells. (C) Quantification of the contribution of GFP⁺ cells to stromal cells in the three regions of the kidney. Z1: control: 39+/-4, mutant: 40+/-4, $p=0.935$; Z2: control: 27+/-10, mutant: 23+/-5, $p=0.504$; Z3: control: 4+/-1, mutant: 17+/-3, $p=0.001$. (D) *in situ* hybridization analysis of GFP expression in *Tbx18*^{cre/+}; *R26*^{mTmG/+} kidneys at different developmental stages as indicated. (E) GFP/RFP epifluorescence analysis of metanephric explants from E11.5 *Tbx18*^{cre/+}; *R26*^{mTmG/+} embryos at 0, 2 and 4 days of culture. GFP (green) marks *Tbx18*⁺ cells and their descendants, RFP (red) marks all other cells in the explants. a: adrenal; k: kidney; u: ureter; ut: ureter tip. (For interpretation of the references to color in this figure legend, the reader is referred to the web version of this article.)

at both stages and the exclusion from SF1⁺ cells (Fig. 11,R). Hence, *Tbx18* is expressed transiently in the coelomic epithelium and in a mesenchymal subdomain of the urogenital ridge.

Tbx18 is expressed in a mesenchymal subregion of the metanephric field before it is restricted to the ureteric mesenchyme

Our previous work showed that during metanephric development *Tbx18* is expressed in a narrow band of mesenchymal cells abutting the mesenchyme of the Wolffian duct and the metanephric kidney at E11.5 before expression becomes confined to the mesenchyme surrounding the ureter from E12.5 onwards (Airik et al., 2006). To determine the onset of *Tbx18* expression in the mesenchymal cells of the metanephric anlage (the metanephric field) and define the relationship to the precursor populations of known metanephric cell lineages, we performed *in situ* hybridization analysis of whole kidney rudiments as well as of adjacent sections through the posterior trunk at E10.5 and E11.5. At each stage, we compared expression of *Tbx18* to that of *Foxd1*, a marker for the stromal lineage of the metanephros (Hatini et al., 1996), to that of *Uncx*, a marker for the cap mesenchyme (Karner et al., 2011), to *Pax2* which marks the cap mesenchyme as well as the Wolffian duct and its epithelial outgrowths (Dressler et al., 1990), and to *Osr1* (Mugford et al., 2008; So and Danielian, 1999).

At E10.5, *Osr1* expression encompassed the mutually exclusive domains of *Tbx18* and *Uncx/Pax2*. Expression of *Foxd1* was scarcely detectable at this stage. At E11.5, *Foxd1* expression surrounded in a

circle-like fashion the cap mesenchyme that was positive for *Osr1*, *Uncx* and *Pax2*. *Tbx18* expression surrounded the ureter stalk in an exclusive fashion. At E12.5, *Tbx18* was restricted to the mesenchyme surrounding the distal ureter whereas expression of *Foxd1* and *Uncx/Pax2/Osr1* was restricted to the stromal and the cap mesenchyme of the kidney, respectively (Fig. 2A). Immunofluorescence analysis of GFP (visualizing TBX18) and FOXD1/UNCX expression on transverse sections of E10.5 and E11.5 *Tbx18*^{GFP/+} embryos confirmed that TBX18 protein was not co-expressed with either of these markers (Fig. 2B). These data show that *Tbx18* expression defines a molecularly distinct sub-population of mesenchymal cells in the early metanephric field.

Tbx18⁺ cells of the urogenital ridge and the early metanephric field contribute to multiple components of the mature urogenital system

To determine the contribution of *Tbx18*⁺ cells in the urogenital ridge and the early metanephric field to the components of the mature urogenital system, we irreversibly labeled the descendants of these populations using a *cre/loxP*-based genetic approach with a *Tbx18*^{cre}-line generated in our laboratory and the sensitive *Rosa26*^{mTmG} reporter (Muzumdar et al., 2007; Trowe et al., 2010). In the *Rosa26*^{mTmG} reporter line cells that have undergone recombination express membrane-bound GFP while non-recombined cells express membrane-bound RFP.

In E18.5 and 3-week old whole urogenital systems, GFP epifluorescence was found in the gonads, the kidneys, the ureters,

the bladder and additionally in the adrenals that are associated with the urogenital system (Fig. 3A–C). To characterize the contribution of *Tbx18*⁺ descendants to the differentiated cell types in these organs, we performed co-immunofluorescence analysis with antibodies directed against GFP and cell-type specific markers on sections of E18.5 *Tbx18*^{cre/+};*Rosa26*^{mTmG/+} embryos. In the testis, GFP expression was found in the tunica albuginea, interstitium and testis cords in a dorsal to ventral gradient (Fig. 3D). Coexpression analysis with cell-type specific markers showed that *Tbx18*⁺ descendants contributed to Leydig cells in the interstitium (SF1) (Luo et al., 1994), to most but not all Sertoli cells (SOX9) (Morais da Silva et al., 1996), to smooth muscle cells of the tunica albuginea (ACTA2) but not to germ cells (DDX4) (Fujiwara et al., 1994) (Fig. 3E–I). In adrenals, GFP⁺ cells were restricted to the SF1⁺ steroidogenic cells of the cortex (Luo et al., 1994) (Fig. 3J–L). Compatible with the notion that *Tbx18*⁺ descendants contribute to steroidogenic cells of the gonad and the adrenal gland, we observed coexpression of the lineage marker GFP with SF1, a marker for the adrenogonadal precursor pool (Bingham et al.,

2006), in the coelomic lining of E10.5 *Tbx18*^{cre/+};*Rosa26*^{mTmG/+} embryos (Supplementary Fig. S1).

In E18.5 kidneys, the distribution of GFP expression appeared graded being more prominent at the medial (where *Tbx18*⁺ cells originally resided) than at the lateral side of the organ (Fig. 3M). In the medial region of the kidney, GFP expression was excluded from cells expressing the epithelial marker CDH1 (Vestweber et al., 1985), the endothelial marker EMCN (Morgan et al., 1999), and the cap mesenchyme marker SIX2 (Karner et al., 2011; Self et al., 2006) indicating that *Tbx18*⁺ descendants do not contribute to the collecting duct system, the endothelial network of the kidney, or the nephron lineage, respectively (Fig. 3N–P). Coexpression in the cortical stroma with FOXD1 and with the smooth muscle marker ACTA2 in arteries and in glomeruli argue that a substantial fraction of interstitial cells, vascular smooth muscle and mesangial cells in the medial kidney region derive from *Tbx18*⁺ progenitors (Fig. 3Q–S). In the ureter, all cells of the mesenchymal coating (fibroblasts of the lamina propria, smooth muscle cells and adventitial fibroblasts) expressed GFP confirming earlier results

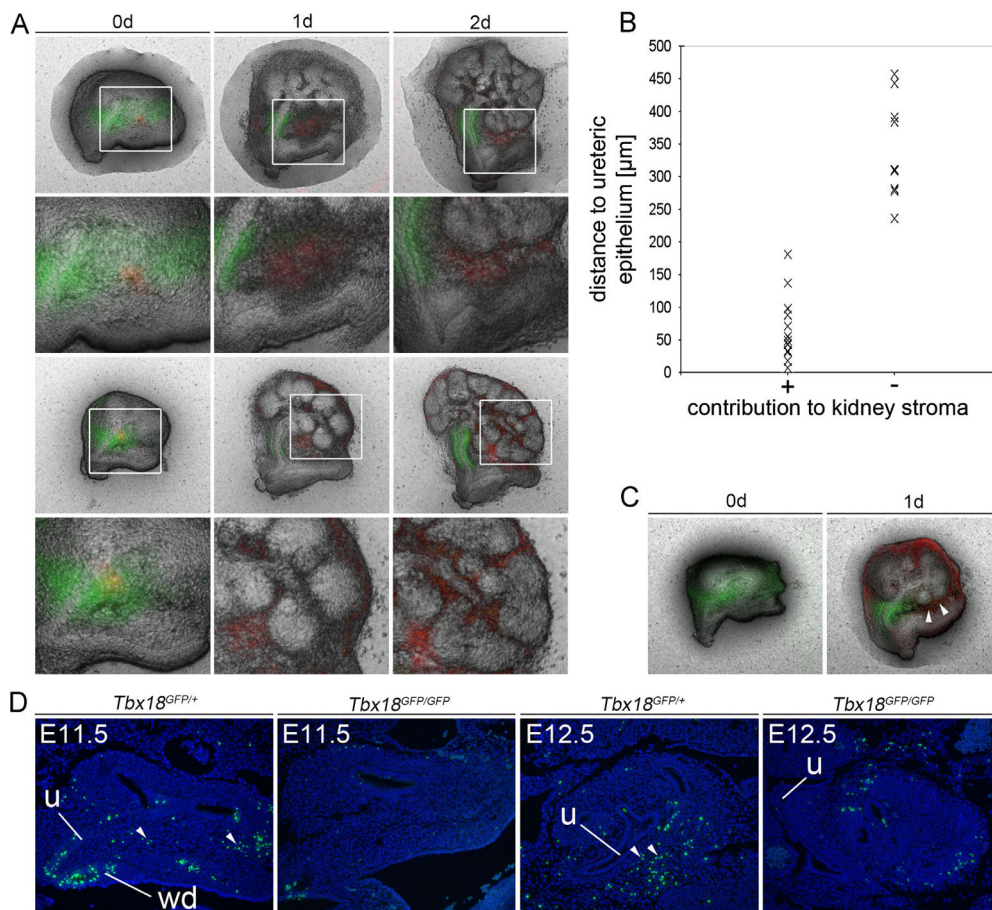


Fig. 5. Lineage analysis and apoptosis of *Tbx18*⁺ mesenchymal cells in early kidney rudiments. (A) Combined brightfield and epifluorescence analysis of metanephric explants from E11.5 *Tbx18*^{GFP/+} embryos at 0, 1 and 2 days of culture. GFP (green) marks the *Tbx18* expression domain, the red fluorescence indicates Dil-injected cell clusters. Shown are two representative examples of Dil-injected cells ending up in the renal stroma (upper row), and of cells localizing to the space between kidneys and the Wolffian duct (lower row). Boxed regions are shown in higher magnifications below. (B) Quantitative evaluation of localization of Dil-injected cells in dependence from the distance from the ureteric epithelium at E11.5. (C) Analysis of cell death by lysotracker staining in explants of E11.5 kidney rudiments from *Tbx18*^{GFP/+} embryos cultured for 0 and 1 day. Arrows point to cell death in the lateral ureteric mesenchyme. (D) Analysis of cell death by the TUNEL assay in E11.5 and E12.5 kidneys rudiments from *Tbx18*^{GFP/+} and *Tbx18*^{GFP/GFP} embryos. Arrows point to cell death in the lateral ureteric mesenchyme. u, ureter; Wd, Wolffian duct. (For interpretation of the references to color in this figure legend, the reader is referred to the web version of this article.)

Part 1 - Tbx18 lineage in urogenital development

32

T. Bohnenpoll et al. / *Developmental Biology* 380 (2013) 25–36

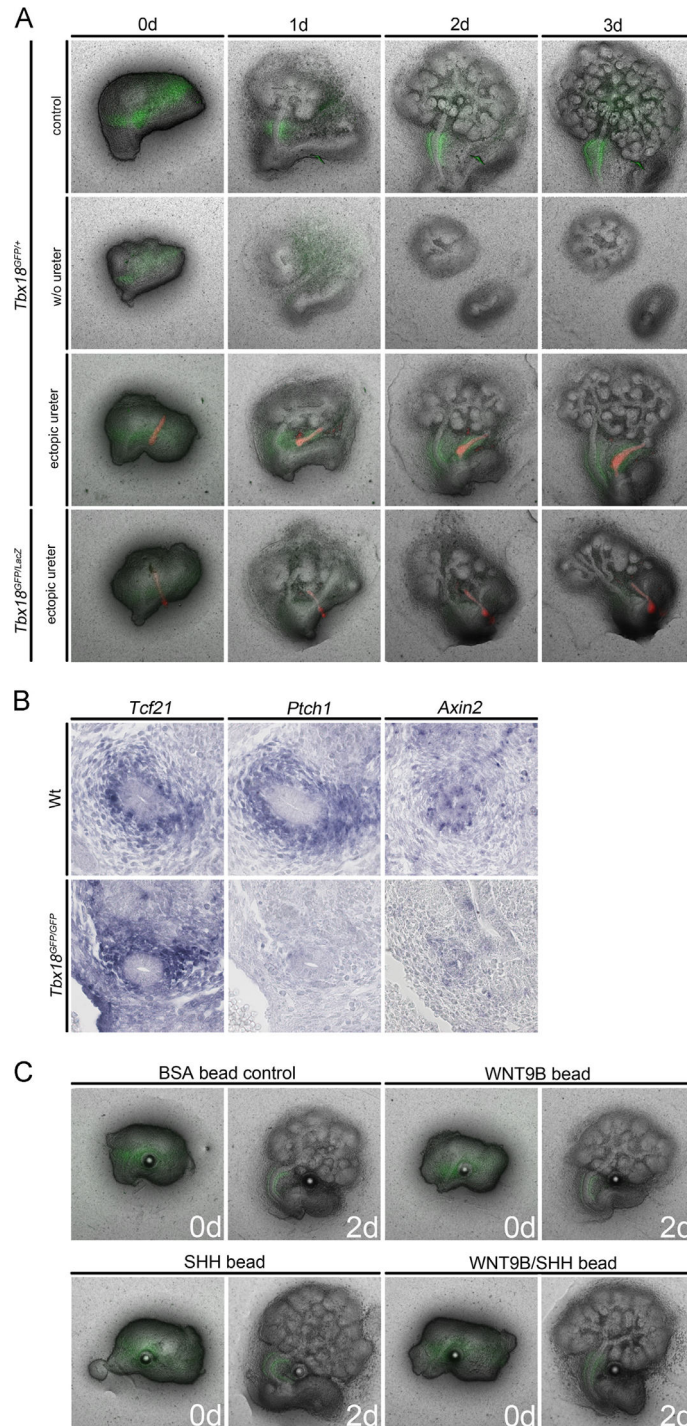


Fig. 6. Regulation of *Tbx18* expression and ureteric fates by signals from the ureteric epithelium. (A) Combined brightfield and GFP/RFP epifluorescence analysis of E11.5 metanephric explants from E11.5 *Tbx18^{GFP/+}* embryos at 0, 1, 2 and 3 days of culture; GFP (green) marks *Tbx18⁺* cells in unmanipulated cultures (control), in cultures from which the ureter was removed (w/o ureter); after transplantation of an RFP⁺ (red) *R26^{mtmG/+}* ureter stripped of mesenchymal cells into the distal domain of *Tbx18⁺* cells (ectopic ureter) in *Tbx18^{GFP/+}* and *Tbx18^{GFP/+GFP}* rudiments. (B) *In situ* hybridization analysis of transverse ureter sections of E12.5 control (wt) and *Tbx18^{GFP/+GFP}* embryos of expression of *Tcf21*, of the target of SHH-signaling, *Ptch1*, and of the target of canonical WNT-signaling, *Axin2*. (C) GFP epifluorescence analysis of explants from E11.5 *Tbx18^{GFP/+}* embryos cultured for 0 and 2 days in the presence of BSA-, WNT9B-, SHH- or WNT9B/SHH-soaked beads. (For interpretation of the references to color in this figure legend, the reader is referred to the web version of this article.)

of our group that the ureteric mesenchyme completely derives from *Tbx18*⁺ mesenchymal cells (Fig. 3T–V) (Trowe et al., 2012). In the bladder, GFP expression was graded from dorsal to ventral within the smooth muscle cell layer but was absent from the urothelium (Fig. 3W–Y).

We conclude, that *Tbx18*⁺ cells in the developing urogenital system are multipotent and contribute to all mesenchymal cell types in the ureter but also to a large degree to the stromal, mesangial and smooth muscle cells of the medial region of the kidney, to the bladder mesenchyme, to the cortical steroidogenic cells of the adrenal gland and to somatic cells of the gonads.

Tbx18 is required for ureteric differentiation of mesenchymal cells

Our previous analysis has shown that *Tbx18* is required for differentiation of the ureteric mesenchyme into smooth muscle cells but has not addressed a critical involvement of the gene in the development of the other organs of the urogenital system, to which *Tbx18*⁺ descendants largely contribute. We, therefore, analyzed *Tbx18*-deficient embryos (*Tbx18*^{cre/lacZ}; *R26*^{mTmG/+}) at E18.5, i.e. shortly before these mice die due to skeletal defects, for histological and molecular changes in the development of these organs. Analysis of the adrenal gland by histological staining, co-immunofluorescence of the lineage marker GFP and the marker of steroidogenic cells SF1, and quantification of GFP⁺ cells in the cortex did not detect any difference in the distribution and differentiation of *Tbx18*⁺ descendants in wildtype and *Tbx18*-deficient adrenals at this stage. Expression of *Akr1c18* and *Cyp11b1*, markers of the inner cortical layer (Lalli, 2010), and of *Wnt-4*, a marker of the outer cortical layer (Heikkila et al., 2002), was unaffected in the mutant showing that zonation into medulla and inner and outer cortex occurred normally (Supplementary Fig. S2). Histological staining and co-expression analysis with subsequent quantification of the previously used differentiation markers SOX9 (Sertoli cells), DDX4 (germ cells), and SF1 (Leydig cells) did not detect any difference between wildtype and *Tbx18*-deficient testes at this stage either (Supplementary Fig. S3). Differentiation of mesenchymal and epithelial lineages was also unaffected in the bladder and the kidney in the absence of *Tbx18* (Supplementary Figs. S4,S5).

However, in the kidney, the contribution of GFP⁺ cells to both the medullary and cortical stroma on the lateral side was enhanced, whereas the few GFP⁺ cells of the ureter failed to differentiate into smooth muscle cells (Fig. 4A–C). *In situ* hybridization of the lineage marker *Gfp* on sections of kidneys of earlier stages revealed that *Tbx18*⁺ descendants dislocalized laterally onto the kidney as early as E12.5 (Fig. 4D). To further visualize the altered contribution to stromal cells in *Tbx18*-deficient kidneys, we explanted E11.5 metanephric rudiments and followed the GFP epifluorescence in culture (Fig. 4E). In the control (*Tbx18*^{cre/+}; *R26*^{mTmG/+}) GFP⁺ cells localized to the ureteric mesenchyme and the stromal cells of the kidney particularly those of the medial cortex. In *Tbx18*-deficient embryos (*Tbx18*^{cre/lacZ}; *R26*^{mTmG/+}), GFP expression was reduced around the short ureter but strongly enhanced in the medullary stroma around the distorted pelvic region. Of note, GFP⁺ cells now surrounded branching ureteric epithelium unlike in the control (Fig. 4E). We conclude from this analysis that *Tbx18* is required in uncommitted precursor cells to adopt the ureteric fate. In absence of *Tbx18* these cells contribute to the renal stroma.

A spatially restricted subset of Tbx18⁺ mesenchymal cells contributes to the definite ureteric mesenchyme after E11.5

As *Tbx18* is exclusively required within the ureteric mesenchymal lineage, we wished to learn about the mechanisms that

confine *Tbx18* expression in the early metanephric field, and suppress the stromal in favor of the ureteric mesenchymal fate. To determine whether *Tbx18*⁺ cells of the early metanephric field contribute randomly or in a spatially defined manner to the ureteric mesenchyme, we isolated kidney rudiments of E11.5 *Tbx18*^{GFP/+} embryos and explanted them onto filter membranes. The red fluorescent dye Dil was injected at defined distances from the ureteric epithelium onto small cell clusters within the *Tbx18*⁺ domain (as visualized by GFP fluorescence from the *Tbx18*^{GFP} allele) and the distribution of the red fluorescence was determined after 2 days (Fig. 5A, Supplementary Fig. S6). Two outcomes were observed: Dil injected into mesenchymal cells in a distance of up to 200 μm from the ureteric epithelium contributed to the kidney stroma whereas Dil injected more distally ended up as an amorphous mass in between the Wolffian duct and the kidney. Localization of Dil⁺ cells to the GFP⁺ ureteric mesenchyme was never observed (Fig. 5B). Lysotracker staining of E11.5 metanephric rudiments explanted for 1 day detected apoptotic cells in the lateral domain of the ureteric mesenchyme that had lost *Tbx18* expression at this time but not in those adjacent to the ureteric epithelium (Fig. 5C). To exclude a culture artefact, we also analyzed apoptosis by TUNEL staining in sections of E11.5 and E12.5 embryos. At both stages we detected apoptosis in mesenchymal cells lateral to but not adjacent to the short ureter stalk. Intriguingly, apoptosis in this domain was completely lost in *Tbx18*-deficient embryos (Fig. 5D).

We conclude that only a minor fraction of the mesenchymal cells initially positive for *Tbx18* contribute to the definite ureteric mesenchyme, most likely those in direct proximity to the epithelium (that we were unable to label by this technique). Cells within a 200-μm range of the ureteric epithelium contribute to the kidney stroma whereas cells further away undergo apoptosis. In *Tbx18*-deficient embryos, lateral *Tbx18*⁺ descendants fail to undergo apoptosis but may additionally contribute to the renal stroma.

Epithelial signals impose a ureteric fate onto Tbx18⁺ cells

Given the finding that only cells in direct vicinity of the ureteric epithelium are likely to contribute to the definitive ureteric mesenchyme, we wished to test the role of epithelial signals in maintaining *Tbx18* expression and directing a ureteric fate to cells in the early metanephric field, and performed tissue recombination experiments in cultured explants of metanephric rudiments of E11.5 *Tbx18*^{GFP/+} embryos (Fig. 6A). In a control experiment, GFP expression was confined to the mesenchymal tissue layer covering the ureteric epithelium after 3 days of culture. Removal of the ureter from E11.5 kidney explants resulted in a dispersal of GFP⁺ cells and their complete loss after 3 days. We then transplanted an RFP-labeled ureteric epithelium (obtained from E12.5 *R26*^{mTmG/+} embryos) into the *Tbx18*⁺ domain in a position distant from the ureteric epithelium of the host tissue. Interestingly, GFP expression was maintained in the lateral mesenchyme and GFP⁺ cells accumulated around the ectopic RFP⁺ ureteric epithelium. In contrast, when a RFP-labeled ureteric epithelium was transplanted into the lateral GFP⁺ domain of kidney explants of E11.5 *Tbx18*^{GFP/lacZ} embryos, GFP⁺ cells did not accumulate around the ectopic ureter (Fig. 6A). Together, these results strongly suggest that epithelial signals are required and sufficient to maintain *Tbx18* expression and to impose a ureteric fate onto *Tbx18*⁺ cells. Epithelial signals do not act in a distance to induce a condensation process but merely seem to impinge onto the adjacent layer of mesenchymal cells. In absence of *Tbx18*, mesenchymal cells can no longer respond to signals from the ureteric epithelium.

We have recently shown that canonical (*Ctnnb1*-dependent) WNT signaling is required to maintain *Tbx18* expression and induce smooth muscle differentiation in the ureteric mesenchyme

(Trowe et al., 2012). The latter process also requires SHH signals from the epithelial compartment (Yu et al., 2002). In *Tbx18*-deficient ureters, *Tcf21*⁺-mesenchymal cells surrounding the ureter did not express *Axin2* and *Ptch1*, targets of the canonical WNT- and SHH-signals that are secreted from the epithelial compartment in the mutant (Fig. 6B). We conclude that *Tbx18* is required in uncommitted precursor cells to respond to epithelial signals and to adopt the ureteric fate.

To address the question whether WNT and/or SHH signals are sufficient to maintain *Tbx18* expression in the lateral domain in which it is lost after E11.5, we explanted E11.5 kidney rudiments and implanted beads soaked with SHH and/or WNT9B protein (*Wnt9b* is co-expressed with *Wnt7b* in the ureteric epithelium) into this domain (Trowe et al., 2012). Neither BSA control nor WNT9B-, SHH- or WNT9B/SHH-beads maintained GFP, i.e. *Tbx18* expression, in the lateral domain (Fig. 6C), arguing that WNTs cooperate with other as yet unknown epithelial signals to maintain *Tbx18* expression and possibly determine the ureteric fate.

Discussion

Tbx18⁺ progenitors contribute to multiple cell types in the urogenital system

We have demonstrated that descendants of *Tbx18*⁺ cells contribute to a variety of cell types within the urogenital system including cells within the gonads, the kidney, ureter, bladder and adrenal gland. Our expression analysis together with the genetic lineage tracing of *Tbx18*⁺ cells argue that cellular contribution to the adrenal gland and gonads on one hand and to the kidney, ureter and bladder on the other hand reflect two independent expression domains of *Tbx18*; one in the urogenital ridge and the other one in the metanephric field, and that the latter represents a novel subpool of progenitors from which the ureteric mesenchyme will eventually arise.

Transient expression in the epithelial lining of the urogenital ridge around E9.5 is likely to present a common precursor pool for the gonads and the adrenals. In fact, the contribution to interstitial, Sertoli and tunica albuginea cells in the gonad and steroidogenic cells of the adrenal cortex is virtually identical to that identified by a genetic approach based on expression of *Sf1*, a marker for this primordium (Bingham et al., 2006). *Tbx18* expression in the epithelial lining of the ridge is transient and seems to slightly precede that of *Sf1* in this domain. Compatible with expression in the unseparated progenitor pool for both tissues, we recently noted sex reversal and loss of adrenals in mice with conditional *Tbx18*^{cre}-mediated deletion of *Ctnnb1* (Trowe et al., 2012). In fact, identical phenotypes were observed upon an *Sf1*^{cre}-mediated deletion of this mediator of the canonical branch of WNT signaling in mice (Kim et al., 2008; Liu et al., 2009). At this point, we do not have the technical means to independently evaluate the contribution of the mesenchymal expression domain of *Tbx18* in the early urogenital ridge. However, since this domain does not overlap with *Pax2* in the mesonephros, we suggest that it does not mark progenitors for mesonephric tubules but for stromal cells that are associated with these structures.

In contrast to our initial expectations, we found that the *Tbx18*⁺ cells that are located in the metanephric field between the mesenchymal populations of the metanephros and the Wolffian duct, are not yet specified to a ureteric mesenchymal fate but are a multipotent population that contributes to interstitial cells of the kidney (cortical and medullary stromal cells, mesangial cells and vascular smooth muscle cells), to all mesenchymal cells of the ureter and to a subset of smooth muscle cells of the bladder. Most notably, our expression analysis as well as the fate mapping clearly

shows that the *Tbx18*⁺ lineage is at all time points separated from the *Six2*⁺*Uncx*⁺ progenitors from which nephrons will develop. *Tbx18* expression does not overlap with the stromal marker *Foxd1* at E11.5. However, *Foxd1* is not expressed at E10.5 in the metanephric field strongly suggesting that *Tbx18* expression at this stage encompasses progenitors of renal stromal cells as well as of the ureteric mesenchyme. Hence, within the *Osr1*⁺ metanephric field two lineages are established at E10.5: the *Six2*⁺*Uncx*⁺ nephron lineage and the *Tbx18*⁺ lineage of kidney stromal cells/ureter and bladder mesenchyme. Between E10.5 and E11.5 the *Tbx18*⁺ and *Foxd1*⁺ lineages are completely separated. *Tbx18*⁺ cells lying in direct proximity to the ureteric epithelium will maintain *Tbx18* and differentiate into all mesenchymal cell types of the ureter. Cells which loose *Tbx18* expression will either die or contribute to the renal stroma and the bladder mesenchyme. Due to lack of appropriate markers and adequate culture settings we cannot firmly state when the mesenchymal lineages of the ureter and bladder separate but assume that it occurs around the same time.

Tbx18-Cre cell lineage tracing with a BAC-based approach recently reported contribution of *Tbx18*⁺ descendants to smooth muscle cells of the bladder and the ureter in the mature urogenital system. The more restricted contribution in this genetic setting may relate to a less sensitive detection system used but more likely reflects the lack of regulatory elements in the BAC used for construction of a *Tbx18*-Cre transgene (Wang et al., 2009). Our *Tbx18*^{cre} allele was constructed by inserting a *cre* orf into the start codon of the *Tbx18* locus (Trowe et al., 2010). Analysis of *cre* expression in the urogenital system as well as at extrarenal sites showed that expression of *cre* faithfully mimics endogenous expression of *Tbx18* strongly arguing that all control elements of *Tbx18* are preserved and direct appropriate expression of *cre* from this allele (Christoffels et al., 2009; Trowe et al., 2012). Furthermore, the sensitive *Rosa26*^{mtmG} reporter line allows a cellular resolution of all recombination events. Hence, we are convinced that our genetic lineage tracing system is technically sound and provides a true image of the widespread distribution of *Tbx18*⁺ descendants in the urogenital system.

Tbx18⁺ cells do not condense to form the definitive ureteric mesenchyme

We previously suggested that the band of *Tbx18*⁺ mesenchymal cells in the E11.5 metanephric field condenses around the ureteric epithelium to form the definite ureteric mesenchyme until E12.5. Our genetic lineage tracings as well as our Dil injection in the *Tbx18*⁺ domain at E11.5 contradict this “condensation” model but suggest that only a minor fraction of the cells initially positive for *Tbx18* become the precursors for smooth muscle cells and fibroblasts of the ureter. In fact, the majority of cells in this domain switch off *Tbx18* expression, and depending on the distance from the ureter contribute to the kidney stroma (the more proximal ones) or localize to the tissue in between the kidney and the Wolffian duct (the more distal ones). The latter population undergoes apoptosis, a process that may aid in severing the connections between the two organs. Only the few cells in proximity to the ureteric epithelium maintain *Tbx18* expression. Our further experiments suggest that the ureteric mesenchyme is specified between E11.5 and E12.5 by signals from the ureteric epithelium. Data from canonical WNT pathway manipulation presented in this study as well in a recent report from our lab strongly suggest that WNT signals are required to maintain but are not sufficient to induce *Tbx18* expression (Trowe et al., 2012). We suggest that other signals from the epithelium, but not SHH, cooperate with WNT signals to maintain *Tbx18* expression and specify a ureteric fate to allow further differentiation of ureteric fibroblasts and smooth muscle cells.

Our analysis of *Tbx18*-deficient embryos has shown that *Tbx18* is not required for development of any of the components of the urogenital system except the ureter. *Tbx18* seems to act in a sub-pool of mesenchymal precursors of the metanephric field to favor a ureteric at the expense of a renal stromal fate. Since target genes for signals from the ureteric epithelium (*i.e.* SHH and WNTs) are not activated in *Tbx18*-deficient cells, we suggest that *Tbx18* acts as a pre-patterning gene to make the cells competent to receive signals emanating from the epithelial compartment. However, our analysis has also shown that transient *Tbx18* expression in mesenchymal cells of the early metanephric field is required to induce apoptosis in the lateral domain to avoid the formation of ectopic ligaments between the gonads, the kidney and the ureter as observed in *Tbx18*-deficient urogenital systems.

Acknowledgments

This work was supported by a grant from the Deutsche Forschungsgemeinschaft (German Research Foundation) to A.K. (DFG Ki728/7-1). We would like to thank Rolf Kemler, Andrew P. McMahon, Dietmar Vestweber, Tamara Rabe and Ahmed Mansouri for antibodies.

Appendix A. Supporting information

Supplementary data associated with this article can be found in the online version at <http://dx.doi.org/10.1016/j.ydbio.2013.04.036>.

References

- Airik, R., Bussen, M., Singh, M.K., Petry, M., Kispert, A., 2006. Tbx18 regulates the development of the ureteral mesenchyme. *J. Clin. Invest.* 116, 663–674.
- Airik, R., Trowe, M.O., Foik, A., Farin, H.F., Petry, M., Schuster-Gossler, K., Schweizer, M., Scherer, G., Kist, R., Kispert, A., 2010. Hydronephrosis due to loss of Sox9-regulated smooth muscle cell differentiation of the ureteric mesenchyme. *Hum. Mol. Genet.* 19, 4918–4929.
- Bingham, N.C., Verma-Kurvari, S., Parada, L.F., Parker, K.L., 2006. Development of a steroidogenic factor 1/Cre transgenic mouse line. *Genesis* 44, 419–424.
- Boyle, S., Misfeldt, A., Chandler, K.J., Deal, K.K., Southard-Smith, E.M., Mortlock, D.P., Baldwin, H.S., de Caestecker, M., 2008. Fate mapping using Cited1-CreERT2 mice demonstrates that the cap mesenchyme contains self-renewing progenitor cells and gives rise exclusively to nephronic epithelia. *Dev. Biol.* 313, 234–245.
- Brenner-Anantharam, A., Cebrían, C., Guillaume, R., Hurtado, R., Sun, T.T., Herzlinger, D., 2007. Tailbud-derived mesenchyme promotes urinary tract segmentation via BMP4 signaling. *Development* 134, 1967–1975.
- Bussen, M., Petry, M., Schuster-Gossler, K., Leitges, M., Gossler, A., Kispert, A., 2004. The T-box transcription factor Tbx18 maintains the separation of anterior and posterior somite compartments. *Genes Dev.* 18, 1209–1221.
- Christoffels, V.M., Grieskamp, T., Norden, J., Mommersteeg, M.T., Rudat, C., Kispert, A., 2009. Tbx18 and the fate of epicardial progenitors. *Nature* 458, E8–E9; discussion E9–10.
- Christoffels, V.M., Mommersteeg, M.T., Trowe, M.O., Prall, O.W., de Gier-de Vries, C., Soufan, A.T., Bussen, M., Schuster-Gossler, K., Harvey, R.P., Moorman, A.F., Kispert, A., 2006. Formation of the venous pole of the heart from an Nkx2-5-negative precursor population requires Tbx18. *Circ. Res.* 98, 1555–1563.
- Dressler, G.R., Deutsch, U., Chowdhury, K., Nornes, H.O., Gruss, P., 1990. Pax2, a new murine paired-box-containing gene and its expression in the developing excretory system. *Development* 109, 787–795.
- Fujiwara, Y., Komiya, T., Kawabata, H., Sato, M., Fujimoto, H., Furusawa, M., Noce, T., 1994. Isolation of a DEAD-family protein gene that encodes a murine homolog of *Drosophila vasa* and its specific expression in germ cell lineage. *Proc. Natl. Acad. Sci. USA* 91, 12258–12262.
- Gao, X., Chen, X., Taglienti, M., Rumballe, B., Little, M.H., Kreidberg, J.A., 2005. Angioblast-mesenchyme induction of early kidney development is mediated by Wt1 and Vegfa. *Development* 132, 5437–5449.
- Grote, D., Souabni, A., Busslinger, M., Bouchard, M., 2006. Pax 2/8-regulated *Gata 3* expression is necessary for morphogenesis and guidance of the nephric duct in the developing kidney. *Development* 133, 53–61.
- Guillaume, R., Bressan, M., Herzlinger, D., 2009. Paraxial mesoderm contributes stromal cells to the developing kidney. *Dev. Biol.* 329, 169–175.
- Hatano, O., Takakusu, A., Nomura, M., Morohashi, K., 1996. Identical origin of adrenal cortex and gonad revealed by expression profiles of Ad4BP/SF-1. *Genes Cells* 1, 663–671.
- Hatini, V., Huh, S.O., Herzlinger, D., Soares, V.C., Lai, E., 1996. Essential role of stromal mesenchyme in kidney morphogenesis revealed by targeted disruption of Winged Helix transcription factor BF-2. *Genes Dev.* 10, 1467–1478.
- Heikkilä, M., Peltoketo, H., Leppaluoto, J., Ilves, M., Vuolteenaho, O., Vainio, S., 2002. Wnt-4 deficiency alters mouse adrenal cortex function, reducing aldosterone production. *Endocrinology* 143, 4358–4365.
- Humphreys, B.D., Lin, S.L., Kobayashi, A., Hudson, T.E., Nowlin, B.T., Bonventre, J.V., Valerius, M.T., McMahon, A.P., Duffield, J.S., 2010. Fate tracing reveals the pericyte and not epithelial origin of myofibroblasts in kidney fibrosis. *Am. J. Pathol.* 176, 85–97.
- Ikeda, Y., Shen, W.H., Ingraham, H.A., Parker, K.L., 1994. Developmental expression of mouse steroidogenic factor-1, an essential regulator of the steroid hydroxylases. *Mol. Endocrinol.* 8, 654–662.
- James, R.G., Kamei, C.N., Wang, Q., Jiang, R., Schultheiss, T.M., 2006. Odd-skipped related 1 is required for development of the metanephric kidney and regulates formation and differentiation of kidney precursor cells. *Development* 133, 2995–3004.
- Karner, C.M., Das, A., Ma, Z., Self, M., Chen, C., Lum, L., Oliver, G., Carroll, T.J., 2011. Canonical Wnt9b signaling balances progenitor cell expansion and differentiation during kidney development. *Development* 138, 1247–1257.
- Keegan, C.E., Hammer, G.D., 2002. Recent insights into organogenesis of the adrenal cortex. *Trends Endocrinol. Metab.* 13, 200–208.
- Kim, A.C., Reuter, A.L., Zubair, M., Else, T., Serecky, K., Bingham, N.C., Lavery, G.G., Parker, K.L., Hammer, G.D., 2008. Targeted disruption of beta-catenin in Sf1-expressing cells impairs development and maintenance of the adrenal cortex. *Development* 135, 2593–2602.
- Kobayashi, A., Valerius, M.T., Mugford, J.W., Carroll, T.J., Self, M., Oliver, G., McMahon, A.P., 2008. Six2 defines and regulates a multipotent self-renewing nephron progenitor population throughout mammalian kidney development. *Cell Stem Cell* 3, 169–181.
- Kraus, F., Haenig, B., Kispert, A., 2001. Cloning and expression analysis of the mouse T-box gene Tbx18. *Mech. Dev.* 100, 83–86.
- Lalli, E., 2010. Adrenal cortex ontogenesis. *Best Pract. Res. Clin. Endocrinol. Metab.* 24, 853–864.
- Levinson, R.S., Batourina, E., Choi, C., Vorontchikhina, M., Kitajewski, J., Mendelsohn, C.L., 2005. Foxd1-dependent signals control cellularity in the renal capsule, a structure required for normal renal development. *Development* 132, 529–539.
- Little, M.H., McMahon, A.P., 2012. Mammalian kidney development: principles, progress, and projections. *Cold Spring Harbor Perspect. Biol.* 4.
- Liu, C.F., Bingham, N., Parker, K., Yao, H.H., 2009. Sex-specific roles of beta-catenin in mouse gonadal development. *Hum. Mol. Genet.* 18, 405–417.
- Luo, X., Ikeda, Y., Parker, K.L., 1994. A cell-specific nuclear receptor is essential for adrenal and gonadal development and sexual differentiation. *Cell* 77, 481–490.
- Moorman, A.F., Houweling, A.C., de Boer, P.A., Christoffels, V.M., 2001. Sensitive nonradioactive detection of mRNA in tissue sections: novel application of the whole-mount *in situ* hybridization protocol. *J. Histochem. Cytochem.* 49, 1–8.
- Morais da Silva, S., Hacker, A., Harley, V., Goodfellow, P., Swain, A., Lovell-Badge, R., 1996. Sox9 expression during gonadal development implies a conserved role for the gene in testis differentiation in mammals and birds. *Nat. Genet.* 14, 62–68.
- Morgan, S.M., Samulowitz, U., Darley, L., Simmons, D.L., Vestweber, D., 1999. Biochemical characterization and molecular cloning of a novel endothelial-specific sialomucin. *Blood* 93, 165–175.
- Mugford, J.W., Sipila, P., McMahon, J.A., McMahon, A.P., 2008. Osr1 expression demarcates a multi-potent population of intermediate mesoderm that undergoes progressive restriction to an Osr1-dependent nephron progenitor compartment within the mammalian kidney. *Dev. Biol.* 324, 88–98.
- Muzumdar, M.D., Tasic, B., Miyamichi, K., Li, L., Luo, L., 2007. A global double-fluorescent Cre reporter mouse. *Genesis* 45, 593–605.
- Neidhardt, L.M., Kispert, A., Herrmann, B.G., 1997. A mouse gene of the paired-related homeobox class expressed in the caudal somite compartment, and in the developing vertebral column, kidney and nervous system. *Dev. Genes Evol.* 207, 330–339.
- Pedersen, A., Skjong, C., Shawlot, W., 2005. Lim 1 is required for nephric duct extension and ureteric bud morphogenesis. *Dev. Biol.* 288, 571–581.
- Saxen, I., 1987. *Organogenesis of the Kidney*. Cambridge University Press, Cambridge, UK.
- Schneider, C.A., Rasband, W.S., Eliceiri, K.W., 2012. NIH image to image J: 25 years of image analysis. *Nat. Methods* 9, 671–675.
- Self, M., Lagutin, O.V., Bowling, B., Hendrix, J., Cai, Y., Dressler, G.R., Oliver, G., 2006. Six2 is required for suppression of nephrogenesis and progenitor renewal in the developing kidney. *EMBO J.* 25, 5214–5228.
- So, P.L., Danielian, P.S., 1999. Cloning and expression analysis of a mouse gene related to *Drosophila odd-skipped*. *Mech. Dev.* 84, 157–160.
- Trowe, M.O., Airik, R., Weiss, A.C., Farin, H.F., Foik, A.B., Bettenhausen, E., Schuster-Gossler, K., Taketo, M.M., Kispert, A., 2012. Canonical Wnt signaling regulates smooth muscle precursor development in the mouse ureter. *Development* 139, 3099–3108.
- Trowe, M.O., Shah, S., Petry, M., Airik, R., Schuster-Gossler, K., Kist, R., Kispert, A., 2010. Loss of Sox9 in the periotic mesenchyme affects mesenchymal expansion and differentiation, and epithelial morphogenesis during cochlea development in the mouse. *Dev. Biol.* 342, 51–62.

Part 1 - Tbx18 lineage in urogenital development

36

T. Bohnenpoll et al. / *Developmental Biology* 380 (2013) 25–36

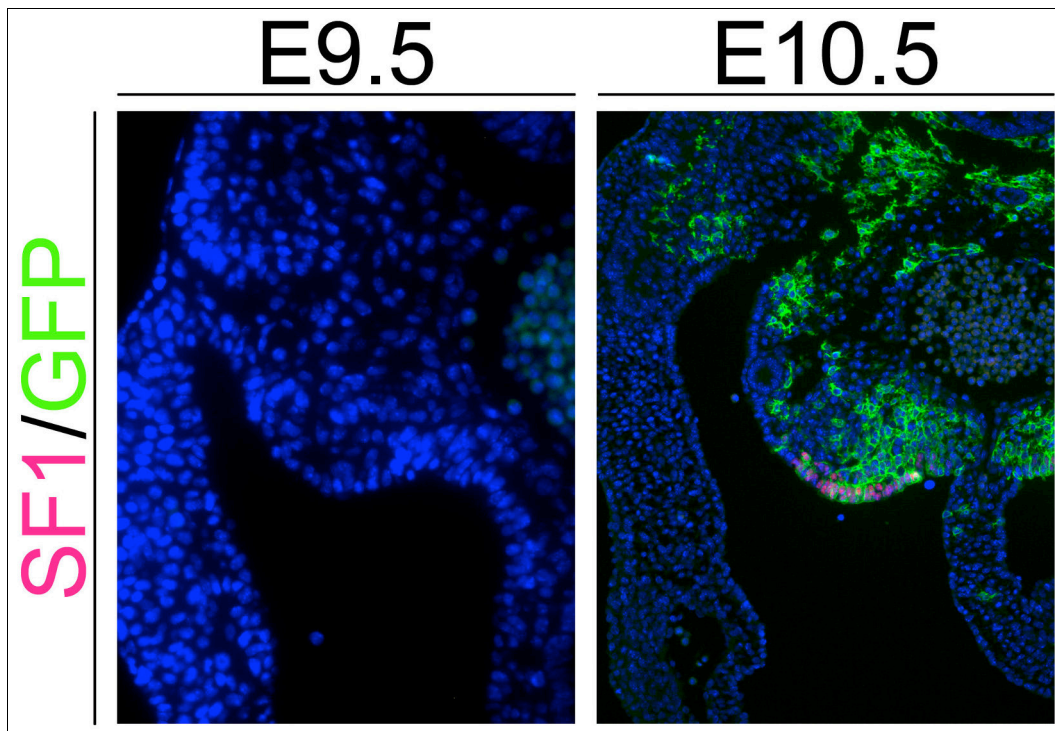
- Vestweber, D., Kemler, R., Ekblom, P., 1985. Cell-adhesion molecule uvomorulin during kidney development. *Dev. Biol.* 112, 213–221.
- Wang, C., Gargollo, P., Guo, C., Tang, T., Mingin, G., Sun, Y., Li, X., 2011. Six1 and Eya1 are critical regulators of peri-cloacal mesenchymal progenitors during genitourinary tract development. *Dev. Biol.* 360, 186–194.
- Wang, Q., Lan, Y., Cho, E.S., Maltby, K.M., Jiang, R., 2005. Odd-skipped related 1 (Odd1) is an essential regulator of heart and urogenital development. *Dev. Biol.* 288, 582–594.
- Wang, Y., Tripathi, P., Guo, Q., Coussens, M., Ma, L., Chen, F., 2009. Cre/lox recombination in the lower urinary tract. *Genesis* 47, 409–413.
- Wilkinson, D.G., Nieto, M.A., 1993. Detection of messenger RNA by *in situ* hybridization to tissue sections and whole mounts. *Methods Enzymol.* 225, 361–373.
- Yu, J., Carroll, T.J., McMahon, A.P., 2002. Sonic hedgehog regulates proliferation and differentiation of mesenchymal cells in the mouse metanephric kidney. *Development* 129, 5301–5312.

Supplementary Figures

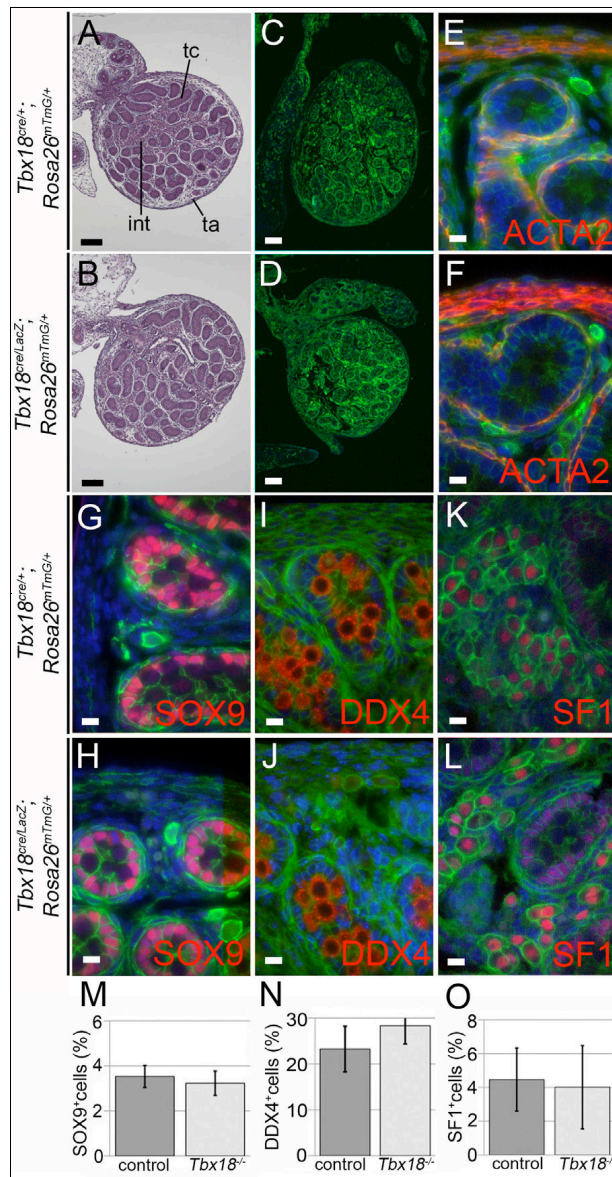
for

***Tbx18* expression demarcates multipotent precursor populations in the developing urogenital system but is exclusively required within the ureteric mesenchymal lineage to suppress a renal stromal fate**

Tobias Bohnenpoll¹, Eva Bettenhausen¹, Anna-Carina Weiss, Anna B. Foik, Mark-Oliver Trowe, Patrick Blank, Rannar Airik, and Andreas Kispert*

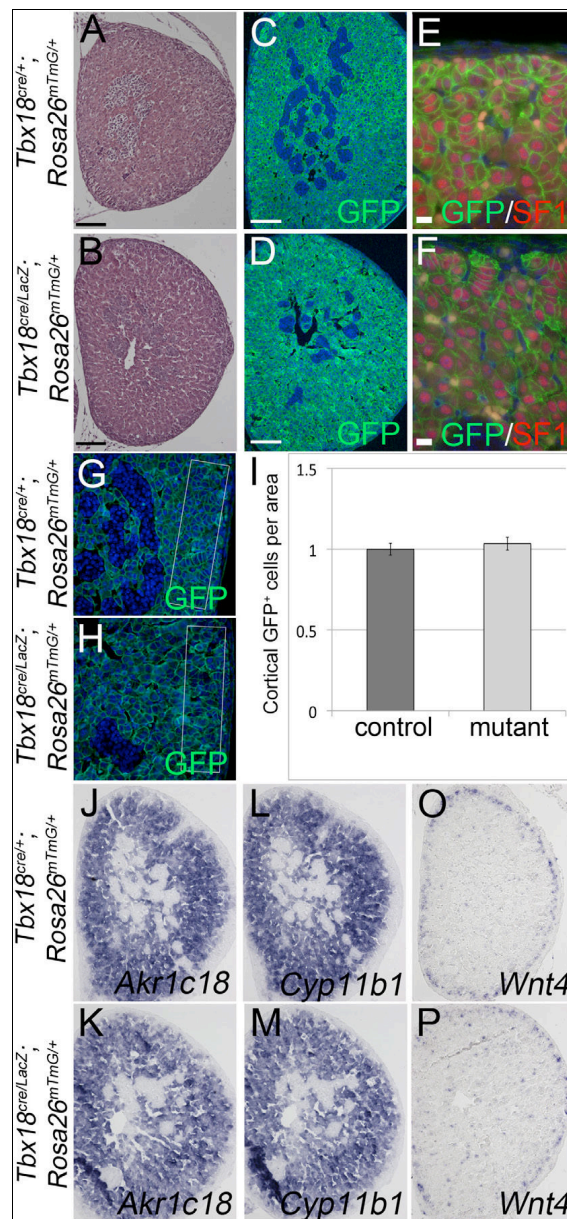


Supplementary Fig. S1. *Tbx18*⁺-descendants are positive for SF1 in the coelomic lining at E10.5. (Co-)immunofluorescence analysis of expression of the lineage marker GFP (green) and the marker for the adrenogonadal primordium, SF1 (red), on transverse sections through the posterior trunk of E9.5 and E10.5 *Tbx18*^{cre/+}; *R26*^{mTmG/+} embryos. At E9.5, SF1 protein is not yet expressed in the coelomic lining and recombination of the lineage reporter has not yet occurred. At E10.5, cells formerly positive for *Tbx18* in the coelomic lining express SF1.

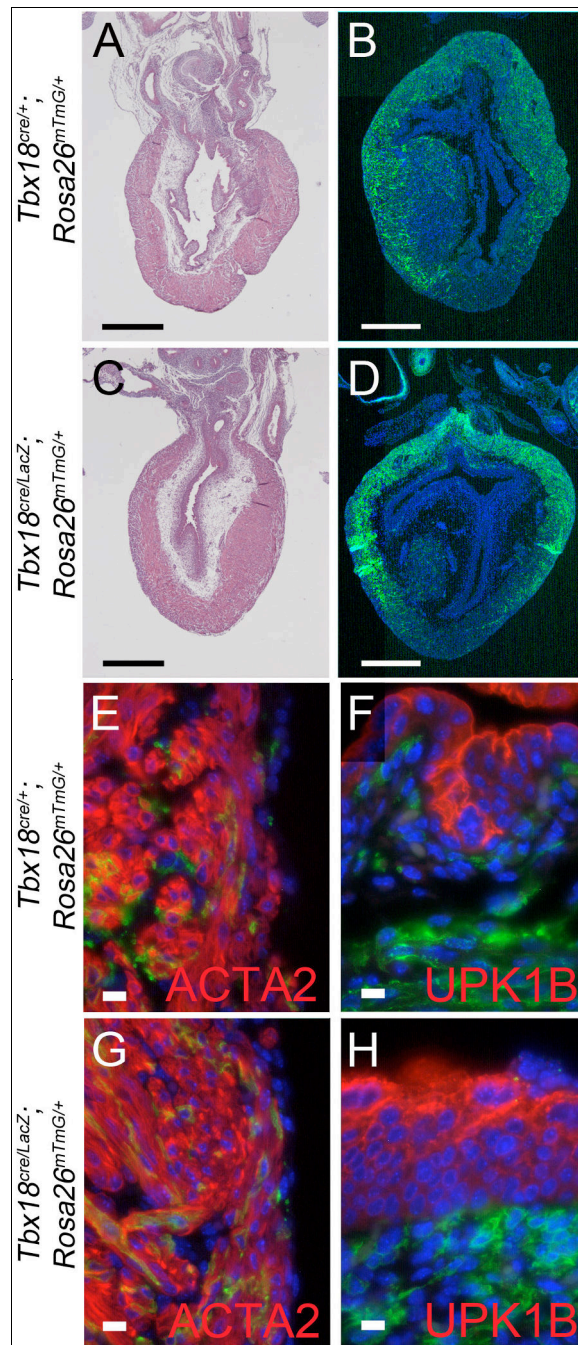


Supplementary Fig. S2. Loss of *Tbx18* does not affect testis development. (A,B) Histological analysis by haematoxylin and eosin staining of sagittal testis sections in E18.5 control ($Tbx18^{cre/+}; R26^{mTmG/+}$) and $Tbx18$ -deficient embryos ($Tbx18^{cre/lacZ}; R26^{mTmG/+}$) does not detect changes of the testicular tissue organization. (C-L) (Co-)immunofluorescence analysis of E18.5 testis does not detect changes in the number and distribution of smooth muscle cells of the capsule (ACTA2), of Sertoli cells (SOX9), of germ cells (DDX4) and of Leydig cells (SF1) between control and $Tbx18$ -deficient embryos. Scale bars represent 100 μ m (A,B,C,D) and 10 μ m (E-L). (M-O) Quantification of SOX9⁺ Sertoli cells, DDX4⁺ germ cells and SF1⁺ Leydig cells in the testis. (M) SOX9⁺ cells/all cells in the counted area (in%), control: 3.5 \pm 0.5, mutant: 3.2 \pm 0.5 p=0.515. (N) DDX4⁺ cells/testis cord cells (somatic and germ cells) (in %). control: 23.3 \pm 5.0, mutant: 28.3 \pm 4.0 p=0.093. (O) SF1⁺ Leydig cells/all interstitial cells (in %), control: 4.5 \pm 1.9, mutant: 4.0 \pm 2.5 p=0.801.

Part 1 - Tbx18 lineage in urogenital development

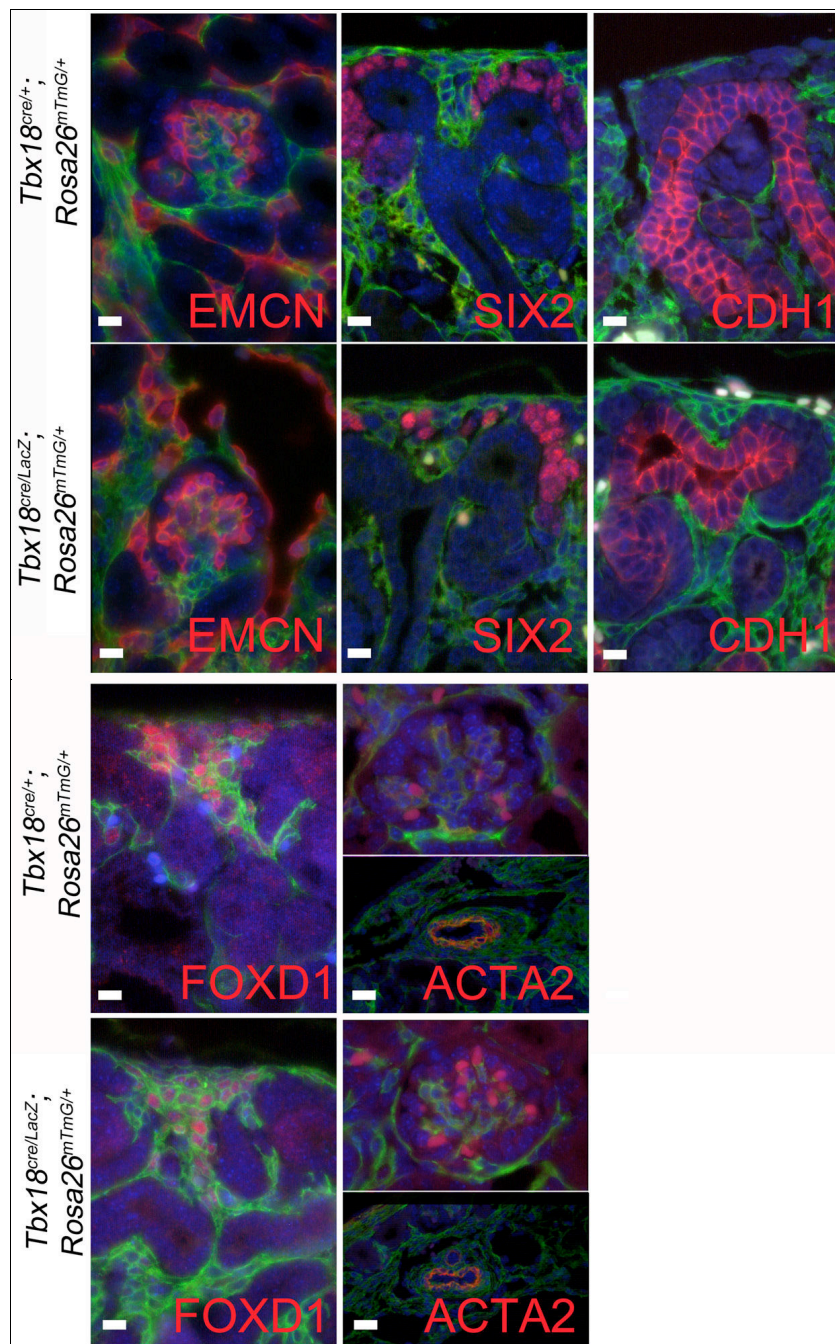


Supplementary Fig. S3. Loss of *Tbx18* does not affect adrenal development at E18.5. (A,D) Histological analysis by haematoxylin and eosin staining, (B,E) immunofluorescence analysis of expression of the lineage marker GFP, (C,F) co-immunofluorescence analysis of expression of the lineage marker GFP and of the steroidogenic marker SF1, on sections of control (*Tbx18^{cre/+};R26^{mTmG/+}*) and *Tbx18*-deficient embryos (*Tbx18^{cre/lacZ};R26^{mTmG/+}*) does not detect changes in adrenal development. Size bars represent 0.1 mm (A-D) and 10 μ m (C,F). (G-I) Immunofluorescence analysis of cells expressing the lineage marker GFP in a defined cortical area and subsequent quantification of GFP⁺ cells (control is set to 1) reveals unchanged contribution of *Tbx18*⁺ descendants to the cortical area of the *Tbx18*-deficient adrenal gland. Control: 1+/-0.037, mutant: 1.034+/-0.04, p=0.26 (J-M) *In situ* hybridization analysis of markers of the inner cortical region shows normal zonation in the mutant adrenal gland. Genotypes, probes and antigens are as shown.

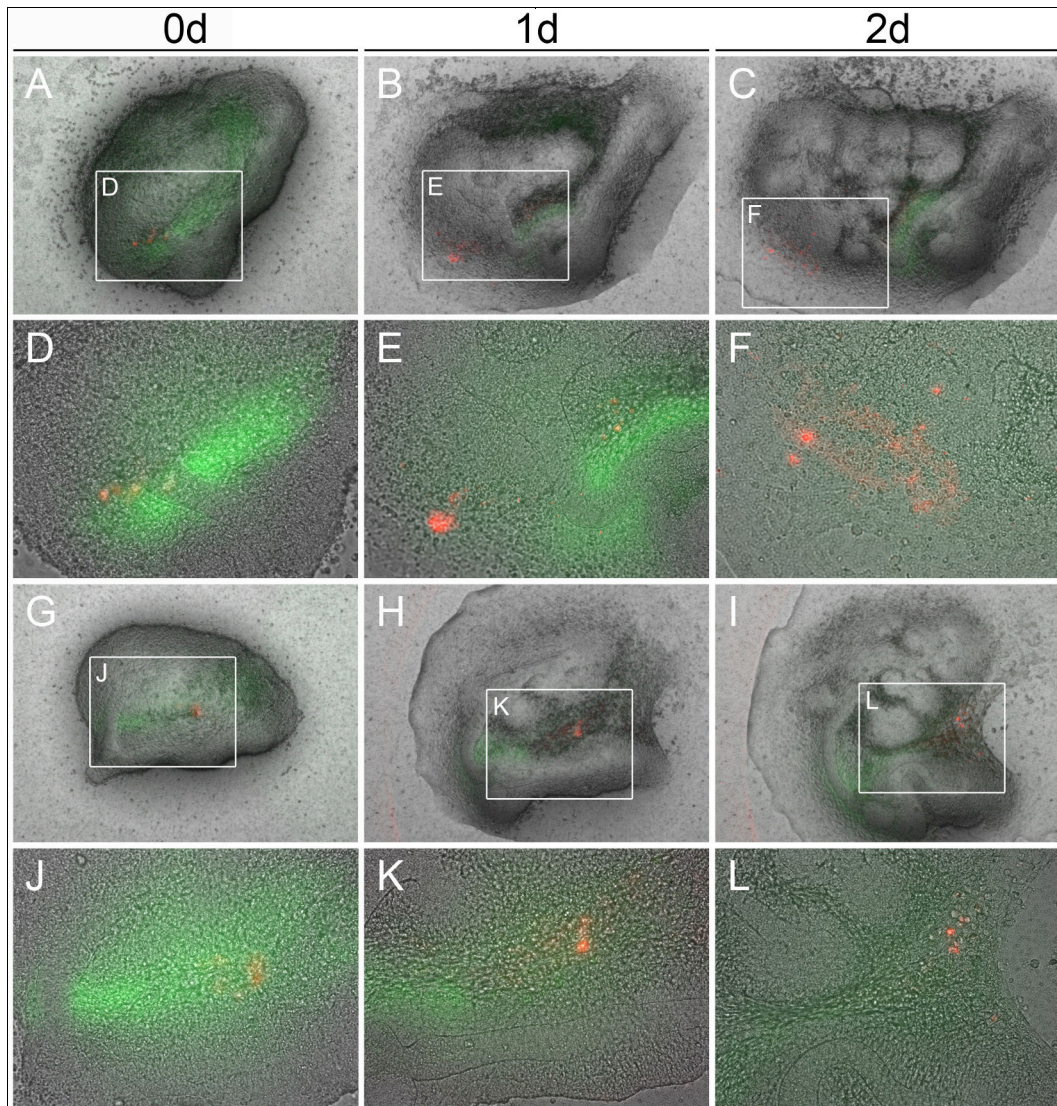


Supplementary Fig. S4. Loss of *Tbx18* does not affect bladder development. (A,C) Histological analysis by haematoxylin and eosin staining, (B,D) immunofluorescence analysis of expression of the lineage marker GFP, (E,G) co-immunofluorescence analysis of expression of the lineage marker GFP and the smooth muscle marker ACTA2, (F,H) co-immunofluorescence analysis of expression of the lineage marker GFP and of the urothelial marker UPK1B on sections of control (*Tbx18*^{cre/+};*R26*^{mTmG/+}) and *Tbx18*-deficient embryos (*Tbx18*^{cre/lacZ};*R26*^{mTmG/+}) does not detect changes in contribution of *Tbx18*⁺ descendants and cellular differentiation in the bladder. Size bars represent 0.5 mm (A-D) and 10 μm (E-H).

Part 1 - *Tbx18* lineage in urogenital development



Supplementary Fig. S5. Loss of *Tbx18* does not affect differentiation of renal cell lineages. Co-immunofluorescence analysis of expression of the lineage marker GFP, with the endothelial marker EMCN, the cap mesenchyme marker SIX2, the epithelial marker CDH1, the cortical stroma marker FOXD1 and the smooth muscle marker ACTA2 on sections of control (*Tbx18*^{cre/+}; *R26*^{mTmG/+}) and *Tbx18*-deficient embryos (*Tbx18*^{cre/lacZ}; *R26*^{mTmG/+}) does not detect changes in contribution of *Tbx18*⁺ descendants and cellular differentiation in the kidney. Size bars represent 10 μ m.



Supplementary Figure S6. Lineage analysis of *Tbx18*⁺ mesenchymal cells in early kidney rudiments. (A) Combined brightfield and epifluorescence analysis of metanephric explants from E11.5 *Tbx18*^{GFP/+} embryos at 0, 1 and 2 days of culture. GFP (green) marks the *Tbx18* expression domain, the red fluorescence indicates Dil-injected cell clusters. Shown are two representative examples of Dil-injected cells localizing to the space between kidneys and the Wolffian duct (lower row). Boxed regions are shown in higher magnifications below.

Part 2 - Lineage diversification in the ureter

Diversification of cell lineages in ureter development

Tobias Bohnenpoll¹, Sarah Feraric¹, Marvin Nattkemper¹,
Anna-Carina Weiss¹, Carsten Rudat¹, Max Meuser¹, Mark-Oliver Trowe¹
and Andreas Kispert^{1,§}

¹ Institut für Molekularbiologie, Medizinische Hochschule Hannover, 30627 Hannover, Germany

§ Author for correspondence:

Email: kispert.andreas@mh-hannover.de

Tel: +49511 5324017

Fax: +49511 5324283

Published in Journal of the American Society of Nephrology (J Am Soc Nephrol (2016), ePub ahead of print)

Reprinted with permission (see Appendix).

Diversification of Cell Lineages in Ureter Development

Tobias Bohnenpoll, Sarah Feraric, Marvin Nattkemper, Anna-Carina Weiss, Carsten Rudat, Max Meuser, Mark-Oliver Trowe, and Andreas Kispert

Institut für Molekularbiologie, Medizinische Hochschule Hannover, Hannover, Germany

ABSTRACT

The mammalian ureter consists of a mesenchymal wall composed of smooth muscle cells and surrounding fibrocytes of the tunica adventitia and the lamina propria and an inner epithelial lining composed of layers of basal, intermediate, and superficial cells. How these cell types arise from multipotent progenitors is poorly understood. Here, we performed marker analysis, cell proliferation assays, and genetic lineage tracing to define the lineage relations and restrictions of the mesenchymal and epithelial cell types in the developing and mature mouse ureter. At embryonic day (E) 12.5, the mesenchymal precursor pool began to subdivide into an inner and outer compartment that began to express markers of smooth muscle precursors and adventitial fibrocytes, respectively, by E13.5. Smooth muscle precursors further diversified into lamina propria cells directly adjacent to the ureteric epithelium and differentiated smooth muscle cells from E16.5 onwards. Uncommitted epithelial progenitors of the ureter differentiated into intermediate cells at E14.5. After stratification into two layers at E15.5 and three cell layers at E18.5, intermediate cells differentiated into basal cells and superficial cells. In homeostasis, proliferation of all epithelial and mesenchymal cell types remained low but intermediate cells still gave rise to basal cells, whereas basal cells divided only into basal cells. These studies provide a framework to further determine the molecular mechanisms of cell differentiation in the tissues of the developing ureter.

J Am Soc Nephrol 28: ●●-●●, 2016. doi: 10.1681/ASN.2016080849

The mammalian ureter has a compartmentalized tissue architecture that is functionally adapted to mediate efficient urinary drainage from the renal pelvis to the bladder. The outer mesenchymal compartment harbors a thick layer of peristaltically active smooth muscle cells (SMCs), the tunica muscularis, that is ensheathed by flexible and anchoring fibroelastic material, the tunica adventitia on the outside and the lamina propria on the inside. The inner compartment is a highly distensible epithelium that provides sealing to the luminal space. This urothelium features a single layer of cuboidal basal cells (B cells) that is attached to the lamina propria *via* a basement membrane, one or two layers of intermediate cells (I cells) that resemble B cells in shape and size, and a luminal layer of large squamous superficial cells (S cells) that exert a barrier function at least partly due to expression of uroplakins (UPKs) that form crystalline plaques on the apical surface.^{1,2}

The differentiated cell types of the two ureteric tissue compartments arise from multipotent precursors

during embryonic development. In the mouse, these precursor pools are established around embryonic day (E) 11.5 when the distal aspect of an epithelial diverticulum of the nephric duct, the ureteric bud, and its surrounding mesenchyme adopt a distal ureteric rather than a proximal renal fate. For the next days, the mesenchymal and epithelial progenitors multiply to support ureter elongation. At E16.5, *i.e.*, shortly after onset of urine production in the kidney, expression of smooth muscle (SM) structural proteins and of UPKs testifies that SMC and S cell differentiation

Received August 5, 2016. Accepted November 8, 2016.

Published online ahead of print. Publication date available at www.jasn.org.

Correspondence: Prof. Andreas Kispert, Institut für Molekularbiologie, OE5250, Medizinische Hochschule Hannover, Carl-Neuberg-Str. 1, 30625 Hannover, Germany. Email: kispert.andreas@mh-hannover.de

Copyright © 2016 by the American Society of Nephrology

has been initiated. Around birth, the three epithelial and mesenchymal cell layers can be histologically clearly distinguished.^{3,4} Embryologic experiments have shown that the survival, patterning, and subsequent differentiation of the primitive ureteric epithelium and its surrounding mesenchyme depend on each other. Genetic analysis has identified some of the trans-acting signals and the downstream transcription factors that regulate these cellular programs.⁴ However, how the different cell types arise in time and how they relate to each other has been poorly studied.

Here, we set out to probe the developmental origin and relationship of the different epithelial and mesenchymal cell types of the mouse ureter. We describe the temporal profile of cell differentiation and proliferation in the ureter, and trace the fate of the two progenitor pools. We provide evidence that I cells are precursors for both B and S cells in development.

RESULTS

Cell Differentiation Occurs in a Temporally Controlled and Coordinated Manner in the Epithelial and Mesenchymal Tissue Compartments of the Embryonic Ureter

Previous work reported expression of cell-type-specific genes at selected stages of ureter development but did not address the precise temporal profile of the mesenchymal and epithelial differentiation programs.^{3,5,6} We therefore wished to correlate histologic changes with expression profiles of cell-type-specific marker sets in either tissue compartment at all stages of embryonic ureter development.

In the mature ureteric mesenchyme, adventitial fibrocytes are marked by expression of periostin (POSTN), whereas SMCs can be identified by transgelin (TAGLN) and actin, alpha 2, smooth muscle, aorta (ACTA2) expression.^{6,7} For the cells of the lamina propria no specific protein marker has been described, but they can be identified as mesenchymal cells negative for SMC markers adjacent to the ureteric epithelium (Figure 1, A–C, P40 panel). We have recently shown that the T-box transcription factor gene *Tbx18* is expressed in the undifferentiated ureteric mesenchyme, and that the descendants of this expression domain constitute the ureteric mesenchymal wall throughout development and in adulthood.^{8,9} To detect and quantify cell differentiation in the ureteric mesenchyme, we therefore analyzed coexpression of cell-type-specific markers with a membrane-bound GFP reporter by immunofluorescence on proximal ureter sections in mice double heterozygous for a *cre* knock-in in the *Tbx18* locus and the *Rosa26^{mTmG}* reporter line (*Tbx18^{cre/+};R26^{mTmG/+}*) (Figure 1, A–E).^{10,11}

At E12.5, two histologically distinct cell populations were present in the GFP⁺ ureteric mesenchyme. Cells adjacent to the ureteric epithelium were densely packed and spherical, whereas the outermost layers contained loosely organized, radially oriented, and spindle-shaped cells. Differentiation

markers were not expressed at this stage. At E13.5, the number of GFP⁺ mesenchymal cells was strongly increased and the outermost spindle-shaped cells started to express POSTN. POSTN expression expanded to cover most cells of the outer mesenchymal compartment at E14.5. At E15.5, few TAGLN⁺ACTA2⁺ SMCs appeared in the dense inner mesenchyme that was surrounded by POSTN⁺ adventitial fibrocytes. At E16.5, a contiguous SMC layer had developed that was separated from the urothelium by a TAGLN[−] layer of lamina propria cells. Most of the spindle-shaped outer fibrocytes were POSTN⁺. At E18.5, the ureteric mesenchyme was fully patterned and differentiated in TAGLN[−]GFP⁺ lamina propria cells, a dense TAGLN⁺ACTA2⁺GFP⁺ SMC layer, and radially organized POSTN⁺GFP⁺ adventitial fibrocytes. The ratio of these cell types was dramatically changed at P40 by relative expansion of the lamina propria and the SMC layer and reduction of the tunica adventitia (Figure 1, A–E, Supplemental Table 1A).

Work in the bladder has shown that combinatorial expression of cytokeratin 5 (KRT5), of an isoform of the transcription factor p63 (Δ NP63), and of UPKs distinguishes the three urothelial cell types in this tissue.¹² We confirmed for the adult ureter that B cells are KRT5⁺ Δ NP63⁺UPK1B[−], I cells are KRT5[−] Δ NP63⁺UPK1B⁺, and S cells are KRT5[−] Δ NP63[−]UPK1B⁺, with levels of UPK1B being significantly lower in I than in S cells (Figure 1, F and G, P40 panel); hence, that these markers can be used to profile urothelial differentiation in this organ (Figure 1, F–J). At E12.5, the mono-layered urothelium was negative for all of these differentiation markers. Δ NP63 expression occurred in single cells at E13.5 but was expressed in increasing cell numbers at E14.5 and labeled the majority of cells of the now double-layered urothelium at E15.5. Expression of *Upk1b* mRNA was weakly found throughout the urothelium at these stages as well characterizing these cells as I cells. At E15.5, single cells on the luminal side were negative for Δ NP63 which correlated with the advent of superficial UPK1B expression. At E16.5, the urothelium was composed of two to three layers. Coexpression of KRT5 and high levels of Δ NP63 indicated the presence of B cells that were intermingled with I cells (KRT5[−] Δ NP63⁺UPK1B^{+(low)}) in the basal layer. UPK1B expression was strong in the intermediate and apical layer. The abundance of B cells significantly increased from E16.5 to E18.5, and B cells constituted the majority of urothelial cells at P40. The relative number of KRT5[−] Δ NP63⁺UPK1B^{+(low)} I cells significantly decreased from E16.5 to E18.5 and remained at low abundance in the adult. KRT5[−] Δ NP63[−]UPK1B^{+(high)} S cells were clearly identifiable at E16.5 and E18.5, but decreased in abundance until P40 (Figure 1, F–J, Supplemental Table 1B). Interestingly, the relaxed adult urothelium showed a pyramidal topology on sections with large binucleated S cells at the tip, small I cells in the middle, and numerous B cells at the base (Figure 1, F–J, Supplemental Figure 1).

Comparative analysis of mesenchymal and epithelial differentiation markers at proximal, medial, and distal levels of the ureter revealed that the expression patterns of differentiation

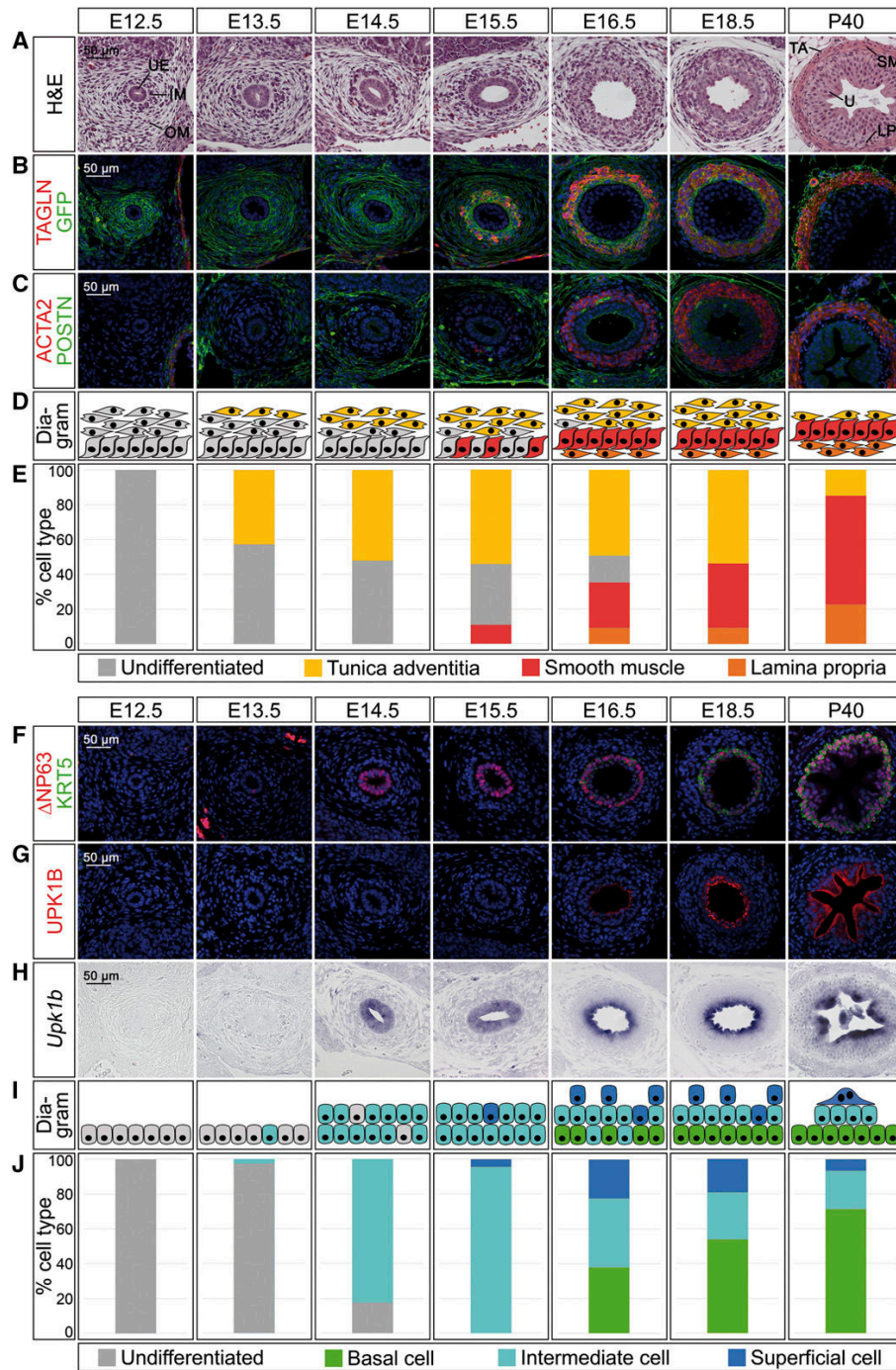


Figure 1. Cell differentiation in ureter development occurs in a temporally and spatially controlled manner. (A–E) Time course of cell differentiation in the ureteric mesenchyme. (A) Hematoxylin and eosin (H&E) staining on transverse sections of the proximal ureter. At E12.5, the inner and outer mesenchymal region (IM and OM) and the ureteric epithelium (UE) are indicated. At P40, the three subregions of the mesenchyme, the lamina propria (LP), the smooth muscle (SM), and the tunica adventitia (TA) are marked adjacent to the urothelium (U). (B and C) Coimmunofluorescence analysis of expression of the SMC marker TAGLN and the lineage marker GFP (B) and of the SMC marker ACTA2 and the adventitial marker POSTN (C) on transverse sections of the proximal ureter in *Tbx18^{cre/+};R26^{mTmG/+}* mice. Nuclei are counterstained

markers are spatially conserved but are activated with a delay of 1–2 days at more distal levels (Supplemental Figures 2 and 3).

We conclude that differentiated cell types arise in a distinct order and in a proximal to distal wave along the ureteric tube. In the mesenchyme adventitial fibrocytes precede SMCs and lamina propria cells, whereas in the epithelial compartment I cells differentiate before B and S cells.

Proliferation Rates Explain Differential Cell-Type Expansion in the Developing Ureter

Our analysis has shown that the different epithelial and mesenchymal cell types of the ureter start to differentiate at different time points and change in abundance over time. To find out if this relates to differences in the temporal profiles of cell-cycle activity, we determined cell proliferation during ureter development and homeostasis using the BrdU incorporation assay.

At E12.5 and E14.5, proliferation rates reached 20%–23% in both the ureteric epithelium and the inner and outer region of the ureteric mesenchyme, showing that the precursor pools coordinately drive the expansion of the early organ rudiment (Figure 2, A and B, Supplemental Table 2A). From E16.5 onwards, the three mesenchymal and epithelial cell types could be molecularly distinguished. In the mesenchyme, the cells of the lamina propria maintained high proliferation rates similar to precursors at the previous stages, whereas SMCs reduced proliferation from 19% at E16.5 to 13% at E18.5, and adventitial fibrocytes from 12% to 8% in line with the relative expansion of SM and lamina cells at the expense of adventitial cells at these stages (Figure 1E). At P40, SMCs were quiescent, whereas cells of the lamina and adventitia divided at a very low rate (0.3% and 0.8%) (Figure 2, C and D, Supplemental Table 2B).

In the epithelial compartment, B and S cells maintained high proliferation at E16.5, whereas I cells proliferated at approximately half the rate (9%). At E18.5, proliferation rates were further reduced with S cells being more proliferative than B and I cells. In the adult ureter, only B cells divided occasionally, whereas S and I cell proliferation was under the detection limit (Figure 2, E and F, Supplemental Table 2C). Together, these findings suggest that mesenchymal and epithelial cell-types withdraw at different time-points from the cell cycle, explaining their changing ratios particularly at late embryonic and at postnatal stages.

Adventitial Cells are Separated Early in Mesenchymal Development Whereas Lamina Propria Cells Derive from SMC Precursors

Our expression analysis showed that the homogenous mesenchymal progenitor pool is separated into a histologically and molecularly distinct inner and outer domain as early as E12.5. To determine whether this subdivision represents a compartment boundary between prospective adventitial fibrocytes and SMCs, and to define the origin of the lamina propria cells, we performed genetic lineage tracing experiments using *cre* lines that are specific to the outer or inner mesenchymal domain. To detect the descendants of outer mesenchymal cells, we took advantage of the fact that *Foxd1* is expressed in this domain exclusively at E12.5 and E14.5 (Supplemental Figure 4A). Marker analysis on sections of proximal E12.5 and E18.5 ureters double heterozygous for a *Foxd1*^{cre} allele¹³ and the *R26*^{mTmG} reporter (*Foxd1*^{cre/+}; *R26*^{mTmG/+}) at E12.5 and E18.5 showed that the descendants of this expression domain localized to the outer mesenchymal ring at E12.5 and E18.5, and expressed POSTN but not the SMC markers TAGLN and ACTA2 (Figure 3A), clearly indicating that outer mesenchymal cells are lineage-restricted to become adventitial fibrocytes as early as E12.5.

Axin2 is expressed at E12.5 and subsequent stages in the inner ring of mesenchymal cells in the ureter as a response to WNT signals emitted from the adjacent epithelium (Supplemental Figure 4B).⁶ To trace the descendants of this *Axin2*⁺ domain, we crossed mice with a *creERT2* knock-in in the *Axin2* locus¹⁴ with the *R26*^{mTmG} reporter line and induced recombination by a single oral administration of 4 mg tamoxifen. To confirm the region-specificity of the labeling reaction, we treated *Axin2*^{creERT2/+}; *R26*^{mTmG/+} embryos at E12.5 and E13.5 and analyzed the distribution of GFP⁺ cells in the inner and outer mesenchymal compartment 24 hours later. In embryos injected at E12.5, 23% of the GFP⁺ cells were detected in the outer compartment, 77% in the inner compartment; in E13.5 embryos, the relation was 6%–94%, indicating that the labeling reaction in E13.5 ureters almost exclusively occurred in the inner ring (Figure 3, B and C, Supplemental Table 3). When *Axin2*^{creERT2/+}; *R26*^{mTmG/+} embryos were analyzed at E18.5, GFP⁺ descendants localized to 71% to the SMC layer, to 18% to the lamina propria, and to 11% to the tunica adventitia when tamoxifen administration was done at E12.5. For embryos tamoxifen-treated at E13.5 the numbers were 73% and 17%, whereas only 10% of labeled cells were

with DAPI (blue). (D) Schematic representation of cell differentiation in the ureteric mesenchyme. Fibrocytes of the tunica adventitia (yellow) are defined as POSTN⁺GFP⁺, SMCs (red) as TAGLN⁺ACTA2⁺GFP⁺, and lamina propria cells (orange) as TAGLN⁻GFP⁺. (E) Quantification of differentiated cell types in the ureteric mesenchyme on the basis of marker expression as explained in (D). For numbers see Supplemental Table 1A. (F–J) Time course of epithelial differentiation in the ureter. (F and G) Coimmunofluorescence analysis of expression of the B cell marker KRT5, the B and I cell marker ΔNP63 (F), and the I and S cell marker UPK1B (G) with DAPI-stained nuclei (blue), and (H) *in situ* hybridization for *Upk1b* expression on transverse sections of the proximal ureter in *Tbx18*^{cre/+}; *R26*^{mTmG/+} mice. (I) Schematic representation of cell expansion and differentiation in the ureteric epithelium. B cells (green) are defined as KRT5⁺ΔNP63⁺UPK1B⁻*Upk1b*⁻, I cells (turquoise) as KRT5⁻ΔNP63⁺UPK1B^{+(low)}*Upk1b*⁺, and S cells (blue) as KRT5⁻ΔNP63⁻UPK1B^{+(high)}*Upk1b*⁺. (J) Quantification of differentiated cell types in the ureteric epithelium on the basis of marker expression as explained in (I). For numbers see Supplemental Table 1B.

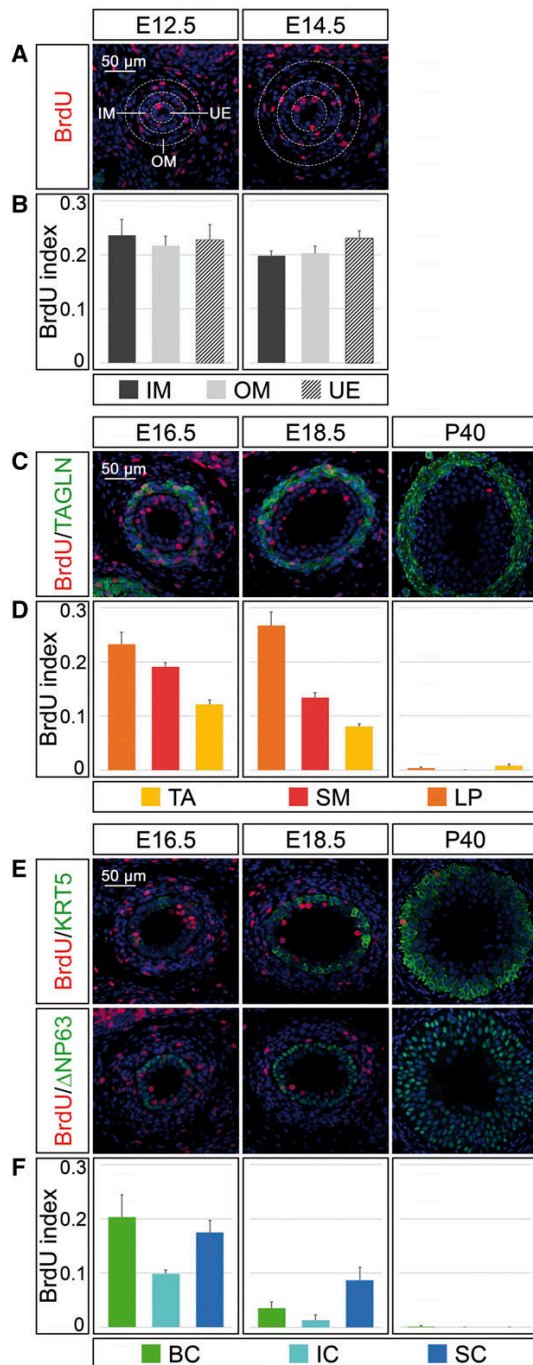


Figure 2. Proliferation rates explain differential cell-type expansion in the developing ureter. (A) Coimmunofluorescence analysis on proximal ureter sections at E12.5 and E14.5 for BrdU and the nuclear counterstain DAPI (blue). White dotted lines demarcate the ureteric epithelium (UE), and the inner and outer mesenchymal cell populations (IM and OM). (B) Quantification of cell proliferation by the BrdU index in the areas indicated in (A). (C)

detected in the tunica adventitia (Figure 3, B and C, Supplemental Table 3). We conclude that *Axin2*⁺ inner mesenchymal cells are precursors of SMCs, and that lineage restriction to adventitial fibrocytes occurs around E12.5 to E13.5. Lamina propria cells derive from inner mesenchymal SMC progenitors by switching off the SMC program at E14.5 to E16.5.

I Cells are Progenitors of B and S Cells in Development

The ureteric epithelium derives from the distal aspect of the ureter bud that emerges as an outgrowth of the nephric duct around E10.5. To confirm that the distal ureter stalk indeed harbors precursors for all epithelial cell types of the mature ureter, we performed genetic lineage tracing on the basis of *cre* lines mediating recombination in all of these precursors. *Pax2* and *Shh* are genes that are expressed throughout the ureteric epithelium at E12.5 and at subsequent stages (Supplemental Figure 4, C and D). A transgenic line, in which *cre* was expressed under *Pax2* regulatory elements (*Pax2-cre*),^{15,16} mediated full recombination of the *R26^{mTmG}* reporter allele in the ureteric epithelium at E12.5; a line harboring a *cre* knock-in into the *Shh* locus¹⁷ did so partially (Figure 4, A and B). In *Pax2-cre/+;R26^{mTmG/+}* and *Shh^{cre/+};R26^{mTmG/+}* ureters analyzed at E18.5, GFP⁺ cells populated all three ureteric cell layers, whereas a contribution to the ureteric mesenchyme was never observed (Figure 4, A and B).

Our expression analysis further demonstrated that the epithelial compartment of the ureter remains undifferentiated until E13.5 and expresses markers for I cells from E14.5 onwards. S cells and B cells were only detected from E15.5 and E16.5 onwards, respectively, suggesting that I cells are precursors for both S and B cells in development. To validate this hypothesis, we used cell-type-specific *creERT2* lines and traced their descendants in ureter explant cultures after 4-hydroxytamoxifen-induced stage-specific recombination of the *R26^{mTmG}* reporter allele.

To trace the fate of B cells we used a *creERT2* lineage tracing system on the basis of the B cell-specific expression of the *Krt5* gene.^{12,18} When ureters from *Krt5^{creERT2/+};R26^{mTmG/+}* embryos were explanted at E14.5, treated with 4-hydroxytamoxifen, and analyzed after 10 days GFP⁺ cells were not detected, compatible

Coimmunofluorescence analysis on proximal ureter sections at E16.5, E18.5, and P40 for BrdU, the nuclear counterstain DAPI (blue), and the SM marker TAGLN. (D) Quantification of cell proliferation by the BrdU index in TAGLN⁺ outer mesenchymal cells of the tunica adventitia (TA), in TAGLN⁺ smooth muscle cells (SM), and in TAGLN⁻ inner mesenchymal cells of the lamina propria (LP). (E) Coimmunofluorescence on proximal ureter sections at E16.5, E18.5, and P40 for BrdU, the nuclear counterstain DAPI (blue), and the B cell marker KRT5 (upper row) and BrdU, the nuclear counterstain DAPI (blue), and the B and I cell marker ΔNP63 (lower row). (F) Quantification of cell proliferation by the BrdU index in KRT5⁺ B cells (BC), in KRT5⁺ΔNP63⁺ I cells (IC), and KRT5⁻ΔNP63⁻ S cells (SC). For numbers see Supplemental Table 2, A–C.

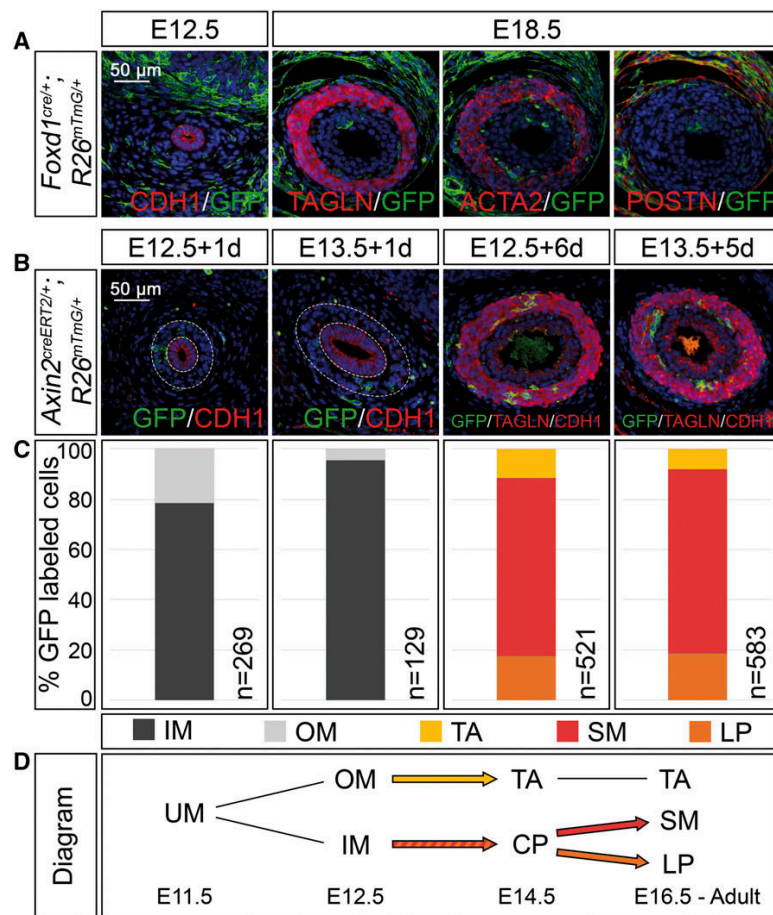


Figure 3. Adventitial cells are separated early in mesenchymal development whereas lamina propria cells derive from SMC precursors in the ureter. (A) Coimmunofluorescence analysis on transverse sections of the proximal ureter for the lineage marker GFP and the epithelial marker CDH1 at E12.5, with the SMC markers TAGLN and ACTA2, and the adventitial cell marker POSTN at E18.5 shows recombination in outer fibrocytes only in *Foxd1^{cre/+};R26^{mTmG/+}* embryos. (B) Coimmunofluorescence of the lineage marker GFP with the epithelial marker CDH1 and the SMC marker TAGLN on proximal sections of ureters from *Axin2^{creERT2/+};R26^{mTmG/+}* embryos that were tamoxifen-induced at E12.5 or E13.5 and harvested after 1 and 6 or 5 days to detect localization of recombined cells. (C) Relative distribution of GFP⁺ cells localized to the inner and outer ureteric mesenchyme (IM and OM), and to the tunica adventitia (TA), the smooth muscle (SM), and the lamina propria (LP) in ureters shown in (B). The number of counted GFP⁺ cells (n) is given. For additional numbers see Supplemental Table 3. (D) Schematic representation of the lineage relations in the ureteric mesenchyme. Abbreviations are as explained in (C). Inner mesenchymal cells contribute to the SM layer and the lamina propria but not to the tunica adventitia. UM, undifferentiated mesenchyme; CP, common precursor.

with the fact that KRT5 expression only occurs around E16.5. When ureters from E16.5 and E18.5 embryos were treated and analyzed after 8 and 6 days, respectively, GFP⁺ cells were present and unambiguously expressed the B cell marker KRT5, suggesting a lineage restriction of the B cell population (Figure 4, C and D, Supplemental Table 4A).

Because *cre* lines specific for I cells are not established, we used a *Upk3a-GCE/+* line,^{12,19} that labels I and S cells but not B cells (Supplemental Figure 5), to trace I cell descendants. Irrespective of whether ureters of *Upk3a-GCE/+;R26^{mTmG/+}* embryos were explanted at E14.5 and analyzed after 10 days, explanted at E16.5 and analyzed after 8 days, or explanted at E18.5 and analyzed after 6 days, GFP⁺ cells differentiated in roughly equal ratio into KRT5⁺ B cells and KRT5⁻ UPK1B⁺ I and S cells, suggesting that I cells are B cell progenitors in development (Figure 4, E and F, Supplemental Table 4B).

To detect the fate of *Krt5*- and *Upk3a*-expressing cells under homeostatic conditions, we injected *Krt5^{creERT2/+};R26^{mTmG/+}* and *Upk3a-GCE/+;R26^{mTmG/+}* mice at P100 with three doses of 5 mg tamoxifen on alternating days and analyzed for GFP expression after 4 weeks. In *Krt5^{creERT2/+};R26^{mTmG/+}* ureters, all lineage-labeled cells coexpressed KRT5, indicating that B cells give only rise to B cells. In *Upk3a-GCE/+;R26^{mTmG/+}* ureters, lineage-labeled cells expressed in roughly equal ratio KRT5 or UPK1B, indicating that I cells still give rise to B cells (and probably S cells) in homeostasis (Figure 4, C–F, Supplemental Table 4, A and B).

DISCUSSION

Early Lineage Restriction in the Ureteric Mesenchyme Separates Adventitial Fibrocytes from a Common Precursor of SMCs and Subepithelial Fibrocytes

Our previous work has shown that all mesenchymal cell types of the ureter derive from a *Tbx18*⁺ mesenchymal progenitor pool that surrounds the distal portion of the ureter bud and separates the metanephric blastema from the nephric duct around E11.5.⁹ Shortly after, at E12.5, this homogeneous cell population is subdivided into an inner compartment of densely packed, spherical cells and an outer compartment of loosely organized, spindle-shaped, and radially oriented cells, implying that mesenchymal cells of the two domains have acquired different fates. Our findings support such an early lineage restriction in the ureteric mesenchyme. First, differential gene expression occurs around E12.5 in the two mesenchymal subregions. The

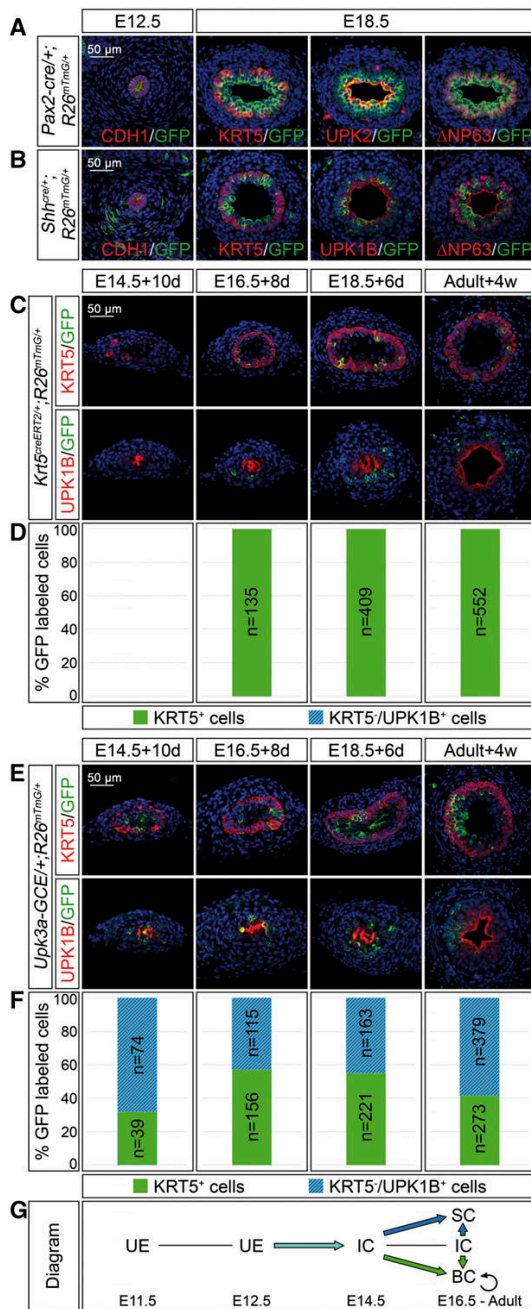


Figure 4. I cells are progenitors of B and S cells in ureter development and homeostasis. (A and B) Coimmunofluorescence analysis on transverse sections of the proximal ureter of the lineage marker GFP with the epithelial marker CDH1 at E12.5, and the B cell marker KRT5, the B and I cell marker ΔNP63, and the S cell markers UPK1B/UPK2 in *Pax2-cre/+;R26^{mTmG/+}* embryos (A) and in *Shh^{cre/+};R26^{mTmG/+}* embryos (B) shows that *Pax2⁺* and *Shh⁺* cells of the early ureteric bud contribute to all urothelial cell types in the ureter but not the surrounding mesenchyme. (C and

outer domain expresses *POSTN* and *Foxd1*, whereas the inner region is positive for *Axin2*. Second, and more importantly, lineage tracing of *Foxd1⁺* cells showed that these cells exclusively contribute to adventitial fibrocytes at E18.5, whereas *Axin2⁺* cells differentiate into cells of the lamina propria and the SM layer. Our marker and proliferation analyses argue that adventitial fibrocytes arise first and become terminally differentiated before the other mesenchymal cell-types around E16.5 to E18.5. In contrast, *Axin2⁺* cells exist as bipotent precursors from E12.5 to E15.5, and differentiate into SMCs and subepithelial fibrocytes around E16.5. The descent of lamina propria and SMCs from a common precursor is also supported by the observation that lamina cells initially also express *ACTA2* but downregulate it afterward. Lamina cells and SMCs maintain high proliferation rates at least until E18.5, arguing that they only terminally differentiate postnatally. Given the maintenance of cell division at low rates in both fibrocyte populations in adults, it is tempting to speculate that adventitial fibrocytes replenish themselves whereas lamina cells serve as precursors for themselves and for SMCs.

Tissue separation experiments provided compelling evidence that SMC differentiation in the ureter, and in many other visceral tubular organs, depends on signals from the adjacent epithelium.²⁰ Our own work has recently shown that canonical WNT signaling is required to initiate SM precursor development and to suppress an adventitial fate in the ureter.⁶ Because *Axin2* is a direct transcriptional target of this signaling pathway,²¹ this suggests that only cells adjacent to the ureteric epithelium that perceive a WNT signal escape from the default program to become adventitial fibrocytes, and differentiate into SM progenitors instead. It is interesting to note that *Axin2* expression persists after E14.5 only in cells directly in contact with the ureteric epithelium, *i.e.*, in lamina propria cells, supporting our idea that these cells represent a persisting pool of SM progenitors. Whether downregulation of WNT signaling is a prerequisite for SM progenitors to differentiate

E) Coimmunofluorescence analysis of the lineage marker GFP with the B cell marker KRT5 (upper panel) and the S cell marker UPK1B (lower panel) on transverse sections of ureters isolated at E14.5, E16.5, and E18.5, induced with 500 nM 4-hydroxytamoxifen for the first 24 hours and cultured for 10, 8, and 6 days; and in adult ureters 4 weeks after tamoxifen administration in *Krt5^{creERT2/+};R26^{mTmG/+}* mice (C) and *Upk3a-GCE/+;R26^{mTmG/+}* mice (E). (D and F) The bar diagrams display the percentage of lineage-labeled (GFP⁺) cells contributing to KRT5⁺UPK1B⁻ B cells or to KRT5⁺UPK1B⁺ I and S cells in the ureter of *Krt5^{creERT2/+};R26^{mTmG/+}* mice (D) and of *Upk3a-GCE/+;R26^{mTmG/+}* mice (F) at the indicated stages and conditions. The number of counted GFP⁺ cells (n) is given. For additional numbers see Supplemental Table 4, A and B. (G) Schematic representation of the lineage relations of urothelial cell types. KRT5⁺ cells only give rise to B cells whereas UPK3A⁺ cells give rise to B, I, and S cells. BC, basal cell; IC, intermediate cell; SC, superficial cell; UE, undifferentiated epithelium.

into SMCs is an attractive possibility that can be experimentally tested.

I Cells are Progenitors for B and S Cells in Urothelial Development and Homeostasis

Here, we have shown that all cell types of the mature urothelium derive from a common *Pax2*⁺ *Shh*⁺ precursor in the ureter bud. Differentiated cell-types arise from this precursor in a strict temporal sequence. At E14.5, all epithelial cells bear the molecular signature of an I cell. With the onset of stratification at E15.5, single apical cells express S cell markers. At E16.5, KRT5⁺ cells appear in the basal layer but subsequently expand and constitute the main cell-type of the mature urothelium. The sequential appearance of differentiated cell types suggests that I cells are a common precursor for S and B cells. This hypothesis is further supported by our genetic lineage tracing experiments. Whereas *Upk3a*⁺ cells contributed to all cell-types throughout development and in adult tissue homeostasis, *Krt5*⁺ cells only replicated themselves. Interestingly, proliferation rates of I cells were low compared with that of B and S cells, suggesting that they first differentiate along their respective lineages and then expand. Of course, our analysis cannot exclude that I cells are heterogeneous and harbor distinct subpopulations that give rise to B and S cells, respectively. Identification of additional biomarkers, possibly by single cell transcriptome analysis, may help to resolve such an issue in the future.

So far, urothelial progenitors have only been studied in the bladder, mostly under conditions of regeneration. Even though the urothelium of the bladder and the ureter are derived from different germ layers, our study and a recent report suggest that stratification and differentiation follow a similar time course in both organs, thus, might be controlled by a common molecular program.¹² However, the nature of the urothelial progenitors in the bladder has been controversially discussed. Although initially B cells were thought to be progenitors for the other urothelial cell types,²² Gandhi and colleagues suggested I cells to be S cell progenitors only and defined B cells as a unipotent, self-renewing population of unknown descent.¹² A recent work identified a KRT14⁺ subpopulation of B cells to give rise to all urothelial cell types after injury.²³ Whether the injury conditions ablate S and I cells so much that B cells are reprogrammed to compensate for their loss remains to be seen. Unlike the bladder, where KRT14 expression occurs in a large fraction of KRT5⁺ B cells both in the embryonic and adult urothelium, KRT14 is not expressed in the embryonic ureter and is found at very low levels in few B cells in the mature ureteric urothelium (Supplemental Figure 6). This indicates that B cells in both organs are of different heterogeneity, and that a KRT14⁺ subpopulation of B cells might be of less relevance for urothelial homeostasis and regeneration in the ureter.

The molecular pathways that regulate the specification, differentiation, and maintenance of the urothelium remain obscure. Retinoic acid signaling has been implied in the specification of

the bladder urothelium from an endodermal precursor,¹² whereas BMP4 was reported to be involved in the maintenance of basal cell differentiation.²⁴ Whether these signaling pathways are involved in urothelial development of the ureter as well should be a focus of future research.

CONCISE METHODS

Animals

Gt(ROSA)26Sor^{tm4}(ACTB-tdTomato-EGFP)Luo (synonym: R26^{mTmG}),¹⁰ *Krt5*^{tm1.1}(cre/ERT2)Blh (synonym: *Krt5*^{creERT2}),¹⁸ *Tg*(*Upk3a-GFP/cre/ERT2*)26*Amc* (synonym: *Upk3a-GCE*),¹⁹ *Foxd1*^{tm1}(GFP/cre)*Amc* (synonym: *Foxd1*^{cre}),¹³ *Shh*^{tm1}(EGFP/cre)*Cjt* (synonym: *Shh*^{cre}),¹⁷ and *Axin2*^{tm1}(cre/ERT2)*Rnu* (synonym: *Axin2*^{creERT2})¹⁴ mouse lines were all obtained from the Jackson Laboratory. *Tbx18*^{tm4}(*cre*)*Akis* (synonym: *Tbx18*^{cre})¹¹ and *Tg*(*Pax2-cre*)1*AKis* (synonym: *Pax2-cre*)^{15,16} were previously generated in the laboratory. All lines were maintained on an NMRI outbred background. Embryos for gene expression and proliferation assays were derived from matings of NMRI wildtype mice, or from matings of males heterozygous for the *cre* driver with R26^{mTmG/mTmG} females. For timed pregnancies, vaginal plugs were checked in the morning after mating, and noon was defined as E0.5. Embryos and urogenital systems were dissected in PBS. Ureters for explant cultures were dissected in L-15 Leibovitz medium (Biochrom). Specimens were fixed in 4% PFA/PBS, transferred to methanol, and stored at -20°C before immunofluorescence or *in situ* hybridization analyses. PCR genotyping was performed on genomic DNA prepared from yolk sac or tail biopsies. For conditional lineage tracing experiments, tamoxifen (Sigma) was dissolved in pure ethanol at 100 mg/ml and then emulsified in corn oil (Sigma) to a final concentration of 12.5 mg/ml. Within 1 week, three times 5 mg of tamoxifen were given to 14-week-old mice *via* oral gavage. Urogenital systems were harvested 4 weeks thereafter. All animal work conducted for this study was performed according to European and German legislation.

Histologic Analysis

Embryos, urogenital systems, and ureters were paraffin-embedded and sectioned to 5 μm. Hematoxylin and eosin staining was performed according to standard procedures.

In Situ Hybridization Analysis

Nonradioactive *in situ* hybridization analysis of gene expression was performed on 10 μm paraffin sections of the proximal ureter with digoxigenin-labeled antisense riboprobes.²⁵ At least three embryos of each genotype were used for each analysis.

Immunofluorescence Detection of Antigens

For immunofluorescence analysis on 5 μm paraffin sections polyclonal rabbit-anti-TAGLN (1:250, ab14106; Abcam), monoclonal mouse-anti-GFP (1:250, 11814460001; Roche), polyclonal rabbit-anti-GFP (1:250, sc-8334; Santa Cruz), monoclonal mouse-anti-ACTA2 (1:250, A5228; Sigma-Aldrich), polyclonal rabbit-anti-ΔNP63 (1:250, 619001; BioLegend), polyclonal rabbit-anti-KRT5 (1:250, PRB-160P; Covance), monoclonal mouse-anti-KRT14 (1:250, ab7800; Abcam), monoclonal mouse-anti-UPK1B (1:250, WH0007348M2;

Sigma-Aldrich), polyclonal rabbit-anti-POSTN (1:250, ab14041; Abcam), monoclonal mouse-anti-BrdU (1:250, 1170376; Roche), or polyclonal rabbit-anti-CDH1 (1:250, gift from Rolf Kemler) were used as primary antibodies. Biotinylated goat-anti-rabbit IgG (1:250, 111065033; Dianova), Alexa488-conjugated goat-anti-rabbit IgG (1:500, A11034; Molecular Probes), and Alexa555-conjugated goat-anti-mouse IgG (1:500, A21422; Molecular Probes) were used as secondary antibodies. The signals of BrdU, Δ NP63 and POSTN primary antibodies were amplified using the Tyramide Signal Amplification system (NEL702001KT; Perkin Elmer). For coimmunofluorescence with primary antibodies from the same host (Δ NP63 and KRT5) detection was performed sequentially and epitopes of the first antibody were blocked with goat-anti-rabbit Fab (1:250, 111007003; Dianova). Before staining, paraffin sections were deparaffinized and cooked for 15 minutes in antigen unmasking solution (H-3300; Vector Laboratories). Nuclei were stained with 4',6-diamidino-2-phenylindole (DAPI). At least three embryos of each genotype were used for each analysis.

Three-Dimensional Reconstruction of S cells

For three-dimensional reconstruction of S cells in the adult ureter 28 consecutive 5 μ m transverse paraffin sections were stained for CDH1 and DAPI as described above. CDH1 and DAPI signals were used to highlight cell boundaries and nuclei that were reconstructed with the Amira 5.3.3 software (FEI).

Cell Proliferation Assay

Cell proliferation rates in wildtype ureters ($n=3$ per stage) were investigated by the detection of incorporated BrdU on 5 μ m paraffin sections similar to published protocols.²⁶ For embryonic stages the BrdU incorporation time was 1 hour; for adult ureters incorporation time was 10 hours due to low cell division rates. For each specimen 12 sections of the proximal ureter were assessed. The BrdU-labeling index was defined as the number of BrdU-positive nuclei relative to the total number of nuclei as detected by DAPI counterstaining in arbitrarily or molecularly defined compartments of the ureter. Data were expressed as mean \pm SD.

Organ Cultures

Ureters were dissected from the embryo, explanted on 0.4 μ m polyester membrane Transwell supports (Corning), and cultured at the air-liquid interface for 24 hours with DMEM/F12 (Gibco) supplemented with 10% FCS (Biochrom), 1 \times penicillin/streptomycin (Gibco), 1 \times pyruvate (Gibco), and 1 \times Glutamax (Gibco). 4-Hydroxytamoxifen (H7904; Sigma-Aldrich) was added to the medium at a final concentration of 500 nM for the first 24 hours of culture to induce recombination. Culture medium was replaced every day.

Image Analysis

Sections were photographed using a Leica DM5000 microscope with Leica DFC300FX digital camera or a Leica DM6000 microscope with Leica DFC350FX digital camera and afterward processed in Adobe Photoshop CS4.

ACKNOWLEDGMENTS

We thank Rolf Kemler for the anti-CDH1 antiserum.

This work was supported by a grant from the Deutsche Forschungsgemeinschaft (DFG KI728/9-1) to A.K.

DISCLOSURES

None.

REFERENCES

- Velardo JT: Histology of the ureter. In: *The ureter*, 2nd Ed., edited by Bergman H, New York, Springer-Verlag, 1981
- Yu J, Manabe M, Wu XR, Xu C, Surya B, Sun TT: Uroplakin I: A 27-kD protein associated with the asymmetric unit membrane of mammalian urothelium. *J Cell Biol* 111: 1207–1216, 1990
- Weiss RM, Guo S, Shan A, Shi H, Romano RA, Sinha S, Cantley LG, Guo JK: Brg1 determines urothelial cell fate during ureter development. *J Am Soc Nephrol* 24: 618–626, 2013
- Bohnenpoll T, Kispert A: Ureter growth and differentiation. *Semin Cell Dev Biol* 36: 21–30, 2014
- Airik R, Trowe MO, Foik A, Farin HF, Petry M, Schuster-Gossler K, Schweizer M, Scherer G, Kist R, Kispert A: Hydronephrosis due to loss of Sox9-regulated smooth muscle cell differentiation of the ureteric mesenchyme. *Hum Mol Genet* 19: 4918–4929, 2010
- Trowe MO, Airik R, Weiss AC, Farin HF, Foik AB, Bettenhausen E, Schuster-Gossler K, Taketo MM, Kispert A: Canonical Wnt signaling regulates smooth muscle precursor development in the mouse ureter. *Development* 139: 3099–3108, 2012
- Sorococ K, Kostoulas X, Cullen-McEwen L, Hart AH, Bertram JF, Caruana G: Expression patterns and roles of periostin during kidney and ureter development. *J Urol* 186: 1537–1544, 2011
- Airik R, Bussen M, Singh MK, Petry M, Kispert A: Tbx18 regulates the development of the ureteral mesenchyme. *J Clin Invest* 116: 663–674, 2006
- Bohnenpoll T, Bettenhausen E, Weiss AC, Foik AB, Trowe MO, Blank P, Airik R, Kispert A: Tbx18 expression demarcates multipotent precursor populations in the developing urogenital system but is exclusively required within the ureteric mesenchymal lineage to suppress a renal stromal fate. *Dev Biol* 380: 25–36, 2013
- Muzumdar MD, Tasic B, Miyamichi K, Li L, Luo L: A global double-fluorescent Cre reporter mouse. *Genesis* 45: 593–605, 2007
- Trowe MO, Shah S, Petry M, Airik R, Schuster-Gossler K, Kist R, Kispert A: Loss of Sox9 in the periotic mesenchyme affects mesenchymal expansion and differentiation, and epithelial morphogenesis during cochlea development in the mouse. *Dev Biol* 342: 51–62, 2010
- Gandhi D, Molotkov A, Batourina E, Schneider K, Dan H, Reiley M, Laufer E, Metzger D, Liang F, Liao Y, Sun TT, Aronow B, Rosen R, Mauney J, Adam R, Rosselot C, Van Batavia J, McMahon AP, McMahon J, Guo JJ, Mendelsohn C: Retinoid signaling in progenitors controls specification and regeneration of the urothelium. *Dev Cell* 26: 469–482, 2013
- Humphreys BD, Lin SL, Kobayashi A, Hudson TE, Nowlin BT, Bonventre JV, Valerius MT, McMahon AP, Duffield JS: Fate tracing reveals the pericyte and not epithelial origin of myofibroblasts in kidney fibrosis. *Am J Pathol* 176: 85–97, 2010
- van Amerongen R, Bowman AN, Nusse R: Developmental stage and time dictate the fate of Wnt/ β -catenin-responsive stem cells in the mammary gland. *Cell Stem Cell* 11: 387–400, 2012
- Kuschert S, Rowitch DH, Haenig B, McMahon AP, Kispert A: Characterization of Pax-2 regulatory sequences that direct transgene expression in the Wolffian duct and its derivatives. *Dev Biol* 229: 128–140, 2001

Part 2 - Lineage diversification in the ureter

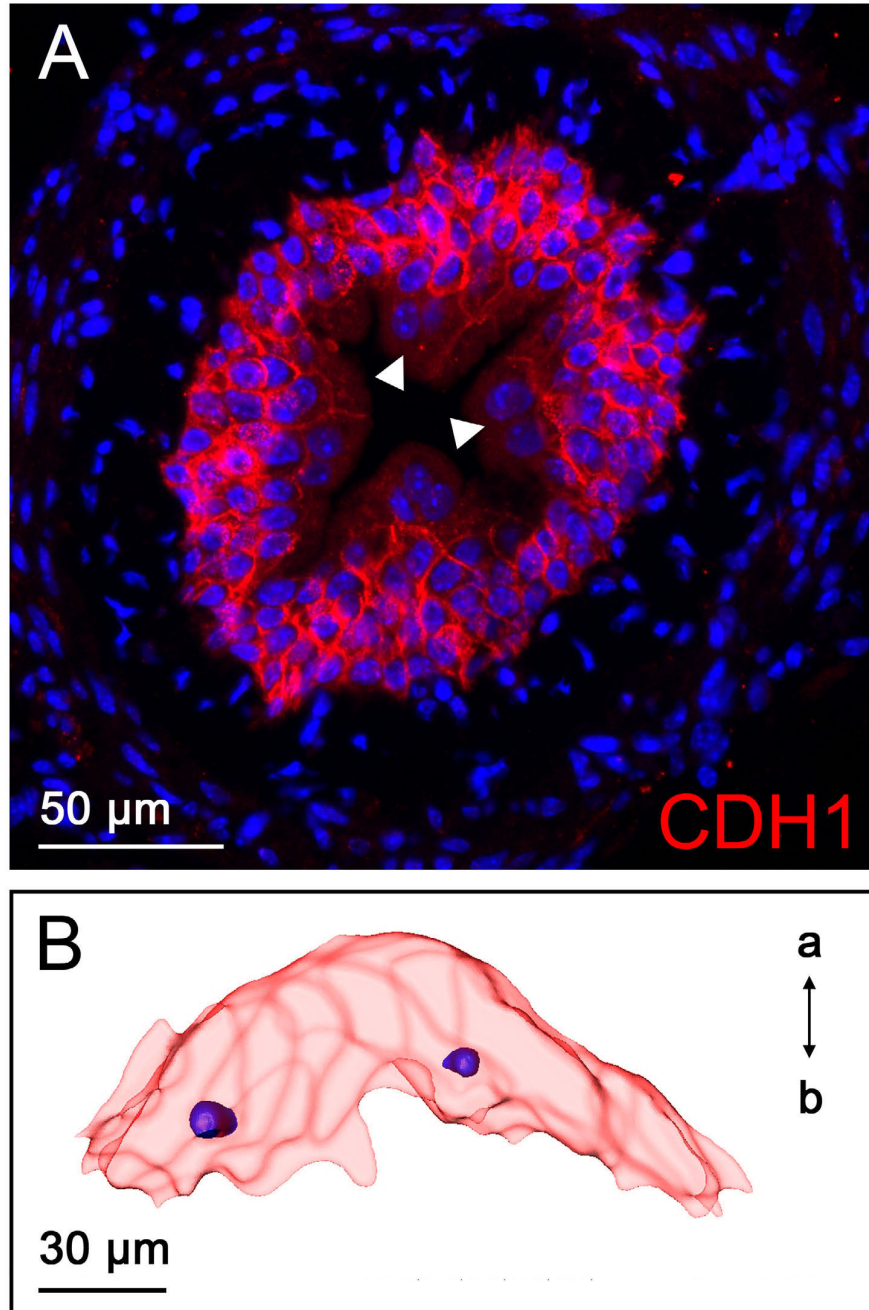
BASIC RESEARCH | www.jasn.org

16. Trowe MO, Maier H, Petry M, Schweizer M, Schuster-Gossler K, Kispert A: Impaired stria vascularis integrity upon loss of E-cadherin in basal cells. *Dev Biol* 359: 95–107, 2011
17. Harfe BD, Scherz PJ, Nissim S, Tian H, McMahon AP, Tabin CJ: Evidence for an expansion-based temporal Shh gradient in specifying vertebrate digit identities. *Cell* 118: 517–528, 2004
18. Van Keymeulen A, Rocha AS, Ousset M, Beck B, Bouvencourt G, Rock J, Sharma N, Dekoninck S, Blanpain C: Distinct stem cells contribute to mammary gland development and maintenance. *Nature* 479: 189–193, 2011
19. McMahon AP, Aronow BJ, Davidson DR, Davies JA, Gaido KW, Grimmond S, Lessard JL, Little MH, Potter SS, Wilder EL, Zhang P, GUDMAP project: GUDMAP: the genitourinary developmental molecular anatomy project. *J Am Soc Nephrol* 19: 667–671, 2008
20. Cunha GR: Epithelial-stromal interactions in development of the urogenital tract. *Int Rev Cytol* 47: 137–194, 1976
21. Jho EH, Zhang T, Domon C, Joo CK, Freund JN, Costantini F: Wnt/beta-catenin/Tcf signaling induces the transcription of *Axin2*, a negative regulator of the signaling pathway. *Mol Cell Biol* 22: 1172–1183, 2002
22. Shin K, Lee J, Guo N, Kim J, Lim A, Qu L, Mysorekar IU, Beachy PA: Hedgehog/Wnt feedback supports regenerative proliferation of epithelial stem cells in bladder. *Nature* 472: 110–114, 2011
23. Papafotiou G, Paraskevopoulou V, Vasilaki E, Kanaki Z, Paschalidis N, Klinakis A: KRT14 marks a subpopulation of bladder basal cells with pivotal role in regeneration and tumorigenesis. *Nat Commun* 7: 11914, 2016
24. Mysorekar IU, Mulvey MA, Hultgren SJ, Gordon JI: Molecular regulation of urothelial renewal and host defenses during infection with uropathogenic *Escherichia coli*. *J Biol Chem* 277: 7412–7419, 2002
25. Moorman AF, Houweling AC, de Boer PA, Christoffels VM: Sensitive nonradioactive detection of mRNA in tissue sections: Novel application of the whole-mount in situ hybridization protocol. *J Histochem Cytochem* 49: 1–8, 2001
26. Bussen M, Petry M, Schuster-Gossler K, Leitges M, Gossler A, Kispert A: The T-box transcription factor *Tbx18* maintains the separation of anterior and posterior somite compartments. *Genes Dev* 18: 1209–1221, 2004

This article contains supplemental material online at <http://jasn.asnjournals.org/lookup/suppl/doi:10.1681/ASN.2016080849/-/DCSupplemental>.

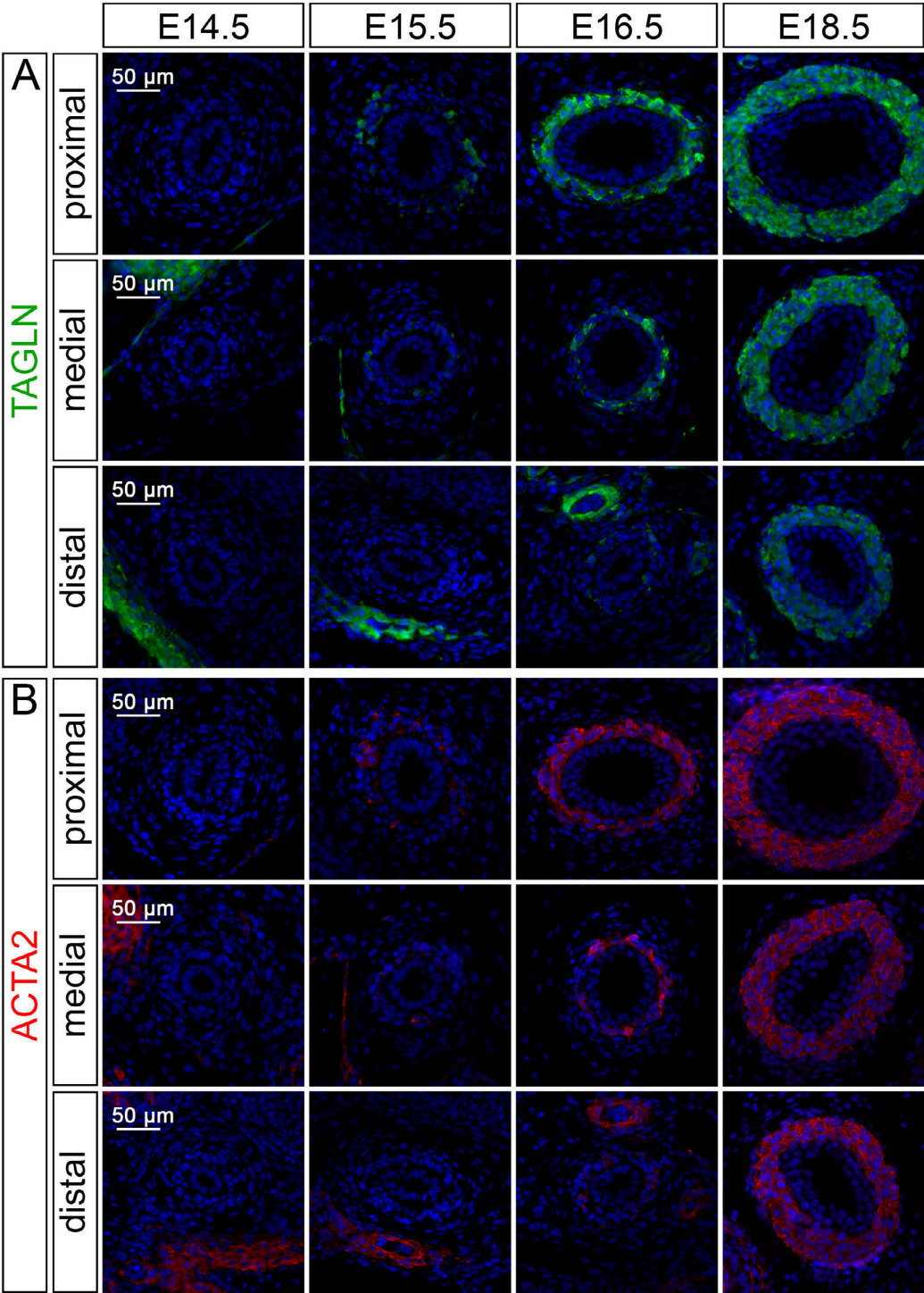
Supplemental Data

Supplemental Figures

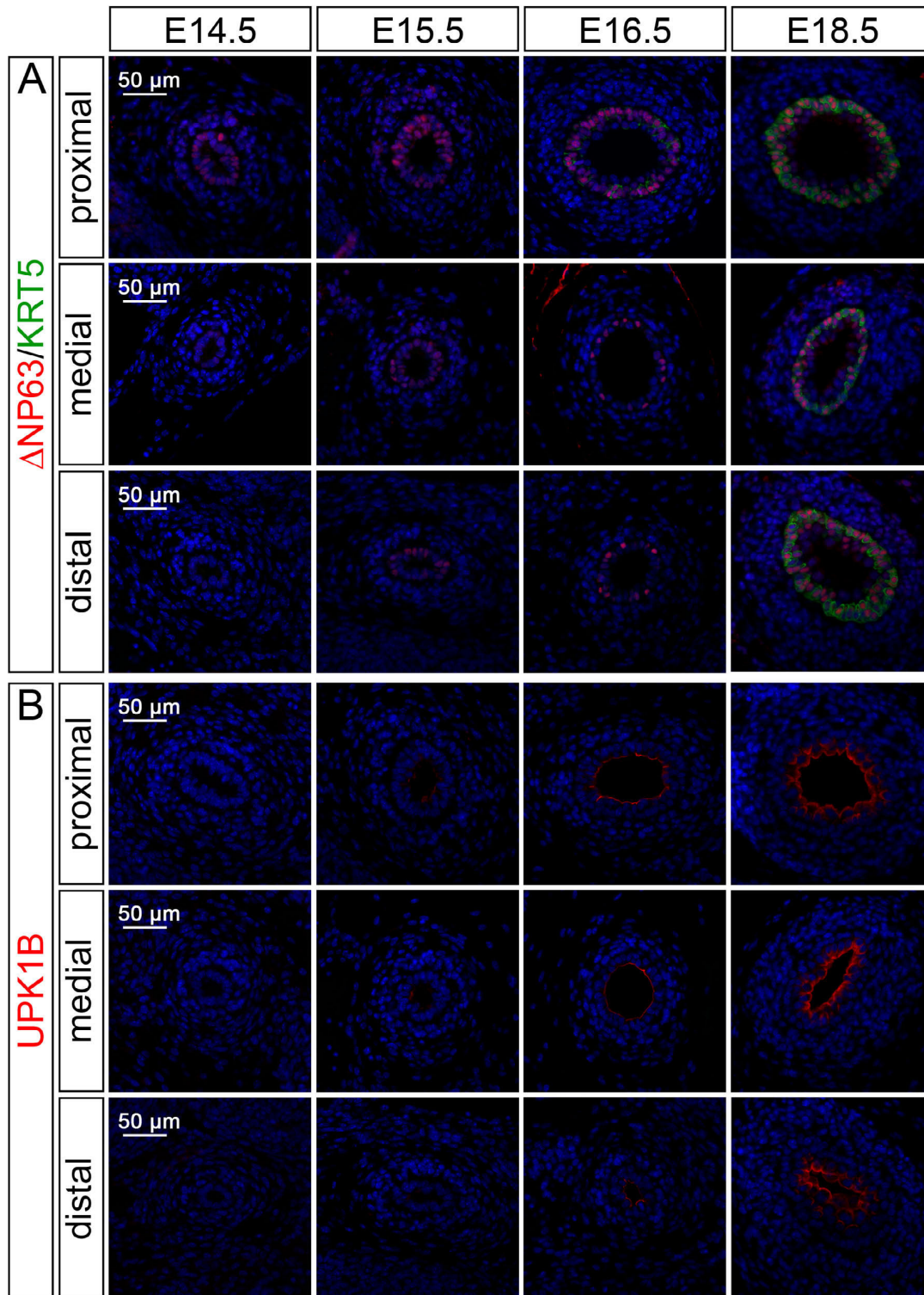


Supplemental Figure 1. S-cells in the ureter are binucleate. (A) Immunofluorescence analysis of CDH1 expression with nuclear DAPI counterstain (blue) on transverse sections of a proximal ureter at P220. White arrowheads point towards binucleated S-cells. (B) Three-dimensional reconstruction of a single S-cell harboring two nuclei based on serial sections of an adult ureter stained as in (A). a, apical; b, basal.

Part 2 - Lineage diversification in the ureter

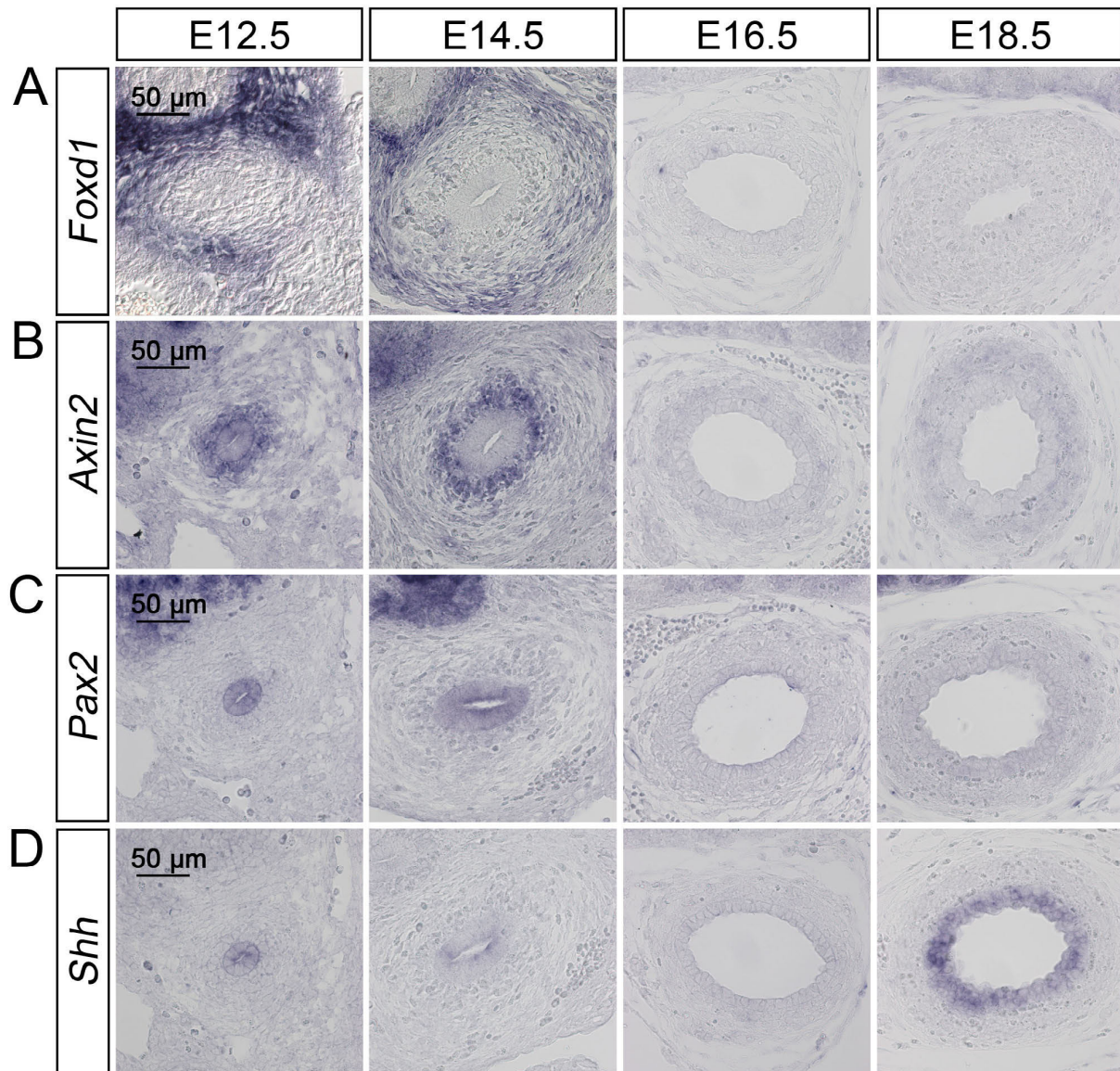


Supplemental Figure 2. Cellular differentiation in the ureteric mesenchyme proceeds in a proximal to distal fashion. Immunofluorescence analysis of the SMC markers TAGLN (A) and ACTA2 (B) with nuclear DAPI (blue) on transverse sections of E14.5, E15.5, E16.5 and E18.5 ureters sectioned each at a proximal (upper row), medial (middle row) and distal (lower row) level. Expression of differentiation markers at the proximal ureter level precedes their expression at more distal levels by approximately one day.

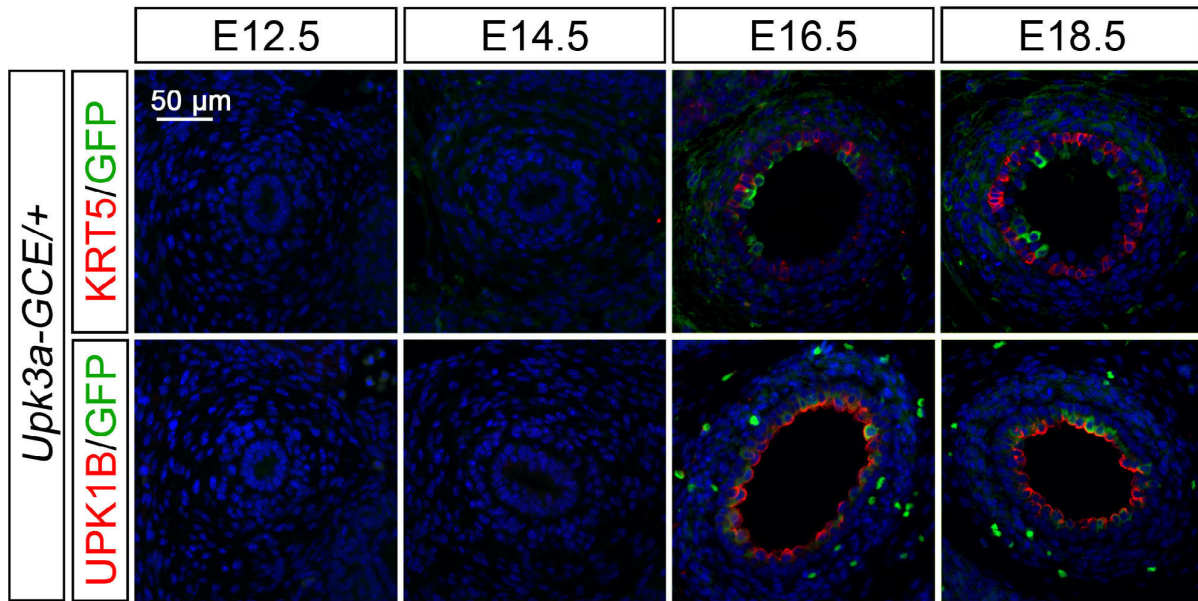


Supplemental Figure 3. Cellular differentiation in the ureteric epithelium proceeds in a proximal to distal fashion. Immunofluorescence analysis of the urothelial markers Δ NP63/KRT5 (A) and UPK1B (B) with nuclear DAPI (blue) on transverse sections of E14.5, E15.5, E16.5 and E18.5 ureters sectioned each at a proximal (upper row), medial (middle row) and distal (lower row) level. Expression of differentiation markers at the proximal ureter level occurs approximately one day earlier than at the distal level.

Part 2 - Lineage diversification in the ureter

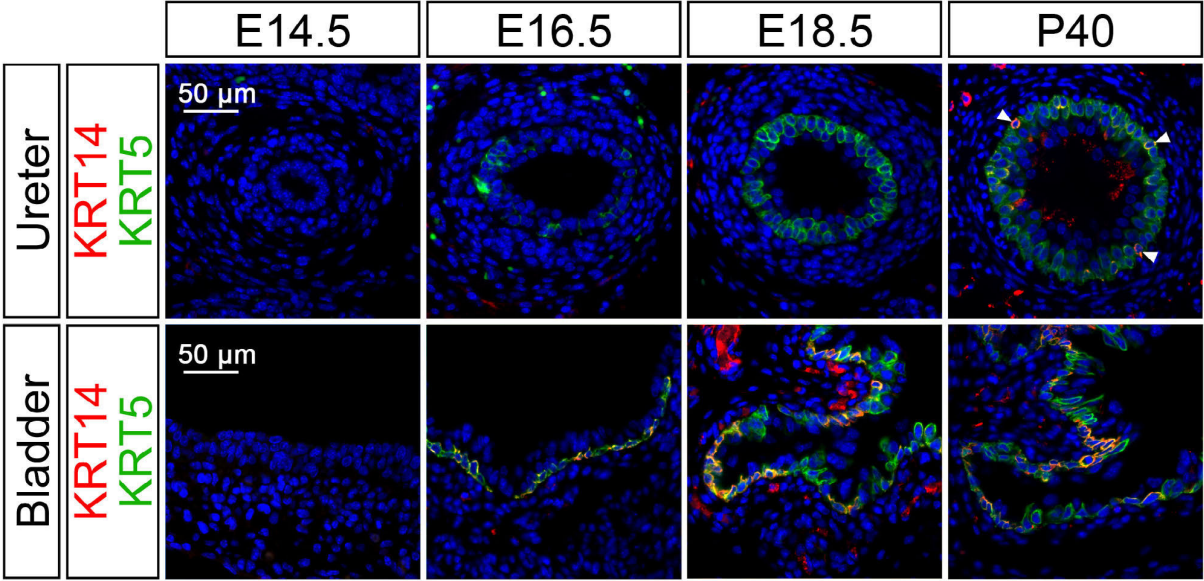


Supplemental Figure 4. Gene expression during ureter development confirms specificity of *cre* driver lines. (A-D) *In situ* hybridization analysis of gene expression on proximal sections of the mouse ureter at the indicated stages. (A) *Foxd1* expression is restricted to the outer mesenchymal domain at E12.5 and E14.5 while (B) *Axin2* mRNA is found only in the inner mesenchymal domain at these two stages. (C) *Pax2* expression is confined to the ureteric epithelium at E12.5 and E14.5. (D) *Shh* mRNA is expressed in the ureteric epithelium from E12.5 to E18.5 with reduced expression at E16.5.



Supplemental Figure 5. The *Upk3a-GCE* driver line mediates *loxP*-recombination in I- and S-cells but not in B-cells. Co-immunofluorescence analysis of expression of cytoplasmic GFP in the GFP-creRT2 fusion protein expressed from the *Tg(Upk3a-GFP/cre/ERT2)26Amc* (*Upk3a-GCE*) transgene with nuclear DAPI (blue) and the B-cell marker KRT5 (upper row) and the I- and S-cell marker UPK1B (lower row) on proximal sections of a ureter at the indicated embryonic stages. GFP and KRT5 expression is mutually exclusive while GFP overlaps with UPK1B showing that the GFP-creERT2 fusion protein, thus, cre activity is confined to I- and S-cells.

Part 2 - Lineage diversification in the ureter



Supplemental Figure 6. KRT14 expression marks a small subpopulation of KRT5⁺ B-cells in the adult ureter. Co-immunofluorescence analysis of expression of KRT14 and the B-cell marker KRT5 with nuclear DAPI counterstain (blue) on transverse sections of the proximal ureter (upper row) and on mid-sagittal sections of the bladder (lower row) at the indicated stages. In the ureter, KRT14 expression is found in few KRT5⁺ B-cells in the P40 adult only (white arrowheads) whereas KRT14 marks a large subpopulation of KRT5⁺ B-cells in the bladder from E16.5 onwards.

Supplemental Tables

Stage	Undiff. (%)	TA-cells (%)	SM-cells (%)	LP-cells (%)
E12.5	100	0	0	0
E13.5	57.1 ± 6.1	42.9 ± 6.1	0	0
E14.5	47.8 ± 3.3	52.2 ± 3.3	0	0
E15.5	34.6 ± 8.1	54.3 ± 2.2	11.1 ± 8.3	0
E16.5	15.5 ± 7.2	49.2 ± 4.5	26.2 ± 6.2	9.1 ± 1.1
E18.5	0	53.7 ± 3.6	37.0 ± 2.3	9.3 ± 1.4
P40	0	15.0 ± 1.1	62.6 ± 2.9	22.4 ± 2.8

Supplemental Table 1A. Distribution of mesenchymal cell types during ureter development. Values are displayed in % as mean ± sd of undifferentiated cells (Undiff.), adventitial cells (TA-cells), smooth muscle cells (SM-cells) and *Lamina propria* cells (LP-cells) with respect to the total cell number. Quantification is based on 6 sections from three individuals at each stage.

Stage	Undiff. (%)	B-cells (%)	I-cells (%)	S-cells (%)
E12.5	100	0	0	0
E13.5	97.4 ± 4.3	0	2.6 ± 4.3	0
E14.5	17.5 ± 8.9	0	82.5 ± 8.9	0
E15.5	0	0	95.5 ± 1.6	4.5 ± 1.6
E16.5	0	37.9 ± 9.8	39.5 ± 8.8	22.5 ± 2.4
E18.5	0	53.8 ± 5.1	26.9 ± 4.8	19.4 ± 3.8
P40	0	71.3 ± 3.2	21.8 ± 3.6	6.9 ± 1.5

Supplemental Table 1B. Distribution of epithelial cell types during ureter development. Values are displayed in % as mean ± sd of undifferentiated cells (Undiff.), basal cells (B-cells), intermediate cells (I-cells) and superficial cells (S-cells) with respect to the total cell number. Quantification is based on 6 sections from three individuals at each stage.

Part 2 - Lineage diversification in the ureter

Stage	IM	OM	UE
E12.5	0.236 ± 0.030	0.217 ± 0.017	0.228 ± 0.028
E14.5	0.198 ± 0.009	0.202 ± 0.014	0.230 ± 0.013

Supplemental Table 2A. Proliferation rates in the developing ureter at E12.5 and E14.5. Shown are the BrdU indices for the inner mesenchymal domain (IM), the outer mesenchymal domain (OM) and the ureteric epithelium (UE). The BrdU index is displayed as mean ± sd, 12 sections from three individuals were used for quantification.

Stage	LP	SMC	TA
E16.5	0.233 ± 0.022	0.191 ± 0.008	0.122 ± 0.007
E18.5	0.267 ± 0.025	0.134 ± 0.009	0.081 ± 0.004
P40	0.003 ± 0.002	0	0.008 ± 0.003

Supplemental Table 2B. Proliferation rates in the ureteric mesenchyme at E16.5, E18.5 and at P40. Shown are the BrdU indices for the inner *Lamina propria* (LP), the smooth muscle cells (SMC) and the *Tunica adventitia* (TA). The BrdU index is displayed as mean ± sd, 8 sections from three individuals were used for quantification.

Stage	BC	IC	SC
E16.5	0.203 ± 0.040	0.098 ± 0.008	0.175 ± 0.022
E18.5	0.035 ± 0.012	0.014 ± 0.009	0.087 ± 0.024
P40	0.001 ± 0.002	0	0

Supplemental Table 2C. Proliferation rates in the ureteric epithelium at E16.5, E18.5 and at P40. Shown are the BrdU indices for basal cells (BC), intermediate cells (IC) and superficial cells (SC). The BrdU index is displayed as mean ± sd, 8 sections from three individuals were used for quantification.

Stage	IM (%)	OM (%)	Numbers
E12.5 + 1d	76.7 ± 5.3	23.3 ± 5.3	269
E13.5 + 1d	94.3 ± 3.5	5.7 ± 3.5	129

Supplemental Table 3A. Lineage labelling in the ureteric mesenchyme of *Axin2^{creERT/+};R26^{mTmG/+}* embryos that were Tamoxifen-induced at E12.5 or E13.5 and analysed for distribution of recombined GFP⁺ cells 24 h later. Values are displayed in % as mean ± sd of all GFP-labelled cells found in the inner (IM) or outer (OM) mesenchymal compartment of the ureter. Additionally, the total number of GFP⁺ cells detected in a total of four individuals is displayed.

Stage	LP (%)	SMC (%)	TA (%)	Numbers
E12.5 + 6d	18.0 ± 2.8	70.7 ± 0.6	11.3 ± 2.6	521
E13.5 + 5d	17.1 ± 4.4	73.2 ± 4.0	9.7 ± 4.6	583

Supplemental Table 3B. Lineage tracing in the ureteric mesenchyme of *Axin2^{creERT/+};R26^{mTmG/+}* embryos that were tamoxifen-induced at E12.5 or E13.5 and analysed for distribution of recombined GFP⁺ cells 6 or 5 days later. Values are displayed in % as mean ± sd of all GFP-labelled cells found in the *Lamina propria* (LP), smooth muscle layer (SMC) or *Tunica adventitia* (TA) of the ureter. Additionally, the total number of GFP⁺ cells detected in a total of four individuals is displayed.

Part 2 - Lineage diversification in the ureter

Stage	KRT5 ⁺ UPK1B ⁻ (%)	KRT5 ⁻ UPK1B ⁺ (%)	Numbers
E14.5 + 10d	0	0	0
E16.5 + 8d	100	0	135
E18.5 + 6d	100	0	409
Adult + 4w	100	0	552

Supplemental Table 4A. Lineage tracing in *Krt5^{creERT2/+};R26^{mTmG/+}* ureter explants from E14.5, E16.5 and E18.5 mice cultured for 10 d, 8 d, and 6 d, respectively, and in adult mice after 4 weeks of labelling. First row: KRT5⁺UPK1B⁻. Values are displayed in % as mean ± sd of all GFP-labelled cells found in the KRT5⁺UPK1B⁻ basal cell layer. Second row: KRT5⁻UPK1B⁺. Values are displayed in % as mean ± sd of all GFP-labelled cells found in the KRT5⁻UPK1B⁺ intermediate and superficial cell layers. Third row: Numbers. Total number of GFP⁺ cells detected in a total of three individual ureters.

Stage	KRT5 ⁺ UPK1B ⁻ (%)	KRT5 ⁻ UPK1B ⁺ (%)	Numbers
E14.5 + 10d	31.7 ± 14.4	68.3 ± 14.4	113
E16.5 + 8d	57.1 ± 9.4	42.9 ± 9.4	271
E18.5 + 6d	55.0 ± 13.4	45.0 ± 13.4	384
Adult + 4w	41.7 ± 1.2	58.3 ± 1.2	652

Supplemental Table 4B. Lineage tracing in *Upk3a-GCE/+;R26^{mTmG/+}* ureter explants from E14.5, E16.5 and E18.5 mice cultured for 10 d, 8 d, and 6 d, respectively, and in adult mice after 4 weeks of labelling. First row: KRT5⁺UPK1B⁻. Values are displayed in % as mean ± sd of all GFP-labelled cells found in the KRT5⁺UPK1B⁻ basal cell layer. Second row: KRT5⁻UPK1B⁺. Values are displayed in % as mean ± sd of all GFP-labelled cells found in the KRT5⁻UPK1B⁺ intermediate and superficial cell layers. Third row: Numbers. Total number of GFP⁺ cells detected in a total of three individual ureters.

Part 3 - SHH signaling in ureter development

A SHH-FOXF1-BMP4 signaling axis regulating growth and differentiation of epithelial and mesenchymal tissues in ureter development

Tobias Bohnenpoll¹, Anna B. Wittern¹, Tamrat M. Mamo¹, Anna-Carina Weiss¹, Karin Schuster-Gossler¹, Carsten Rudat¹, Marc-Jens Kleppa¹, Mark-Oliver Trowe¹ and Andreas Kispert^{1,§}

¹ Institut für Molekularbiologie, Medizinische Hochschule Hannover, 30627 Hannover, Germany

§ Author for correspondence:

Email: kispert.andreas@mh-hannover.de

Tel: +49511 5324017

Fax: +49511 5324283

Manuscript under revision at PLOS Genetics.

Abstract

The differentiated cell types of the epithelial and mesenchymal tissue compartments of the mature ureter arise in a precisely coordinated temporal and spatial sequence from uncommitted precursor cells of the distal ureteric bud and its surrounding mesenchyme. How cellular programs are coupled between the two progenitor pools has remained largely unexplored. Here, we showed that conditional deletion of the gene encoding the Hedgehog (HH) signal transducer Smoothed (*Smo*) in the early ureteric mesenchyme of the mouse resulted in apoptosis of outer mesenchymal cells, reduced proliferation of inner mesenchymal and epithelial cells and failure of the latter two populations to differentiate into smooth muscle and urothelial cell types, respectively. Complementary expression of a constitutively active form of SMO led to adventitial cell survival and enhanced proliferation but did not affect patterning and differentiation of inner mesenchymal and epithelial cells. We identified the Forkhead transcription factor gene *Foxf1* as a target of HH signaling in the ureteric mesenchyme. Expression of a repressor version of FOXF1 in the ureteric mesenchyme completely recapitulated the mesenchymal and epithelial proliferation and differentiation defects associated with loss of HH signaling; re-expression of a wildtype version of FOXF1 in the inner mesenchymal layer restored these cellular programs when HH signaling was inhibited. We further showed that expression of *Bmp4* in the ureteric mesenchyme depends on HH signaling and *Foxf1*, and that exogenous BMP4 rescued cell proliferation and epithelial differentiation in ureters with abrogated HH signaling or FOXF1 function. We conclude that SHH is the crucial epithelial signal that couples the proliferation and differentiation programs in the two tissue compartments of the developing ureter via a FOXF1-BMP4 regulatory module.

Author summary

The mammalian ureter is a simple tube with a specialized multi-layered epithelium, the urothelium, and a surrounding coat of fibroblasts and peristaltically active smooth muscle cells. Beside its important function in urinary drainage the ureter represents a simple model system to study epithelial and mesenchymal tissue interactions in organ development. The differentiated cell types of the ureter coordinately arise from precursor cells of the distal ureteric bud and its surrounding mesenchyme. How their survival, growth and differentiation is regulated and coordinated within and between the epithelial and mesenchymal tissue compartments is largely unknown. Previous work has identified sonic hedgehog (SHH) as a crucial epithelial signal for growth and differentiation of the ureteric mesenchyme, but the entirety of the cellular functions and the molecular mediators of its mesenchymal signaling pathway have remained obscure. Here we showed that epithelial SHH acts paracrine in the ureteric mesenchyme to activate a FOXF1-BMP4 regulatory module that directs growth and differentiation of both ureteric tissue compartments. HH signaling additionally acts in outer mesenchymal cells as a survival factor. Thus, SHH is an epithelial signal that coordinates various cellular programs in early ureter development.

Introduction

The ureter is a pivotal component of the urinary system by warranting the efficient removal of the urine from the renal pelvis to the bladder. This task is accomplished by the compartmentalized organization of the straight tube into an outer flexible but rigid peristaltically active mesenchymal coat with contractile smooth muscle cells (SMCs) and surrounding fibrocytes of the inner *Lamina propria* and the outer *Tunica adventitia*, and a highly distensible yet tightly sealing specialized inner epithelial lining. This urothelium features at the luminal side large binucleate superficial (S-) cells that exert barrier function at least partly due to expression of uroplakins (UPKs) that form crystalline plaques on the surface. Underneath are two layers of smaller intermediate (I-) and basal (B-) cells that serve as precursors in injury conditions and tether the underlying fibrocytes, respectively [1-4].

Although the tissue architecture of the ureter is obviously much less complex compared to the adjacent kidney, our knowledge on the cellular and molecular programs that drive the growth and differentiation of this organ from a simple embryonic rudiment have only recently begun to be elucidated [5]. Cell lineage and marker analyses in the mouse have shown that the different epithelial and mesenchymal cell types of the ureter arise in a highly coordinated fashion from uncommitted progenitors that are established around embryonic day (E)11.5 from two independent precursor pools in the early metanephric field: the distal portion of the ureteric bud and its surrounding mesenchyme [4]. At E12.5, the initially homogenous ureteric mesenchyme is radially subdivided into an inner layer of large cuboidal cells, and an outer layer of tangentially oriented loosely organized cells. While the latter start to differentiate into adventitial fibrocytes from E13.5 onwards, the first maintain a bipotential character until E15.5 when they differentiate into SMCs, and subepithelial fibrocytes of the *Lamina propria*. Urothelial differentiation starts around E14.5 with the establishment of a common progenitor for S- and B-cells, the I-cell that expresses Δ NP63 and low levels of UPKs. At E15.5, first luminal cells downregulate Δ NP63 and express high levels of UPKs to become S-cells. KRT5⁺ B-cells are first recognized at E16.5. They substantially expand thereafter to constitute the major cell type of the adult urothelium [4].

Survival, growth and differentiation of the ureteric mesenchyme and epithelium are tightly coupled and rely on the exchange of signals between and within the two tissues [5-7]. While our knowledge of the signaling systems that underlie urothelial development has remained scarce, WNTs, BMP4 and SHH have been identified as crucial signals for SMC differentiation in the mesenchyme [8-11]. The latter is expressed in the ureteric epithelium throughout development

and is thought to act in a paracrine fashion onto the adjacent mesenchyme. Deletion of *Shh* from the epithelium resulted in reduced mesenchymal proliferation and delayed SMC differentiation, and culminated in hydroureter, i.e. dilatation of the ureter by urinary pressure [8]. The molecular targets of SHH signaling are poorly understood. So far, expression of the genes encoding the transcription factor TSHZ3 and the signaling molecule BMP4 have been described to depend on SHH pathway activity in the ureteric mesenchyme [8, 12]. Both genes are essential for SMC differentiation arguing that they mediate some part of SHH function [9, 12]. Canonical WNT signaling is also required for SMC differentiation and may act in parallel to SHH in this process [10].

Here, we further explore the cellular and molecular functions of HH signaling in the ureteric mesenchyme. We show that HH signaling is not only required for mesenchymal proliferation and differentiation but also acts as a mesenchymal survival factor and is essential for growth and differentiation of the ureteric epithelium. We provide evidence for a mesenchymal FOXF1-BMP4 module acting downstream of HH signaling in the execution of these programs.

Results

Conditional inactivation of *Smo* in the ureteric mesenchyme results in hydroureter formation due to functional insufficiencies of its tissue compartments

To investigate the functional requirement of HH signaling in ureter development, we employed a conditional gene inactivation approach using a *Tbx18^{cre}* line [13] and a floxed allele of *Smo* (*Smo^{fl}*) [14] which encodes a unique signal transducer of this pathway [15]. As previously reported, *Tbx18^{cre}* mediates recombination in the undifferentiated ureteric mesenchyme from E10.5 onwards, i.e. in the precursors of all differentiated cell types of the ureteric wall [10, 16]. At E18.5, urogenital systems of *Tbx18^{cre/+};Smo^{fl/fl}* (*Smo^{LOF}*) mice displayed with full penetrance in both sexes complete bilateral hydroureter (Fig 1A-1D). Histological analyses revealed a reduced pelvic space in mutant kidneys. The ureter was strongly dilated and featured a monolayered urothelium that was surrounded by fibroelastic material (Fig 1E-1H). Expression of the structural components of the SMC layer ACTA2, MYH11 and *Tnnt2* as well as of the key regulator of the SMC transcriptional program *Myocd* was completely absent in the mutant ureter (Fig 1I-1P). Differentiation of urothelial cell types was also severely compromised in the mutant ureter as indicated by a strong decrease in expression of the B- and I-cell markers KRT5 and Δ NP63, and absence of superficial UPK1B expression (Fig 1Q-1T). To test for the continuity of the ureteric lumen and the patency of the uretero-pelvic and vesicular junctions, we injected ink into the renal pelvis. Under conditions of increased hydrostatic pressure, the ink readily drained to the bladder both in control and *Smo^{LOF}* urogenital systems. Furthermore, the ureters in *Smo^{LOF}* embryos terminated in the bladder neck as in the control, arguing together that physical obstruction does not cause or contribute to the hydroureter phenotype in *Smo^{LOF}* urogenital systems (Fig 1U-1X). Control ureters explanted at E14.5 and cultured for 4 days elongated and performed unidirectional peristaltic contractions within 2 days of culture. In contrast, *Smo^{LOF}* ureters were strongly hypoplastic when explanted and degenerated in culture without showing any signs of contractile activity (Fig 1Y-1Z'). Hence, lack of *Smo*, i.e. of HH signaling, in the ureteric mesenchyme results in tissue hypoplasia, a complete lack of differentiated mesenchymal and epithelial cell types and hydroureter formation at birth.

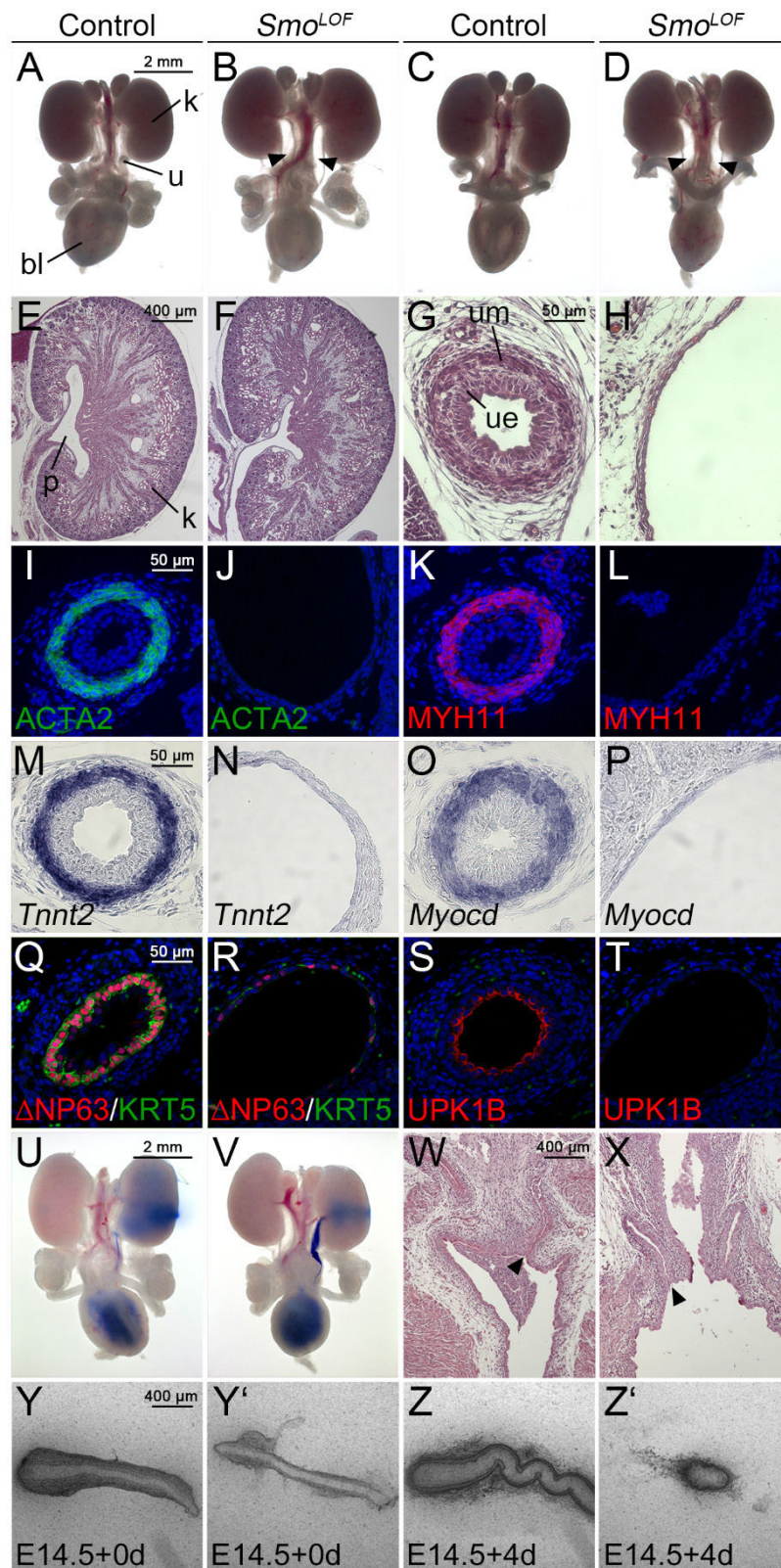


Figure 1: *Tbx18^{cre/+};Smo^{fl/fl} (Smo^{LOF})* embryos exhibit severe ureter defects at E18.5. (A-D) Morphology of whole urogenital systems of male (A,B) and female (C,D) embryos. Arrows point to hydroureters in *Smo^{LOF}* embryos. (E-H) Hematoxylin and Eosin (HE) stainings on midsagittal sections of the kidney (E,F) and of the proximal ureter (G,H). (I-T) Cytodifferentiation of the ureteric mesenchyme (I-P) and urothelium (Q-T) is compromised in *Smo^{LOF}* embryos as shown by immunofluorescence (I-L,Q-T) or RNA *in situ* hybridization (M-P) analysis on transverse sections of the proximal ureter. (U-X) Absence of physical obstruction in the *Smo^{LOF}* ureter as revealed by ink injection experiments (U,V) and HE stainings of the vesicoureteral junction (W,X). (Y-Z') Explants of E14.5 ureters after 0d and 4d of culture. Genotypes and markers are as shown.

Smo^{LOF} ureters show early hypoplasia and do not initiate the SMC and urothelial differentiation programs

To characterize the onset and progression of the growth and differentiation defects in *Smo*^{LOF} ureters, we performed histological and molecular analysis at earlier embryonic stages (Fig 2A-2F). At E12.5, *Smo*^{LOF} ureters appeared histologically unremarkable. The mono-layered ureteric epithelium was surrounded by up to two layers of spherical, densely packed mesenchymal cells with a clear compartment boundary to the outer spindle-shaped and radially oriented cells as in the control, indicating that initial tissue patterning of the ureteric mesenchyme was normal (Fig 2A, left panel). At E14.5, the urothelium of control embryos started to stratify and appeared occasionally double-layered, the compartmentalization of the ureteric mesenchyme was enhanced. In contrast, the *Smo*^{LOF} urothelium remained mono-layered and the mesenchymal cell mass was sparse (Fig 2A, middle panel). At E16.5, the onset of substantial urine production in the embryonic kidney, *Smo*^{LOF} mutants showed a strongly dilated ureter with a mono-layered urothelium surrounded by loosely packed fibrocytes (Fig 2A, right panel).

To characterize the initiation and progression of ureteric SMC differentiation we analyzed the expression of the regulatory gene *Myocd* as well as of the SMC structural genes *Myh11* and *Tagln*. *Myocd* expression was homogenously strong in the wildtype at E14.5 and E16.5 whereas *Myh11* and *Tagln* expression was spotty at E14.5 and became stronger at E16.5. *Smo*^{LOF} ureters never expressed any of these markers, indicating that SMC differentiation was not initiated in the mutants (Fig 2B-2D). Urothelial differentiation started in the wildtype at E14.5 with the expression of Δ NP63 and continued at E16.5 with the appearance of Δ NP63⁺KRT5⁺ B-cells and UPK1B⁺ Δ NP63⁻ S-cells. In *Smo*^{LOF} mutant ureters, only few cells expressed Δ NP63 at low levels at E16.5, KRT5 expression and UPK1B was not observed (Fig 2E and 2F). Taken together, *Smo*^{LOF} ureters develop severe mesenchymal and epithelial hypoplasia and fail to initiate the SMC and urothelial differentiation programs.

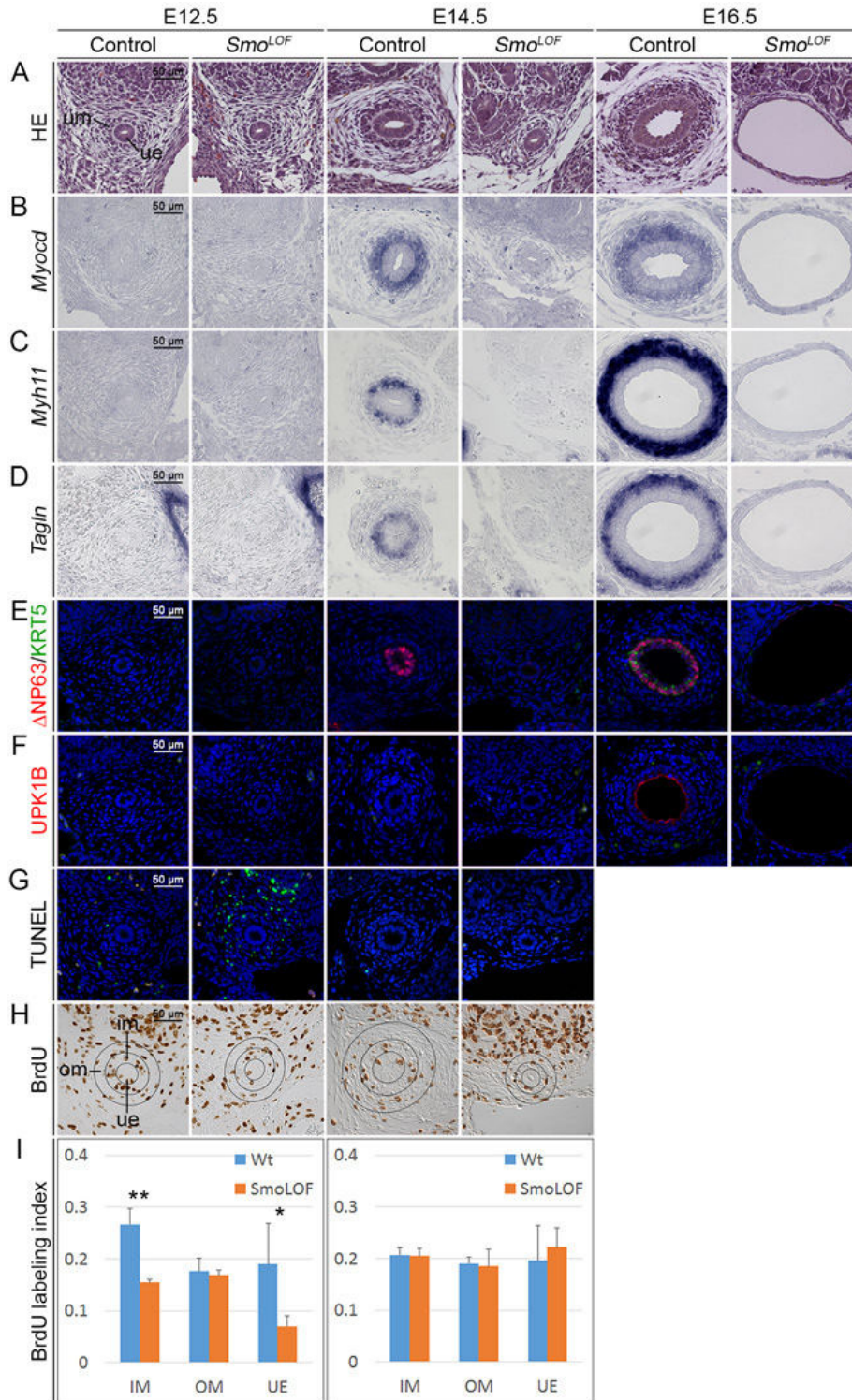


Figure 2: Ureter anomalies arise early in *Tbx18*^{cre/+};*Smo*^{fl/fl} (*Smo*^{LOF}) embryos.

(A) Hematoxylin and Eosin (HE) stainings of transverse sections of the proximal ureter at E12.5, E14.5, and E16.5. (B-D) Cytodifferentiation of the ureteric mesenchyme into SMCs as detected by *in situ* hybridization of expression of SMC marker genes, and (E,F) cytodifferentiation of the ureteric epithelium as detected by immunofluorescence of B-, I- and S-cell markers fail in *Smo*^{LOF} embryos. Nuclei are counterstained with DAPI (blue). (G) Cell death as detected by the TUNEL assay (green) occurs in the outer mesenchymal region of *Smo*^{LOF} ureters at E12.5. Nuclei are counterstained with DAPI. (H) Determination of cellular proliferation by the BrdU incorporation assay on transverse sections of the proximal ureter at E12.5 and E14.5. Black circles in H mark the epithelium (ue) and the inner (im) and outer (om) mesenchymal compartments of the ureter that were analyzed to quantify proliferation. Proliferation in *Smo*^{LOF} embryos is reduced in the inner mesenchymal region and the epithelium of the E12.5 ureter. (I) Quantification of BrdU-positive cells. E12.5 (n=3), wildtype versus mutant: IM, 0.267±0.030 vs 0.155±0.006, P=0.007; OM, 0.176±0.025 vs 0.169±0.009, P=0.709; UE, 0.190±0.079 vs 0.071±0.019, P=0.019. E14.5 (n=4), wildtype versus mutant: IM, 0.208±0.015 vs 0.205±0.014, P=0.839; OM, 0.191±0.013 vs 0.185±0.033, P=0.774; UE, 0.196±0.068 vs 0.222 ±0.037, P=0.526. Values are displayed as mean ± sd. *, P≤0.05; **, P≤0.01; two-tailed Student's t-test.

HH signaling is required for survival and proliferation programs in the undifferentiated ureteric tissues

To address the cellular causes for the severe tissue hypoplasia observed in *Smo*^{LOF} ureters, we examined survival and proliferation in the epithelial and mesenchymal tissue compartments (Fig 2G-2I). We used the terminal dUTP nick end-labeling (TUNEL) assay to detect apoptotic bodies. At E12.5, only few apoptotic bodies were detected in control specimens whereas *Smo*^{LOF} ureters showed numerous strong signals specifically in the outer mesenchymal compartment. At E14.5, no signals were detected in either control or mutant ureters (Fig 2G). To assess proliferation rates, we performed bromodeoxyuridine (BrdU) incorporation assays. At E12.5, *Smo*^{LOF} ureters showed significantly decreased proliferation in the inner mesenchymal compartment and the epithelium; outer mesenchymal cells proliferated at normal rates. At E14.5, no changes in proliferation were observed in *Smo*^{LOF} ureters (Fig 2H and 2I). We conclude that *Smo* is required for the survival of the outer mesenchymal compartment and the proliferation of inner mesenchymal and epithelial cells, specifically at E12.5.

Smo^{GOF} ureters develop severe mesenchymal hyperplasia but show normal tissue patterning and differentiation

The analysis of the *Smo* loss-of-function phenotype revealed a critical requirement of HH signaling in survival, growth and differentiation of the ureter. To test for a possible sufficiency in these cellular processes we performed a complementary gain-of-function study by conditional (*Tbx18*^{cre}-mediated) misexpression of a constitutive active form of *Smo* from the *Rosa26* locus (*R26*^{*SmoM2*}) [17] in the ureteric mesenchyme. *Tbx18*^{cre/+}; *R26*^{*SmoM2*/+} (*Smo*^{GOF}) embryos died around E12.5 possibly due to cardiovascular defects. To circumvent this lethality and enable an endpoint analysis of ureter differentiation, we explanted E11.5 kidney rudiments and cultured them for 8 days. We took advantage of a membrane-bound GFP reporter from the *Rosa26*^{*mTmG*} reporter line [18] to visualize the descendants of the undifferentiated ureteric mesenchyme after *Tbx18*^{cre}-mediated recombination. In *Tbx18*^{cre/+}; *R26*^{*mTmG*/+} control explants, GFP⁺ cells initially localized to a band of mesenchymal cells that surrounded the ureter stalk and separated the metanephric mesenchyme from the nephric duct. In the following days, GFP⁺ cells became restricted to a condensed cell layer directly adjacent to the ureteric epithelium and to stromal cells of the medial kidney cortex as previously reported [16].

In *Smo^{GOF} (Tbx18^{cre/+};R26^{mTmG/SmoM2})* explants, GFP⁺ cells localized to these domains as well but additionally persisted in the lateral ureteric mesenchymal region to form a large ectopic cell mass after 4 and 8 days of culture (Fig 3A and 3B). Histological analysis on proximal ureter sections of *Smo^{GOF} E11.5 + 8d* explants confirmed severe mesenchymal hyperplasia (Fig 3C and 3D). Coimmunofluorescence analysis of GFP and the SMC markers TAGLN and ACTA2 revealed correct tissue compartmentalization into a GFP⁺TAGLN⁻ACTA2⁻ *Lamina propria* adjacent to the urothelium, a GFP⁺TAGLN⁺ACTA2⁺ SMC layer and an outer coat of GFP⁺TAGLN⁻ACTA2⁻ adventitial fibroblasts. All three tissue compartments, particularly the adventitial layer were massively expanded in *Smo^{GOF}* explants (Fig 3E-3H). Urothelial differentiation as analyzed by Δ NP63 and UPK1B expression was unaltered (Fig 3I and 3J). Markers of the *Lamina propria* (*Aldh1a2*, *Colla2*) and the *Tunica adventitia* (*Colla2* and *Fbln2*) showed normal spatial restriction but highlighted adventitial hyperplasia in *Smo^{GOF}* ureters (Fig 3K-3P). *Dpt* expression which marks terminal differentiation of adventitial fibroblasts *in vivo* [10] was not detectable in explant cultures indicating that terminal differentiation of fibrocytes is hampered in this experimental setting (Fig 3Q and 3R). We conclude that mis- and overactivation of HH signaling in the ureteric mesenchyme leads to massive mesenchymal hyperplasia but does not affect tissue patterning or cell differentiation programs.

HH signaling is sufficient to induce survival and proliferation of the ureteric mesenchyme

To unravel the cellular cause of tissue hyperplasia in *Smo^{GOF}* ureters, we analyzed both histology, cell proliferation and apoptosis at the onset of ureter development. At E12.5, *Smo^{GOF}* ureters were shortened and surrounded by a large mass of fibrous tissue (Fig 4A and 4B). On the histological level, the subdivision of the ureteric mesenchyme into an inner region with large cuboidal cells and an outer region of more loosely organized tangentially oriented cell bodies was normal but the outer mesenchymal domain appeared strongly expanded (Fig 4C and 4D). The BrdU incorporation assay revealed significantly increased proliferation in the epithelium and the inner mesenchymal domain of *Smo^{GOF}* ureters at E12.5 (Fig 4E-4G). Incorporation of LysoTracker (DND-99), a chromogenic marker for programmed cell death [19], into whole E11.5 explants after 1 day of culture indicated absence of apoptotic cells in the entire ureteric mesenchyme, with the lateral aspect of *Smo^{GOF}* explants being most prominently affected (Fig 4H and 4I).

Part 3 - SHH signaling in ureter development

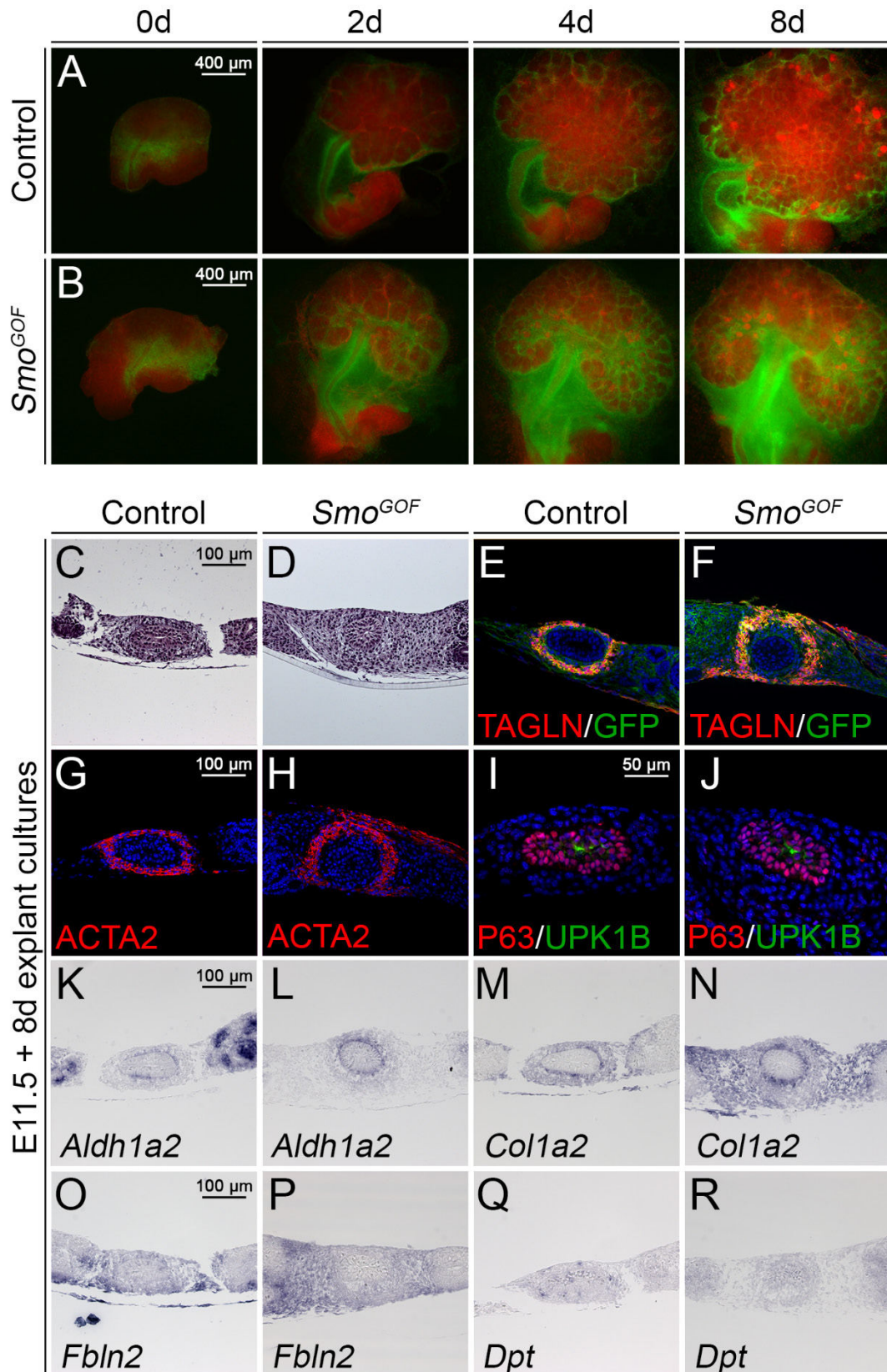


Figure 3: Conditional activation of *Smo* in the ureteric mesenchyme leads to mesenchymal hyperplasia but normal tissue patterning and differentiation. (A,B) GFP/RFP epifluorescence in E11.5 kidney/ureter explants of *Tbx18^{cre/+};R26^{mTmG/+}* (control) and *Tbx18^{cre/+};R26^{mTmG/SmoM2}* (*Smo*^{GOF}) embryos after 0, 2, 4 and 8 d of culture. (C-R) Analysis of proximal sections of ureter explants of E11.5 wildtype and *Tbx18^{cre/+};R26^{mTmG/SmoM2}* embryos cultured for 8 d by Hematoxylin and Eosin staining (C,D), immunofluorescence of SMC markers TAGLN and ACTA2 (E-H) and urothelial markers Δ NP63/UPK1B (I,J), and *in situ* hybridization analysis of fibroblast markers *Aldh1a2*, *Col1a2*, *Fbln2*, *Dpt* (K-R).

Moreover, mesenchyme mechanically separated from the ureteric epithelium and cultured for 6 days in the presence of 2 μM of the SMO agonist purmorphamine [20] survived while DMSO treated control explants disappeared (Fig 4J and 4K).

These experiments show that tissue hyperplasia after mis- and overactivation of HH signaling in the ureteric mesenchyme is caused by a combination of reduced cell death in adventitial precursors and increased cell proliferation in SMC progenitors and the epithelial compartment.

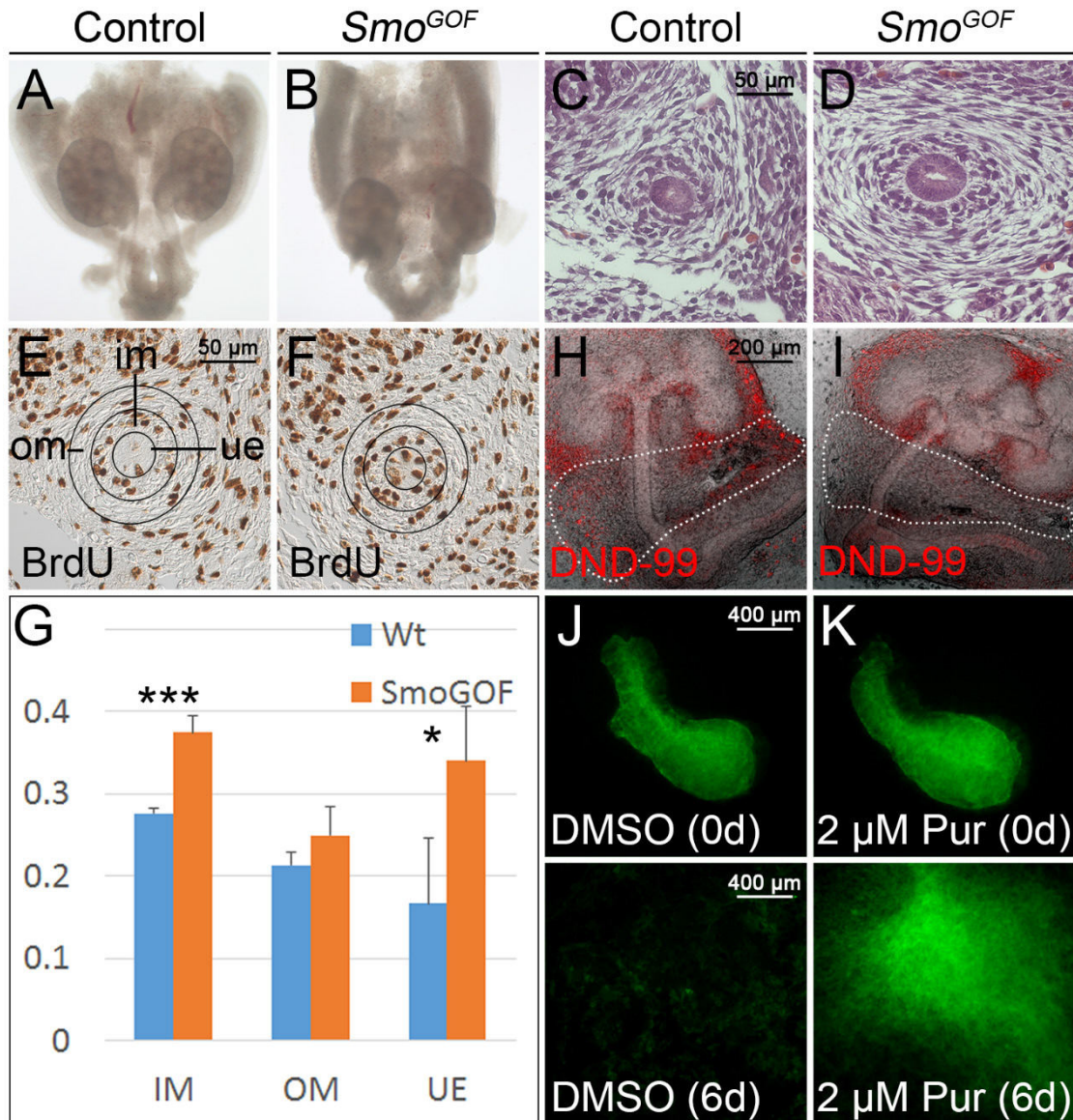


Figure 4: HH signaling is sufficient to maintain survival and proliferation of the ureteric mesenchyme. (A,B) Morphology of whole urogenital systems of wildtype (control) and *Tbx18^{cre/+};R26^{mTmG/SmoM2}* (*Smo^{GOF}*) embryos at E12.5. (C,D) Hematoxylin and Eosin staining on transverse sections of the proximal ureter at E12.5. (E,F) Determination of cellular proliferation by the BrdU incorporation assay on transverse sections of the proximal ureter at E12.5. Black circles in E and F mark the epithelium (ue) and the inner (im) and outer (om) mesenchymal compartments of the ureter that were analyzed to quantify proliferation. (G) Quantification of BrdU-positive cells. E12.5 (n=4), wildtype versus mutant: IM, 0.276±0.006 vs 0.375±0.020, P=0.0001; OM, 0.214±0.015 vs 0.250±0.034, P=0.0966; UE, 0.167±0.080 vs 0.341±0.066, P=0.0211. Values are displayed as mean ± sd. *, P≤0.05; ***, P≤0.001 two-tailed Student's t-test. (H,I) Analysis of cell death by Lysotracker (DND-99) incorporation of E11.5 control and *Smo^{GOF}* explants after 1 day of culture. (J,K) GFP epifluorescence of E12.5 *Tbx18^{cre/+};R26^{mTmG/+}* ureteric mesenchyme that was mechanically separated from the ureteric epithelium and cultured for 6 days with DMSO or 2 μM Purmorphamine (Pur).

A number of genes critical for ureteric SMC differentiation completely or partially depend on HH signaling

In order to analyze molecular changes that may have caused the defective differentiation of SMCs after abrogation of SHH signaling in the ureteric mesenchyme, we screened expression of a panel of genes that have been implicated in the early development of the ureteric mesenchyme and the initiation of the SMC program [5], by *in situ* hybridization analysis on sections of both *Smo^{LOF}* and *Smo^{GOF}* ureters (Fig 5).

In E12.5 wild-type ureters, *Ptch1*, a direct target of HH signaling [21], *Bmp4*, *Tshz3*, *Tcf21*, *Tbx18* and *Sox9* were expressed throughout the mesenchymal compartment with increased levels in cells adjacent to the epithelium. Expression of the target of canonical WNT signaling, *Axin2* {Jho, 2002 #36}, was confined to the inner mesenchymal region. Expression of *Ptch1*, a transcriptional target of HH signaling [21], was completely lost in *Smo^{LOF}* ureters and expanded at high levels to the outer mesenchymal region in *Smo^{GOF}* ureters, confirming the suitability of our HH inactivation and misexpression approaches. *Bmp4* expression was lost in *Smo^{LOF}* ureters, and increased in the inner mesenchymal ring in *Smo^{GOF}* ureters. Expression of *Axin2* was not affected by either condition. *Tshz3*, *Tcf21*, *Tbx18* and *Sox9* exhibited reduced expression in the ureteric mesenchyme in *Smo^{LOF}* ureters, and were weakly expanded to the outer mesenchymal domain in *Smo^{GOF}* ureters. In E14.5 *Smo^{LOF}* ureters, expression of *Ptch1* and *Bmp4* was lost while expression of *Axin2*, *Tshz3*, *Tcf21*, *Tbx18* and *Sox9* was maintained at low levels in the inner mesenchymal region (Fig 5). Together, these assays show that HH signaling is required but not sufficient to induce *Bmp4* expression in the ureteric mesenchyme. Other genes relevant for SMC differentiation including *Tcf21*, *Tbx18*, *Tshz3* and *Sox9* partially depend on HH signaling, while canonical WNT signaling acts upstream or in parallel to this pathway in the ureteric mesenchyme.

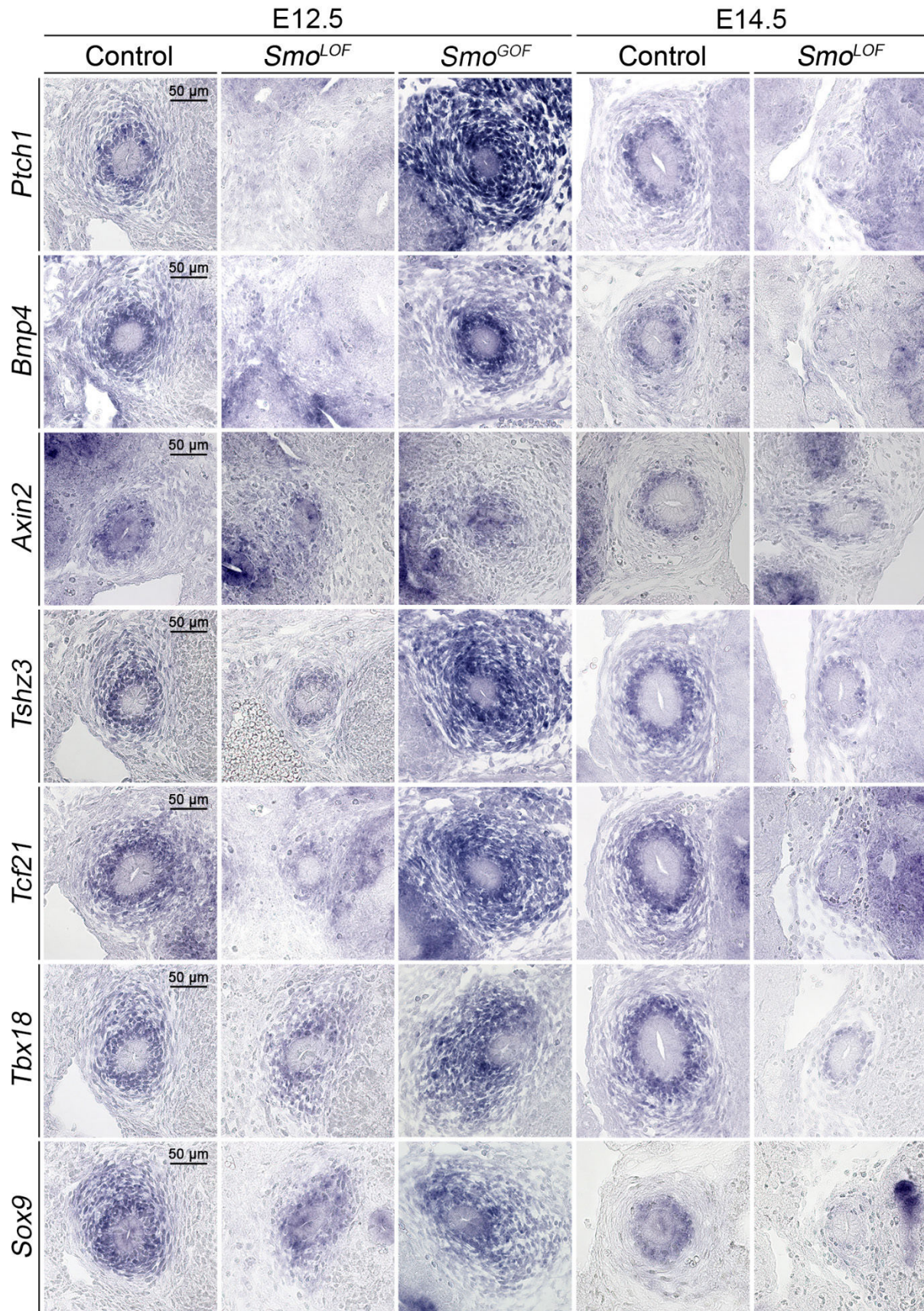


Figure 5: Molecular characterization detects altered marker expression in the *Smo*^{LOF} and *Smo*^{GOF} ureteric mesenchyme. RNA *in situ* hybridization analysis on transverse sections of the proximal ureter region of control, *Smo*^{LOF} and *Smo*^{GOF} embryos at E12.5, and of control and *Smo*^{LOF} embryos at E14.5.

Foxf1 is a target of HH signaling in the ureteric mesenchyme

To get further insight into the spectrum of genes controlled by HH signaling in the ureteric mesenchyme, we wished to determine the global transcriptional changes caused by inhibition of the pathway in the ureter. Rather than comparing mutant (*Smo^{LOF}*) and wildtype ureters, we deemed that pharmacological inhibition of HH signaling by the SMO antagonist cyclopamine [22, 23] in ureter explant cultures would provide a better handle to identify primary transcriptional changes. Treatment of E12.5 ureters with 10 μ M cyclopamine led to a robust downregulation of expression of the direct target of HH signaling *Ptch1* in the ureteric mesenchyme (S1 Fig). Moreover, administration of 10 μ M cyclopamine to E11.5 kidney/ureter explants for 2 days led to a complete loss of ureteric SMC differentiation after 8 days of culture while inhibition in later time intervals left this differentiation program unaffected (S2 Fig). Since these findings delimited the requirement of HH signaling in the ureteric mesenchyme to E11.5 to E13.5, we decided to treat E12.5 ureters with 10 μ M cyclopamine for 18 h to perform microarray profiling of differential gene expression with untreated controls.

Using an intensity threshold of 150, we identified in two independent pools of treated and untreated ureters a small set of 20 genes that were consistently more than 2-fold downregulated and only one gene that was upregulated in expression in cyclopamine treated ureters (Fig 6A and S1 Table). Among the downregulated transcripts were the three *bona fide* SHH target genes *Hhip* (-11.9x), *Ptch1* (-3.2x) and *Gli1* (-2.3x), confirming the specificity of our assay [21, 24-27]. Another group of prominently downregulated transcripts comprised three members of the forkhead transcription factor family, *Foxf1* (-5.3x), *Foxl1* (-3.9x) and *Foxf2* (-3.3x), which have been reported to be primary SHH target genes in several other contexts [28-30] (Fig 6B). Interestingly, we did not find *Tcf21*, *Tshz3*, *Tbx18* and *Bmp4* in the list of top-downregulated genes suggesting that their change in expression in *Smo^{LOF}* ureters is secondary in nature. To validate our microarray results and determine the spatial expression of selected candidates we performed *in situ* hybridization analysis on proximal sections of E12.5 control *Smo^{LOF}* and *Smo^{GOF}* and of E14.5 control and *Smo^{LOF}* ureters (Fig 6C and S3 Fig). *Hhip* expression was barely detectable at E12.5 and E14.5 in the ureteric mesenchyme of wildtype embryos but was abrogated in *Smo^{LOF}* and weakly induced in *Smo^{GOF}* ureters. *Gli1* was strongly expressed in the entire ureteric mesenchyme at E12.5 in the control and completely lost in *Smo^{LOF}* and induced in *Smo^{GOF}* ureters. At E14.5, the expression in the inner mesenchymal compartment was HH signaling-dependent whereas outer mesenchymal cells expressed normal levels of *Gli1*. *Foxf1* expression

was detectable at E14.5 in the inner mesenchymal compartment of wildtype embryos. Expression was completely lost in *Smo^{LOF}* ureters at this stage but was not induced in *Smo^{GOF}* ureters at E12.5. Expression of *Ddit4l* (-3.2x) and *Avpr1a* (-2.5x) was detected in the inner mesenchymal compartment of controls at E12.5, and was down-regulated in *Smo^{LOF}* but not induced in *Smo^{GOF}* ureters (Fig 6C). The sensitivity of the method was not sufficient to detect expression of *Foxl1*, *Foxf2*, *Crym*, *Ndp* and *Wif1* (S3 Fig). Together, these assays identify *Foxf1*, *Ddit4l* and *Avpr1a* as novel targets of SHH signaling in the ureteric mesenchyme.

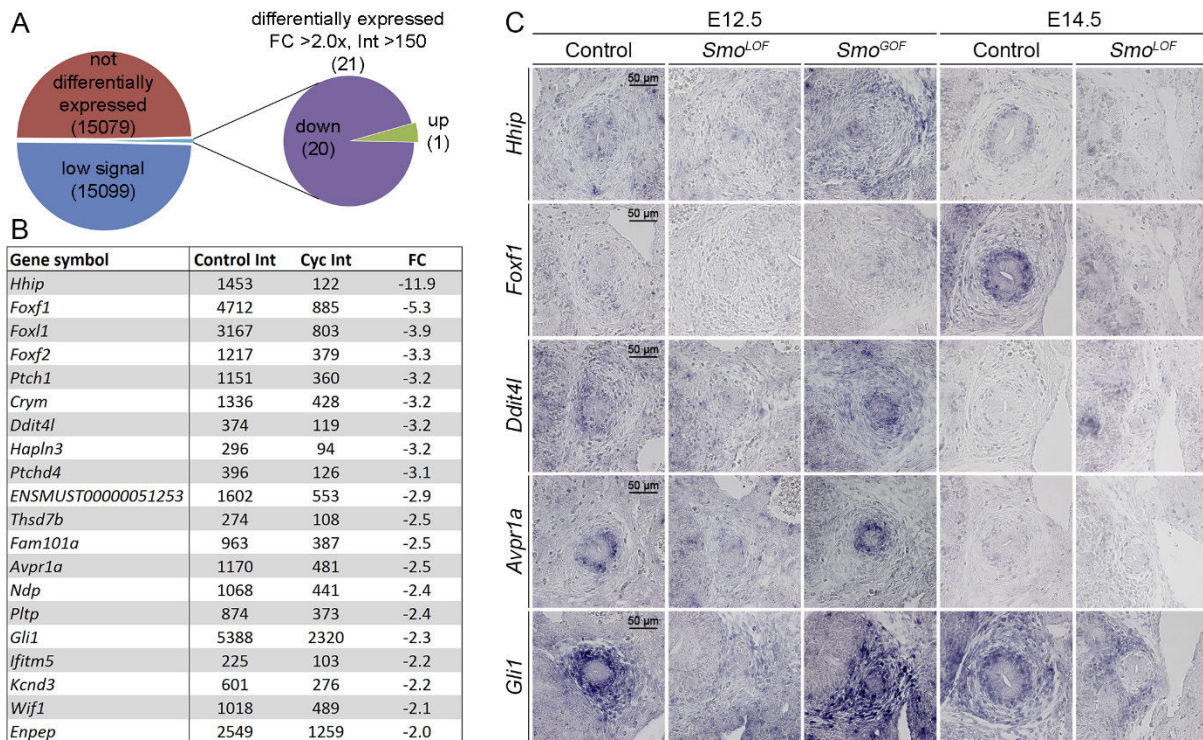


Figure 6: Microarray analysis detects transcriptional changes after loss of HH signaling in the ureteric mesenchyme. (A) Pie-chart summarizing the results from the microarray analysis of E12.5 ureters explanted and treated with DMSO or 10 μ M cyclopamine for 18 h filtered with an intensity (Int) threshold of 150 and a fold change (FC) cut-off of 2.0. (B) Table of the downregulated transcripts. Shown are average intensities of transcripts in control and cyclopamine treated ureters and average fold changes (FC) of RNA intensities between the pools in two independent experiments. (C) *In situ* hybridization analysis of expression of microarray candidates on proximal ureter sections of control, *Tbx18^{cre/+}; Smo^{fl/fl}* (*Smo^{LOF}*) and *Tbx18^{cre/+}; R26^{mTmG}/SmoM2* (*Smo^{GOF}*) ureters at E12.5 and E14.5.

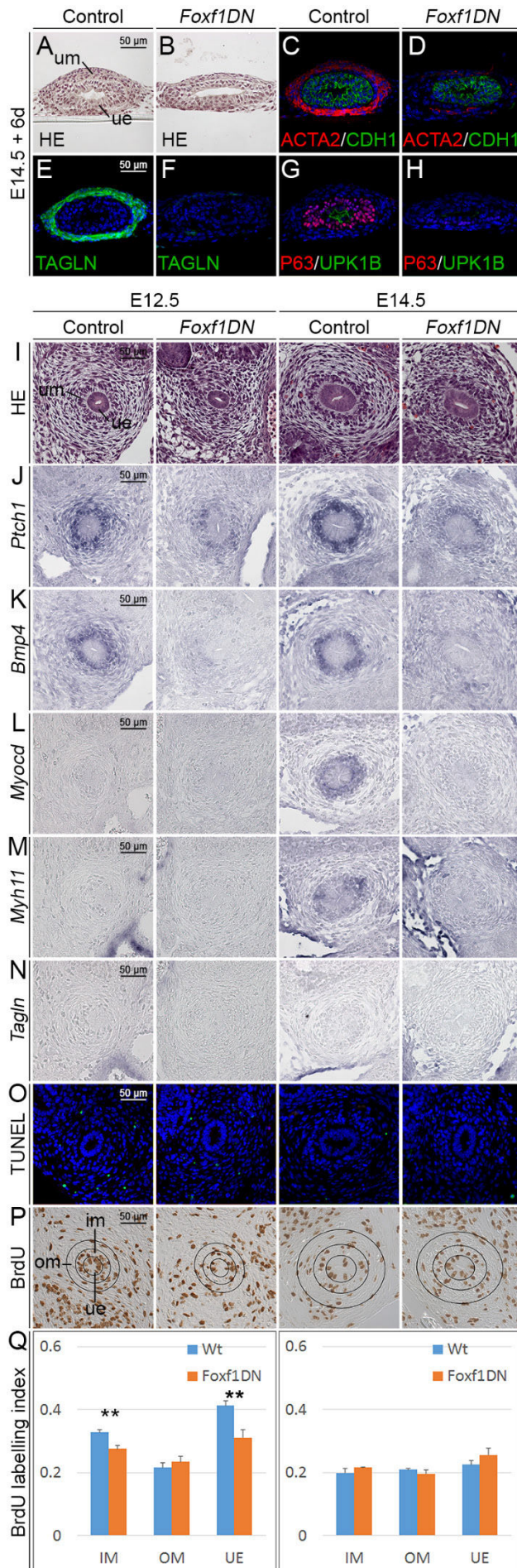
Foxf1 is required for proliferation and cell differentiation in the developing ureter

Previous work identified prominent functions for *Foxf1* and *Foxf2* as targets of epithelial SHH signals in SMC differentiation of the intestinal mesenchyme [29]. Given that *Foxf1* is expressed in the ureteric mesenchyme at E14.5, i.e. prior to the onset of SMC and S-cell differentiation, we wondered whether this transcription factor mediates part of the function of HH signaling in these programs in the ureteric mesenchyme. To test this hypothesis, we used a conditional *Cre/loxP*-based transgenic approach to misexpress a dominant negative version of FOXF1 in the ureteric mesenchyme *in vivo*. We deemed such a strategy more efficient than a conditional knockout considering the possible redundancy of *Foxf1* and *Foxf2*. We generated the dominant negative version of FOXF1 by fusing the open reading frame of this transcriptional activator to a cDNA fragment harboring the strong transcriptional repression domain of the *Drosophila* ENGRAILED (ENG) protein [31, 32]. This coding region was followed by a fragment encoding an IRES-GFP sequence to allow visualization of misexpressing cells. The bicistronic transgene-cassette was integrated in the ubiquitously expressed X-chromosomal Hypoxanthine guanine phosphoribosyl transferase (*Hprt*) locus (*Hprt^{Foxf1DN}*) [33, 34]. Transgene expression was driven by the *Tbx18^{cre}* line. Due to random X-chromosome inactivation, female *Tbx18^{cre/+};Hprt^{Foxf1DN/+}* embryos possessed a mosaic expression. Male *Tbx18^{cre/+};Hprt^{Foxf1DN/y}* (*Foxf1DN*) embryos expressed the transgene in a uniform manner and were subsequently used for phenotypic analysis.

Since *Foxf1DN* embryos died shortly after E14.5, we explanted E14.5 control and *Foxf1DN* ureters and cultured them for 6 days to assess tissue integrity and terminal differentiation. Hematoxylin and eosin staining of sections demonstrated mesenchymal hypoplasia and a reduction of the urothelium from three to two cell layers in cultured *Foxf1DN* ureters (Fig 7A and 7B). Immunofluorescence analysis revealed a strong reduction of TAGLN and ACTA2 expression and absence of Δ NP63/UPK1B indicating severely compromised mesenchymal and epithelial cell differentiation in *Foxf1DN* ureters at this stage (Fig 7C-7F).

To characterize the onset of these phenotypical changes, we analyzed earlier embryonic stages of *Foxf1DN* ureters. Hematoxylin and eosin stainings at E12.5 and E14.5 revealed no dramatic effects on overall tissue size in the epithelial and mesenchymal compartments of the mutant ureter. However sub-division of the ureteric mesenchyme into inner cuboidal SMC precursors and outer spindle shaped adventitial fibrocytes appeared less clear (Fig 7I).

Part 3 - SHH signaling in ureter development



Part 3 - SHH signaling in ureter development

Expression of the HH target gene *Ptch1* was strongly reduced in the inner mesenchymal region at E12.5 and E14.5 indicating a possible role of FOXF1 as a feed-back activator of SHH signaling (Fig 7J). Strikingly, *Foxf1* was required to maintain *Bmp4* expression at E12.5 and E14.5, suggesting that *Foxf1* mediates *Bmp4* expression downstream of HH signaling (Fig 7K). *Tshz3*, *Tcf21*, *Tbx18* and *Sox9* that only partially depend in their expression on HH signaling, were normally expressed in *Foxf1DN* mutants, as was *Axin2* (S4 Fig). Importantly, SMC differentiation as analyzed by *Myocd*, *Myh11* and *Tagln* expression was not initiated in *Foxf1DN* ureters at E14.5 (Fig 7L-7N). Apoptosis in the ureter was not changed at either stage while proliferation in the inner mesenchymal region and the epithelium was reduced at E12.5 in *Foxf1DN* embryos (Fig 7O-7Q). We conclude that FOXF1 acts upstream of *Bmp4*, and is required to mediate the proliferation and differentiation but not the survival function of HH signaling in the ureteric mesenchyme.

FOXF1 suffices to induce the ureteric differentiation program downstream of HH signaling

To stringently test which of the various cellular function of HH signaling in the ureter is mediated by FOXF1, we wished to restore *Foxf1* expression in ureter explants in which HH signaling was abolished by administration of cyclopamine. For this purpose, we employed the *Hprt* strategy again to generate an allele for conditional misexpression of *Foxf1* (*Hprt^{Foxf1}*). Since *Tbx18^{cre/+};Hprt^{Foxf1/y}* male embryos showed early embryonic lethality prior to the onset of kidney development at E10.5, we used an inducible *Axin2^{creERT2}* line that mediates recombination specifically in the inner mesenchymal domain of the ureter [4]. *Axin2^{creERT2/+};Hprt^{Foxf1/y}* ureters explanted at E12.5 and cultured for 3 days in the presence of 500 nM 4-Hydroxy-Tamoxifen showed robust expression of *Foxf1* in the inner mesenchymal region and restored *Bmp4* expression after cyclopamine treatment proving the suitability of our approach (S5 Fig). E12.5 *Axin2^{creERT2/+};Hprt^{Foxf1/y}* ureters cultured for 6 days in the presence of 500 nM 4-Hydroxy-Tamoxifen with or without 10 μ M cyclopamine were morphologically indistinguishable from wildtype controls indicating that reconstitution of *Foxf1* expression was not able to alleviate cyclopamine induced tissue hypoplasia in this setting (Fig 8A). However, SMC differentiation as analyzed by ACTA2 and TAGLN expression and urothelial differentiation as analyzed by Δ NP63 and UPK1B expression was rescued in cyclopamine treated *Axin2^{creERT2/+};Hprt^{Foxf1/y}* explants, indicating that FOXF1 controls these differentiation programs downstream of HH signaling (Fig 8B-8D).

Part 3 - SHH signaling in ureter development

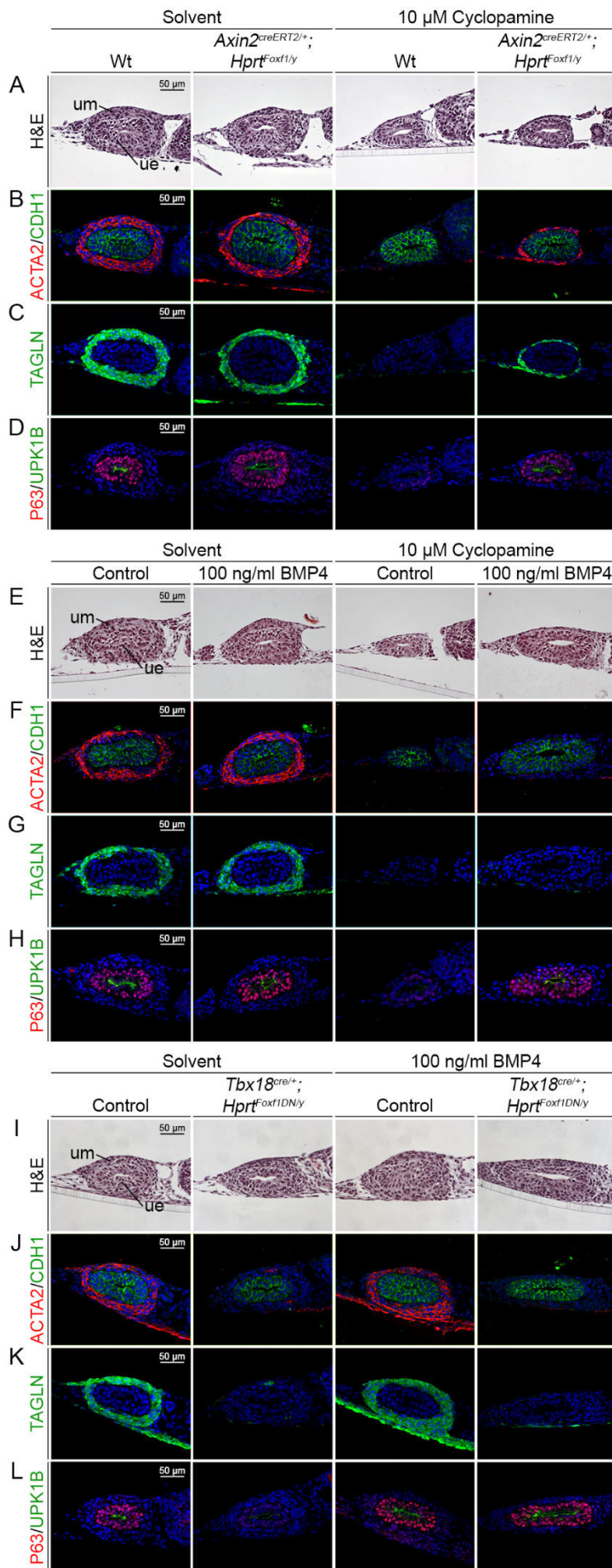


Figure 8: Analysis of the epistatic relations of HH signaling, FOXF1 and BMP4 in cytodifferentiation of the ureter. (A-L) Analysis of proximal sections of ureters explanted from E12.5 wildtype, *Axin2^{creERT2/+}; Hprt^{Foxf1/y}* or *Tbx18^{cre/+}; Hprt^{Foxf1DN/y}* embryos and cultured for 6 d in the presence or absence of 10 μ M cyclopamine and/or 100 ng/ μ l BMP4 or solvent by Hematoxylin and Eosin staining (A,E,I), by immunofluorescence (B-D,F-H,J-L) for the SMC markers ACTA2 and TAGLN with the epithelial marker CDH1 (B,C,F,G,J,K), and for the urothelial markers Δ NP63/UPK1B (D,H,L).

Part 3 - SHH signaling in ureter development

To investigate whether this effect was solely mediated by FOXF1-dependent BMP4, we cultured E12.5 ureters for 6 days with or without 100 ng/ml BMP4 and 10 μ M cyclopamine. Interestingly, BMP4 was able to reduce cyclopamine-induced epithelial and mesenchymal hypoplasia and to completely restore epithelial differentiation. However, it was not sufficient to induce SMC differentiation (Fig 8E-8H). Similarly, BMP4 administration to E12.5 *Tbx18^{cre/+};Hprt^{Foxf1DN/y} (Foxf1DN)* explants did not rescue SMC differentiation but restored urothelial differentiation after 6 days of culture (Fig 8I-8L).

We conclude that FOXF1 is required and sufficient to induce SMC and urothelial differentiation downstream of HH signaling. BMP4 controls epithelial and mesenchymal growth as well as urothelial differentiation downstream of FOXF1 but is on its own not sufficient to induce the SMC program (Fig 9).

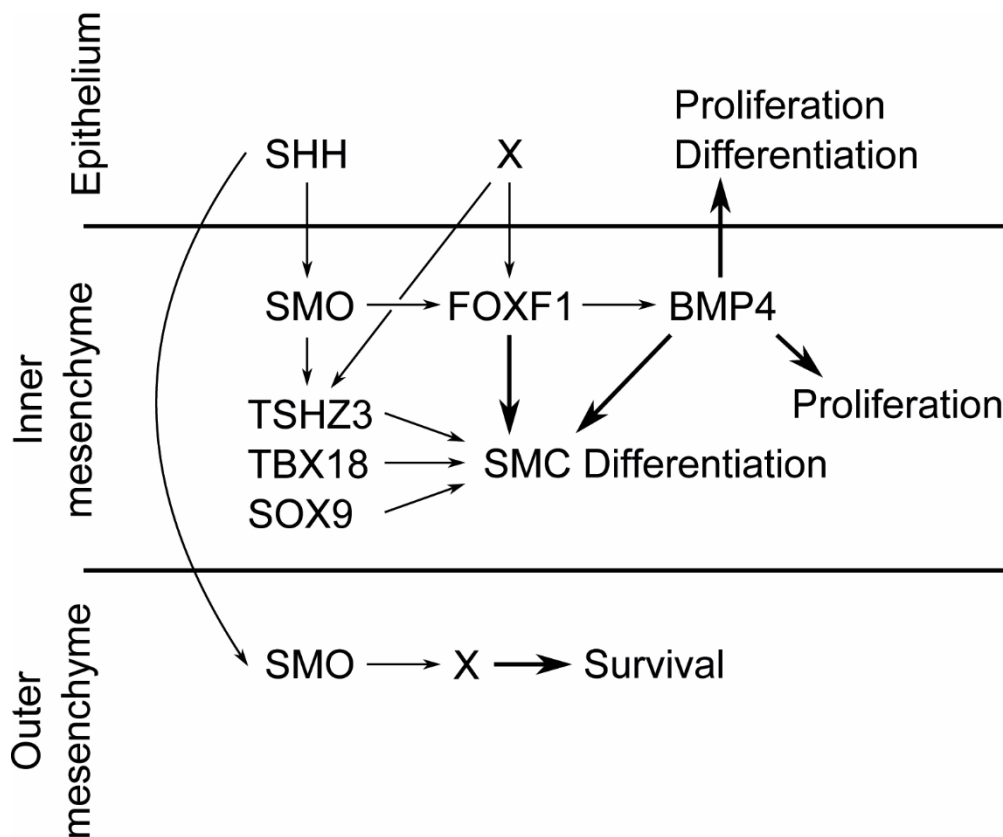


Figure 9: Model of how SHH and HH signaling direct various cellular programs in early ureter development. SHH is secreted from the ureteric epithelium and activates in the mesenchyme a SMO-dependent signaling pathway that induces expression of *Foxf1* in the inner mesenchymal domain. FOXF1, in turn activates expression of *Bmp4*. BMP4 regulates mesenchymal and epithelial proliferation, and epithelial differentiation. SMC differentiation depends both on *Bmp4* and *Foxf1*, and gets additional input from other transcription factors including TBX18, TSHZ3 and SOX9. Note that *Foxf1* as well as these other transcription factor genes require an additional (epithelial) signaling input to upregulate and confine them to the inner mesenchymal domain. SMO-mediated HH signaling also directs cell survival in the outer mesenchymal domain but this activity is independent of *Foxf1*.

Discussion

SHH has previously been characterized as an essential epithelial signal for proliferation and SMC differentiation of mesenchymal cells in the ureter. Here, we provided genetic evidence that mesenchymal HH signaling controls proliferation and differentiation both in the inner region of the mesenchyme as well as in the ureteric epithelium, and that these programs are relayed by a FOXF1-BMP4 module. HH signaling also regulates survival of outer mesenchymal cells, which however employs other effector genes. We conclude that SHH is the crucial signal for coordinated tissue growth and cell differentiation in early ureter development (Fig 9).

HH signaling promotes coordinated proliferation and differentiation of mesenchymal and epithelial progenitors in the ureter

It was previously reported that global or conditional loss of *Shh* in the ureteric epithelium leads to reduced mesenchymal proliferation and delayed SMC differentiation [8, 11]. Our study showed that deletion of HH signaling in the mesenchymal compartment leads to a reduction of proliferation rates in the inner mesenchymal region at E12.5 and to a failure to initiate SMC differentiation at E14.5. Together, these studies argue that epithelial SHH regulates in a paracrine fashion the proliferation and SMC differentiation of adjacent mesenchymal cells. The difference in the severity of SMC defects in the conditional loss-of-function models may derive from variable efficiency of cre recombination or different genetic backgrounds. Alternatively, it may indicate that other HH family members provide a minor but relevant input to SMO-mediated signaling in the ureter. A paradigm for this is found in the intestinal epithelium where SHH and IHH cooperatively signal to the underlying mesenchyme [35, 36].

Misexpression of a constitutively active form of SMO in the entire ureteric mesenchyme resulted in increased cell proliferation in the inner mesenchymal region and the epithelium indicating that the level of SHH is a limiting factor in this program. However, it did not result in ectopic or enhanced SMC differentiation in the outer mesenchymal layer. Together with our recent finding that loss of canonical WNT signaling in the ureteric mesenchyme abrogates the SMC investment of the ureter [10], it seems plausible that initiation of SMC differentiation depends on the combinatorial input of both epithelial SHH and WNT signals and that the short range signaling activity of the latter is decisive to restrict the program to mesenchymal cells

Part 3 - SHH signaling in ureter development

adjacent to the ureteric epithelium. WNT signals may also impinge on mesenchymal proliferation since proliferation rates were reduced but not stalled in mice with mesenchyme specific loss of both WNT and HH signaling in the ureter [10].

In contrast to previous studies [8, 11], we also analyzed the consequence of abrogation of HH signaling for epithelial development. To our excitement, we found that proliferation and differentiation of the epithelial compartment was similarly affected than that of the mesenchyme; proliferation was reduced at E12.5 and epithelial differentiation was not initiated at E14.5 resulting in epithelial hypoplasia and a complete lack of urothelial cell types at E18.5. While it is possible that epithelial SHH uses paracrine and autocrine signaling pathways to regulate proliferation rates in the mesenchyme and epithelium, respectively, our approach to manipulate the signaling pathway in the mesenchyme disfavors an autocrine mode of HH signaling and rather suggests that mesenchymal HH signaling uses a relay signal to affect epithelial cell cycle progression and differentiation.

Since cell density and cell number can affect cellular differentiation programs [37], the argument may arise that epithelial and mesenchymal differentiation defects are secondary to the severe hypoplasia found in *Smo*-deficient ureters. However, our genetic rescue experiments showed robust SMC and urothelial differentiation despite massive mesenchymal hypoplasia, indicating that HH controlled cell differentiation is a direct and cell-autonomous process that does not rely on cell number.

All in all, our data suggest that SHH and HH signaling play a much more crucial role in early ureter development than previously thought, namely by directing and coordinating proliferation and differentiation of the mesenchymal and epithelial tissue compartments required for elongation and functionality of this simple tube.

HH signaling employs a FOXF1-BMP4 module to mediate mesenchymal and epithelial proliferation and differentiation programs in the ureter

The three Forkhead transcription factor genes *Foxf1*, *Foxl1* and *Foxf2* are expressed in numerous sites of the embryo including the foregut, the lung, the vessels and the palate adjacent to sources of SHH protein [38-41]. HH-dependency of these expression domains and the presence of GLI1 binding sites in the regulatory regions of *Foxf1* and *Foxl1* characterized these genes as direct targets of HH signaling [30, 40, 42]. Individual or combined loss of *Foxf1*, *Foxf2* and *Foxl1* in these organs system led to severe defects that are characterized by tissue hypoplasia and cell immaturity [29, 30]. These defects, at least in some organs, resemble those of mice

with loss of SHH and/or IHH, arguing that these FOX proteins are downstream mediators of HH signaling [35, 41, 43, 44]. Similarly, an intricate relationship was reported between HH and BMP signaling. *Hh* and *Bmp* genes are coexpressed at many diverse sites of cell-cell interaction in the mouse embryo and similar phenotypes of mutant mice suggest the existence of a HH-BMP signaling relay [45, 46]. Which aspects and to what extent FOX and BMP proteins mediate HH signaling at these embryonic sites has, however, remained unclear.

Here, we showed that *Foxf1* is expressed in the ureteric mesenchyme and that this expression depends on HH signaling. Intriguingly, *Foxf1* expression was upregulated at E14.5, i.e. shortly before the onset of SMC and epithelial differentiation while mesenchymal HH signaling is present from at least E11.5 onwards in the ureteric mesenchyme. Together with the observation that ectopic HH signaling (i.e. activated SMO) in the outer mesenchymal region is not sufficient to induce *Foxf1* in this domain, this argues that *Foxf1* expression requires a critical second input from the epithelial compartment around E13.5. Alternatively, a mesenchymal activity may counteract HH activation of *Foxf1* expression until that stage. Conditional misexpression of a variant of FOXF1 encoding a strong transcriptional repressor in the ureteric mesenchyme completely recapitulated the proliferation and differentiation defects of *Smo* loss-of-function mutants in the inner mesenchymal domain and the epithelium of the developing ureter. Moreover, mesenchymal expression of FOXF1 partially ameliorated tissue hypoplasia and completely rescued the mesenchymal and epithelial differentiation defects in cyclopamine treated ureters arguing together that FOXF1 is the crucial and unique mesenchymal mediator of inputs from SHH and other epithelial signals in the control of these cellular programs. Our molecular analyses showed that expression of *Tbx18*, *Sox9* and *Tshz3*, genes previously implicated in SMC differentiation in the ureteric mesenchyme partially depend on HH signaling but not on *Foxf1* arguing that they act in parallel to *Foxf1* in this program. Reduced expression of *Ptch1* in *Foxf1*^{DN} ureters points to a role for FOXF1 as a feed-back activator of HH signaling.

Our molecular analyses have shown that expression of *Bmp4* in the ureteric mesenchyme strictly depends on HH signaling and FOXF1 activity in this tissue. While the function of BMP4 in the control of cell proliferation has remained unclear, a number of studies have indicated that abrogation of BMP4 activity compromises SMC and S-cell differentiation in the ureter [8, 9, 47, 48]. Our rescue experiment provided clear evidence that BMP4 or a similar BMP activity acts downstream of HH signaling and FOXF1 activity to mediate the pro-proliferative function in both tissue compartments as well as induce epithelial differentiation. While FOXF1 rescued the SMC defect of HH signaling mutants, BMP4 did not, suggesting that BMP4 can only mediate parts of the *Foxf1* function in this program. Together, we identified a SHH-FOXF1-BMP4

Part 3 - SHH signaling in ureter development

axis controlling proliferation and differentiation in the mesenchymal and epithelial tissues of the ureter.

SHH-FOXF1-BMP4 and human congenital renal anomalies

Given the requirement of the SHH-FOXF1-BMP4 regulatory axis for SMC differentiation in the ureter and the severity of the hydroureter formation associated with their complete or partial loss in the mouse, it is obvious that the components of this axis represent candidate genes for human congenital anomalies of the kidney and urinary tract (CAKUT). In fact, heterozygous loss-of-function mutations in *BMP4* and *GLI* transcription factor genes have been identified in patients with ureter anomalies, and hypo- and dysplastic kidneys [49, 50]. Since these genes are expressed and required in numerous embryonic programs, renal defects are often associated with a whole spectrum of other organ malformations. The VATER/VACTERL association describes such a combination of congenital anomalies including vertebral defects, anorectal malformations, cardiac defects, tracheoesophageal fistula with or without esophageal atresia, renal malformations, and limb defects. Given that loss of HH signaling in mice recapitulates the spectrum of VATER/VACTERL phenotypes [51], and that *Foxf1* is a functional target of HH signaling in most of the effected organ systems including the urinary tract as shown here, points to the relevance *FOXF1* as an attractive candidate gene for at least a subset of VATER/VACTERL cases. Targeted sequencing in 123 patients with VATER/VACTERL or VATER/VACTERL-like phenotype detected a *FOXF1* *de novo* mutation in one patient. *In situ* hybridization analyses in mouse embryos identified *Foxf1* expression in the development of most VATER/VACTERL organ systems except the urinary tract [52], questioning the significance of mutations in *FOXF1* for renal disease manifestations [53]. With our finding that *Foxf1* is expressed and functionally required in ureter development in the mouse, the gene is back on the list of candidates for the VATER/VACTERL association of phenotypic changes.

HH signaling promotes survival of mesenchymal progenitor cells in the developing ureter in a FOXF1-independent fashion

Our study found that conditional deletion of the unique HH signal transducer *Smo* in the ureteric mesenchyme results in a massive increase of programmed cell death in the outer mesenchymal domain at E12.5, and severe ureter hypoplasia from E14.5 onwards. Moreover, expression of a

conditionally activated form of SMO completely abolished apoptosis in the lateral mesenchymal domain at E11.5 and led to massive tissue hyperplasia of this region from which adventitial fibrocytes normally arise. Importantly, pharmacological activation of SMO was sufficient to trigger survival of isolated ureteric mesenchyme. Together, these findings demonstrate that HH signaling is required and sufficient to maintain cell survival in the outer region of the undifferentiated ureteric mesenchyme.

It is interesting to note that this domain of cells is relatively distant from the source of SHH signals in the ureteric epithelium. It is therefore possible that HH signaling occurs here in a ligand-independent fashion as previously found in other biological contexts [54, 55]. Alternatively, SHH may act as a long-range signal similarly to the situation reported for the ventral spinal cord where notochord- and floorplate-derived SHH controls cell survival at a distance [56]. Strong support for the second possibility is provided by two findings. First, tissue separation and recombination experiments demonstrated that survival of mesenchymal tissues in the developing urinary system relies on epithelial signals [7, 10, 16]. Second, mice with a conditional or global deletion of *Shh* from the ureteric epithelium also exhibited a severe thinning of the epithelial and mesenchymal tissue compartments [8, 11]. The finding that tissue hypoplasia in these mutants appeared less severe compared to our approach can be due to different genetic backgrounds or different cre activities in the conditional approaches, while the reported lack of apoptosis may simply reflect the fact that analysis was performed at E14.5 and not E12.5 as in our study.

While our functional experiments provided compelling evidence that FOXF1 mediates the proliferation and differentiation function of HH signaling in the ureter, it seems unlikely that this or other Forkhead factors also account for the anti-apoptotic activity of this pathway in the outer mesenchymal domain. First, *Foxf1*, *Foxf2* and *Foxl1* were not detectably expressed in the ureteric mesenchyme at E11.5 to E12.5 when this HH activity occurs. Second, apoptosis of outer mesenchymal cells was not detected in mutants with expression of the repressor version of FOXF1 in the ureteric mesenchyme. Third and most importantly, FOXF1 was not sufficient to rescue tissue hypoplasia after abrogation of HH signaling.

Exogenous BMP4 at least partly rescued tissue hypoplasia of cyclophamide treated ureters. Since the phenotypic consequences of the complete loss of *Bmp4* in the ureter have only been poorly analyzed, and *in vitro* studies provided conflicting results on pro- or anti-apoptotic activities in the ureter and kidney [47], it remains unclear whether BMP4 contributes to the cell survival in outer mesenchymal cells [8, 9, 57, 58]. In other developmental contexts (e.g. the spinal cord) it was shown that HH signaling directly regulates the expression of the anti-apoptotic gene *Bcl2*

Part 3 - SHH signaling in ureter development

[56]. Our microarray analysis showed that *Bcl2* is slightly reduced upon cyclopamine treatment of ureter explants (S1 Table) making it a possible contributor of the pro-survival role of HH signaling. We detected strong reduction of expression of *Ddit4l* whose homologue DDIT4 in at least some biological contexts was reported to exert an anti-apoptotic function [59, 60] making it another candidate for this function.

While molecular mediators of the anti-apoptotic function of HH signaling in the early ureteric mesenchyme are currently unresolved, the tight spatial and temporal regulation of this activity may be instrumental in defining the size of adventitial precursor pool as well as severing the ureter from the kidney. In any case, the finding that HH signaling suffices to maintain ureteric mesenchymal cells *in vitro*, may open avenues for easier manipulation of these progenitors in the future.

Materials and methods

Generation of *Hprt^{Foxf1}* and *Hprt^{Foxf1DN}* alleles

The *Foxf1* open reading frame was PCR-amplified from cDNA with primer pairs Foxf1-for (*NheI*) ATG CAC TAG TAT GTC CGC GCC CGA CAA GC and Foxf1-rev (*NdeI*) ATG CCA TAT GTC ACA TCA CAC ACG GCT TGA TG or Foxf1 Δ Stop-rev (*NdeI*) ATG CCA TAT GCA TCA CAC ACG GCT TGA TG with the latter introducing a mutated stop codon. A DNA fragment encoding the engrailed repressor domain (ENG) was PCR-amplified from the *pCS2⁺.Engrailed* plasmid [32] with primer pairs Eng-for (*NdeI*) GAG ACA TAT GGC CCT GGA GGA TCG C and Eng+Stop-rev (*NdeI*) GAG ACA TAT GCT AGA GGC TCG AGA GGG ATC C. Restriction sites introduced via primers were used to insert PCR products into *NheI-NdeI* sites of a shuttle vector containing *IRES-GFP* to generate *FOXF1-IRES-GFP* (for *Hprt^{Foxf1}*) and *FOXF1ENG-IRES-GFP* (for *Hprt^{Foxf1DN}*) constructs. These constructs were then subcloned into the *pMP8.CAG-Stop* vector [61] using restriction enzymes *SwaI* and *MluI*. To target the *Hprt* locus, linearized constructs were electroporated into E14TG2a embryonic stem cells that carry a deficient *Hprt* locus enabling HAT selection after correct targeting and restoration of the locus [33, 34]. Correctly targeted ES cell clones were selected with HAT (Gibco) in a concentration of 1:300. Surviving colonies were expanded and genotyped by PCR. To test the functionality of the expression cassette in candidate ES clones, GFP epifluorescence was analyzed 6 d after electroporation with a *cre*-expression plasmid (*pCAG::turbo-cre*, kind gift from Achim Gossler). Verified ES clones were microinjected into CD1 mouse blastocysts. Chimeric males were obtained and mated to NMRI females to produce heterozygous F1 females.

Mouse strains and husbandry

Smo^{tm2Amc} (synonym: *Smo^{fl}*) [14], *Gt(ROSA)26Sor^{tm1(Smo/EYFP)Amc}* (synonym: *R26^{SmoM2}*) [17], *Gt(ROSA)26Sor^{tm4(ACTB-tdTomato-EGFP)Luo}* (synonym: *R26^{mTmG}*) [18 and *Axin2tm1(cre/ERT2)Rnu* (synonym: *Axin2creERT2*) {van Amerongen, 2012 #47] mouse lines were all obtained from the Jackson Lab. The *Tbx18^{tm4(cre)Akis}* (synonym: *Tbx18^{cre}*) mouse line was previously generated in the lab [62]. All lines were maintained on an NMRI outbred background. *Tbx18^{cre/+};Smo^{fl/fl}* (synonym: *Smo^{LOF}*) embryos were obtained from matings of *Tbx18^{cre/+};Smo^{fl/+}* males and

Part 3 - SHH signaling in ureter development

Smo^{fl/fl} females. *Tbx18^{cre/+};R26^{mTmG/SmoM2}* (synonym: *Smo^{GOF}*) and *Tbx18^{cre/+};R26^{mTmG/+}* embryos were derived from matings of *Tbx18^{cre/+};R26^{mTmG/mTmG}* males and *R26^{SmoM2/SmoM2}* and NMRI females, respectively. *Tbx18^{cre/+};Hprt^{Foxf1DN/y}* (synonym: *Foxf1DN*) and *Tbx18^{cre/+};Hprt^{Foxf1/y}* embryos were obtained from matings of *Tbx18^{cre/+}* males with *Hprt^{Foxf1DN/Foxf1DN}* and *Hprt^{Foxf1/Foxf1}* females, respectively. *Axin2^{creERT2/+};Hprt^{Foxf1/y}* embryos were obtained from matings of *Axin2^{creERT2/+}* and *Foxd1^{cre/+}* males with *Hprt^{Foxf1/Foxf1}* females, respectively. For all matings cre negative littermates were used as controls. For timed pregnancies, vaginal plugs were checked in the morning after mating, and noon was defined as embryonic day (E) 0.5. Embryos and urogenital systems were dissected in PBS. Ureters for explant cultures were dissected in L-15 Leibovitz medium (Biochrom). Specimens were fixed in 4% PFA/PBS, transferred to methanol and stored at -20°C prior to immunofluorescence or *in situ* hybridization analyses. PCR genotyping was performed on genomic DNA prepared from yolk sac or tail biopsies. All mice were bred and maintained in the central animal facility of the Medizinische Hochschule Hannover (Hannover, Germany) according to institutional guidelines. All experiments were performed with approval by the State of Lower Saxony.

Histological and expression analyses

Embryos, urogenital systems and ureters were paraffin-embedded and sectioned to 5 µm. Hematoxylin and eosin staining was performed according to standard procedures.

Non-radioactive *in situ* hybridization analysis of gene expression was performed on whole-mount specimens or 10-µm paraffin sections of the proximal ureter with digoxigenin-labeled antisense riboprobes [63, 64].

For immunofluorescence analysis on 5-µm paraffin sections polyclonal rabbit-anti-TAGLN (1:250, ab14106, Abcam), monoclonal mouse-anti-GFP (1:250, 11814460001, Roche), monoclonal mouse-anti-ACTA2 (1:250, A5228, Sigma-Aldrich), polyclonal rabbit-anti-ΔNP63 (1:250, 619001, Biolegend), monoclonal mouse-anti-BrdU (1:250, 1170376, Roche) or polyclonal rabbit antisera against CDH1 (1:250, gift from Rolf Kemler) and MYH11 (1:250, gift from Robert Adelstein) were used as primary antibodies. Biotinylated goat-anti-rabbit IgG (1:250, 111065033, Dianova), Alexa488-conjugated goat-anti-rabbit IgG (1:500, A11034, Molecular Probes) and Alexa555-conjugated goat-anti-mouse IgG (1:500, A21422, Molecular Probes) were used as secondary antibodies. The signal of the ΔNP63 antibody was amplified using the Tyramide Signal Amplification (TSA) system (NEL702001KT, Perkin Elmer). Before staining, paraffin sections were deparaffinized and cooked for 15 min in antigen unmasking

solution (H-3300, Vector Laboratories). Nuclei were stained with 4',6-diamidino-2-phenylindole (DAPI).

At least three specimens of each genotype were used for each of these analyses.

Cellular assays

Cell proliferation rates were analyzed by the detection of incorporated BrdU on 5 μ m paraffin sections according to published protocols [65]. A minimum of 12 sections of the proximal ureter from 3 independent specimens was analyzed per genotype. The BrdU-labeling index was defined as the number of BrdU-positive nuclei relative to the total number of nuclei as detected by DAPI counterstaining in arbitrarily defined compartments of the ureter. Data were expressed as mean \pm standard deviation. The two-tailed Student's t-test was used to test for significance. $P \leq 0.05$ was regarded as significant, $P \leq 0.005$ as highly significant and $P \leq 0.001$ as extremely significant.

Apoptosis was analyzed on 5 μ m paraffin sections using the ApopTag Plus Fluorescein *In Situ* Apoptosis Detection Kit (Chemicon). Alternatively, LysoTracker Red DND-99 (Thermo Scientific) was used to detect cell death in organ cultures. Briefly, E11.5 kidney rudiments were cultured for 1 d and incubated for 1 h with 2.5 μ M LysoTracker prior to documentation.

Organ cultures

Kidney rudiments or ureters were dissected from the embryo, explanted on 0.4 μ m polyester membrane Transwell supports (Corning) and cultured at the air-medium interface with DMEM/F12 (Gibco) supplemented with 10% FCS (Biochrom), 1x Penicillin/Streptomycin (Gibco), 1x Pyruvate (Gibco) and 1x Glutamax (Gibco). For pharmacological manipulation of SHH signaling cyclopamine (Selleckchem) and purmorphamine (Millipore) were used at a final concentration of 10 μ M and 2 μ M, respectively. Recombinant mouse BMP4 (R&D Systems) was used at a final concentration of 100 ng/ml. To induce recombination with the *Axin2^{creERT2}* line 4-Hydroxytamoxifen (H7904, Sigma-Aldrich) was added to the medium at a final concentration of 500 nM for the first 24 h of culture. Culture medium was replaced every day.

Part 3 - SHH signaling in ureter development

Microarray

Two independent pools of 50 E12.5 ureters were cultured with DMSO or 10 μ M cyclopamine for 18 h. Total RNA was extracted with peqGOLD RNAPure (PeqLab) and was sent to the Research Core Unit Transcriptomics of Hannover Medical School where RNA was Cy3-labeled and hybridized to Agilent Whole Mouse Genome Oligo v2 (4x44K) Microarrays. To identify differentially expressed genes, normalized expression data was filtered using Excel based on an intensity threshold of 150 and a more than 2 fold change in both pools.

Image analysis

Sections and organ cultures were photographed using a Leica DM5000 microscope with Leica DFC300FX digital camera or a Leica DM6000 microscope with Leica DFC350FX digital camera. Urogenital systems were documented using a Leica M420 microscope with a Fujix HC-300Z digital camera. Figures were prepared with Adobe Photoshop CS4.

Acknowledgements

We thank Achim Gossler for the turbo-cre plasmid.

References

1. Velardo JT. Histology of the ureter. In: Bergman H, editor. The ureter. 2nd ed. New York: Springer-Verlag; 1981.
2. Yu J, Manabe M, Wu XR, Xu C, Surya B, Sun TT. Uroplakin I: a 27-kD protein associated with the asymmetric unit membrane of mammalian urothelium. *J Cell Biol.* 1990;111(3):1207-16.
3. Gandhi D, Molotkov A, Batourina E, Schneider K, Dan H, Reiley M, et al. Retinoid signaling in progenitors controls specification and regeneration of the urothelium. *Dev Cell.* 2013;26(5):469-82.
4. Bohnenpoll T, Feraric S, Nattkemper M, Weiss AC, Rudat C, Meuser M, et al. Diversification of Cell Lineages in Ureter Development. *J Am Soc Nephrol.* 2016.
5. Bohnenpoll T, Kispert A. Ureter growth and differentiation. *Semin Cell Dev Biol.* 2014;36:21-30.
6. Cunha GR, Young P, Higgins SJ, Cooke PS. Neonatal seminal vesicle mesenchyme induces a new morphological and functional phenotype in the epithelia of adult ureter and ductus deferens. *Development.* 1991;111(1):145-58.
7. Baskin LS, Hayward SW, Young P, Cunha GR. Role of mesenchymal-epithelial interactions in normal bladder development. *J Urol.* 1996;156(5):1820-7.
8. Yu J, Carroll TJ, McMahon AP. Sonic hedgehog regulates proliferation and differentiation of mesenchymal cells in the mouse metanephric kidney. *Development.* 2002;129(22):5301-12.
9. Wang GJ, Brenner-Anantharam A, Vaughan ED, Herzlinger D. Antagonism of BMP4 signaling disrupts smooth muscle investment of the ureter and ureteropelvic junction. *J Urol.* 2009;181(1):401-7.
10. Trowe MO, Airik R, Weiss AC, Farin HF, Foik AB, Bettenhausen E, et al. Canonical Wnt signaling regulates smooth muscle precursor development in the mouse ureter. *Development.* 2012;139(17):3099-108.
11. Haraguchi R, Matsumaru D, Nakagata N, Miyagawa S, Suzuki K, Kitazawa S, et al. The hedgehog signal induced modulation of bone morphogenetic protein signaling: an essential signaling relay for urinary tract morphogenesis. *PLoS One.* 2012;7(7):e42245.
12. Caubit X, Lye CM, Martin E, Core N, Long DA, Vola C, et al. Teashirt 3 is necessary for ureteral smooth muscle differentiation downstream of SHH and BMP4. *Development.* 2008;135(19):3301-10.
13. Airik R, Trowe MO, Foik A, Farin HF, Petry M, Schuster-Gossler K, et al. Hydronephrosis due to loss of Sox9-regulated smooth muscle cell differentiation of the ureteric mesenchyme. *Hum Mol Genet.* 2010;19(24):4918-29.

Part 3 - SHH signaling in ureter development

14. Long F, Zhang XM, Karp S, Yang Y, McMahon AP. Genetic manipulation of hedgehog signaling in the endochondral skeleton reveals a direct role in the regulation of chondrocyte proliferation. *Development*. 2001;128(24):5099-108.
15. Murone M, Rosenthal A, de Sauvage FJ. Sonic hedgehog signaling by the patched-smoothed receptor complex. *Curr Biol*. 1999;9(2):76-84.
16. Bohnenpoll T, Bettenhausen E, Weiss AC, Foik AB, Trowe MO, Blank P, et al. Tbx18 expression demarcates multipotent precursor populations in the developing urogenital system but is exclusively required within the ureteric mesenchymal lineage to suppress a renal stromal fate. *Dev Biol*. 2013;380(1):25-36.
17. Jeong J, Mao J, Tenzen T, Kottmann AH, McMahon AP. Hedgehog signaling in the neural crest cells regulates the patterning and growth of facial primordia. *Genes Dev*. 2004;18(8):937-51.
18. Muzumdar MD, Tasic B, Miyamichi K, Li L, Luo L. A global double-fluorescent Cre reporter mouse. *Genesis*. 2007;45(9):593-605.
19. Fogel JL, Thein TZ, Mariani FV. Use of LysoTracker to detect programmed cell death in embryos and differentiating embryonic stem cells. *J Vis Exp*. 2012;(68).
20. Li XJ, Hu BY, Jones SA, Zhang YS, Lavaute T, Du ZW, et al. Directed differentiation of ventral spinal progenitors and motor neurons from human embryonic stem cells by small molecules. *Stem Cells*. 2008;26(4):886-93.
21. Ingham PW, McMahon AP. Hedgehog signaling in animal development: paradigms and principles. *Genes Dev*. 2001;15(23):3059-87.
22. Cooper MK, Porter JA, Young KE, Beachy PA. Teratogen-mediated inhibition of target tissue response to Shh signaling. *Science*. 1998;280(5369):1603-7.
23. Chen JK, Taipale J, Cooper MK, Beachy PA. Inhibition of Hedgehog signaling by direct binding of cyclopamine to Smoothed. *Genes Dev*. 2002;16(21):2743-8.
24. Chuang PT, McMahon AP. Vertebrate Hedgehog signalling modulated by induction of a Hedgehog-binding protein. *Nature*. 1999;397(6720):617-21.
25. Lee J, Platt KA, Censullo P, Ruiz i Altaba A. Gli1 is a target of Sonic hedgehog that induces ventral neural tube development. *Development*. 1997;124(13):2537-52.
26. Vokes SA, Ji H, McCuine S, Tenzen T, Giles S, Zhong S, et al. Genomic characterization of Gli-activator targets in sonic hedgehog-mediated neural patterning. *Development*. 2007;134(10):1977-89.
27. Vokes SA, Ji H, Wong WH, McMahon AP. A genome-scale analysis of the cis-regulatory circuitry underlying sonic hedgehog-mediated patterning of the mammalian limb. *Genes Dev*. 2008;22(19):2651-63.
28. Mahlapuu M, Enerback S, Carlsson P. Haploinsufficiency of the forkhead gene Foxf1, a target for sonic hedgehog signaling, causes lung and foregut malformations. *Development*. 2001;128(12):2397-406.

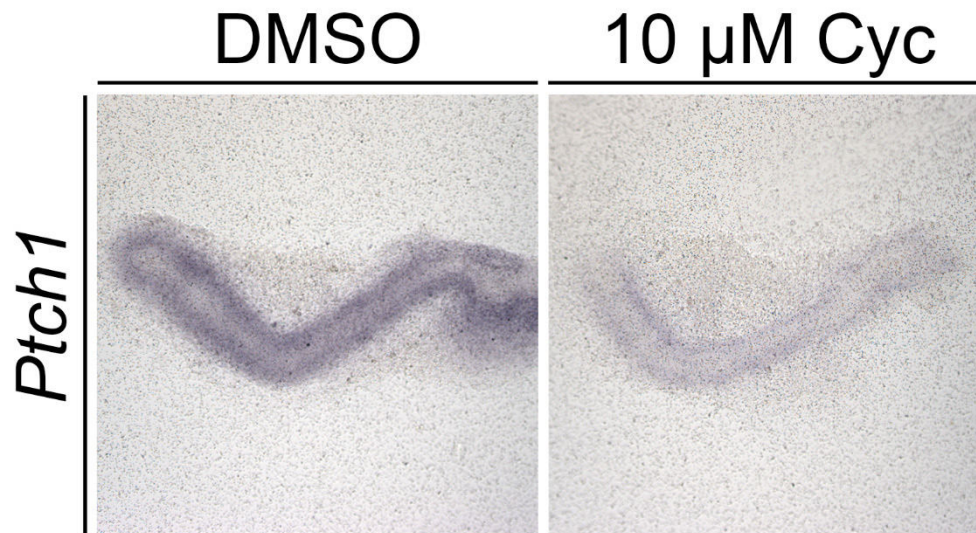
29. Ormestad M, Astorga J, Landgren H, Wang T, Johansson BR, Miura N, et al. Foxf1 and Foxf2 control murine gut development by limiting mesenchymal Wnt signaling and promoting extracellular matrix production. *Development*. 2006;133(5):833-43.
30. Madison BB, McKenna LB, Dolson D, Epstein DJ, Kaestner KH. FoxF1 and FoxL1 link hedgehog signaling and the control of epithelial proliferation in the developing stomach and intestine. *J Biol Chem*. 2009;284(9):5936-44.
31. Smith ST, Jaynes JB. A conserved region of engrailed, shared among all en-, gsc-, Nk1-, Nk2- and msh-class homeoproteins, mediates active transcriptional repression in vivo. *Development*. 1996;122(10):3141-50.
32. Kessler DS. Siamois is required for formation of Spemann's organizer. *Proc Natl Acad Sci U S A*. 1997;94(24):13017-22.
33. Hooper M, Hardy K, Handyside A, Hunter S, Monk M. HPRT-deficient (Lesch-Nyhan) mouse embryos derived from germline colonization by cultured cells. *Nature*. 1987;326(6110):292-5.
34. Preusse K, Tveriakhina L, Schuster-Gossler K, Gaspar C, Rosa AI, Henrique D, et al. Context-Dependent Functional Divergence of the Notch Ligands DLL1 and DLL4 In Vivo. *PLoS Genet*. 2015;11(6):e1005328.
35. Madison BB, Braunstein K, Kuizon E, Portman K, Qiao XT, Gumucio DL. Epithelial hedgehog signals pattern the intestinal crypt-villus axis. *Development*. 2005;132(2):279-89.
36. Zacharias WJ, Madison BB, Kretovich KE, Walton KD, Richards N, Udager AM, et al. Hedgehog signaling controls homeostasis of adult intestinal smooth muscle. *Dev Biol*. 2011;355(1):152-62.
37. Buckingham M. How the community effect orchestrates muscle differentiation. *Bioessays*. 2003;25(1):13-6.
38. Mahlapuu M, Pelto-Huikko M, Aitola M, Enerback S, Carlsson P. FREAC-1 contains a cell-type-specific transcriptional activation domain and is expressed in epithelial-mesenchymal interfaces. *Dev Biol*. 1998;202(2):183-95.
39. Sato H, Murphy P, Giles S, Bannigan J, Takayasu H, Puri P. Visualizing expression patterns of Shh and Foxf1 genes in the foregut and lung buds by optical projection tomography. *Pediatr Surg Int*. 2008;24(1):3-11.
40. Seo H, Kim J, Park GH, Kim Y, Cho SW. Long-range enhancers modulate Foxf1 transcription in blood vessels of pulmonary vascular network. *Histochem Cell Biol*. 2016;146(3):289-300.
41. Xu J, Liu H, Lan Y, Aronow BJ, Kalinichenko VV, Jiang R. A Shh-Foxf-Fgf18-Shh Molecular Circuit Regulating Palate Development. *PLoS Genet*. 2016;12(1):e1005769.
42. Hoffmann AD, Yang XH, Burnicka-Turek O, Bosman JD, Ren X, Steimle JD, et al. Foxf genes integrate tbx5 and hedgehog pathways in the second heart field for cardiac septation. *PLoS Genet*. 2014;10(10):e1004604.

Part 3 - SHH signaling in ureter development

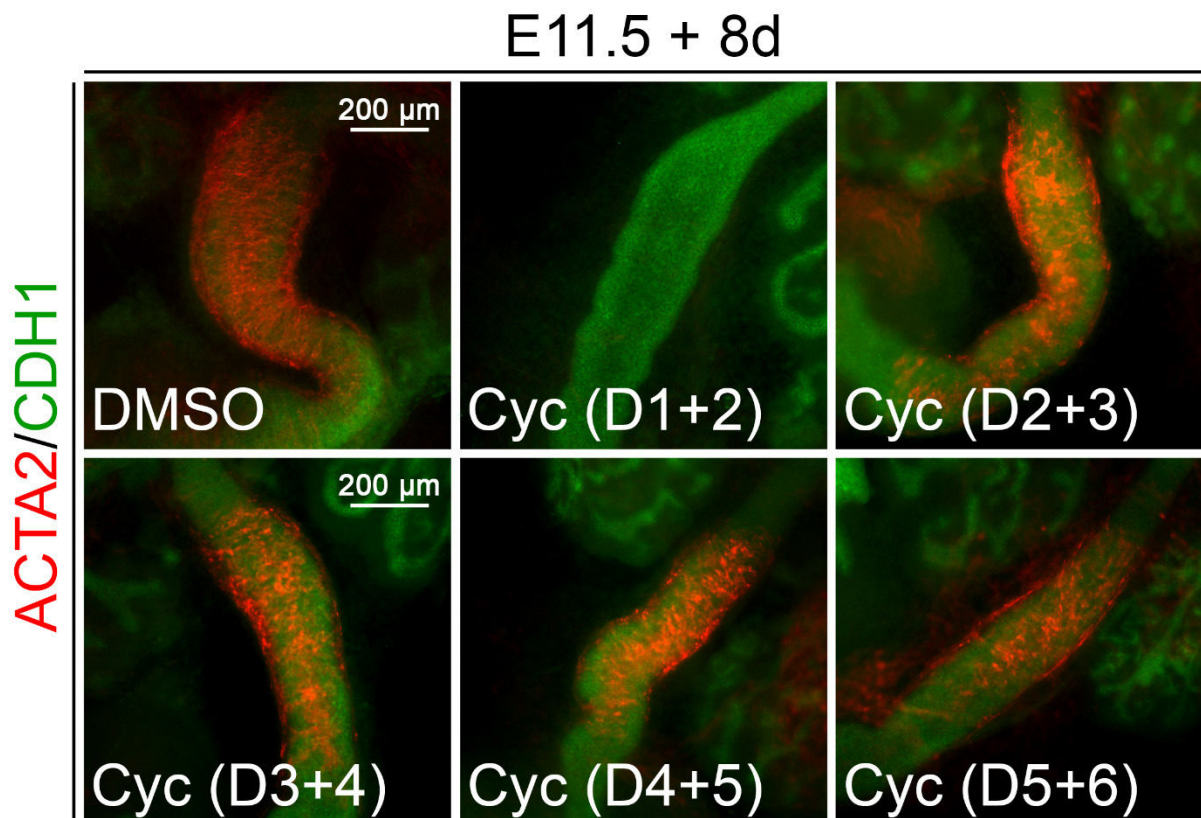
43. van den Brink GR. Hedgehog signaling in development and homeostasis of the gastrointestinal tract. *Physiol Rev.* 2007;87(4):1343-75.
44. Mao J, Kim BM, Rajurkar M, Shivdasani RA, McMahon AP. Hedgehog signaling controls mesenchymal growth in the developing mammalian digestive tract. *Development.* 2010;137(10):1721-9.
45. Bitgood MJ, McMahon AP. Hedgehog and Bmp genes are coexpressed at many diverse sites of cell-cell interaction in the mouse embryo. *Dev Biol.* 1995;172(1):126-38.
46. Ishizuya-Oka A, Hasebe T. Sonic hedgehog and bone morphogenetic protein-4 signaling pathway involved in epithelial cell renewal along the radial axis of the intestine. *Digestion.* 2008;77 Suppl 1:42-7.
47. Miyazaki Y, Oshima K, Fogo A, Ichikawa I. Evidence that bone morphogenetic protein 4 has multiple biological functions during kidney and urinary tract development. *Kidney Int.* 2003;63(3):835-44.
48. Brenner-Anantharam A, Cebrian C, Guillaume R, Hurtado R, Sun TT, Herzlinger D. Tailbud-derived mesenchyme promotes urinary tract segmentation via BMP4 signaling. *Development.* 2007;134(10):1967-75.
49. Hall JG, Pallister PD, Clarren SK, Beckwith JB, Wiglesworth FW, Fraser FC, et al. Congenital hypothalamic hamartoblastoma, hypopituitarism, imperforate anus and postaxial polydactyly--a new syndrome? Part I: clinical, causal, and pathogenetic considerations. *Am J Med Genet.* 1980;7(1):47-74.
50. Weber S, Taylor JC, Winyard P, Baker KF, Sullivan-Brown J, Schild R, et al. SIX2 and BMP4 mutations associate with anomalous kidney development. *J Am Soc Nephrol.* 2008;19(5):891-903.
51. Kim J, Kim P, Hui CC. The VACTERL association: lessons from the Sonic hedgehog pathway. *Clin Genet.* 2001;59(5):306-15.
52. Hilger AC, Halbritter J, Pennimpede T, van der Ven A, Sarma G, Braun DA, et al. Targeted Resequencing of 29 Candidate Genes and Mouse Expression Studies Implicate ZIC3 and FOXF1 in Human VATER/VACTERL Association. *Hum Mutat.* 2015;36(12):1150-4.
53. Reutter H, Hilger AC, Hildebrandt F, Ludwig M. Underlying genetic factors of the VATER/VACTERL association with special emphasis on the "Renal" phenotype. *Pediatr Nephrol.* 2016;31(11):2025-33.
54. Onishi H, Kai M, Odate S, Iwasaki H, Morifuji Y, Ogino T, et al. Hypoxia activates the hedgehog signaling pathway in a ligand-independent manner by upregulation of Smo transcription in pancreatic cancer. *Cancer Sci.* 2011;102(6):1144-50.
55. Lei J, Ma J, Ma Q, Li X, Liu H, Xu Q, et al. Hedgehog signaling regulates hypoxia induced epithelial to mesenchymal transition and invasion in pancreatic cancer cells via a ligand-independent manner. *Mol Cancer.* 2013;12:66.

56. Cayuso J, Ulloa F, Cox B, Briscoe J, Marti E. The Sonic hedgehog pathway independently controls the patterning, proliferation and survival of neuroepithelial cells by regulating Gli activity. *Development*. 2006;133(3):517-28.
57. Miyazaki Y, Oshima K, Fogo A, Hogan BL, Ichikawa I. Bone morphogenetic protein 4 regulates the budding site and elongation of the mouse ureter. *J Clin Invest*. 2000;105(7):863-73.
58. Cain JE, Nion T, Jeulin D, Bertram JF. Exogenous BMP-4 amplifies asymmetric ureteric branching in the developing mouse kidney in vitro. *Kidney Int*. 2005;67(2):420-31.
59. Wang Z, Malone MH, Thomenius MJ, Zhong F, Xu F, Distelhorst CW. Dexamethasone-induced gene 2 (dig2) is a novel pro-survival stress gene induced rapidly by diverse apoptotic signals. *J Biol Chem*. 2003;278(29):27053-8.
60. Brugarolas J, Lei K, Hurley RL, Manning BD, Reiling JH, Hafen E, et al. Regulation of mTOR function in response to hypoxia by REDD1 and the TSC1/TSC2 tumor suppressor complex. *Genes Dev*. 2004;18(23):2893-904.
61. Singh R, Hoogaars WM, Barnett P, Grieskamp T, Rana MS, Buermans H, et al. Tbx2 and Tbx3 induce atrioventricular myocardial development and endocardial cushion formation. *Cell Mol Life Sci*. 2012;69(8):1377-89.
62. Trowe MO, Shah S, Petry M, Airik R, Schuster-Gossler K, Kist R, et al. Loss of Sox9 in the periotic mesenchyme affects mesenchymal expansion and differentiation, and epithelial morphogenesis during cochlea development in the mouse. *Dev Biol*. 2010;342(1):51-62.
63. Wilkinson DG, Nieto MA. Detection of messenger RNA by in situ hybridization to tissue sections and whole mounts. *Methods Enzymol*. 1993;225:361-73.
64. Moorman AF, Houweling AC, de Boer PA, Christoffels VM. Sensitive nonradioactive detection of mRNA in tissue sections: novel application of the whole-mount in situ hybridization protocol. *J Histochem Cytochem*. 2001;49(1):1-8.
65. Bussen M, Petry M, Schuster-Gossler K, Leitges M, Gossler A, Kispert A. The T-box transcription factor Tbx18 maintains the separation of anterior and posterior somite compartments. *Genes Dev*. 2004;18(10):1209-21.

Supporting information

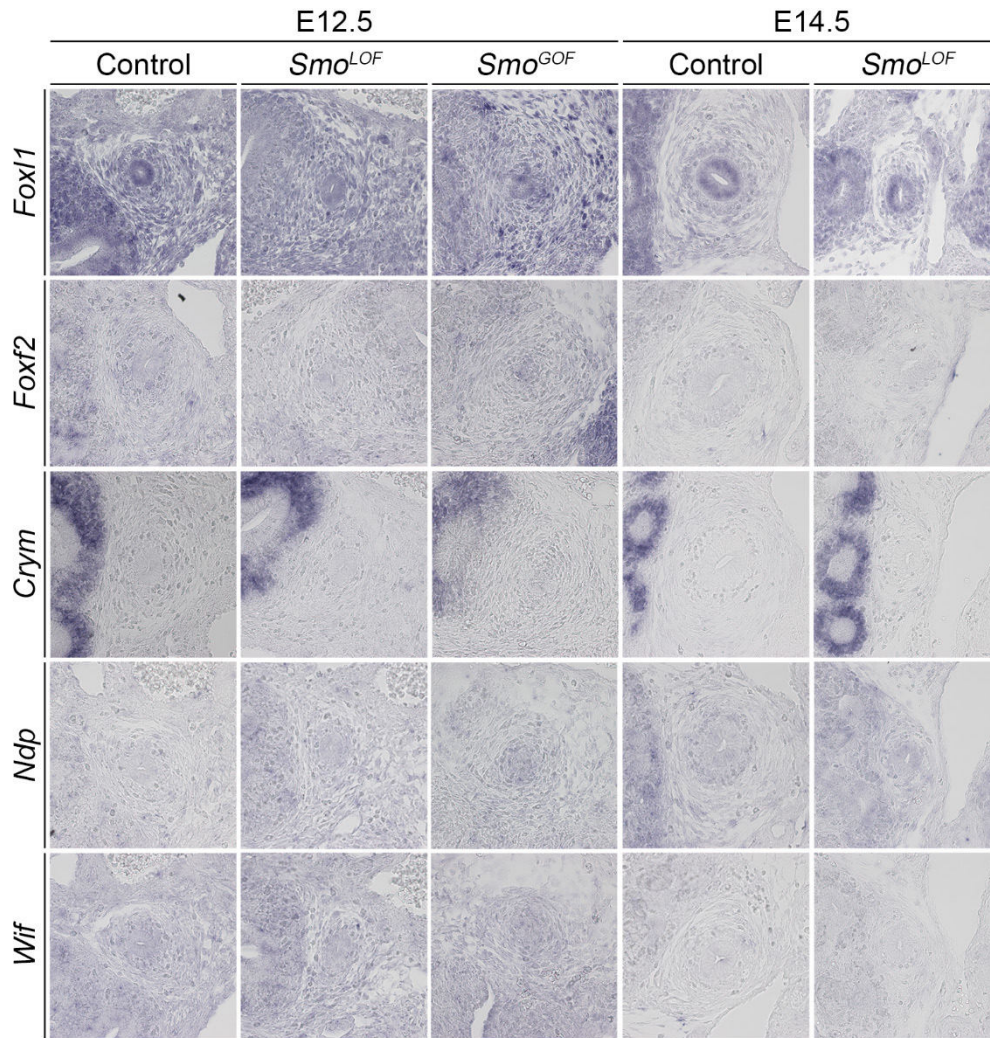


S1 Figure: 10 μM Cyclopamine is sufficient to largely inhibit HH signaling in ureter explant cultures. Wildtype ureters were isolated at E12.5, cultured for 18 h in the presence of DMSO or 10 μM cyclopamine (Cyc) and subjected to *in situ* hybridization analysis of expression of the SHH target gene *Ptch1*. Reduced expression of *Ptch1* in the cyclopamine treated culture indicates that HH signaling is severely compromised under these conditions.



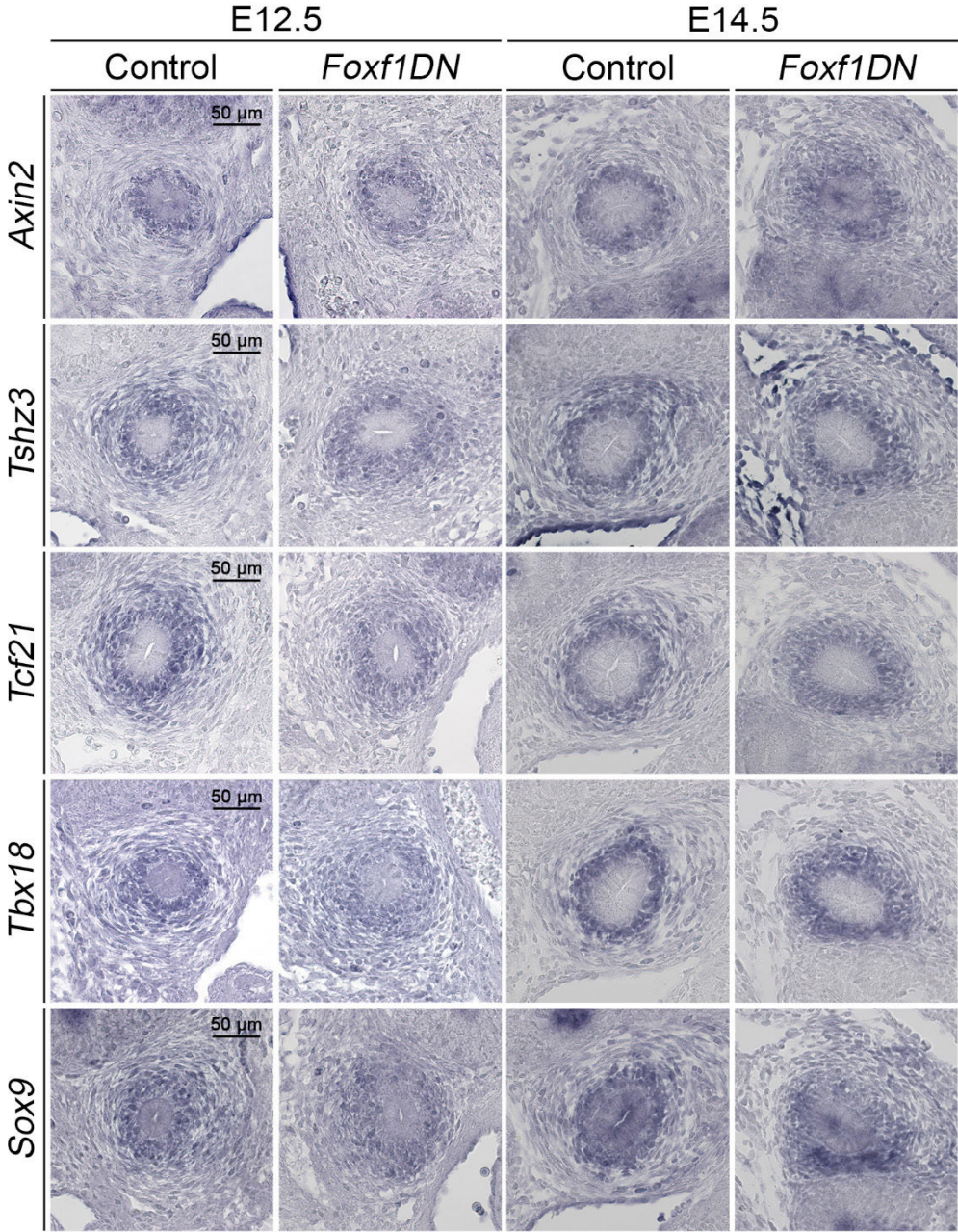
S2 Figure: HH signaling acts at E11.5 to E13.5 in ureter development. Wildtype ureters were isolated at E11.5 and cultured for 8 days in the presence of DMSO or 10 μM Cyclopamine in intervals of 2 days (D) as indicated. Immunofluorescence of the SMC marker ACTA2 (in red) in presence of the epithelial counterstain CDH1 (in green) shows that only treatment of the ureter explants at day 1 and 2 of the culture abrogates SMC differentiation in the ureter.

Part 3 - SHH signaling in ureter development

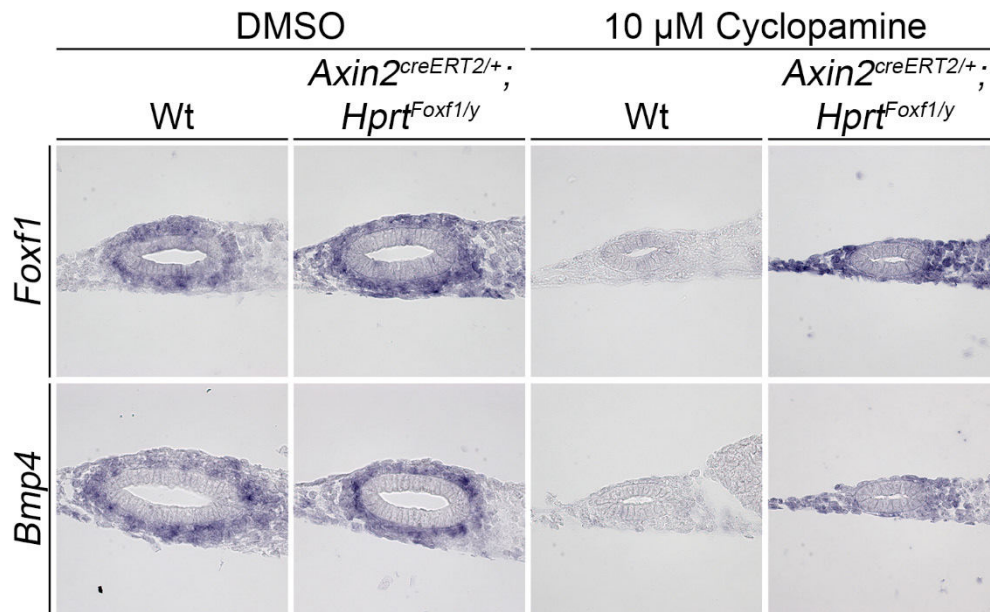


S3 Figure: *In situ* hybridization analysis of genes downregulated in microarrays of cyclopamine treated ureters. Note that specific expression of *Foxl1*, *Foxf2*, *Crym*, *Ndp* and *Wif* was not detected in the ureter of wildtype, *Tbx18^{cre/+};Smo^{fl/fl}* (*Smo^{LOF}*) and *Tbx18^{cre/+};R26^{mTmG}/Smo^{M2}* (*Smo^{GOF}*) embryos at E12.5 and E14.5.

Part 3 - SHH signaling in ureter development



S4 Figure: Molecular analysis of marker gene expression in control and *Tbx18^{cre/+};Hprt^{Foxf1DN/y} (Foxf1DN)* ureters at E12.5 and E14.5. *In situ* hybridization on proximal ureter sections shows that markers of the inner domain of the ureteric mesenchyme, *Axin2*, *Tshz3*, *Tcf21*, *Tbx18* and *Sox9* are not changed in their expression in *Foxf1DN* ureters.



S5 Figure: FOXF1 induces expression of *Bmp4* in the ureteric mesenchyme. Analysis of proximal sections of ureters explanted from E12.5 wildtype and *Axin2*^{creERT2/+};*Hprt*^{Foxf1/y} embryos and cultured for 3 d in the presence or absence of 10 μ M cyclopamine or DMSO solvent by *in situ* hybridization for expression of *Foxf1* and *Bmp4*. Abrogation of HH signaling by cyclopamine leads to loss of *Foxf1* and *Bmp4* expression in the ureteric mesenchyme. *Axin2*^{creERT2/+} mediated recombination of the *Hprt*^{Foxf1/y} allele results in robust expression of *Foxf1* and induction of *Bmp4* showing that FOXF1 is required and sufficient for *Bmp4* expression in the ureteric mesenchyme.

Part 3 - SHH signaling in ureter development

S1 Table: List of transcripts identified by microarray analysis as dependent in their expression on HH signaling in the developing ureter. Shown are two lists of transcripts with reduced and enhanced expression after an 18-h treatment of E12.5 ureter explants with 10 μ M cyclopamine. Two groups each of untreated and cyclopamine-treated ureters are shown with their intensities, and the resulting fold changes in expression upon comparison. Intensity thresholds were 200 for the controls; fold changes were larger than 1.4.

Identifier	Gene Name	Intensity Control 1	Intensity Cyclopamine 1	Intensity Control 2	Intensity Cyclopamine 2	Fold change 1	Fold change 2	Average fold change
NM_020259	Hhip	1581	123	1326	121	-12.9	-11.0	-11.9
NM_010426	Foxf1	4668	892	4757	877	-5.2	-5.4	-5.3
NM_008024	Foxl1	3028	771	3306	835	-3.9	-4.0	-3.9
NM_010225	Foxf2	1329	446	1105	311	-3.0	-3.5	-3.3
AK147626	Ptch1	1238	344	1065	377	-3.6	-2.8	-3.2
NM_016669	Crym	1573	390	1098	465	-4.0	-2.4	-3.2
NM_030143	Ddit4l	402	109	345	130	-3.7	-2.6	-3.2
AK136956	Hapln3	301	87	292	102	-3.5	-2.9	-3.2
AK014270	Ptchd4	450	135	343	116	-3.3	-2.9	-3.1
ENSMUST00000051253	ENSMUST00000051253	1748	614	1456	492	-2.8	-3.0	-2.9
NM_172485	Thsd7b	246	103	302	113	-2.4	-2.7	-2.5
NM_028443	Fam101a	1068	380	859	394	-2.8	-2.2	-2.5
NM_016847	Avpr1a	1116	420	1224	543	-2.7	-2.3	-2.5
NM_010883	Ndp	1218	474	919	408	-2.6	-2.3	-2.4
NM_011125	Pltp	888	400	860	346	-2.2	-2.5	-2.4
NM_010296	Gli1	5606	2329	5170	2311	-2.4	-2.2	-2.3
NM_053088	lfitm5	235	110	215	95	-2.1	-2.3	-2.2
NM_001039347	Kcnd3	581	266	621	286	-2.2	-2.2	-2.2
NM_011915	Wif1	1026	476	1009	501	-2.2	-2.0	-2.1
NM_007934	Enpep	2515	1212	2583	1307	-2.1	-2.0	-2.0
NM_001024139	Adams15	1258	650	1332	664	-1.9	-2.0	-2.0
NM_019521	Gas6	2225	1066	1998	1078	-2.1	-1.9	-2.0
NM_021342	Kcne4	300	138	233	132	-2.2	-1.8	-2.0
NM_007472	Aqp1	1077	518	873	473	-2.1	-1.8	-2.0
NM_001099299	Ajap1	785	403	757	383	-1.9	-2.0	-2.0
NM_178642	Ano1	1172	543	1035	595	-2.2	-1.7	-1.9
NM_009856	Cd83	576	267	474	274	-2.2	-1.7	-1.9
NM_013703	Vldlr	4095	2082	3883	2097	-2.0	-1.9	-1.9
NR_033803	6030408816Rik	6137	3162	6232	3372	-1.9	-1.8	-1.9
NM_018874	Pnliprp1	1068	601	914	460	-1.8	-2.0	-1.9
NM_022316	Smoc1	2470	1401	2867	1465	-1.8	-2.0	-1.9
NR_030721	9130206124Rik	580	316	530	295	-1.8	-1.8	-1.8
NM_001085521	Tmem90b	657	329	519	331	-2.0	-1.6	-1.8
NM_011580	Thbs1	2556	1422	2964	1693	-1.8	-1.8	-1.8
NM_008770	Cldn11	4607	2689	4651	2561	-1.7	-1.8	-1.8
NM_001190870	Kcne3	234	130	197	115	-1.8	-1.7	-1.8
NM_025807	Slc16a9	288	166	388	226	-1.7	-1.7	-1.7
NM_144945	Lgi2	611	349	505	296	-1.7	-1.7	-1.7
NM_145741	Gdf10	568	346	607	337	-1.6	-1.8	-1.7
ENSMUST00000055537	Gm22	237	137	218	131	-1.7	-1.7	-1.7
NM_054095	Necab2	1011	613	1000	576	-1.6	-1.7	-1.7
NM_172610	Mpped1	629	387	611	351	-1.6	-1.7	-1.7
NM_148938	Slc1a3	1295	707	1292	842	-1.8	-1.5	-1.7
TC1679329	TC1679329	214	117	262	171	-1.8	-1.5	-1.7
AK017236	5330406M23Rik	193	116	253	150	-1.7	-1.7	-1.7
NM_177410	Bcl2	945	555	756	462	-1.7	-1.6	-1.7
NM_011825	Grem2	191	115	238	143	-1.7	-1.7	-1.7
NM_030060	Batf3	1328	810	1229	731	-1.6	-1.7	-1.7
NM_022435	Sp5	414	261	407	235	-1.6	-1.7	-1.7
NM_001037906	Nell1	895	502	890	581	-1.8	-1.5	-1.7
NM_010500	Ier5	1749	1130	1413	868	-1.5	-1.6	-1.6
NM_153543	Aldh1l2	288	184	414	268	-1.6	-1.5	-1.6
NM_011427	Snai1	1277	825	1393	909	-1.5	-1.5	-1.5
NR_030682	2810410L24Rik	1036	686	1114	728	-1.5	-1.5	-1.5

Part 3 - SHH signaling in ureter development

Identifier	Gene Name	Intensity Control 1	Intensity Control 2	Intensity Cyclopamine 1	Intensity Cyclopamine 2	Fold change 1	Fold change 2	Average fold change
NM_017474	Clca3	234	583	131	312	2.5	2.4	2.4
NM_008605	Mmp12	454	772	346	847	1.7	2.5	2.1
NM_001163032	Synpr	288	533	251	483	1.9	1.9	1.9
NM_133681	Tspan1	267	548	195	336	2.0	1.7	1.9
NM_001126490	Ism1	595	1098	705	1288	1.8	1.8	1.8
NM_010819	Clec4d	348	628	460	855	1.8	1.9	1.8
NM_001204233	Spp1	2787	5073	1798	3259	1.8	1.8	1.8
NM_008469	Krt15	1821	3247	1119	2029	1.8	1.8	1.8
NM_001039195	Gria2	110	195	135	245	1.8	1.8	1.8
NM_007726	Cnr1	434	790	489	842	1.8	1.7	1.8
NM_033605	Dach2	982	1771	924	1580	1.8	1.7	1.8
NM_010518	Igfbp5	16097	28770	18042	30658	1.8	1.7	1.7
NM_013602	Mt1	7461	13221	9088	14905	1.8	1.6	1.7
NM_021384	Rsad2	241	394	326	578	1.6	1.8	1.7
NM_018798	Ubqln2	820	1517	1234	1915	1.8	1.6	1.7
NM_177597	March11	518	899	539	898	1.7	1.7	1.7
NM_008147	Gp49a	529	865	474	835	1.6	1.8	1.7
NM_008509	Lpl	3199	5070	3054	5414	1.6	1.8	1.7
NM_011337	Ccl3	177	288	146	250	1.6	1.7	1.7
NM_011338	Ccl9	740	1194	629	1046	1.6	1.7	1.6
ENSMUST00000093859	Grin3a	747	1289	734	1109	1.7	1.5	1.6
NM_013532	Lilrb4	1014	1611	993	1620	1.6	1.6	1.6
NR_004414	Rnu2-10	526	823	569	906	1.6	1.6	1.6
XR_035383	A730089K16Rik	316	496	324	494	1.6	1.5	1.5
NM_009807	Casp1	205	316	192	299	1.5	1.6	1.5
NM_053155	Clmn	1189	1855	1347	2026	1.6	1.5	1.5

Part 4 - RA signaling in ureter development

Retinoic acid signaling maintains epithelial and mesenchymal progenitors in the developing mouse ureter

Tobias Bohnenpoll¹, Anna-Carina Weiss¹, Maurice Labuhn¹
and Andreas Kispert^{1,§}

¹ Institut für Molekularbiologie, Medizinische Hochschule Hannover, 30627 Hannover, Germany

§ Author for correspondence:

Email: kispert.andreas@mh-hannover.de

Tel: +49511 5324017

Fax: +49511 5324283

Manuscript in preparation

Abstract

The differentiated cell types of the two tissue compartments of the mature ureter arise from multipotent progenitors in embryonic development. In the mesenchyme, adventitial fibrocytes differentiate first in an outer domain, then common progenitors in an inner region give rise to smooth muscle and lamina propria cells. In the epithelium, uncommitted cells first become intermediate cells from which both basal and superficial cells develop. How the progenitor cells are maintained and differentiate in a precisely coordinated temporal and spatial fashion has remained enigmatic. Here, we have addressed the role of retinoic acid (RA) signaling in ureter development. Using comprehensive expression analysis of components and target genes of RA signaling, we showed that the pathway acts both in the mesenchymal and epithelial progenitor pools from embryonic day 11.5 to E14.5. Pharmacological pathway inhibition in ureter explant cultures resulted in an expansion of smooth muscle cells at the expense of lamina propria fibroblast in the mesenchymal wall of the ureter, and an expansion of superficial cells at the expense of intermediate cells in the urothelium; pharmacological activation experiments gave complementary results. A precocious differentiation of smooth muscle cells, basal cells and superficial cells from their uncommitted progenitors was identified as a cause for these cellular composition defects. We conclude that RA signaling acts specifically in the undifferentiated ureter to temporally and spatially restrict differentiation and to maintain ureteric progenitors. Finally, we identified transcriptional targets of RA signaling that may account for this activity.

Introduction

The mammalian ureter is a tubular organ dedicated to the efficient removal of the urine from the renal pelvis to the bladder. Its outer mesenchymal coat is highly flexible and peristaltically active due to a three-layered organization of an outer fibroblastic tunica adventitia, a medial accumulation of smooth muscle cells (SMCs) and an inner lamina propria with fibroblasts. The inner epithelial compartment, the urothelium, is a three-tiered dilatable yet sealing tissue with a single layer of cuboidal basal cells (B-cells), one or two layers of similarly shaped intermediate cells (I-cells), and a luminal layer of large squamous superficial cells (S-cells) [1].

The ordered array of differentiated cell types of the mature ureter arises by a complex program of patterning, proliferation and differentiation from epithelial and mesenchymal precursor cells in early embryogenesis. In the mouse, a diverticulum of the nephric duct emerges around E10.5 at the level of the future hindlimbs and invades the adjacent mesenchymal tissue. While the proximal aspect of the bud and the surrounding mesenchyme will form the different tissues of the kidney, the distal cell populations are specified towards a ureteric fate. From E12.5 to E14.5, the ureteric mesenchyme is subdivided into an inner and outer region that will differentiate from E15.5 onwards in a proximal to distal wave into SMCs and adventitial fibroblasts, respectively. The lamina propria can be recognized from E16.5 onwards as a cell-sparse layer in between the ureteric epithelium and the SMCs. The ureteric epithelium remains single-layered and undifferentiated until E14.5. Around this stage, intermediate cell markers are switched on and stratification occurs. At E16.5, the luminal layer of epithelial cells starts S-cell differentiation while individual cells of the basal layer initiate B-cell differentiation. Around birth, three distinct layers with differentiated B-, I- and S- cells can be distinguished [2].

While the signals and factors that maintain the precursor character of the ureteric tissues have remained enigmatic, embryological and genetic experiments have shown that mesenchymal and epithelial differentiation is coupled by trans-acting signaling activities. SMC differentiation depends on epithelial Sonic Hedgehog (SHH) and WNT signals while SHH-dependent BMP4 signaling has autocrine effects on mesenchymal differentiation as well as paracrine functions on epithelial growth [3-6].

Retinoic acid (RA) signaling is a conserved paracrine pathway with diverse functions in cellular proliferation and differentiation programs both in embryogenesis and in adult tissue homeostasis [7, 8]. RA is locally produced from dietary retinol (vitamin A) by two consecutive oxidation steps catalyzed by retinol and retinaldehyde dehydrogenases [8]. Tissue-availability of RA is further controlled by specific expression of RA-degrading enzymes of the cytochrome P450 26

subfamily (CYP26A1-C1) [9]. RA binds to nuclear RA receptors (RARs) that form heterodimers with retinoid X receptors (RXRs) which triggers the exchange of co-repressor against coactivator complexes to activate the expression of target genes [10, 11]. Previous studies have indicated diverse roles of RA signaling in the excretory system. RA from the pericloacal mesenchyme regulates ureter-bladder connectivity by inducing apoptosis of the most distal aspect of the nephric duct [12]. RA signaling is active in the renal stroma to regulate branching morphogenesis [13, 14]. Studies in the bladder have recently uncovered a role for the signal in urothelial specification [15].

Here, we analyze the functional involvement of RA signaling in the development of the murine ureter. We uncover a critical role for this pathway in the maintenance of progenitor cells in the early ureter and identify RA-responsive genes that may account for this function.

Results

RA signaling is active in early ureter development

To determine the spatiotemporal profile of RA signaling in ureter development, we first analyzed by *in situ* hybridization on proximal ureter sections of embryonic ureters the expression of genes responsible for the local production of RA from retinaldehyde (*Aldh1a1*, *Aldh1a2*, *Aldh1a3*). *Aldh1a2* was found throughout the ureteric mesenchyme at E11.5. Expression was down-regulated at the proximal ureter at E12.5 but persisted at the distal most aspect of the organ as well as in the renal stroma until E18.5 as shown by additional analysis of whole urogenital systems. At E18.5, *Aldh1a2* expression was newly activated in the lamina propria. *Aldh1a3* expression was restricted to the epithelium of the nephric duct and the ureteric bud at E11.5. Expression was maintained in the renal collecting duct system but was lost in the ureter except its distal most aspect at subsequent stages (Figure 1, A-C, Supplemental Figure 1). We next screened for expression of genes encoding RARs (*Rara*, *Rarb*, *Rarg*) and RXRs (*Rxra*, *Rxrb*, *Rxrg*) that account for transcriptional activation of target genes upon RA binding. Expression of all three *Rar* genes was found in the ureteric epithelium and mesenchyme at E11.5 and E12.5. Expression of *Rarb*, a direct transcriptional target of this pathway [16], was maintained at E14.5 particularly in the inner mesenchymal domain whereas expression of *Rara* and *Rarg* was down-regulated at this stage (Figure 1, D-F). Expression of all three *Rxr* genes was detected at E11.5 to E14.5 both in the ureteric epithelium and mesenchyme. *Rxra* was increased in the ureteric epithelium at E14.5 and was maintained in this domain until E18.5 (Figure 1, G-I). Together this analysis shows that RA is synthesized in both tissue compartments of the ureter at E11.5, and that RA signaling occurs therein until E14.5, i.e. prior to the onset of ureteric cell differentiation.

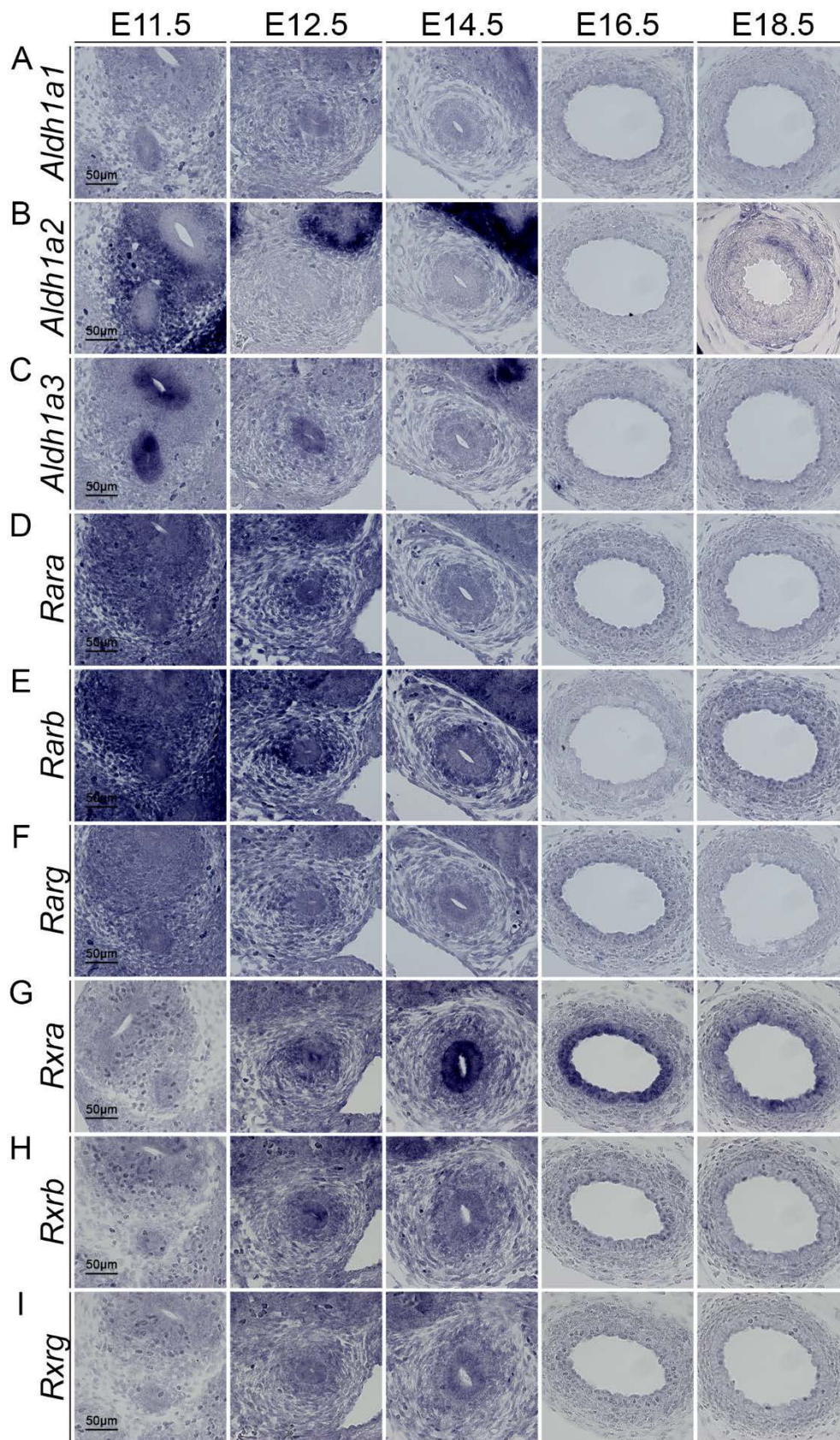


Figure 1: Retinoic acid signaling is active in early ureter development. *In situ* hybridization analysis on transverse sections of the proximal ureter of wild-type embryos for expression of genes encoding RA synthesizing genes (A-C), RA receptors (D-F) and retinoid X receptors (G-I). Stages are as indicated. k, kidney; u, ureter; ue, ureteric epithelium; um, ureteric mesenchyme; us, ureter stalk; wd, Wolffian duct.

RA signaling controls differentiation of the ureteric mesenchyme

Given the complexity of RAR and RXR expression in ureter development, we choose pharmacological pathway manipulation in explant cultures rather than a genetic approach to address the functional involvement of RA signaling in ureter development. To inactivate RA signaling we used the pan RAR antagonist BMS493 in a concentration of 1 μ M after showing that this concentration abolished expression of the RA target gene *Rarb* in E11.5 explants after 18 h of treatment [17]. (Over-)activation of the pathway was reached by 1 μ M RA in the same interval (Supplemental Figure 2). We explanted ureter rudiments at E11.5, E12.5, E14.5, E16.5 and E18.5 and cultured them for 14 d, 12 d, 10 d, 8 d and 6 d to obtain similar end-points for histological and molecular analysis.

We first investigated the effect of RA manipulation on mesenchymal cell types. We have recently shown that the T-box transcription factor gene *Tbx18* is expressed in the undifferentiated ureteric mesenchyme, and that the descendants of this expression domain constitute the ureteric mesenchymal wall throughout development and in adulthood [18, 19]. We therefore used mice double heterozygous for a *cre* knock-in the *Tbx18* locus and the *Rosa26^{mTmG}* reporter line (*Tbx18^{cre/+};Rosa26^{mTmG/+}*) [20, 21] for visualization of the ureteric mesenchyme by GFP expression.

Brightfield and GFP epifluorescence analysis throughout the culture period showed that the ureter elongated and became peristaltically active under all conditions. GFP epifluorescence around the ureter was strongly decreased under BMS treatment in ureter explants at E11.5, E12.5 and E14.5 while RA administration resulted in increased width of the ureteric wall in explants at these stages (Supplemental Figures 3-7). Histological and GFP expression analysis of proximal ureter segments at the culture end-points confirmed mesenchymal hypoplasia by BMS493-treatment and hyperplasia by RA treatment at E11.5 to E14.5 (Figure 2).

To detect and quantify cell differentiation in the ureteric mesenchyme, we analyzed co-expression of the SMC marker Transgelin (TAGLN) with the GFP reporter by immunofluorescence on sections of ureter explants of *Tbx18^{cre/+};Rosa26^{mTmG/+}* mice. Adventitial fibroblasts were defined as GFP⁺TAGLN⁻ outer ring cells, SMCs as GFP⁺TAGLN⁺ intermediary cells and lamina propria cells as GFP⁺TAGLN⁻ inner ring cells of the mesenchymal wall. Inhibition of RA signaling in cultures of E11.5 to E14.5 ureter explants resulted in a relative increase of SMCs largely at the expense of lamina propria cells. At the same stages RA treatment led to a reduction of SMCs and increased lamina formation (most obviously at E12.5). In E16.5 and E18.5 explants, neither BMS nor RA treatment affected the width or the composition of differentiated

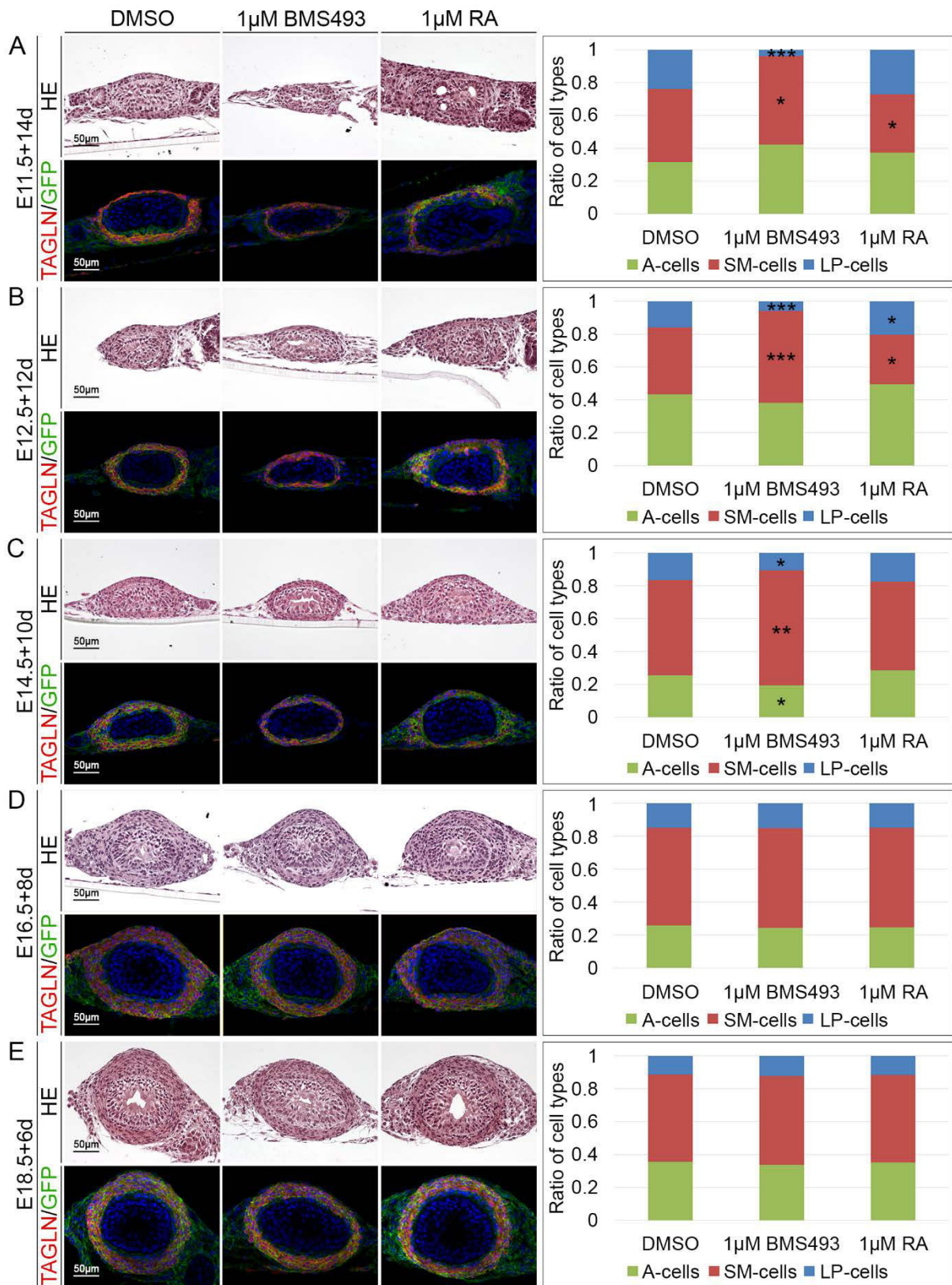


Figure 2: RA signaling controls ureteric mesenchymal differentiation. Hematoxylin and eosin (upper panel) and co-immunofluorescence analysis of GFP and TAGLN (lower panel) on transverse proximal sections of E11.5+14d (A), E12.5+12d (B), E14.5+10d (C), E16.5+8d (D) and E18.5+6d (E) *Tbx18^{cre/+};R26^{mTmG/+}* ureter explants that were treated with DMSO, 1 µM BMS493 or 1 µM RA. The bar graph displays ratios of differentiated cell types that were quantified based on the immunofluorescence analysis. For numbers and statistics see Supplemental Table 1. * p<0.01; ** p<0.001; *** p<0.0001.

Part 4 - RA signaling in ureter development

cell types in the mesenchymal wall of the ureter (Figure 2, Supplemental Table 1). Hence, RA signaling is required in the undifferentiated ureteric mesenchyme from E11.5 to E14.5 to expand adventitial and most importantly lamina fibrocytes and inhibit SMC differentiation.

RA signaling controls urothelial differentiation

The three cell types of the mature ureteric epithelium can be distinguished by combinatorial expression of the intracytoplasmic protein KRT5, the nuclear protein Δ NP63 and the cell surface protein UPK1B. B-cells are $KRT5^+\Delta NP63^+UPK1B^-$, I-cells are $KRT5^-\Delta NP63^+UPK1B^{+low}$ and S-cells are $KRT5^-\Delta NP63^-UPK1B^{+high}$ [2]. Inhibition of RA signaling by BMS493 treatment resulted in E11.5, E12.5 and in E14.5 but not in E16.5 and E18.5 explants in a large expansion of S-cells at the expense of I-cells. Enhanced and prolonged RA signaling by RA administration prevented B-cell differentiation, reduced S-cell differentiation and expanded the pool of I-cells. In E16.5 and E18.5 explants, RA treatment expanded I-cells at the expense of B-cells (Figure 3, Supplemental Table 2). Given our recent finding that in the ureter I-cells are precursors for both B- and S-cells [2], this analysis suggests that RA signaling is required from E11.5 to at least E14.5 to prevent premature differentiation of I- into S- and B-cells.

RA signaling has a minor function in proliferation control

We next addressed a potential function of RA signaling in the proliferation and survival of the epithelial and mesenchymal tissue compartments in the ureter by performing bromodeoxyuridine (BrdU) incorporation assays (Figure 4, A-C, upper row, Supplemental Table 3) and terminal dUTP nick end-labeling (TUNEL) assays (Figure 4 A-C, lower row) on E11.5, E12.5 and E14.5 *Tbx18^{cre/+};R26^{mTmG/+}* explants that were cultured in the presence of 1 μ M BMS493 or 1 μ M RA for 1 day. At E11.5 inhibition of RA signaling resulted in a significant decrease of proliferation of the inner mesenchymal compartment of the ureter but left the outer mesenchymal and epithelial cells unaltered. Activation of RA signaling showed no effect on proliferation rates, as did inhibition or activation experiments at E12.5 and E14.5. Moreover, apoptosis was not altered under RA loss- and gain-of-function conditions. We conclude that RA signaling has a minor function in proliferation control at E11.5 only.

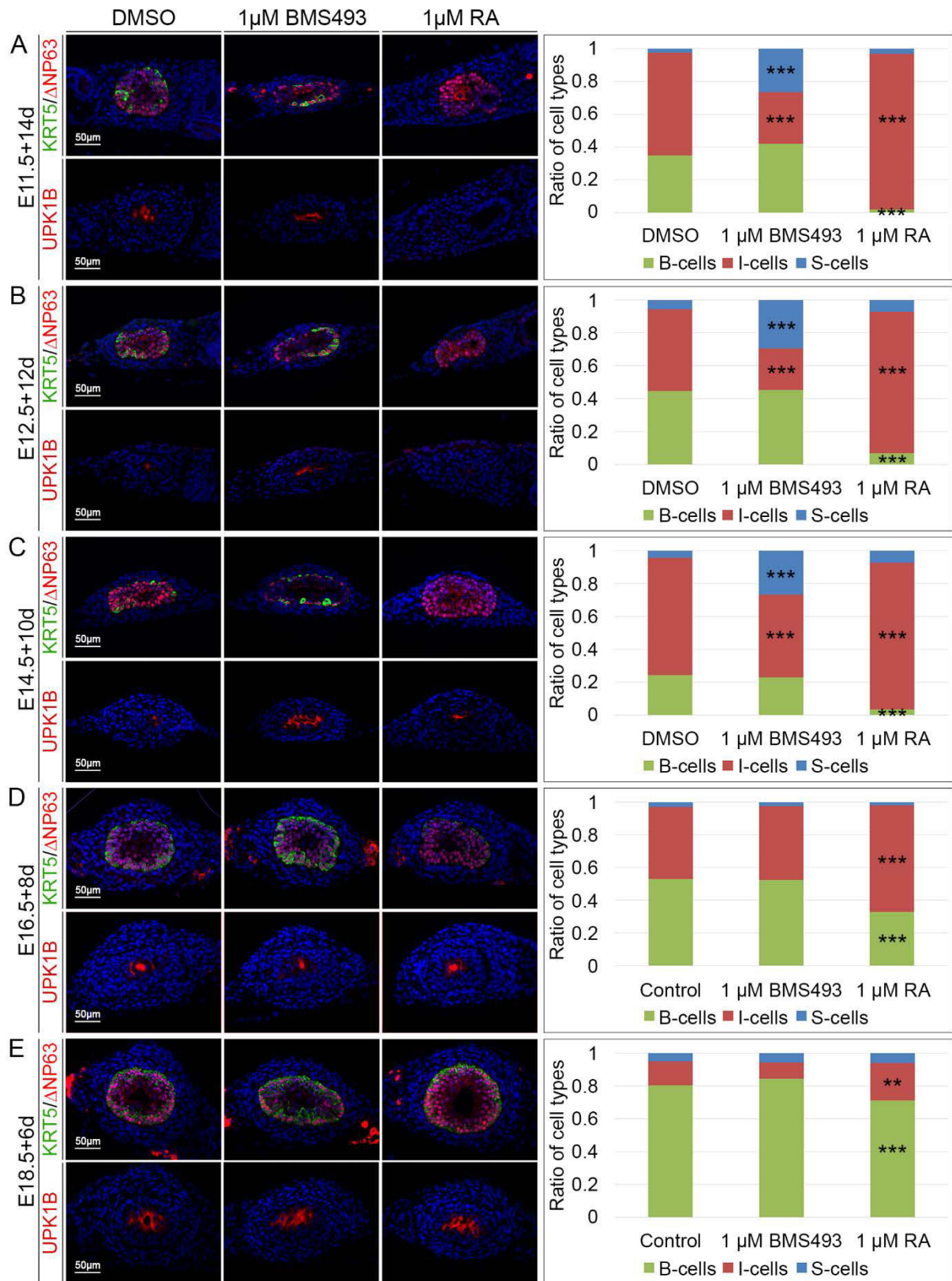


Figure 3: RA signaling controls urothelial differentiation. Co-immunofluorescence analysis of KRT5 and Δ NP63 (upper panel) and UPK1B (lower panel) on transverse proximal sections of E11.5+14d (A), E12.5+12d (B), E14.5+10d (C), E16.5+8d (D) and E18.5+6d (E) wildtype ureter explants that were treated with DMSO, 1 μ M BMS493 or 1 μ M RA. The bar diagram displays ratios of differentiated cell types that were quantified based on the immunofluorescence analysis. For numbers and statistics see Supplemental Table 2. ** $p \leq 0.001$; *** $p \leq 0.0001$.

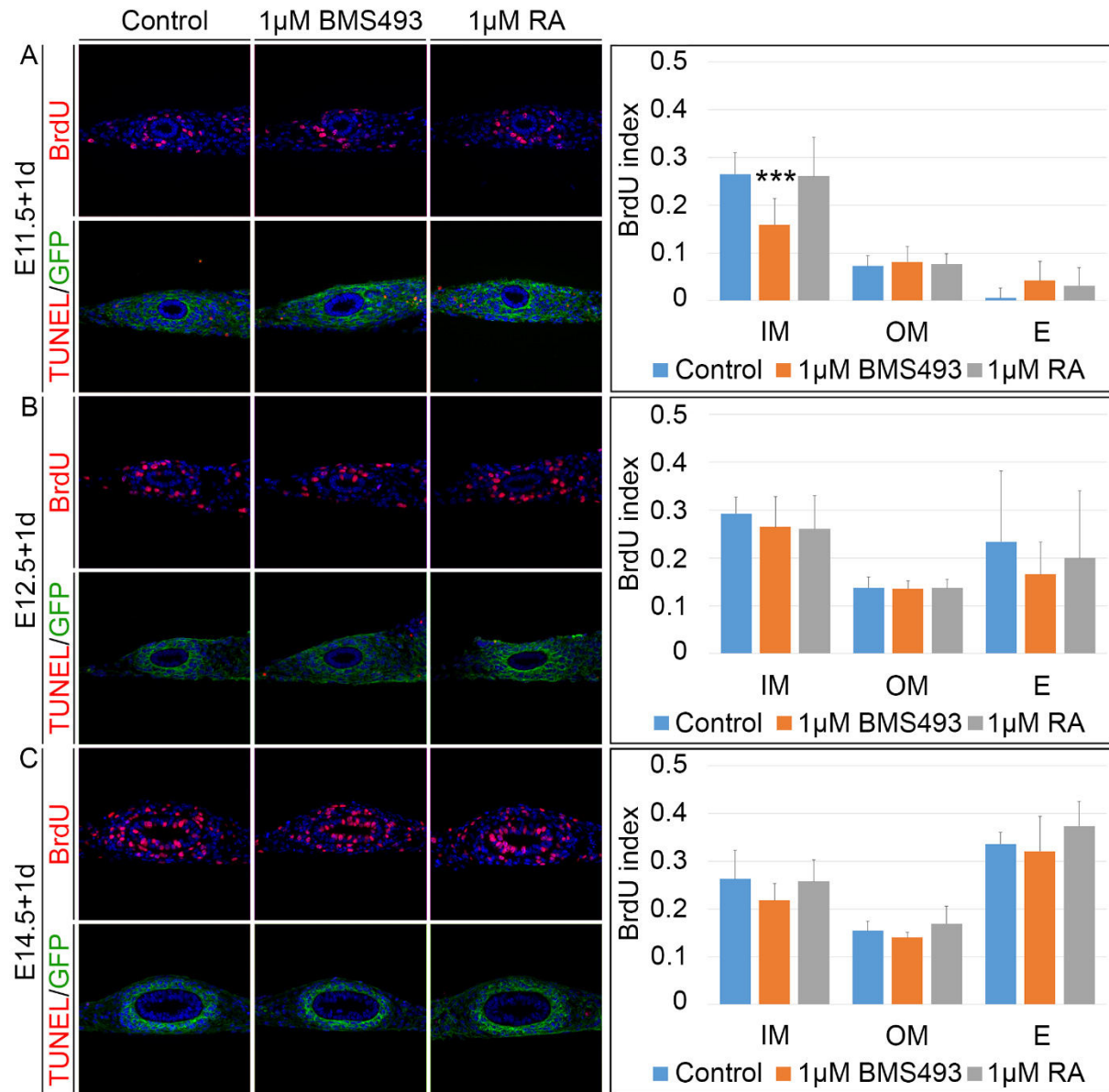


Figure 4: RA signaling affects proliferation in a minor way. Determination of cellular proliferation by BrdU incorporation assay (upper row) and apoptosis by TUNEL/GFP assay (lower row) on transverse sections of the proximal ureter of E11.5 (A), E12.5 (B) and E14.5 (C) *Tbx18^{cre/+};R26^{mTmG/+}* explants that were cultured in the presence of DMSO, 1µM BMS493 or 1µM RA for 1 day. The bar diagrams display the BrdU incorporation indices in arbitrarily defined compartments of the ureter under given conditions. For numbers and statistics see Supplemental Table 3. *** $p \leq 0.0001$. E, epithelium; IM inner mesenchyme; OM, outer mesenchyme.

RA signaling prevents precocious differentiation of ureteric progenitors

To further test whether RA signaling contributes to the maintenance of precursor cells, we explanted E12.5 ureters and cultured them for different intervals to score the onset of cell differentiation in the mesenchymal and epithelial compartments. SMC differentiation, as analyzed by TAGLN (Figure 5A, upper row) and ACTA2 (Figure 5A, lower row) immunofluorescence, was initiated after 4 days in control cultures. TAGLN showed a comparable expression in BMS493 treated cultures after 4 and 5 days, but ACTA2 expression was considerably stronger

under these conditions at both time-points. Expression of UPK1B and KRT5 indicated onset of S-cell and B-cell differentiation after 4 and 11 days, respectively, in control cultures. Both markers were expressed 1 day earlier in BMS493 treated cultures (Figure 5B, upper and lower row). Hence, RA signaling is required to prevent precocious differentiation in either tissue compartment of the ureter.

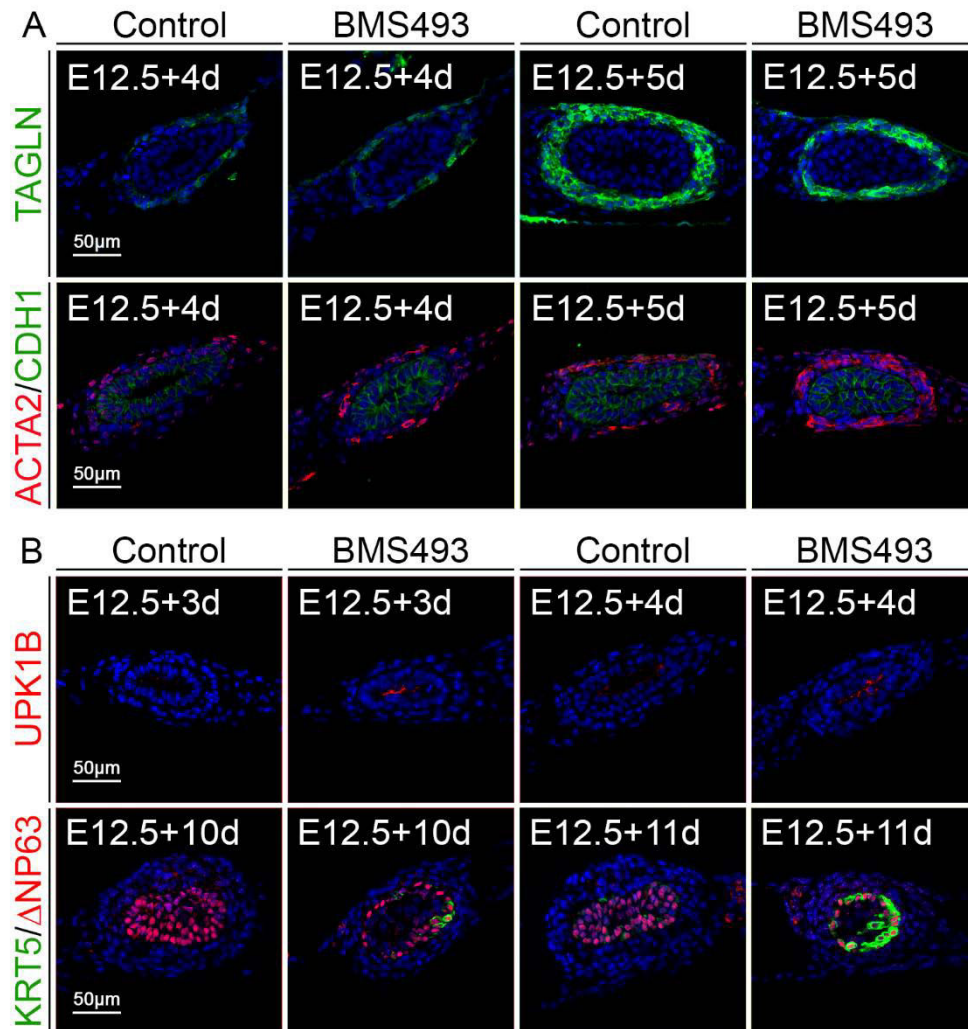


Figure 5: RA signaling prevents precocious differentiation in the ureter. (A) Immunofluorescence analysis for TAGLN (upper row) and co-immunofluorescence analysis of ACTA/CDH1 (lower row) on E12.5 ureter explants that were cultured for 3 and 4 days in presence of DMSO or 1 µM BMS493. (B) Immunofluorescence analysis for UPK1B (upper row) and co-immunofluorescence analysis of KRT5/ANP63 (lower row) on E12.5 ureter explants that were culture for 3 and 4 days (UPK1B) or 10 and 11 days (KRT5/ANP63) in the presence of DMSO or 1 µM BMS493.

Characterization of the RA-responsive transcriptome in early ureter development

To get more insights into the phenotypic changes and the underlying molecular program that is controlled by RA signaling in the early ureter, we treated E12.5 ureters with 1 μ M BMS493 or 1 μ M RA for 18 h and performed microarray analysis of differential gene expression compared to untreated controls. We first addressed our hypothesis that RA signaling maintains the progenitor status in the mesenchymal and epithelial compartments of the ureter by examining transcripts that were negatively regulated by RA signaling (Figure 6A, Supplemental Table 4). Among the most affected transcripts were several cytokeratins which are known to be expressed in urothelial B-cells, including *Krt6b*, *Krt6a*, *Krt14* and *Krt5* [2, 22, 23] as well as transcripts encoding for structural components of SMCs, including *Actg2*, *Acta1*, *Actc1* and *Tagln* (Figure 6B, Supplemental Table 4) confirming a functional requirement of RA signaling in preventing precocious cell differentiation in the ureter.

To identify potential RA target genes that may account for this function, we next focused on positively regulated transcripts (Figure 6C, Supplemental Table 5). Among the most deregulated transcripts were the well-established RA target genes *Dhrs3* and *Rarb* (Figure 6D; Supplemental Table 5) [16, 24]. To validate the RA-responsive expression of candidate genes and to characterize their spatial confinement we performed RNA *in situ* hybridization analysis on explants of E11.5 kidney and ureter rudiments cultured for 1 day in the presence of 1 μ M BMS493 or 1 μ M RA (Figure 6E). As previously shown *Rarb* expression in the ureteric mesenchyme and renal stroma was strongly RA dependent. To our surprise, some genes including *Tnfsf13b*, *Il33*, *Ecm1* and *Hic1* were expressed in the renal stroma but not in the ureter of control explants. BMS493 treatment abolished expression of these genes, while RA treatment enhanced stromal expression and induced expression in the ureteric mesenchyme. Expression of *Tgm5* and *Shisa3* was strong in the ureteric mesenchyme of control explants. BMS493 abolished, RA treatment slightly enhanced this expression. The weak expression of *Shisa3* in the ureteric epithelium and renal collecting ducts was not RA-responsive. *Tgm2* showed a weak and ubiquitous expression in control explants which was slightly reduced upon BMS493 treatment. Administration of RA augmented the overall expression level of *Tgm2* and induced a strong expression in the ureteric mesenchyme. Expression of *Elf5* was restricted to the epithelium of the nephric duct, the ureter and the collecting ducts and was strongly reduced and enhanced upon BMS493 and RA treatment, respectively.

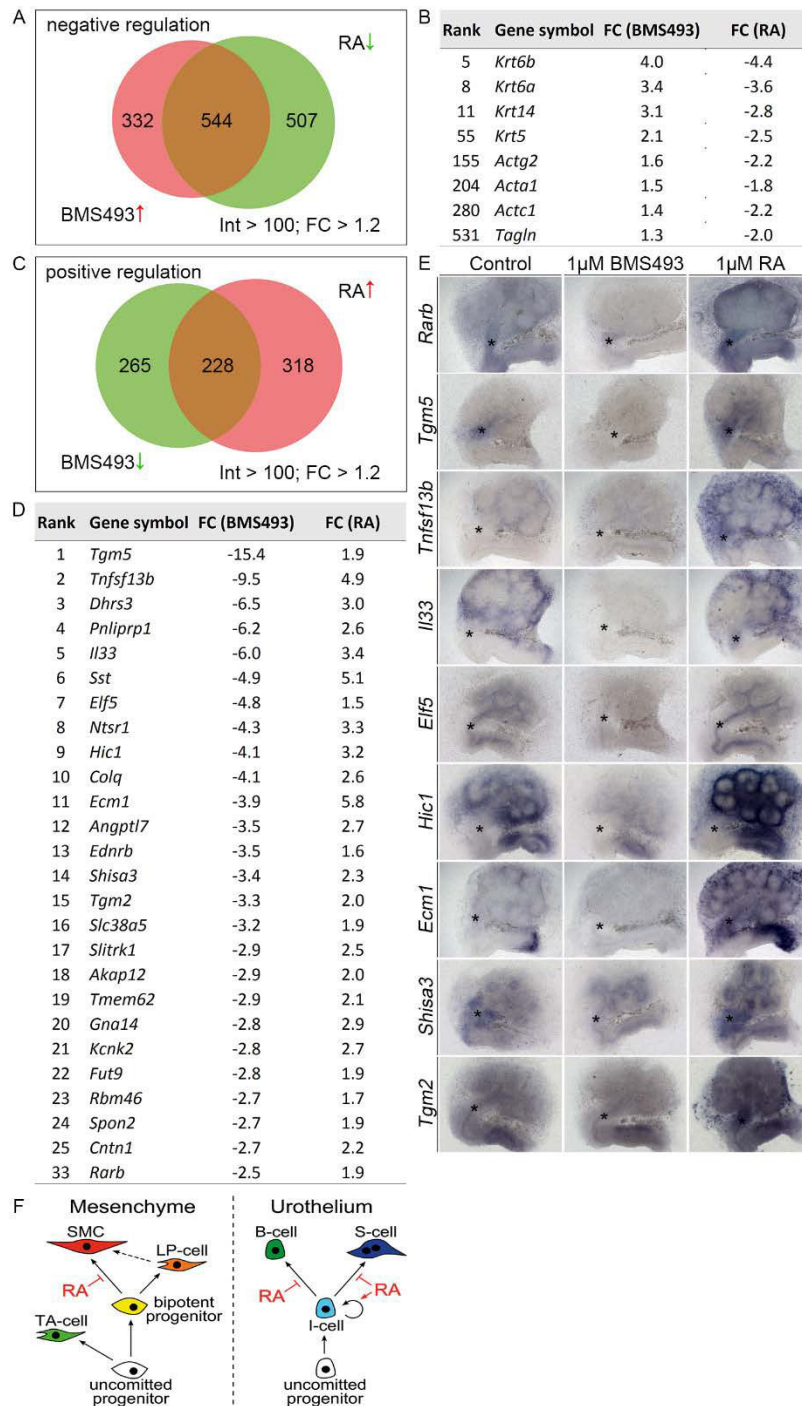


Figure 6: Identification of RA-responsive genes in microarray experiments. Summary of the results from the microarray analysis of E12.5 ureters explanted and treated with DMSO or 1 μ M BMS493 or 1 μ M RA for 18 h filtered with an intensity (Int) threshold of 100 and a fold change (FC) cut-off of 1.2. (A) The Venn diagram displays transcripts that were negatively regulated by RA signaling, i.e. up-regulated upon BMS493 treatment (876, red) or down-regulated upon RA treatment (1051, green). The intersection shows the common group of negatively regulated transcripts (544). (B) Selected differentiation markers of urothelial cells and SMCs which were negatively regulated by RA signaling. Genes were ranked according to their average FC up-regulation upon BMS493 treatment. (C) The Venn diagram displays transcripts which were positively regulated by RA signaling, i.e. down-regulated upon BMS493 treatment (493, green) or up-regulated upon RA treatment (546, red). The intersection shows the common group of positively regulated transcripts (228). (D) Top 25 of the common positively regulated genes were ranked according to their FC down-regulation upon BMS493 treatment. (E) *In situ* hybridization analysis of expression of selected genes which were positively regulated by RA signaling on E11.5 kidney explant cultures, treated with 1 μ M BMS493 or 1 μ M RA for 1 day. (F) Schematic illustration of RA signaling function in the maintenance of ureteric progenitors. In the ureteric mesenchyme (left) uncommitted progenitors diversify into adventitial fibrocytes (AF-cells) and bipotent progenitors of SMCs and lamina propria fibrocytes (LP-cells). RA specifically acts in the bipotent progenitors to prevent precocious differentiation towards the SMC lineage. In the ureteric epithelium (right) uncommitted progenitors give rise to I-cells which are maintained by RA signaling by preventing precocious differentiation towards the B- and S-cell lineage.

Discussion

RA signaling is required for the spatiotemporal control of ureteric SMC differentiation

Ureteric SMCs arise in a temporally and spatially tightly controlled manner from the adluminal mesenchymal cell layer. Differentiation starts around E15.5 in the proximal region of the ureter and progresses distally within the following day [2]. The program depends on epithelial signals, SHH and members of WNT family, that activate autocrine BMP4 signaling in the mesenchymal compartment [4-6]. Intriguingly all of these signaling pathways are active from E11.5 onwards but culminate at E14.5 only in transcriptional activation of *Myocd*, which encodes the master regulator of the SMC differentiation program [25]. While it is conceivable that the delayed expression of *Myocd* results from a gradual build-up of positive signaling inputs, an alternative scenario features the presence of inhibitory activities in the undifferentiated ureteric mesenchyme.

Our findings suggest that RA constitutes such an inhibitory signal that acts in the undifferentiated ureteric mesenchyme to temporally and spatially restrict differentiation, possibly through modulation of the WNT signaling pathway. A comprehensive expression analysis of components and target genes of the pathway revealed that RA signaling is active in the ureteric mesenchyme from E11.5 to E14.5, i.e. until the onset of SMC differentiation. Moreover, RA producing enzyme genes *Aldh1a2* and *Aldh1a3* were transiently expressed in the proximal ureter but maintained in its distal aspect in line with the delayed onset of SMC differentiation at this site. Furthermore, our pharmacological loss- and gain-of-function experiments delimited the functional requirement of RA to the interval E11.5 to E14.5. A relative expansion of SMCs at the expense of lamina propria fibrocytes under RA loss-of-function conditions suggests that the mesenchymal progenitors of the ureter prematurely and preferentially differentiated towards the SMC lineage. This hypothesis was further supported by the relative expansion of lamina propria fibrocytes under RA gain-of-function conditions. Importantly, the analysis of differentiation markers revealed a precocious differentiation of SMCs when RA signaling was inhibited.

Microarray analysis characterized the RA-responsive transcriptome in the early ureter. Interestingly, a considerable number of identified genes including *Tgm5*, *Tnfsf13b*, *Il33*, *Elf5* and *Ecm1* were previously reported to be RA-responsive in a similar assay performed for the renal stroma of the embryonic kidney [14]. *Tnfsf13b* and *Il33* activate NF κ B signaling and have been

reported to control renal branching morphogenesis, while *Ecm1* exerts a similar function via control of GDNF/RET signaling [13, 14]. The present study newly identified the RA-responsive expression of two genes encoding antagonists of the WNT signaling pathway in the ureter. *Hic1* encodes for a transcriptional repressor that attenuates canonical WNT signaling by sequestration of TCF-4 and CTNNB1 in specific nuclear compartments [26]. *Sisha3* encodes a member of the SHISA family of proteins that inhibit WNT signaling by retention of WNT receptors in the endoplasmic reticulum and/or by promoting CTNNB1 degradation [27, 28]. Thus, a negative modulation of mesenchymal WNT signaling by RA represents a potential molecular mechanism to control the timing of ureteric SMC differentiation.

Since uncommitted mesenchymal progenitors first diversify into adventitial fibrocytes and bipotent progenitors of SMCs and lamina propria fibrocytes, we conclude that RA is specifically required in the bipotent progenitor to prevent precocious differentiation towards the SMC lineage. The late re-expression of *Ald1a2* in the lamina propria suggests that this cell population constitutes a SMC progenitor in homeostasis and regeneration (Figure 6 F).

RA signaling maintains urothelial progenitors by preventing precocious differentiation

Our previous work has shown that I-cells arise in the ureteric epithelium at E13.5 and differentiate into S-cells and B-cells at E15.5 and E16.5, respectively [2]. How this strict temporal sequence of differentiation is molecularly regulated has remained elusive. Studies in the developing and regenerating bladder urothelium reported a function of RA signaling in urothelial specification of endodermal precursors [15]. Given the distinct developmental origin of the ureter urothelium from the intermediate mesoderm, it has remained unclear whether this finding also accounts for the ureter. The present study suggests that RA signaling in the ureter urothelium is involved in the temporal control of cellular differentiation rather than in the specification of progenitor cells. First, pharmacological inhibition of RA signaling in ureter explant cultures between E11.5 and E14.5 resulted in a relative expansion of S-cells at the expense of I-cells. Moreover, compared to control specimens S-cells and B-cells differentiated one day earlier under RA loss-of-function conditions. Second, pharmacological overactivation of RA signaling between E11.5 and E14.5 reduced S-cell differentiation, completely blocked B-cell differentiation and resulted in an expansion of I-cells. Even at later time points excessive RA was sufficient to decrease the abundance of B-cells and to expand I-cells.

Part 4 - RA signaling in ureter development

A negative effect of RA signaling on epithelial differentiation and especially on the expression of cytokeratins has been reported in the context of keratinocytes, tracheal and bronchial epithelial cells and the salivary gland epithelium [29-31]. *In vitro* studies of the *Krt5* and *Krt14* promoter identified an unconventional mechanism of RA-mediated direct transcriptional repression that involves ligand bound homodimers of RARs [32]. The precocious upregulation of several cytokeratin genes under RA loss-of-function conditions indicates that such a mechanism may be utilized to control the timing of B-cell differentiation in the urothelium. Alternatively, RA may maintain urothelial progenitors indirectly via intermediate factors. Our transcriptome analysis revealed RA-dependent expression of *Elf5* in the undifferentiated ureteric epithelium. The paralogous gene *Elf3* has been reported to activate urothelial differentiation downstream of PPARG signaling [33]. Recent *in vitro* studies identified an enrichment of ELF5 binding sites in regulatory elements of urothelial differentiation genes [34]. Interestingly, misexpression of *Elf5* in the lung epithelium interferes with terminal differentiation [35]. Moreover, *Elf5* regulates stem cell self-renewal and counteracts precocious differentiation in the trophoblast [36, 37]. It is conceivable that, in contrast to *Elf3*, *Elf5* negatively regulates the urothelial differentiation program.

We conclude that RA signaling acts specifically in the urothelial progenitor, the I-cell, to prevent precocious differentiation of B- and S-cells and to control progenitor self-renewal and maintenance in development and homeostasis (Figure 6 F).

Concise methods

Mice

Gt(ROSA)26So^{tm4}(ACTB-tdTomato-EGFP)Luo (synonym: *R26^{mTmG}*) [20] and *Tbx18^{tm4(cre)Akis}* (synonym: *Tbx18^{cre}*) [21] mouse lines were maintained on an NMRI outbred background. Embryos for gene expression and microarray analysis were derived from matings of NMRI wildtype mice. *Tbx18^{cre/+};R26^{mTmG/+}* embryos were obtained from mating *Tbx18^{cre/+}* males with *R26^{mTmG/mTmG}* females. For timed pregnancies, vaginal plugs were checked in the morning after mating, and noon was defined as embryonic day (E) 0.5. Embryos and urogenital systems were dissected in PBS. Specimens were fixed in 4% PFA/PBS, transferred to methanol and stored at -20°C prior to immunofluorescence or *in situ* hybridization analyses. PCR genotyping was performed on genomic DNA prepared from yolk sac or tail biopsies. All animal work conducted for this study was performed according to European and German legislation.

Organ cultures

Cultures of embryonic ureter and kidney explants were performed as described [2]. BMS493 (#3509, Tocris) or RA (#0695, Tocris) were dissolved in DMSO and added to the medium at a final concentration of 1 μM. Culture medium was replaced every day.

Histological analysis

Embryos, urogenital systems or explant cultures were paraffin-embedded and the proximal ureter was sectioned to 5 μm. Hematoxylin and eosin staining was performed according to standard procedures.

In situ hybridization analysis

Whole-mount *in situ* hybridization was performed following a standard procedure with digoxigenin-labeled antisense riboprobes [38]. Stained specimens were transferred in 80% glycerol prior to documentation. *In situ* hybridization on 10-μm paraffin sections was performed essentially as described [39]. For each marker, at least three independent specimens were analyzed.

Part 4 - RA signaling in ureter development

Immunofluorescent detection of antigens

Immunofluorescent analysis on 5- μ m paraffin sections was done as described [2]. At least three embryos of each genotype were used for each analysis.

Cell proliferation and apoptosis assay

Cell proliferation rates in explant cultures (n=3 per condition) were investigated by the detection of incorporated BrdU on 5 μ m paraffin sections similar to published protocols [40]. Explant cultures were incubated for 2 h with 3.3 μ g/ml BrdU in the culture medium. For each specimen 12 sections of the proximal ureter were assessed. The BrdU-labeling index was defined as the number of BrdU-positive nuclei relative to the total number of nuclei as detected by 4',6-diamidino-2-phenylindole (DAPI) counterstaining in arbitrarily defined compartments of the ureter. Data were expressed as mean \pm standard deviation. Apoptosis was analyzed on 5 μ m paraffin sections using the ApopTag Plus Fluorescein *In Situ* Apoptosis Detection Kit (Chemicon).

Microarray

Three independent pools of 50 E12.5 ureters were cultured with DMSO or 1 μ M BMS493 or 1 μ M RA for 18 h. Total RNA was extracted with peqGOLD RNApure (PeqLab) and was sent to the Research Core Unit Transcriptomics of Hannover Medical School where RNA was Cy3-labeled and hybridized to Agilent Whole Mouse Genome Oligo v2 (4x44K) Microarrays. To identify differentially expressed genes, normalized expression data was filtered using Excel based on an intensity threshold of 100 and a more than 1.2 fold change in all pools.

Image documentation

Sections and organ cultures were photographed using a Leica DM5000 microscope with Leica DFC300FX digital camera or a Leica DM6000 microscope with Leica DFC350FX digital camera. Figures were prepared with Adobe Photoshop CS4.

References

1. Velardo JT. Histology of the Ureter. In: Bergman H, editor. *The Ureter*. 2nd ed. New York: Springer-Verlag; 1981.
2. Bohnenpoll T, Feraric S, Nattkemper M, Weiss AC, Rudat C, Meuser M, et al. Diversification of Cell Lineages in Ureter Development. *J Am Soc Nephrol*. 2016.
3. Miyazaki Y, Oshima K, Fogo A, Ichikawa I. Evidence that bone morphogenetic protein 4 has multiple biological functions during kidney and urinary tract development. *Kidney Int*. 2003;63(3):835-44.
4. Trowe MO, Airik R, Weiss AC, Farin HF, Foik AB, Bettenhausen E, et al. Canonical Wnt signaling regulates smooth muscle precursor development in the mouse ureter. *Development*. 2012;139(17):3099-108.
5. Wang GJ, Brenner-Anantharam A, Vaughan ED, Herzlinger D. Antagonism of BMP4 signaling disrupts smooth muscle investment of the ureter and ureteropelvic junction. *J Urol*. 2009;181(1):401-7.
6. Yu J, Carroll TJ, McMahon AP. Sonic hedgehog regulates proliferation and differentiation of mesenchymal cells in the mouse metanephric kidney. *Development*. 2002;129(22):5301-12.
7. Duester G. Retinoid signaling in control of progenitor cell differentiation during mouse development. *Semin Cell Dev Biol*. 2013;24(10-12):694-700.
8. Rhinn M, Dolle P. Retinoic acid signalling during development. *Development*. 2012;139(5):843-58.
9. Pennimpede T, Cameron DA, MacLean GA, Li H, Abu-Abed S, Petkovich M. The role of CYP26 enzymes in defining appropriate retinoic acid exposure during embryogenesis. *Birth Defects Res A Clin Mol Teratol*. 2010;88(10):883-94.
10. Balmer JE, Blomhoff R. Gene expression regulation by retinoic acid. *J Lipid Res*. 2002;43(11):1773-808.
11. Rochette-Egly C, Germain P. Dynamic and combinatorial control of gene expression by nuclear retinoic acid receptors (RARs). *Nucl Recept Signal*. 2009;7:e005.
12. Batourina E, Tsai S, Lambert S, Sprengle P, Viana R, Dutta S, et al. Apoptosis induced by vitamin A signaling is crucial for connecting the ureters to the bladder. *Nat Genet*. 2005;37(10):1082-9.
13. Paroly SS, Wang F, Spraggon L, Merregaert J, Batourina E, Tycko B, et al. Stromal protein *Ecm1* regulates ureteric bud patterning and branching. *PLoS One*. 2013;8(12):e84155.
14. Takayama M, Miyatake K, Nishida E. Identification and characterization of retinoic acid-responsive genes in mouse kidney development. *Genes Cells*. 2014;19(8):637-49.

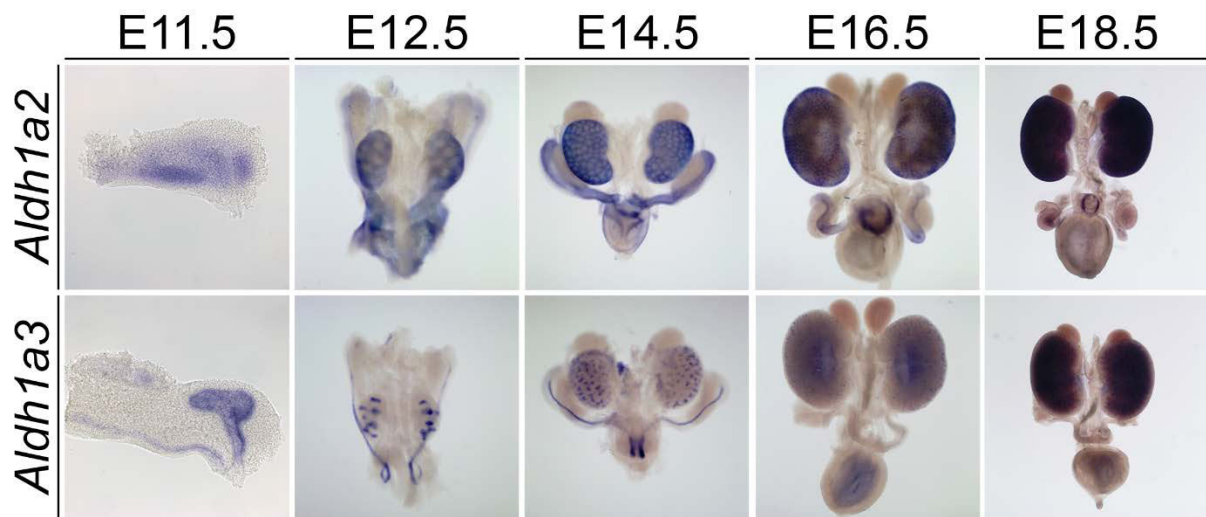
Part 4 - RA signaling in ureter development

15. Gandhi D, Molotkov A, Batourina E, Schneider K, Dan H, Reiley M, et al. Retinoid signaling in progenitors controls specification and regeneration of the urothelium. *Dev Cell*. 2013;26(5):469-82.
16. Mendelsohn C, Ruberte E, LeMeur M, Morriss-Kay G, Chambon P. Developmental analysis of the retinoic acid-inducible RAR-beta 2 promoter in transgenic animals. *Development*. 1991;113(3):723-34.
17. Chazaud C, Dolle P, Rossant J, Mollard R. Retinoic acid signaling regulates murine bronchial tubule formation. *Mech Dev*. 2003;120(6):691-700.
18. Airik R, Bussen M, Singh MK, Petry M, Kispert A. Tbx18 regulates the development of the ureteral mesenchyme. *J Clin Invest*. 2006;116(3):663-74.
19. Bohnenpoll T, Bettenhausen E, Weiss AC, Foik AB, Trowe MO, Blank P, et al. Tbx18 expression demarcates multipotent precursor populations in the developing urogenital system but is exclusively required within the ureteric mesenchymal lineage to suppress a renal stromal fate. *Dev Biol*. 2013;380(1):25-36.
20. Muzumdar MD, Tasic B, Miyamichi K, Li L, Luo L. A global double-fluorescent Cre reporter mouse. *Genesis*. 2007;45(9):593-605.
21. Trowe MO, Shah S, Petry M, Airik R, Schuster-Gossler K, Kist R, et al. Loss of Sox9 in the periotic mesenchyme affects mesenchymal expansion and differentiation, and epithelial morphogenesis during cochlea development in the mouse. *Dev Biol*. 2010;342(1):51-62.
22. Choi W, Porten S, Kim S, Willis D, Plimack ER, Hoffman-Censits J, et al. Identification of distinct basal and luminal subtypes of muscle-invasive bladder cancer with different sensitivities to frontline chemotherapy. *Cancer Cell*. 2014;25(2):152-65.
23. Tai G, Ranjzad P, Marriage F, Rehman S, Denley H, Dixon J, et al. Cytokeratin 15 marks basal epithelia in developing ureters and is upregulated in a subset of urothelial cell carcinomas. *PLoS One*. 2013;8(11):e81167.
24. Feng L, Hernandez RE, Waxman JS, Yelon D, Moens CB. Dhhrs3a regulates retinoic acid biosynthesis through a feedback inhibition mechanism. *Dev Biol*. 2010;338(1):1-14.
25. Wang Z, Wang DZ, Pipes GC, Olson EN. Myocardin is a master regulator of smooth muscle gene expression. *Proc Natl Acad Sci U S A*. 2003;100(12):7129-34.
26. Valenta T, Lukas J, Doubravska L, Fafulek B, Korinek V. HIC1 attenuates Wnt signaling by recruitment of TCF-4 and beta-catenin to the nuclear bodies. *EMBO J*. 2006;25(11):2326-37.
27. Chen CC, Chen HY, Su KY, Hong QS, Yan BS, Chen CH, et al. Shisa3 is associated with prolonged survival through promoting beta-catenin degradation in lung cancer. *Am J Respir Crit Care Med*. 2014;190(4):433-44.
28. Yamamoto A, Nagano T, Takehara S, Hibi M, Aizawa S. Shisa promotes head formation through the inhibition of receptor protein maturation for the caudalizing factors, Wnt and FGF. *Cell*. 2005;120(2):223-35.

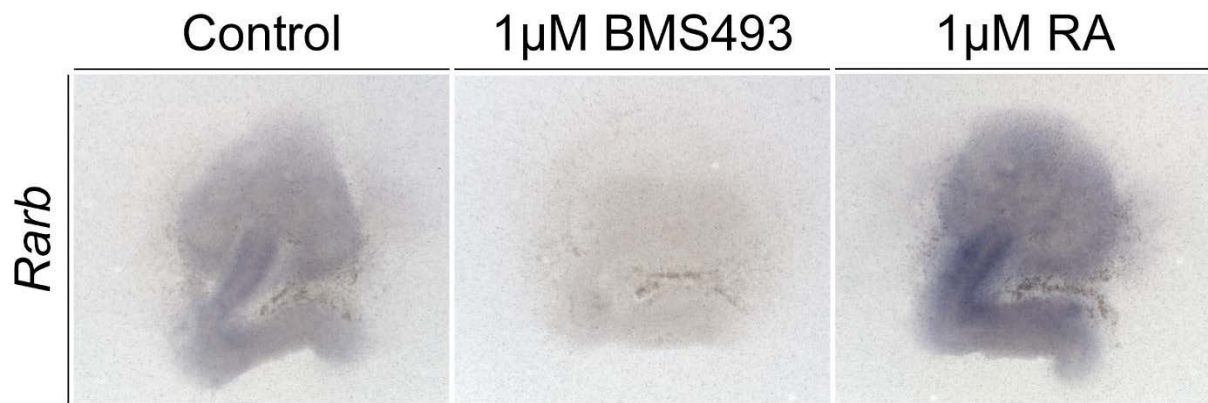
29. Abashev TM, Metzler MA, Wright DM, Sandell LL. Retinoic acid signaling regulates Krt5 and Krt14 independently of stem cell markers in submandibular salivary gland epithelium. *Dev Dyn*. 2017;246(2):135-47.
30. Gilfix BM, Eckert RL. Coordinate control by vitamin A of keratin gene expression in human keratinocytes. *J Biol Chem*. 1985;260(26):14026-9.
31. Lee HY, Dawson MI, Walsh GL, Nesbitt JC, Eckert RL, Fuchs E, et al. Retinoic acid receptor- and retinoid X receptor-selective retinoids activate signaling pathways that converge on AP-1 and inhibit squamous differentiation in human bronchial epithelial cells. *Cell Growth Differ*. 1996;7(8):997-1004.
32. Jho SH, Vouthounis C, Lee B, Stojadinovic O, Im MJ, Brem H, et al. The book of opposites: the role of the nuclear receptor co-regulators in the suppression of epidermal genes by retinoic acid and thyroid hormone receptors. *J Invest Dermatol*. 2005;124(5):1034-43.
33. Bock M, Hinley J, Schmitt C, Wahlicht T, Kramer S, Southgate J. Identification of ELF3 as an early transcriptional regulator of human urothelium. *Dev Biol*. 2014;386(2):321-30.
34. Fishwick C, Higgins J, Percival-Alwyn L, Hustler A, Pearson J, Bastkowski S, et al. Heterarchy of transcription factors driving basal and luminal cell phenotypes in human urothelium. *Cell Death Differ*. 2017.
35. Metzger DE, Stahlman MT, Shannon JM. Misexpression of ELF5 disrupts lung branching and inhibits epithelial differentiation. *Dev Biol*. 2008;320(1):149-60.
36. Latos PA, Sienerth AR, Murray A, Senner CE, Muto M, Ikawa M, et al. Elf5-centered transcription factor hub controls trophoblast stem cell self-renewal and differentiation through stoichiometry-sensitive shifts in target gene networks. *Genes Dev*. 2015;29(23):2435-48.
37. Pearton DJ, Smith CS, Redgate E, van Leeuwen J, Donnison M, Pfeffer PL. Elf5 counteracts precocious trophoblast differentiation by maintaining Sox2 and 3 and inhibiting Hand1 expression. *Dev Biol*. 2014;392(2):344-57.
38. Wilkinson DG, Nieto MA. Detection of messenger RNA by in situ hybridization to tissue sections and whole mounts. *Methods Enzymol*. 1993;225:361-73.
39. Moorman AF, Houweling AC, de Boer PA, Christoffels VM. Sensitive nonradioactive detection of mRNA in tissue sections: novel application of the whole-mount in situ hybridization protocol. *J Histochem Cytochem*. 2001;49(1):1-8.
40. Bussen M, Petry M, Schuster-Gossler K, Leitges M, Gossler A, Kispert A. The T-box transcription factor Tbx18 maintains the separation of anterior and posterior somite compartments. *Genes Dev*. 2004;18(10):1209-21.

Supplementary Material

Supplementary Figures

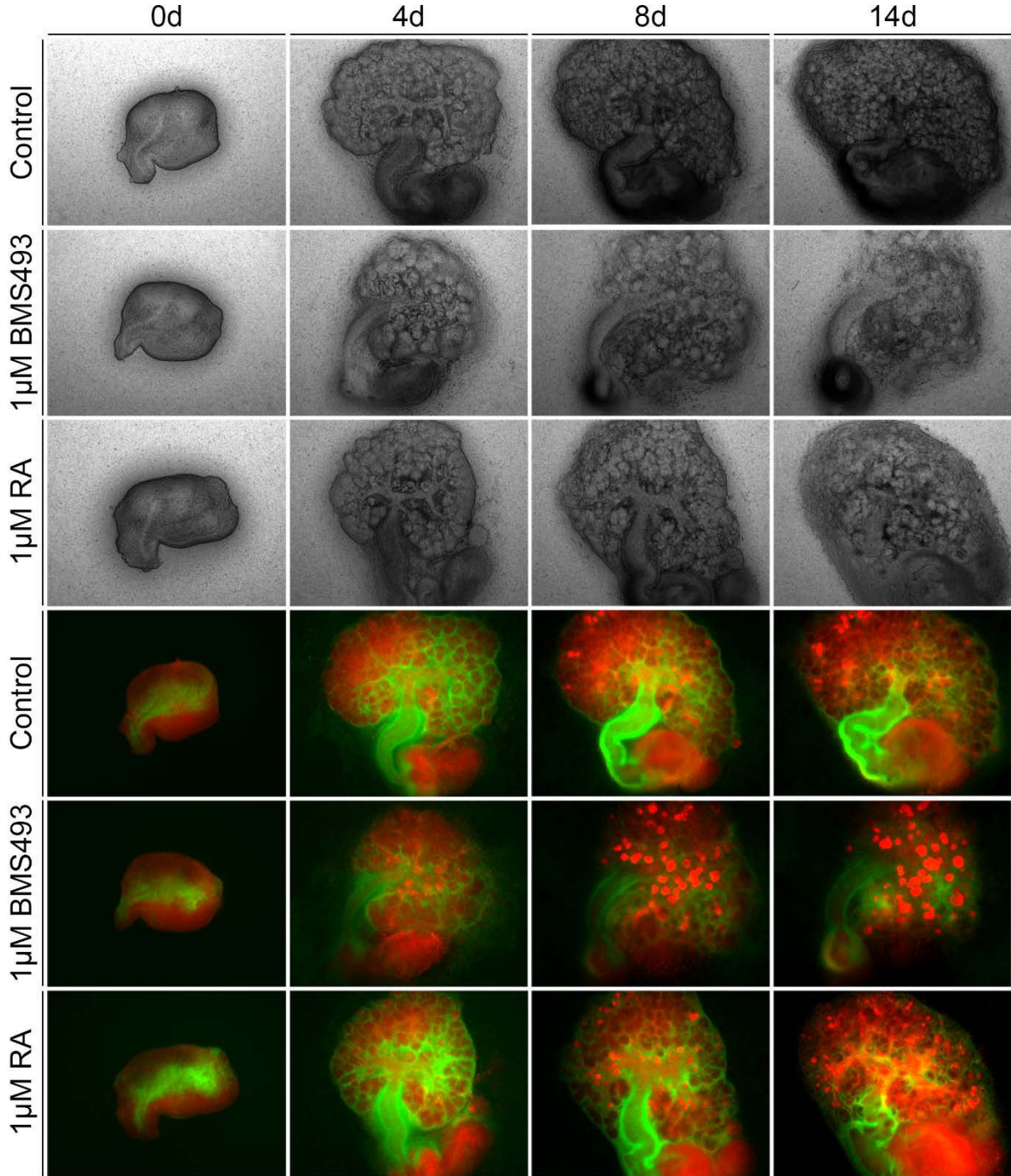


Supplemental Figure 1: *Aldh1a2* and *Aldh1a3* are expressed in urogenital system development. Expression analysis by whole mount *in situ* hybridization of *Aldh1a2* and *Aldh1a3* on E11.5 kidney rudiments and E12.5, E14.5, E16.5 and E18.5 whole urogenital systems. *Aldh1a2* expression is found in the prospective ureteric mesenchyme at E11.5. At subsequent stages expression is confined to the distal ureteric mesenchyme at the ureter-bladder junction and to the renal stroma. *Aldh1a3* is expressed in the nephric duct from E11.5 to E14.5, the distal ureteric epithelium from E11.5 to E14.5 and to the ureteric tip and collecting duct system, respectively, from E11.5 to E18.5.

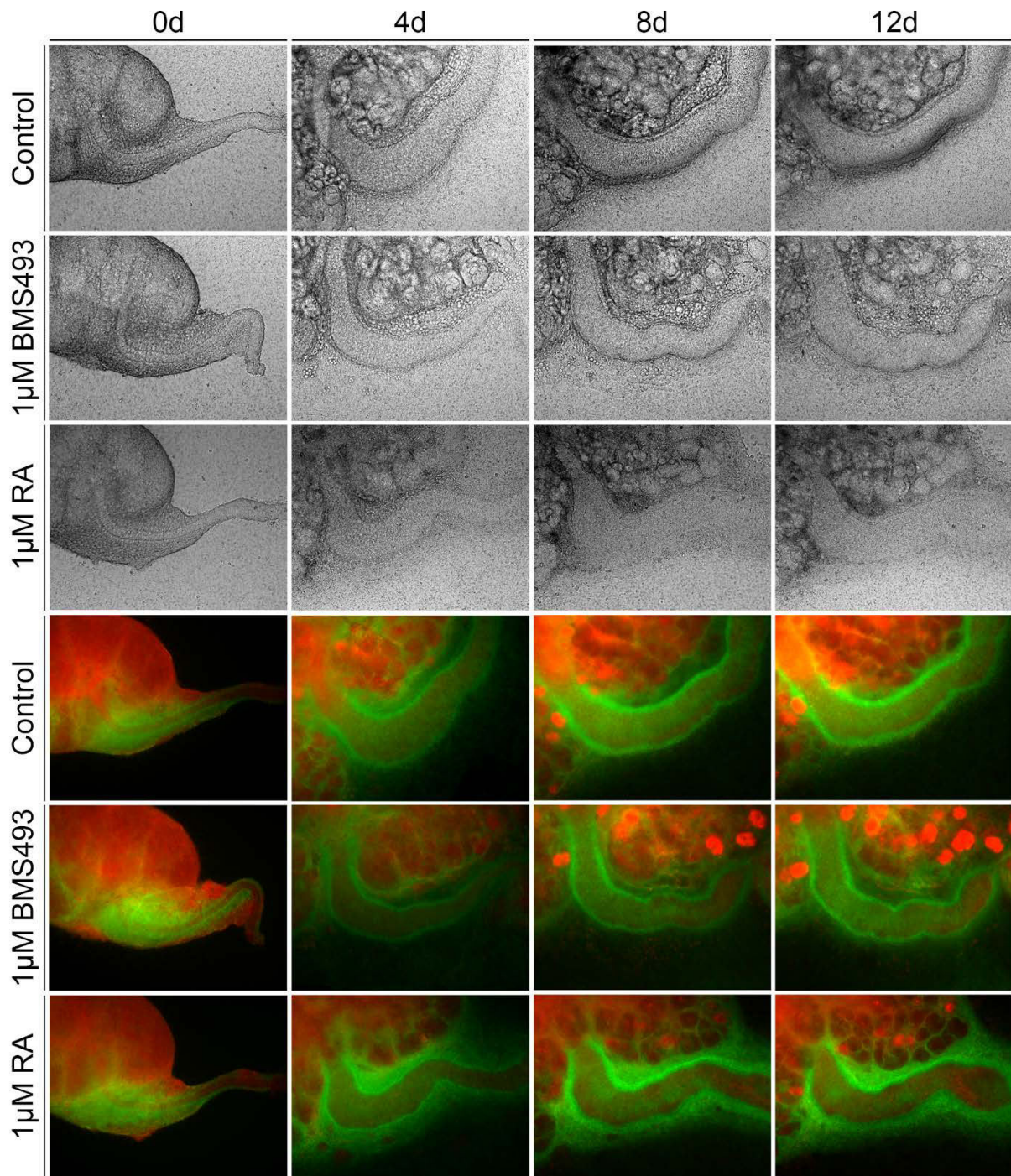


Supplemental Figure 2: 1 μM BMS493 or 1 μM RA are sufficient to inhibit or activate RA signaling in kidney explant cultures. E11.5 kidney rudiments were cultured for 18 h in the presence of DMSO, 1 μM BMS493 or 1 μM RA and subjected to *in situ* hybridization analysis of expression of the RA receptor and RA target gene *Rarb*. Reduced expression upon BMS493 treatment and increased expression upon RA treatment indicates that these conditions are suitable for the manipulation of RA signaling activity.

Part 4 - RA signaling in ureter development

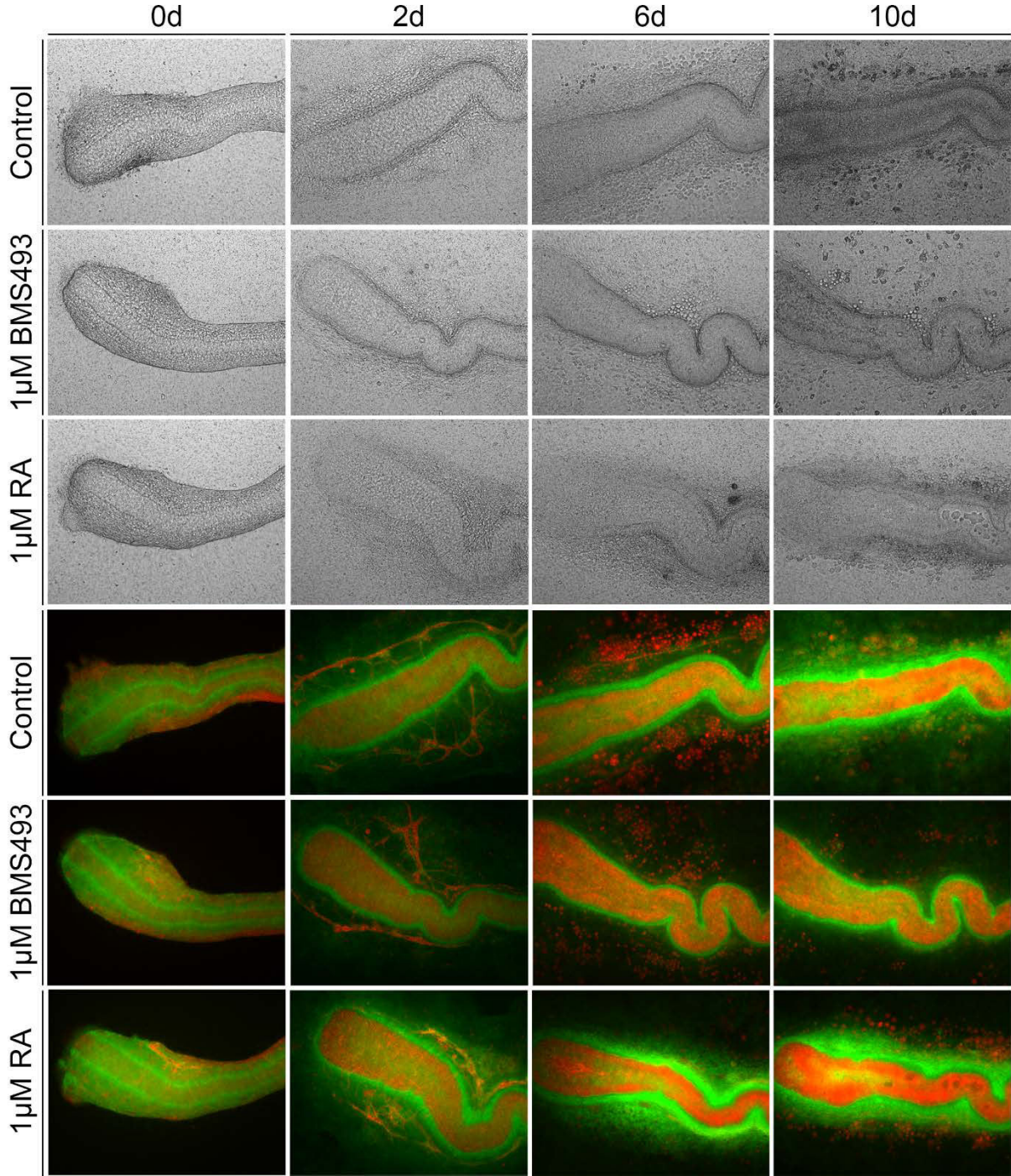


Supplemental Figure 3: Pharmacological manipulation of RA signaling in E11.5 kidney explant cultures. E11.5 *Tbx18^{cre/+};R26^{mTmG/+}* kidney rudiments were explanted and cultured for 14 d in the presence of DMSO, 1 μM BMS493 or 1 μM RA. Brightfield and GFP/RFP epifluorescence images are displayed to visualize explant growth after 0 d, 4 d, 8 d and 14 d of culture under given conditions. GFP expression marks the ureteric mesenchyme and a sub-population of the renal stroma.

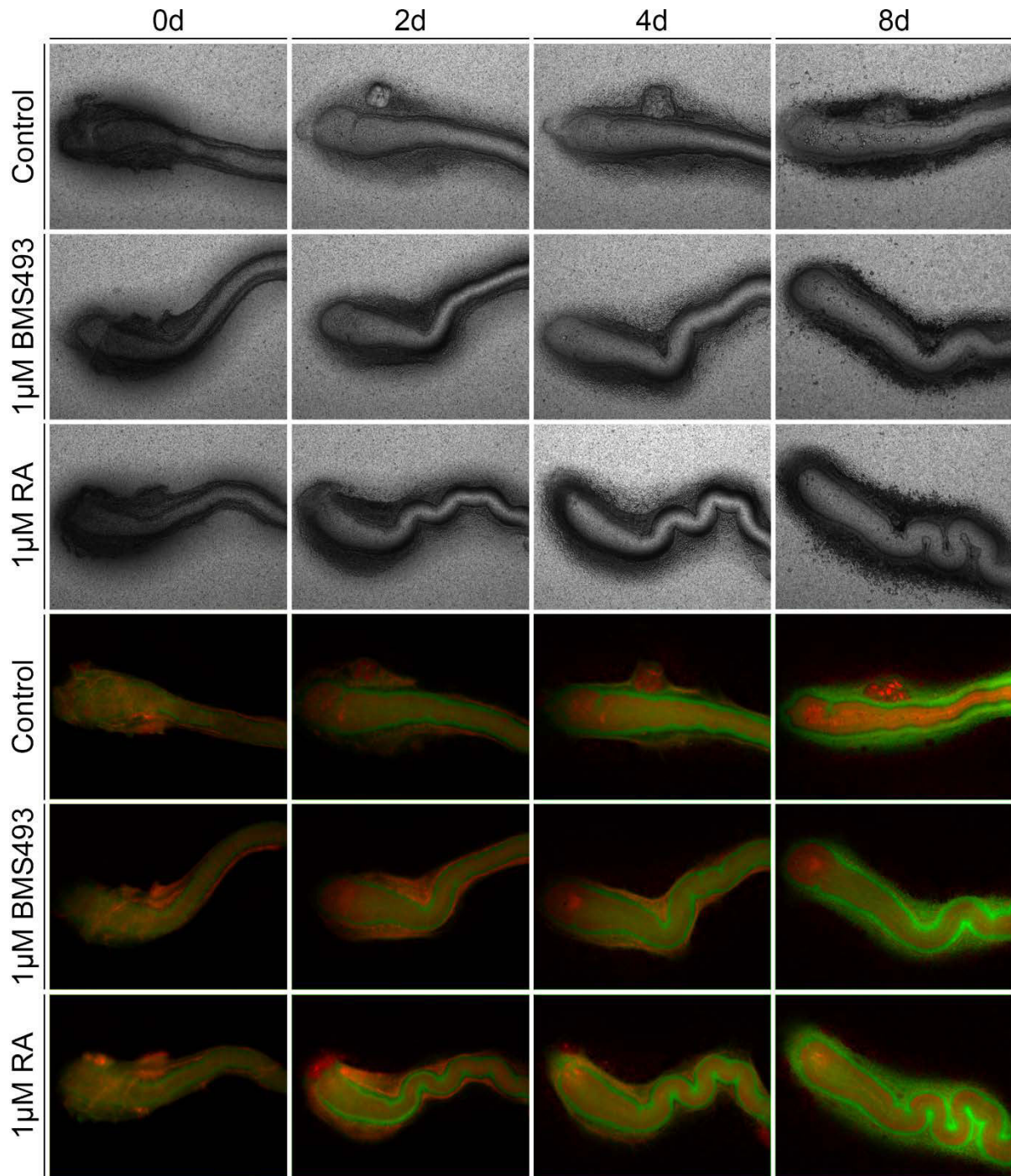


Supplemental Figure 4: Pharmacological manipulation of RA signaling in E12.5 kidney explant cultures. E12.5 *Tbx18^{cre/+};R26^{mTmG/+}* kidney rudiments were explanted and cultured for 12 d in the presence of DMSO, 1 μM BMS493 or 1 μM RA. Brightfield and GFP/RFP epifluorescence images are displayed to visualize explant growth after 0 d, 4 d, 8 d and 12 d of culture under given conditions. GFP expression marks the ureteric mesenchyme and a sub-population of the renal stroma.

Part 4 - RA signaling in ureter development

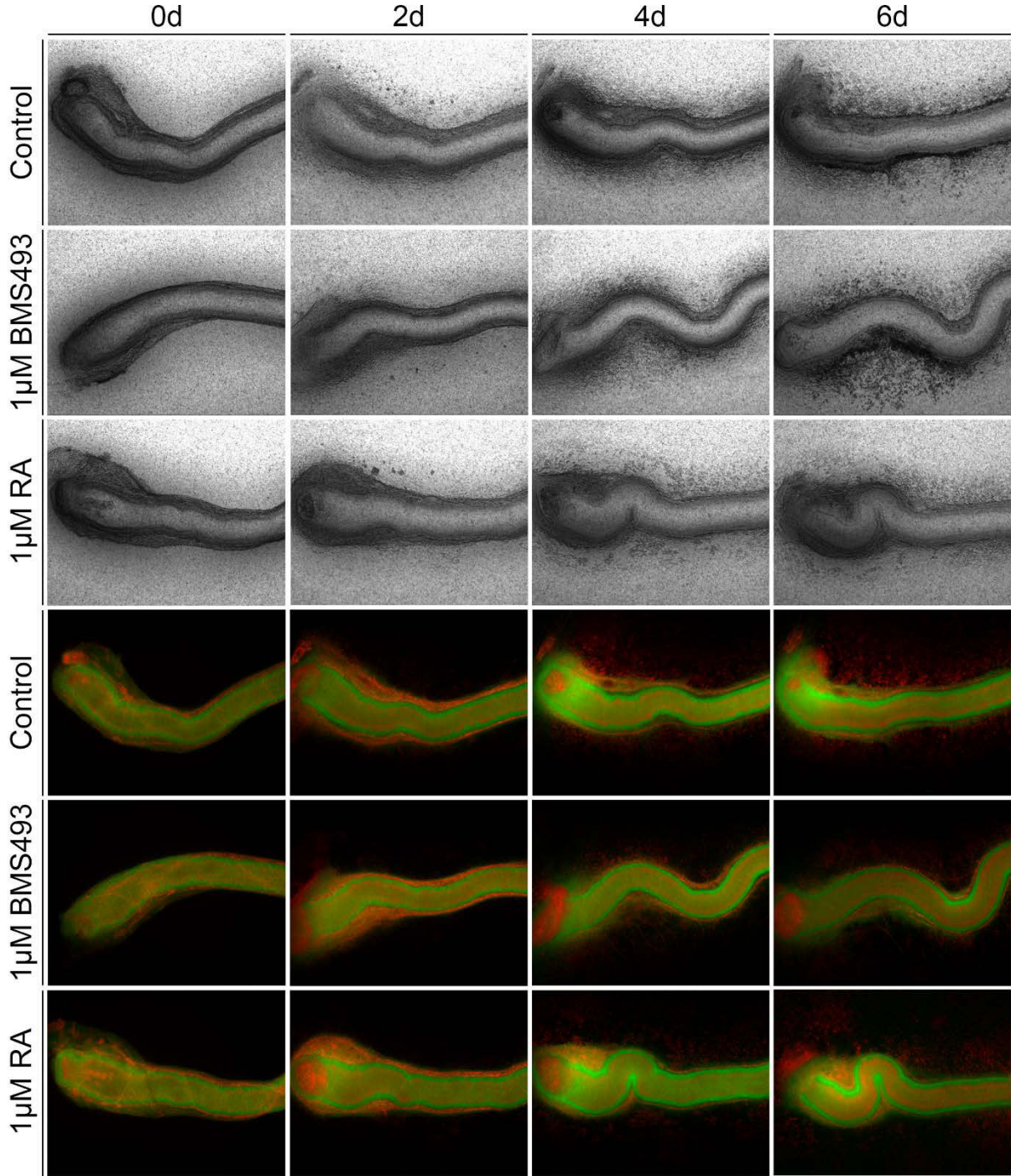


Supplemental Figure 5: Pharmacological manipulation of RA signaling in E14.5 ureter explant cultures. E14.5 *Tbx18^{cre/+};R26^{mTmG/+}* ureters were explanted and cultured for 10 d in the presence of DMSO, 1 μ M BMS493 or 1 μ M RA. Brightfield and GFP/RFP epifluorescence images are displayed to visualize explant growth after 0 d, 2 d, 6 d and 10 d of culture under given conditions. GFP expression marks the ureteric mesenchyme.



Supplemental Figure 6: Pharmacological manipulation of RA signaling in E16.5 ureter explant cultures. E16.5 *Tbx18^{cre/+};R26^{mTmG/+}* ureters were explanted and cultured for 8 d in the presence of DMSO, 1 μM BMS493 or 1 μM RA. Brightfield and GFP/RFP epifluorescence images are displayed to visualize explant growth after 0 d, 2 d, 4 d and 8 d of culture under given conditions. GFP expression marks the ureteric mesenchyme.

Part 4 - RA signaling in ureter development



Supplemental Figure 7: Pharmacological manipulation of RA signaling in E18.5 ureter explant cultures. E18.5 *Tbx18^{cre/+};R26^{mTmG/+}* ureters were explanted and cultured for 6 d in the presence of DMSO, 1 µM BMS493 or 1 µM RA. Brightfield and GFP/RFP epifluorescence images are displayed to visualize explant growth after 0 d, 2 d, 4 d and 6 d of culture under given conditions. GFP expression marks the ureteric mesenchyme.

Supplementary Tables

E11.5 + 14d	A-cells (%)	SM-cells (%)	LP-cells (%)
DMSO	31.6 ± 4.5	44.6 ± 2.6	23.8 ± 3.2
1 μM BMS493	42.4 ± 4.7	53.7 ± 2.6 (p=2.4E-03)	3.9 ± 2.5 (p=6.2E-05)
1 μM RA	37.4 ± 0.6	35.5 ± 2.4 (p=5.4E-03)	27.1 ± 2.4
E12.5 + 12d	A-cells (%)	SM-cells (%)	LP-cells (%)
DMSO	43.5 ± 11.8	40.8 ± 11.7	15.7 ± 2.2
1 μM BMS493	38.1 ± 2.3	56.2 ± 2.1 (p=3.6E-06)	5.7 ± 2.2 (6.1E-05)
1 μM RA	49.5 ± 4.1	30.2 ± 5.2 (p=2.2E-03)	20.3 ± 2.0 (1.0E-02)
E14.5 + 10d	A-cells (%)	SM-cells (%)	LP-cells (%)
DMSO	25.6 ± 3.5	57.9 ± 4.3	16.5 ± 1.1
1 μM BMS493	19.3 ± 2.1 (p=9.2E-03)	70.1 ± 3.0 (p=8.5E-04)	10.6 ± 3.6 (p=7.2E-03)
1 μM RA	28.5 ± 2.8	54.0 ± 5.7	17.5 ± 4.4
E16.5 + 8d	A-cells (%)	SM-cells (%)	LP-cells (%)
DMSO	25.7 ± 2.5	59.5 ± 2.9	14.8 ± 0.8
1 μM BMS493	24.4 ± 2.1	60.5 ± 2.3	15.0 ± 1.6
1 μM RA	24.5 ± 2.1	60.7 ± 2.3	14.8 ± 1.6
E18.5 + 6d	A-cells (%)	SM-cells (%)	LP-cells (%)
DMSO	35.6 ± 2.2	53.0 ± 3.0	11.4 ± 1.3
1 μM BMS493	33.7 ± 3.2	54.0 ± 2.5	12.3 ± 2.9
1 μM RA	35.2 ± 1.4	53.2 ± 1.1	11.6 ± 1.5

Part 4 - RA signaling in ureter development

Supplemental Table 2: Ratios of urothelial cell types under RA loss- and gain-of-function conditions. Values are displayed in % as mean \pm sd of basal cells (B-cells), intermediate cells (I-cells) and superficial cells (S-cells) with respect to the total cell number. Quantification is based on 6 sections of the proximal ureter from 3 individuals of each stage and condition. Student's t-test was applied to test for significant differences between control (DMSO) and test groups (BMS493 or RA). P-values are shown in brackets when $p \leq 0.01$.

E11.5 + 14d	B-cells (%)	I-cells (%)	S-cells (%)
DMSO	35.0 \pm 11.8	62.6 \pm 11.7	2.4 \pm 2.2
1 μ M BMS493	42.0 \pm 7.0	31.5 \pm 10.7 (p=7.2E-04)	26.5 \pm 7.4 (p=1.8E-05)
1 μ M RA	2.0 \pm 1.8 (p=4.8E-05)	95.0 \pm 10.9 (p=4.9E-05)	3.0 \pm 1.2
E12.5 + 12d	B-cells (%)	I-cells (%)	S-cells (%)
DMSO	44.7 \pm 2.3	49.7 \pm 2.3	5.6 \pm 1.5
1 μ M BMS493	45.3 \pm 4.1	25.4 \pm 9.3 (p=2.3E-04)	29.4 \pm 8.2 (p=9.9E-05)
1 μ M RA	6.9 \pm 1.9 (p=3.5E-10)	85.9 \pm 7.1 (p=8.3E-07)	7.1 \pm 5.5
E14.5 + 10d	B-cells (%)	I-cells (%)	S-cells (%)
DMSO	24.3 \pm 5.2	71.5 \pm 7.2	4.2 \pm 3.4
1 μ M BMS493	22.9 \pm 7.9	50.4 \pm 4.9 (p=1.9E-06)	26.7 \pm 5.3 (p=1.2E-08)
1 μ M RA	3.4 \pm 2.9 (p=1.3E-08)	89.2 \pm 4.3 (p=1.1E-05)	7.4 \pm 3.3
E16.5 + 8d	B-cells (%)	I-cells (%)	S-cells (%)
DMSO	53.1 \pm 7.5	44.1 \pm 7.0	2.8 \pm 1.1
1 μ M BMS493	52.3 \pm 6.9	45.3 \pm 7.0	2.3 \pm 0.7
1 μ M RA	32.8 \pm 6.8 (p=1.8E-05)	65.3 \pm 6.7 (p=6.3E-06)	1.9 \pm 0.6
E18.5 + 6d	B-cells (%)	I-cells (%)	S-cells (%)
DMSO	80.4 \pm 3.9	14.6 \pm 3.8	5.0 \pm 1.3
1 μ M BMS493	84.5 \pm 4.4	9.9 \pm 2.8	5.6 \pm 2.2
1 μ M RA	71.3 \pm 2.6 (p=8.4E-04)	22.9 \pm 3.0 (p=2.0E-02)	5.8 \pm 1.2

Part 4 - RA signaling in ureter development

Supplemental Table 3: Proliferation rates in the developing ureter under RA loss- and gain-of-function conditions. Shown are BrdU indices for the inner mesenchymal (IM) and outer mesenchymal compartment (OM) and the ureteric epithelium (E) as mean \pm sd. Quantification is based on 12 sections of the proximal ureter from 3 individuals of each stage and condition. Student's t-test was applied to test for significant differences between control (DMSO) and test groups (BMS493 or RA). ** p=3.350E-05.

E11.5 + 1d	IM	OM	E
DMSO	0.266 \pm 0.045	0.073 \pm 0.022	0.006 \pm 0.021
1 μ M BMS493	0.159 \pm 0.055 **	0.081 \pm 0.033	0.042 \pm 0.04
1 μ M RA	0.261 \pm 0.082	0.077 \pm 0.021	0.032 \pm 0.038
E12.5 + 1d	IM	OM	E
DMSO	0.293 \pm 0.034	0.138 \pm 0.023	0.234 \pm 0.148
1 μ M BMS493	0.265 \pm 0.063	0.136 \pm 0.017	0.166 \pm 0.068
1 μ M RA	0.261 \pm 0.069	0.137 \pm 0.018	0.2 \pm 0.141
E14.5 + 1d	IM	OM	E
DMSO	0.263 \pm 0.061	0.155 \pm 0.020	0.336 \pm 0.024
1 μ M BMS493	0.218 \pm 0.035	0.14 \pm 0.012	0.321 \pm 0.073
1 μ M RA	0.258 \pm 0.046	0.169 \pm 0.037	0.374 \pm 0.052

Part 4 - RA signaling in ureter development

Supplemental Table 4: Transcripts identified by microarray analysis that were negatively regulated by RA in the early ureter. Shown is a list of transcripts that were negatively regulated by RA, i.e. upregulated after BMS493 treatment and down-regulated after RA treatment of E12.5 ureter explants. Three groups for each condition were compared to untreated controls and the resulting fold changes (FC) in expression are displayed. Intensity thresholds were >100 for the BMS493 treated explants; fold changes were larger than 1.2.

Rank	Gene symbol	BMS493 FC 1	BMS493 FC 2	BMS493 FC 3	BMS493 Avg FC	RA FC 1	RA FC 2	RA FC 3	RA Avg FC
1	Corin	4.4	5.3	3.6	4.4	-2.4	-1.8	-1.3	-1.8
2	Pkp1	5.0	4.0	4.2	4.4	-3.6	-3.4	-6.3	-4.4
3	3830417A13Rik	3.8	4.2	4.7	4.2	-5.8	-3.1	-2.9	-4.0
4	S100a4	4.0	4.5	4.0	4.2	-3.7	-2.8	-5.0	-3.8
5	Krt6b	4.4	5.0	2.6	4.0	-2.4	-3.2	-7.8	-4.4
6	Serpib5	4.4	4.6	2.2	3.7	-1.2	-1.8	-9.5	-4.2
7	Col17a1	3.1	4.7	2.9	3.6	-2.1	-1.6	-5.8	-3.2
8	Krt6a	4.0	4.2	2.1	3.4	-2.9	-2.8	-4.9	-3.6
9	Rgcc	3.1	3.5	3.3	3.3	-2.6	-3.9	-6.1	-4.2
10	AK008770	2.6	4.0	3.0	3.2	-1.5	-1.6	-2.0	-1.7
11	Krt14	3.3	3.7	2.3	3.1	-1.7	-2.5	-4.4	-2.8
12	Ly6d	3.2	2.6	2.8	2.9	-1.8	-1.4	-2.7	-2.0
13	Serpine1	3.3	2.9	2.6	2.9	-2.8	-2.5	-7.3	-4.2
14	NrOb1	2.2	2.8	3.5	2.8	-1.3	-1.8	-2.1	-1.7
15	Crlf1	2.7	2.8	2.7	2.7	-1.0	-1.2	-2.7	-1.7
16	Dkk1	2.3	2.6	3.1	2.7	-4.3	-3.5	-4.4	-4.1
17	Gm5476	2.4	3.5	2.1	2.7	-2.0	-2.3	-4.1	-2.8
18	Kcnc2	2.5	2.9	2.5	2.7	-3.0	-2.0	-1.7	-2.2
19	Osr2	3.4	2.6	2.0	2.7	-2.1	-1.4	-2.2	-1.9
20	Ugt2b34	2.3	2.7	3.2	2.7	-4.3	-4.8	-5.0	-4.7
21	Efcab6	2.6	2.9	2.1	2.6	-2.4	-2.4	-2.4	-2.4
22	Ryr3	2.8	2.5	2.5	2.6	-1.6	-1.9	-2.3	-1.9
23	Glis1	2.2	2.4	2.8	2.5	-2.1	-2.0	-1.7	-1.9
24	Mc4r	3.0	2.3	2.2	2.5	-2.6	-2.5	-3.0	-2.7
25	Pcp4l1	2.3	2.4	2.8	2.5	-1.4	-1.2	-1.4	-1.3
26	Penk	2.4	2.2	2.9	2.5	-2.6	-3.2	-3.2	-3.0
27	Rasgrf1	3.4	2.2	2.0	2.5	-8.4	-4.6	-4.9	-5.9
28	Serpina3f	2.2	2.8	2.6	2.5	-1.9	-2.0	-4.5	-2.8
29	Wif1	2.5	2.8	2.3	2.5	-2.4	-2.4	-2.3	-2.4
30	Aard	2.7	2.1	2.3	2.4	-2.2	-2.1	-2.6	-2.3
31	Cbr2	2.8	2.4	2	2.4	-2.3	-2.4	-2.9	-2.5
32	AK137313	2.2	2.4	2.3	2.3	-1.9	-2.2	-1.6	-1.9
33	Col8a1	2.1	2.1	2.8	2.3	-2.7	-5.3	-5.7	-4.6
34	Gm10639	1.8	2.3	2.8	2.3	-2.9	-2.6	-2.7	-2.7
35	Grm7	2	2.7	2.1	2.3	-4.4	-3.7	-4.2	-4.1
36	Higd1c	2.9	2.6	1.4	2.3	-4.9	-4.6	-8.7	-6
37	Lypd3	2.6	2.3	2	2.3	-1.6	-1.4	-2.3	-1.8
38	Serpina3i	2.4	2.7	1.9	2.3	-1.7	-1.7	-5.2	-2.8
39	Slc26a7	2.4	1.9	2.5	2.3	-2.6	-1.7	-2	-2.1
40	8430436N08Rik	2.1	1.9	2.7	2.2	-3.3	-1.4	-7	-3.9
41	C1qtnf7	2.2	2.3	2	2.2	-1.9	-1.6	-1.8	-1.8
42	Cxcl5	1.9	2.4	2.2	2.2	-2.4	-2.1	-4.3	-2.9
43	Gabra1	2.1	1.9	2.5	2.2	-5.3	-5.8	-5.9	-5.7
44	Npy	2.9	2	1.6	2.2	-5.4	-4.9	-5.4	-5.2
45	Nts	2	2.8	1.8	2.2	-3.4	-4	-9.5	-5.6
46	Pde4d	2	2	2.6	2.2	-2.9	-4	-2.2	-3
47	Trim29	2.8	2.2	1.7	2.2	-2.2	-1.4	-3.1	-2.2
48	Vgf	1.9	2.9	1.8	2.2	1	-1.1	-4.6	-1.5
49	Cd55	1.8	2	2.4	2.1	-1.7	-2.1	-1.4	-1.7
50	Dmkn	1.8	2.1	2.3	2.1	-1.6	-1.5	-1.6	-1.6

Part 4 - RA signaling in ureter development

Rank	Gene symbol	BMS493 FC 1	BMS493 FC 2	BMS493 FC 3	BMS493 Avg FC	RA FC 1	RA FC 2	RA FC 3	RA Avg FC
51	Fbp1	2.4	2.4	1.5	2.1	-2.2	-1.7	-2	-2
52	Gsdma	1.9	2	2.3	2.1	-1.5	-1.3	-1.6	-1.5
53	Kcnp4	2.2	2	1.9	2.1	-1.8	-2.7	-3.1	-2.5
54	Krt17	2.3	2.7	1.3	2.1	1.2	-2.1	-6.1	-2.3
55	Krt5	2.4	2.2	1.7	2.1	-2.1	-1.9	-3.7	-2.5
56	Rasd2	1.9	2.6	1.7	2.1	-3.1	-2.5	-2.5	-2.7
57	Rasl10a	2.1	2.1	2	2.1	-1.1	-1.4	-1.5	-1.4
58	Vcam1	2.1	2.2	2	2.1	-2.8	-3	-3.1	-3
59	5031415H12Rik	1.6	2.3	2	2	-2	-1.5	-1.7	-1.7
60	Anxa8	2.1	2.1	1.7	2	-2.4	-2.2	-3.7	-2.8
61	Artn	1.9	2.1	2	2	-1.8	-1.5	-1.8	-1.7
62	Dmrta2	1.7	2	2.2	2	-1.6	-1.5	-1.3	-1.5
63	Daf2	2	1.9	2	2	-1.8	-1.9	-1.7	-1.8
64	Dlx5	1.8	1.7	2.5	2	-2.1	-1.8	-2.1	-2
65	Emp2	1.5	2.8	1.8	2	-1.5	-1.3	-1.4	-1.4
66	Fam65c	2.3	2.1	1.5	2	-2.3	-1.8	-2.9	-2.3
67	Gem	2	2.1	2	2	-1.8	-1.5	-2	-1.8
68	Guca2a	2.2	2.2	1.5	2	-1.6	-1.7	-2.4	-1.9
69	Kcnab1	2	1.9	2.1	2	-2.3	-1.8	-2.8	-2.3
70	Krt16	2	1.6	2.4	2	-1.1	-1.2	-1.5	-1.3
71	Ltbp2	2	2.3	1.8	2	-2.4	-2.2	-4.6	-3.1
72	Meox2	1.5	1.5	3	2	-1.2	-1.2	-1.3	-1.3
73	Mt2	1.9	2	2.1	2	-1.8	-1.9	-1.6	-1.7
74	Pgam2	2	1.9	2	2	-1.5	-1.5	-1.8	-1.6
75	Bfsp2	2.1	1.9	1.8	1.9	-1.8	-1.9	-2.3	-2
76	Cx3cl1	1.8	1.8	1.9	1.9	-1.5	-1.3	-3.1	-1.9
77	Hmcn1	2.1	2	1.7	1.9	-1.9	-1.6	-1.7	-1.8
78	Ifi202b	2	2.2	1.5	1.9	-1.2	-1.3	-3.4	-2
79	Isl2	1.7	1.7	2.4	1.9	-1.4	-1.2	-1.3	-1.3
80	Krtdap	2.1	2	1.6	1.9	-1.1	-1.2	-2.1	-1.5
81	Nfatc2	1.6	2.1	1.9	1.9	-1.5	-1.3	-1.3	-1.4
82	Tcea3	1.9	2.3	1.5	1.9	-1.4	-1.4	-1.4	-1.4
83	Rasgef1a	1.4	2.2	2	1.9	-2.4	-1.9	-2.1	-2.1
84	S100a6	2.1	2	1.5	1.9	-1.7	-1.7	-3	-2.1
85	Svep1	1.8	2.1	1.8	1.9	-2	-1.4	-1.7	-1.7
86	Tfap2a	1.8	2.6	1.3	1.9	-1.7	-1.2	-1.4	-1.4
87	Tfap2c	1.7	1.6	2.4	1.9	-1.4	-1.4	-1.1	-1.3
88	Tox	1.9	1.9	1.9	1.9	-3.1	-2.4	-3.1	-2.9
89	Adamts15	2.1	1.6	1.7	1.8	-1.4	-1.4	-2.3	-1.7
90	Aqp3	1.7	1.6	2.2	1.8	-2.8	-2.7	-1.9	-2.5
91	Arc	1.9	2	1.6	1.8	-1.7	-1.4	-3.8	-2.3
92	Ctgf	1.7	1.9	1.8	1.8	-3	-3.1	-5.1	-3.7
93	Dlk1	2.3	1.9	1.3	1.8	-1.7	-1.4	-2.7	-1.9
94	Egr4	1.5	2.3	1.7	1.8	-3	-2.5	-5.7	-3.7
95	ENSMUST00000064591	2	1.9	1.6	1.8	-1.4	-1.6	-2.5	-1.8
96	Fam81a	1.5	2.4	1.6	1.8	-1.5	-1.8	-1.8	-1.7
97	Figf	1.9	2.1	1.3	1.8	-2.1	-2.1	-2.8	-2.3
98	Gm10387	1.4	2.7	1.2	1.8	-2.5	-2.4	-2	-2.3
99	Gm2115	1.8	1.8	1.8	1.8	-1.5	-1.9	-2	-1.8
100	Gnas	1.8	2.1	1.5	1.8	-2.8	-3.6	-3.5	-3.3

Part 4 - RA signaling in ureter development

Rank	Gene symbol	BMS493 FC 1	BMS493 FC 2	BMS493 FC 3	BMS493 Avg FC	RA FC 1	RA FC 2	RA FC 3	RA Avg FC
101	Gpr165	2.2	1.6	1.5	1.8	-3	-1.6	-1.9	-2.2
102	Hspb2	2	2.1	1.5	1.8	-1.9	-2	-3.3	-2.4
103	Lrrc15	2	2.2	1.2	1.8	-1.7	-1.7	-3.5	-2.3
104	Mdga2	1.4	2.2	1.9	1.8	-1.8	-2.6	-2.3	-2.2
105	Nov	1.8	1.8	1.7	1.8	-2.4	-2.1	-2.8	-2.4
106	Perp	1.9	1.8	1.7	1.8	-2	-1.5	-3	-2.2
107	Ptchd4	1.5	2.2	1.7	1.8	-1.7	-1.5	-2	-1.8
108	Rab38	1.7	1.9	1.8	1.8	-1.7	-2.1	-3.1	-2.3
109	Rgs4	1.6	1.8	1.9	1.8	-3.4	-4.3	-4.5	-4.1
110	Rgs5	1.7	1.8	1.9	1.8	-3.3	-5.5	-5.5	-4.8
111	Six2	1.6	1.7	2	1.8	-2.3	-1.4	-1.9	-1.9
112	Robo2	1.7	1.8	1.9	1.8	-2.2	-2.1	-1.5	-1.9
113	Sgk2	1.4	1.9	2.1	1.8	-3.2	-2.3	-2.6	-2.7
114	Tfap2b	2	2	1.3	1.8	-2.4	-2.4	-2.9	-2.6
115	Sytl2	2	1.5	1.8	1.8	-1.9	-1.6	-1.9	-1.8
116	TC1654523	1.6	2.1	1.6	1.8	-2.1	-1.4	-1.6	-1.7
117	Vnn1	1.4	1.9	2.1	1.8	-1.8	-1.8	-1.7	-1.8
118	Zfp365	1.8	1.8	1.9	1.8	-2.6	-2.2	-2.2	-2.3
119	1700038P13Rik	1.6	1.8	1.6	1.7	-1.6	-1.5	-1.2	-1.4
120	4631405K08Rik	1.7	2.3	1.2	1.7	-2.1	-1.5	-2.2	-1.9
121	Aldh1a2	1.8	1.8	1.6	1.7	-2.3	-1.8	-1.8	-2
122	Ascl2	1.9	1.3	1.9	1.7	-1.5	-1.3	-1.2	-1.3
123	Bgn	2	1.6	1.4	1.7	-1.5	-1.5	-2.4	-1.8
124	Trp63	1.3	2.3	1.6	1.7	-3.3	-2.5	-2.7	-2.8
125	Ctsc	1.7	2	1.4	1.7	-1.9	-1.7	-3.2	-2.3
126	Cyr61	1.6	1.8	1.7	1.7	-1.9	-1.7	-2.5	-2
127	D630013G24Rik	1.5	1.8	1.6	1.7	-1.6	-1.4	-1.3	-1.5
128	Dclk2	2	1.7	1.5	1.7	-1.5	-1.4	-1.4	-1.4
129	Ddah1	1.6	1.8	1.6	1.7	-1.3	-1.4	-2.1	-1.6
130	Dkk2	1.5	1.8	1.7	1.7	-3	-3.4	-4.5	-3.6
131	Egr2	1.6	1.7	2	1.7	-2.6	-2.4	-5.3	-3.4
132	Epha3	1.5	1.5	1.9	1.7	-2.4	-2.8	-2.4	-2.5
133	Gabrb2	1.8	2	1.4	1.7	-3	-2.3	-3.1	-2.8
134	Cited1	1.7	2	1.6	1.7	-1.3	-1.4	-1.2	-1.3
135	Itga7	1.9	1.8	1.5	1.7	-1.4	-1.5	-1.4	-1.4
136	Kcnq5	1.9	1.9	1.5	1.7	-2.1	-1.4	-1.8	-1.8
137	Ms4a7	1.9	2.1	1.1	1.7	-1.5	-1.8	-3.9	-2.4
138	Ndr1	1.9	1.9	1.5	1.7	-1.6	-1.2	-1.7	-1.5
139	Nr4a1	1.8	1.7	1.5	1.7	-1.7	-1.5	-2.5	-1.9
140	Osmr	2	1.8	1.2	1.7	-1.8	-1.4	-3.2	-2.1
141	Pip5k1a	1.6	1.8	1.7	1.7	-1.5	-1.4	-1.5	-1.5
142	Pitx2	1.6	1.8	1.7	1.7	-2	-1.5	-1.8	-1.8
143	Rarres1	1.8	1.5	1.8	1.7	-1.6	-1.6	-2.2	-1.8
144	Serp1b1a	2.1	1.8	1.1	1.7	-1.4	-1.5	-2	-1.6
145	Stc1	1.8	1.6	1.7	1.7	-1.7	-2.2	-1.8	-1.9
146	Tmem132c	1.6	1.8	1.8	1.7	-2	-1.6	-1.5	-1.7
147	Trim47	1.6	1.7	1.7	1.7	-1.8	-1.6	-2.9	-2.1
148	Ttc22	1.8	1.6	1.6	1.7	-1.9	-1.3	-1.8	-1.7
149	Wnt6	1.6	1.6	2	1.7	-1.5	-1.3	-1.3	-1.3
150	Zmat4	1.7	1.9	1.7	1.7	-1.6	-1.3	-2.4	-1.8

Part 4 - RA signaling in ureter development

Rank	Gene symbol	BMS493 FC 1	BMS493 FC 2	BMS493 FC 3	BMS493 Avg FC	RA FC 1	RA FC 2	RA FC 3	RA Avg FC
151	1500015O10Rik	1.5	1.7	1.5	1.6	-2.3	-2.6	-3.9	-2.9
152	2900001G08Rik	1.4	2	1.5	1.6	-1.8	-1.3	-1.5	-1.5
153	A4galt	1.4	1.7	1.7	1.6	-1.6	-1.3	-1	-1.3
154	Ace2	1.7	1.7	1.4	1.6	-6.1	-5.1	-4.9	-5.4
155	Actg2	1.6	1.8	1.5	1.6	-2.1	-1.7	-2.9	-2.2
156	Agtr1a	1.6	1.7	1.5	1.6	-1.6	-1.5	-1.6	-1.6
157	Ankrd1	1.6	1.6	1.5	1.6	-1.2	-1.2	-3.8	-2.1
158	Atp6v0a4	1.5	1.6	1.6	1.6	-1.3	-1.3	-1.3	-1.3
159	Btc	1.8	1.6	1.4	1.6	-2	-1.8	-1.9	-1.9
160	Cacna2d3	1.5	1.5	1.6	1.6	-1.3	-1.2	-1.4	-1.3
161	Calcr1	2	1.4	1.4	1.6	-2.7	-2	-2.3	-2.3
162	Cartpt	1.9	1.7	1.2	1.6	-2.4	-4.1	-4.9	-3.8
163	Cd44	1.7	1.7	1.3	1.6	-1.8	-1.3	-2.1	-1.7
164	Hopx	2.1	1.4	1.3	1.6	-1.7	-1.7	-2.2	-1.9
165	Col5a3	1.7	1.6	1.4	1.6	-1.6	-1.3	-2	-1.6
166	D630010B17Rik	1.6	1.7	1.6	1.6	-1.8	-1.9	-2.1	-1.9
167	Dusp2	1.5	1.5	1.6	1.6	-1.2	-1.2	-1.7	-1.3
168	Fam150b	1.7	1.8	1.3	1.6	-2.8	-3.1	-7.8	-4.6
169	Fas	1.4	1.7	1.5	1.6	-1.9	-2.2	-4.2	-2.7
170	Fgf12	1.8	1.7	1.4	1.6	-1.6	-1.8	-1.4	-1.6
171	Gas2	1.4	1.5	1.8	1.6	-1.6	-1.8	-2.1	-1.8
172	Gfra2	1.7	1.6	1.4	1.6	-2.2	-2.3	-1.9	-2.1
173	Hist2h2bb	1.6	1.8	1.4	1.6	-1.7	-1.4	-1.3	-1.5
174	Itga11	1.4	1.7	1.6	1.6	-2.2	-1.3	-2.1	-1.9
175	Kcnn2	1.7	1.7	1.3	1.6	-1.9	-1.6	-1.8	-1.8
176	Lama3	1.6	1.6	1.5	1.6	-1.3	-1.2	-2.6	-1.7
177	Lgi2	1.7	1.5	1.6	1.6	-1.4	-1.9	-1.5	-1.6
178	Lhfp13	1.9	1.4	1.5	1.6	-1.3	-2.2	-1.9	-1.8
179	Lmo1	1.6	1.6	1.5	1.6	-2.2	-2.8	-3	-2.6
180	Lrrtm1	1.6	1.7	1.4	1.6	-2.1	-2.2	-2.6	-2.3
181	40603	1.5	1.7	1.6	1.6	-1.4	-1.7	-2.2	-1.8
182	Nfkbiz	1.7	2	1.3	1.6	-1.9	-1.5	-2	-1.8
183	Npas4	1.6	1.5	1.5	1.6	-1.5	-1.4	-1.7	-1.5
184	Nrp2	1.6	1.9	1.2	1.6	-1.3	-1.3	-1.7	-1.4
185	Ntrk3	1.7	1.7	1.3	1.6	-1.7	-1.4	-2.2	-1.8
186	Pcdh10	1.7	1.7	1.5	1.6	-1.3	-1.8	-1.7	-1.6
187	Pcdhac2	1.3	2.1	1.4	1.6	-1.4	-1.4	-1.2	-1.3
188	Pdgfrb	1.6	1.6	1.4	1.6	-2.3	-1.8	-1.9	-2
189	Plekha4	1.8	1.6	1.4	1.6	-1.5	-1.4	-2.1	-1.7
190	Ppp1r3d	1.5	1.6	1.7	1.6	-1.4	-1.4	-1.3	-1.4
191	Prrx2	1.5	1.6	1.8	1.6	-1.2	-1.5	-1.5	-1.4
192	Ptchd1	1.6	1.6	1.5	1.6	-2.1	-2.3	-2.2	-2.2
193	Ptgs2	1.6	1.8	1.5	1.6	-1	-2	-4.2	-2.4
194	Rasgrp2	1.7	1.5	1.4	1.6	-1.5	-1.3	-2	-1.6
195	Slc23a3	1.4	1.5	2	1.6	-1.9	-1.9	-1.6	-1.8
196	Hand1	1.9	1.5	1.4	1.6	-1.5	-2	-2.5	-2
197	1500009L16Rik	1.4	1.4	1.6	1.5	-1.3	-1.5	-1.7	-1.5
198	1700040L02Rik	1.3	1.7	1.5	1.5	-1.7	-1.7	-1.5	-1.6
199	1810011O10Rik	1.5	1.4	1.7	1.5	-1.5	-1.7	-2.4	-1.9
200	2010111I01Rik	1.4	1.4	1.7	1.5	-1.4	-1.5	-1.7	-1.5

Part 4 - RA signaling in ureter development

Rank	Gene symbol	BMS493 FC 1	BMS493 FC 2	BMS493 FC 3	BMS493 Avg FC	RA FC 1	RA FC 2	RA FC 3	RA Avg FC
201	5330426P16Rik	1.4	1.4	1.6	1.5	-1.5	-1.5	-1.5	-1.5
202	A_55_P1953377	1.5	1.8	1.1	1.5	-1.6	-1.4	-2.8	-1.9
203	A930009L07Rik	1.4	1.8	1.2	1.5	-3.1	-7.2	-4.8	-5
204	Acta1	1.7	1.4	1.4	1.5	-1.2	-1.3	-2.7	-1.8
205	Hr	1.5	1.9	1.1	1.5	-3	-2.6	-2.6	-2.7
206	Ahrr	1.2	1.5	2	1.5	-2.1	-2.1	-1.1	-1.8
207	AK036131	1.3	1.7	1.4	1.5	-1.3	-1.6	-1.1	-1.3
208	Arid5a	1.5	1.6	1.5	1.5	-1.5	-1.4	-1.7	-1.5
209	Aspn	1.6	1.5	1.5	1.5	-1.8	-1.6	-2	-1.8
210	AY512938	1.4	1.4	1.7	1.5	-1.5	-1.6	-1.3	-1.5
211	Bdnf	1.3	1.5	1.6	1.5	-1.3	-1.4	-2.6	-1.8
212	C1qtnf2	1.8	1.2	1.4	1.5	-1.4	-1.6	-1.7	-1.6
213	Calcr	1.5	1.5	1.4	1.5	-2	-1.7	-1.1	-1.6
214	Cap2	1.7	1.3	1.5	1.5	-1.5	-1.3	-1.4	-1.4
215	Ccdc3	1.5	1.7	1.3	1.5	-1.7	-1.5	-1.7	-1.7
216	Cdkn2b	1.5	1.6	1.3	1.5	-1	-1.6	-2.9	-1.9
217	Col12a1	1.5	1.5	1.6	1.5	-1.5	-1.3	-1.4	-1.4
218	Cryab	1.9	1.3	1.3	1.5	-1.4	-1.7	-2.1	-1.7
219	Dgkk	1.4	1.7	1.4	1.5	-1.8	-2.7	-1.6	-2
220	Dmrta1	1.3	1.6	1.5	1.5	-1.8	-1.9	-1.9	-1.9
221	Fam83g	1.4	1.7	1.4	1.5	-1.5	-1.2	-1.5	-1.4
222	Fbn2	1.6	1.7	1.2	1.5	-1.5	-1.6	-1.4	-1.5
223	Fn1	1.5	1.3	1.6	1.5	-1.4	-1.4	-1.4	-1.4
224	Frzb	1.5	1.6	1.5	1.5	-2	-1.7	-2.1	-1.9
225	Fxyd2	1.2	1.4	1.8	1.5	-1.4	-1.7	-1.6	-1.6
226	Gadd45b	1.6	1.5	1.5	1.5	-1.2	-1.6	-2.3	-1.7
227	Gpr17	1.9	1.6	1.1	1.5	-1.7	-2.5	-2.6	-2.3
228	Gsn	1.4	1.5	1.4	1.5	-1.4	-1.2	-1.3	-1.3
229	Fos	1.4	1.5	1.6	1.5	-1.6	-1.8	-2.4	-1.9
230	Hspb1	1.5	1.2	1.6	1.5	-1.2	-1.5	-1.6	-1.4
231	Htra1	1.3	1.6	1.5	1.5	-1.4	-1.2	-1.7	-1.4
232	Inhba	1.5	1.8	1.3	1.5	-1.1	-1.4	-3.5	-2
233	Inhbb	1.6	1.8	1.3	1.5	-2.7	-1.9	-2.3	-2.3
234	Ism1	1.5	1.6	1.4	1.5	-1.9	-1.5	-1.6	-1.7
235	Itga4	1.5	1.6	1.5	1.5	-1.6	-1.5	-1.5	-1.5
236	Jag1	1.5	1.5	1.4	1.5	-1.5	-1.4	-1.6	-1.5
237	Kctd12	1.5	1.4	1.5	1.5	-2	-2.1	-1.3	-1.8
238	Klc3	1.6	1.4	1.4	1.5	-1.2	-1	-1.6	-1.3
239	Loxl1	1.7	1.4	1.2	1.5	-1.5	-1.3	-1.9	-1.6
240	Lum	1.5	1.4	1.6	1.5	-2.7	-3.5	-3.2	-3.1
241	Ly6c1	1.5	1.7	1.2	1.5	-1.8	-1.6	-3.3	-2.2
242	Magel2	1.6	1.3	1.6	1.5	-1.4	-1.2	-1.4	-1.3
243	Mamdc2	1.6	1.3	1.7	1.5	-2.2	-1.8	-2.2	-2.1
244	Maob	1.3	1.5	1.7	1.5	-2.1	-2.2	-2.2	-2.2
245	Mme	1.6	1.5	1.4	1.5	-2.1	-1.5	-1.5	-1.7
246	Mmrn1	1.4	1.6	1.4	1.5	-1.7	-1.3	-1.8	-1.6
247	NAP061760-1	1.8	1.4	1.3	1.5	-1.2	-1.2	-2.4	-1.6
248	Nppb	1.8	1.5	1.1	1.5	1.3	-1.2	-6	-2
249	Pamr1	1.4	1.7	1.5	1.5	-1.5	-1.2	-1.4	-1.4
250	Pappa2	1.6	1.7	1.1	1.5	-2.2	-1.5	-1.9	-1.9

Part 4 - RA signaling in ureter development

Rank	Gene symbol	BMS493 FC 1	BMS493 FC 2	BMS493 FC 3	BMS493 Avg FC	RA FC 1	RA FC 2	RA FC 3	RA Avg FC
251	Pcdh8	1.5	1.8	1.3	1.5	-2.2	-2.6	-2.2	-2.3
252	Plec	1.5	1.7	1.4	1.5	-1.4	-1.1	-1.3	-1.3
253	Plk3	1.4	1.5	1.5	1.5	-1.2	-1.2	-1.7	-1.3
254	Pmaip1	1.4	1.6	1.4	1.5	-1.4	-1.4	-2.9	-1.9
255	Rasgef1b	1.4	1.5	1.5	1.5	-1.9	-1.7	-1.7	-1.8
256	Rgs7bp	1.2	1.6	1.7	1.5	-1.1	-1.5	-1.3	-1.3
257	Rgs8	1.3	1.7	1.4	1.5	-1.3	-1.1	-1.4	-1.3
258	Rin1	1.4	1.6	1.4	1.5	-1.1	-1	-2.2	-1.5
259	Runx1	1.7	1.3	1.4	1.5	-1.2	-1.1	-2.1	-1.5
260	S100a13	1.4	1.6	1.6	1.5	-1.4	-1.4	-1.6	-1.5
261	S100a14	2.2	1.2	1	1.5	-1.3	-1.3	-1.3	-1.3
262	Sfn	1.7	1.5	1.3	1.5	-1.2	-1.2	-2.3	-1.5
263	Ssfa2	1.7	1.5	1.3	1.5	-1.7	-1.5	-1.7	-1.6
264	Sytl1	1.4	1.4	1.6	1.5	-1.3	-1.3	-1.4	-1.3
265	Thrb	1.3	1.4	1.6	1.5	-1.2	-1.8	-1.7	-1.5
266	Tiam2	1.5	1.7	1.5	1.5	-1.3	-1.2	-1.3	-1.3
267	Tmem100	1.5	1.5	1.4	1.5	-1.3	-1.4	-1.5	-1.4
268	Tmem26	1.6	1.6	1.5	1.5	-1.6	-1.9	-1.7	-1.7
269	Tmem40	1.6	1.5	1.5	1.5	-1.4	-1.4	-2	-1.6
270	Traf1	1.4	1.6	1.4	1.5	-1.4	-1.3	-1.6	-1.5
271	Wnt10a	1.4	2	1.1	1.5	-1.2	-1	-2.5	-1.6
272	1110032F04Rik	1.3	1.4	1.4	1.4	-2	-1.7	-1.6	-1.7
273	1700011H14Rik	1.2	1.6	1.4	1.4	-1.4	-1.4	-1.6	-1.5
274	2610018G03Rik	1.7	1.2	1.5	1.4	-1.4	-1.9	-1.6	-1.6
275	2610316D01Rik	1.5	1.3	1.4	1.4	-1.3	-1.3	-1.6	-1.4
276	9330159M07Rik	1.2	1.3	1.7	1.4	-1.3	-1.6	-1.5	-1.5
277	A_55_P1970825	1.8	1.3	1.3	1.4	-1.9	-2.4	-1.9	-2.1
278	A_55_P1972975	1.2	1.3	1.7	1.4	-1.3	-1.6	-1.8	-1.5
279	A_55_P2180347	1.4	1.2	1.6	1.4	-1.4	-1.5	-1.4	-1.4
280	Actc1	1.5	1.4	1.5	1.4	-2	-2.2	-2.5	-2.2
281	Adamts14	1.4	1.5	1.4	1.4	-1.4	-1.4	-1.8	-1.5
282	Adamts5	1.8	1.2	1.2	1.4	-2.1	-2	-2.2	-2.1
283	Afm	1.2	1.5	1.4	1.4	-1.5	-1.4	-1.5	-1.4
284	Agpat2	1.6	1.3	1.2	1.4	-1.2	-1.2	-1.5	-1.3
285	Ahnak	1.4	1.2	1.5	1.4	-1.4	-1.4	-1.5	-1.4
286	Akr1b7	1.5	1.6	1	1.4	-5.3	-3	-4.6	-4.3
287	Akr1c19	1.5	1.5	1.3	1.4	-1.3	-1.3	-1.5	-1.3
288	Anxa1	1.4	1.2	1.4	1.4	-1.5	-1.8	-2.6	-2
289	Arid5b	1.3	1.4	1.3	1.4	-1.8	-1.3	-1.4	-1.5
290	B930095G15Rik	1.4	1.4	1.3	1.4	-1.4	-1.3	-1.1	-1.3
291	Bai3	1.4	1.4	1.3	1.4	-1.7	-1.4	-1.5	-1.6
292	Trps1	1.3	1.5	1.3	1.4	-1.5	-1.7	-1.3	-1.5
293	Bmp5	1.3	1.6	1.3	1.4	-1.5	-1.6	-1.5	-1.6
294	Btbd17	1.6	1.5	1	1.4	-1.7	-1.8	-2.3	-1.9
295	C2cd4b	1.5	1.3	1.3	1.4	-1.5	-3.4	-2.5	-2.5
296	Cav1	1.6	1.4	1.2	1.4	-1.7	-1.6	-2.9	-2.1
297	Cav2	1.3	1.3	1.4	1.4	-2	-1.9	-2.7	-2.2
298	Cbr3	1.6	1.4	1.1	1.4	-1.3	-1.3	-2	-1.5
299	Cd99	1.4	1.6	1.2	1.4	-1.2	-1.1	-1.5	-1.3
300	Cdc42ep3	1.2	1.4	1.5	1.4	-1.1	-1.4	-1.4	-1.3

Part 4 - RA signaling in ureter development

Rank	Gene symbol	BMS493 FC 1	BMS493 FC 2	BMS493 FC 3	BMS493 Avg FC	RA FC 1	RA FC 2	RA FC 3	RA Avg FC
301	Chmp2b	1.4	1.1	1.7	1.4	-1.4	-1.6	-1.4	-1.5
302	Chst1	1.4	1.5	1.4	1.4	-1.6	-1.5	-1.5	-1.5
303	Ckmt1	1.2	1.4	1.5	1.4	-1.4	-1.2	-1.2	-1.3
304	Clec4n	1.6	1.2	1.3	1.4	-1.2	-1.2	-1.8	-1.4
305	Col2a1	1.5	1.5	1.2	1.4	-1.6	-1.4	-1.5	-1.5
306	Ctla2a	1.2	1.6	1.4	1.4	-1.8	-1.2	-1.9	-1.7
307	Cttnbp2	1.4	1.2	1.7	1.4	-1.7	-1.6	-1.1	-1.4
308	D230018H15Rik	1.1	1.6	1.5	1.4	-1.7	-1.3	-1.4	-1.5
309	D630033O11Rik	1.6	1.4	1.1	1.4	-1.4	-1.4	-1.4	-1.4
310	Dbh	1.5	1.6	1.1	1.4	-2.1	-3.5	-3.5	-3
311	Degs2	1.5	1.3	1.5	1.4	-1.4	-1.5	-1.7	-1.5
312	Dpp4	1.3	1.5	1.5	1.4	-1.4	-1.5	-1.4	-1.4
313	Egr1	1.3	1.5	1.5	1.4	-2	-1.7	-2	-1.9
314	Fbln2	1.4	1.6	1.2	1.4	-1.8	-2	-1.9	-1.9
315	Fbln5	1.3	1.2	1.7	1.4	-2.1	-2.2	-2	-2.1
316	Fgd3	1.4	1.5	1.3	1.4	-1.4	-1.3	-2.2	-1.6
317	Fstl3	1.5	1.3	1.3	1.4	-1	-1.1	-1.7	-1.3
318	Fxyd5	1.5	1.3	1.2	1.4	-1.3	-1.3	-2.2	-1.6
319	Gm10134	1.7	1.5	1	1.4	-1.3	-1.2	-1.4	-1.3
320	Gm17501	1.1	2	1.2	1.4	-1.6	-2.5	-2.6	-2.2
321	Gpc4	1.4	1.5	1.3	1.4	-1.5	-1.2	-2	-1.6
322	Grem2	1.5	1.5	1.4	1.4	-2.3	-2	-1.9	-2.1
323	Grin3a	1.4	1.4	1.5	1.4	-1.3	-1.5	-1.6	-1.5
324	Cited2	1.3	1.2	1.8	1.4	-1.1	-1.7	-1.2	-1.3
325	Foxs1	1.7	1.4	1.2	1.4	-1.5	-1.5	-3	-2
326	Hspa1a	1.4	1.3	1.6	1.4	-1.5	-1.1	-1.2	-1.3
327	Id4	1.5	1.5	1.3	1.4	-1.6	-1.5	-1.7	-1.6
328	Ier3	1.3	1.3	1.7	1.4	-1.6	-1.5	-2.5	-1.9
329	Igfbp2	1.5	1.4	1.3	1.4	-1.1	-1.2	-1.7	-1.4
330	Il1r1	1.5	1.6	1.3	1.4	-1.6	-1.3	-2.1	-1.6
331	Il2rg	1.7	1.4	1.1	1.4	-1.6	-1.1	-1.6	-1.4
332	Junb	1.7	1.3	1.4	1.4	-1.1	-1.1	-2	-1.4
333	Kcnj8	1.6	1.6	1.2	1.4	-1.5	-2.4	-2.3	-2.1
334	Kif21b	1.4	1.6	1.3	1.4	-1.3	-1.2	-1.3	-1.3
335	Klf2	1.2	1.4	1.5	1.4	-1.4	-1.4	-1.4	-1.4
336	Klf8	1.3	1.5	1.6	1.4	-1.4	-1.3	-1.2	-1.3
337	Ldlrad4	1.4	1.5	1.4	1.4	-1.3	-1.2	-2.3	-1.6
338	Ldoc1	1.2	1.4	1.6	1.4	-1.6	-1.3	-1.3	-1.4
339	Lfng	1.6	1.6	1.2	1.4	-1.5	-1.3	-1.9	-1.6
340	Lilrb4	1.5	1.3	1.5	1.4	-1.8	-1.6	-1.7	-1.7
341	Lmna	1.6	1.4	1.2	1.4	-1.4	-1.4	-1.9	-1.6
342	Lox	1.4	1.5	1.4	1.4	-2.5	-1.9	-1.9	-2.1
343	Lrrn3	1.4	1.3	1.6	1.4	-2.1	-2.2	-1.9	-2.1
344	Lxn	1.2	1.6	1.5	1.4	-1.4	-1.4	-1.5	-1.5
345	Ly6a	1.5	1.5	1.2	1.4	-1.6	-1.6	-3.3	-2.2
346	37681	1.6	1.4	1.3	1.4	-1.3	-1.3	-2	-1.5
347	Mef2c	1.5	1.6	1.3	1.4	-1.2	-1.6	-1.7	-1.5
348	Mmd	1.3	1.4	1.4	1.4	-1.4	-1.5	-1.6	-1.5
349	Ms4a6d	1.4	1.2	1.5	1.4	-1.6	-1.4	-2.3	-1.8
350	Myo1g	1.2	1.6	1.5	1.4	-1.6	-1.6	-1.7	-1.6

Part 4 - RA signaling in ureter development

Rank	Gene symbol	BMS493 FC 1	BMS493 FC 2	BMS493 FC 3	BMS493 Avg FC	RA FC 1	RA FC 2	RA FC 3	RA Avg FC
351	Nog	1.7	1.3	1.2	1.4	-1.2	-1.1	-1.9	-1.4
352	Npb	1.2	1.5	1.6	1.4	-1.3	-1.4	-1.5	-1.4
353	Nrbp2	1.4	1.4	1.3	1.4	-1.3	-1.5	-1.4	-1.4
354	Nup62cl	1.4	1.4	1.4	1.4	-1.8	-1.3	-2.4	-1.8
355	Nupr1	1.4	1.6	1.1	1.4	-1.2	-1.3	-2.2	-1.6
356	Ogfrl1	1.5	1.4	1.5	1.4	-1.5	-1.2	-1.2	-1.3
357	Olfml2b	1.5	1.4	1.3	1.4	-1.3	-1.1	-1.5	-1.3
358	Palm3	1.3	1.4	1.5	1.4	-1.3	-1.3	-1.2	-1.3
359	Pdlim2	1.7	1.3	1.3	1.4	-1.4	-1.5	-1.7	-1.6
360	Pdzk1ip1	1.3	1.2	1.5	1.4	-1.5	-1.6	-1.7	-1.6
361	Plac1	1.1	1.5	1.6	1.4	-1.7	-1.4	-1.8	-1.7
362	Plcl1	1.4	1.6	1.2	1.4	-1.4	-1.1	-1.4	-1.3
363	Pnma2	1.3	1.5	1.2	1.4	-1.9	-1.6	-1.7	-1.7
364	Prdm6	1.5	1.4	1.5	1.4	-1.3	-1.6	-1.3	-1.4
365	Prr5l	1.3	1.4	1.4	1.4	-1.4	-1.4	-1.5	-1.5
366	Prss12	1.2	1.3	1.5	1.4	-1.6	-1.2	-2.3	-1.7
367	Ptn	1.6	1.4	1.4	1.4	-2.3	-2.3	-2.3	-2.3
368	Ramp2	1.5	1.4	1.3	1.4	-1.5	-1.5	-1.8	-1.6
369	Rdh10	1.4	1.3	1.6	1.4	-1.8	-1.5	-1.7	-1.7
370	Rem2	1.5	1.6	1.3	1.4	-1.3	-1.1	-1.7	-1.4
371	Rhbdf1	1.3	1.5	1.3	1.4	-1.3	-1.2	-1.5	-1.3
372	Rspo3	1.3	1.3	1.5	1.4	-1.8	-1.9	-1.9	-1.9
373	Runx1t1	1.4	1.4	1.5	1.4	-1.6	-1.8	-1.3	-1.6
374	Rxrg	1.4	1.7	1.2	1.4	-1.5	-1.5	-1.5	-1.5
375	S100a10	1.4	1.2	1.5	1.4	-1.1	-1.6	-1.6	-1.4
376	Sema5b	1.7	1.4	1.1	1.4	-1.5	-1.2	-1.9	-1.5
377	Sfmbt2	1.4	1.3	1.5	1.4	-1.6	-1.7	-1.4	-1.6
378	Smoc2	1.6	1.3	1.4	1.4	-1.7	-1.6	-1.8	-1.7
379	Spry2	1.4	1.3	1.4	1.4	-1.3	-1.3	-2	-1.6
380	Sqrdl	1.4	1.6	1.3	1.4	-1.4	-1.5	-2	-1.6
381	Tacstd2	1.5	1.4	1.3	1.4	-1.6	-1.3	-1.7	-1.5
382	Tcerg1l	1.2	1.8	1.2	1.4	-1.5	-1.5	-1.4	-1.5
383	Tep1	1.4	1.5	1.3	1.4	-1.3	-1.4	-1.2	-1.3
384	Tfpi2	1.4	1.5	1.4	1.4	-1.6	-1.5	-1.6	-1.6
385	Insm2	1.6	1.6	1.1	1.4	-4.7	-9.4	-7.5	-7.2
386	Th	1.5	1.5	1.2	1.4	-1.5	-1.9	-2.5	-2
387	Thbs1	1.4	1.4	1.3	1.4	-1.5	-1.4	-2	-1.7
388	Tm4sf1	1.5	1.6	1.1	1.4	-1.7	-1.8	-4.7	-2.7
389	Tmem171	1.5	1.2	1.4	1.4	-1.5	-1.4	-2.9	-1.9
390	Tnfrsf12a	1.7	1.2	1.3	1.4	-1.5	-1.7	-3.5	-2.2
391	Tril	1.4	1.3	1.4	1.4	-1.6	-1.1	-1.1	-1.3
392	Vav3	1.4	1.5	1.4	1.4	-1.8	-1.4	-1.9	-1.7
393	Sox2	1.6	1.4	1.2	1.4	-2.4	-1.6	-2.2	-2.1
394	1110006E14Rik	1.3	1.5	1.2	1.3	-1.9	-1.5	-1.5	-1.6
395	1110046J04Rik	1.4	1.3	1.2	1.3	-1.3	-1.2	-1.5	-1.3
396	5730416F02Rik	1.4	1.2	1.2	1.3	-1.3	-1.3	-1.5	-1.4
397	6430411K18Rik	1.2	1.6	1.2	1.3	-1.5	-1.7	-2	-1.7
398	6430519N07Rik	1.2	1.4	1.4	1.3	-1.9	-1.6	-1.1	-1.5
399	8430408G22Rik	1.3	1.2	1.3	1.3	-1.5	-1.3	-1.7	-1.5
400	9.13002E+15	1.3	1.4	1.3	1.3	-1.7	-1.4	-1.2	-1.4

Part 4 - RA signaling in ureter development

Rank	Gene symbol	BMS493 FC 1	BMS493 FC 2	BMS493 FC 3	BMS493 Avg FC	RA FC 1	RA FC 2	RA FC 3	RA Avg FC
401	A_55_P2005672	1.3	1.3	1.4	1.3	-1.2	-1.3	-1.6	-1.4
402	A_55_P2092286	1.2	1.6	1.1	1.3	-1.5	-1.5	-1.5	-1.5
403	A930002H24Rik	1	1.2	1.5	1.3	-1.3	-1.5	-1.5	-1.4
404	Acot11	1.1	1.4	1.4	1.3	-1.6	-1.5	-1.7	-1.6
405	Acot9	1.2	1.4	1.1	1.3	-1.4	-1.2	-1.9	-1.5
406	Adam23	1.2	1.6	1.2	1.3	-1.9	-1.3	-1.7	-1.6
407	Adk	1.3	1.4	1.2	1.3	-1.3	-1.2	-1.5	-1.4
408	Adm	1.4	1.3	1.2	1.3	-1.4	-1.5	-2.1	-1.7
409	Agap2	1.1	1.5	1.1	1.3	-1.4	-1.2	-1.2	-1.3
410	Aldh1a1	1.4	1.4	1.1	1.3	-1.6	-1.5	-1.7	-1.6
411	Ankrd29	1.3	1.3	1.2	1.3	-1.4	-1.3	-1.5	-1.4
412	Arl4a	1.3	1.3	1.4	1.3	-1.3	-1.4	-1.8	-1.5
413	Dmrt2	1.1	1.3	1.6	1.3	-2.1	-2.4	-2.9	-2.4
414	Atp1a2	1.4	1.2	1.2	1.3	-1.4	-1.4	-1.3	-1.4
415	Atp6v0d2	1.2	1.4	1.3	1.3	-1.5	-1.4	-2.1	-1.7
416	Bcl10	1.3	1.3	1.3	1.3	-1.3	-1.1	-1.5	-1.3
417	Blnk	1.1	1.5	1.4	1.3	-1.1	-1.1	-1.6	-1.3
418	Capg	1.3	1.3	1.2	1.3	-1.4	-1.2	-1.4	-1.3
419	Caps2	1.2	1.3	1.3	1.3	-1.5	-1.3	-1.2	-1.3
420	Cd109	1.3	1.4	1.3	1.3	-1.3	-1	-1.5	-1.3
421	Chga	1.4	1.5	1	1.3	-2	-3.3	-3.4	-2.9
422	Ell2	1.4	1.3	1.2	1.3	-1.6	-1.4	-1.7	-1.6
423	Clec4d	1.3	1.2	1.3	1.3	-1.6	-1.5	-2.1	-1.7
424	Clic5	1.3	1.4	1.3	1.3	-1.8	-1	-1.2	-1.4
425	Col14a1	1.4	1.3	1.1	1.3	-2.1	-1.6	-2.2	-2
426	Col16a1	1.1	1.6	1.3	1.3	-1.4	-1.2	-1.3	-1.3
427	Col23a1	1.5	1.4	1	1.3	-1.5	-1.4	-1.3	-1.4
428	Col4a2	1.5	1.4	1.1	1.3	-1.3	-1.1	-1.5	-1.3
429	Crim1	1.1	1.3	1.4	1.3	-1.1	-1.5	-1.2	-1.3
430	Crip1	1.4	1.5	1.1	1.3	-1.2	-1.2	-1.6	-1.3
431	Csf1	1.3	1.3	1.2	1.3	-1.1	-1.2	-1.5	-1.3
432	Ctla2b	1.2	1.4	1.2	1.3	-1.7	-1.2	-2.1	-1.7
433	D9Erttd115e	1.2	1.2	1.4	1.3	-1.2	-1.3	-1.4	-1.3
434	Dgat2	1.2	1.3	1.3	1.3	-1.4	-1.2	-1.3	-1.3
435	Dgkh	1.3	1.3	1.4	1.3	-1.4	-1.4	-1.3	-1.4
436	Zcchc12	1.1	1.2	1.4	1.3	-1.3	-1.5	-1.5	-1.4
437	Eif4e3	1.3	1.2	1.3	1.3	-1.4	-1.2	-1.2	-1.3
438	Emb	1.4	1.3	1.3	1.3	-1.5	-1.5	-1.3	-1.5
439	F2r	1.2	1.2	1.5	1.3	-1.3	-1.3	-1.7	-1.4
440	Fam13c	1.3	1.4	1.3	1.3	-1.8	-1.6	-1.5	-1.6
441	Fbxo17	1.3	1.3	1.2	1.3	-1.2	-1.2	-1.5	-1.3
442	Fgfr4	1.3	1.5	1.1	1.3	-1.8	-1.5	-1.4	-1.6
443	Fibin	1.3	1.5	1.2	1.3	-1.2	-1.3	-1.3	-1.3
444	Filip1l	1.5	1.3	1.3	1.3	-1.8	-1.9	-2.3	-2
445	Frmpd4	1.2	1.3	1.4	1.3	-1.7	-1.3	-1.2	-1.4
446	Fxyd3	1.6	1.4	1.1	1.3	-1.6	-1.7	-1.9	-1.7
447	Gch1	1.4	1.2	1.3	1.3	-1.5	-1.6	-2.7	-1.9
448	Gjb3	1.4	1.3	1.2	1.3	-1.4	-1.1	-2	-1.5
449	Glipr1	1.5	1.3	1.1	1.3	-1.3	-1.3	-2.7	-1.7
450	Glt8d2	1.3	1.1	1.5	1.3	-1.3	-1.4	-1.6	-1.4

Part 4 - RA signaling in ureter development

Rank	Gene symbol	BMS493 FC 1	BMS493 FC 2	BMS493 FC 3	BMS493 Avg FC	RA FC 1	RA FC 2	RA FC 3	RA Avg FC
451	Gm13889	1.1	1.6	1.3	1.3	-1.2	-1.2	-1.5	-1.3
452	Gm6403	1.3	1.5	1.2	1.3	-2.4	-2.1	-2.3	-2.3
453	Gm9963	1.6	1.1	1.1	1.3	-1.5	-1.2	-1.4	-1.4
454	Gng11	1.3	1.4	1.2	1.3	-1.3	-1.3	-1.6	-1.4
455	Gp49a	1.6	1.3	1.1	1.3	-2	-1.4	-2.1	-1.9
456	Gpr176	1.3	1.2	1.4	1.3	-1.2	-1.2	-1.6	-1.3
457	Gpr97	1.1	1.6	1.1	1.3	-1.6	-1.5	-1.9	-1.7
458	Grhl3	1.3	1.2	1.4	1.3	-2.3	-1.2	-1.8	-1.8
459	Gsg1l	1.3	1.4	1.3	1.3	-1.5	-1.3	-1.7	-1.5
460	Gxylt2	1.3	1.4	1.3	1.3	-1.3	-1.2	-1.4	-1.3
461	Hmga2	1.2	1.2	1.5	1.3	-1	-1.5	-1.4	-1.3
462	Hmga2-ps1	1.2	1.3	1.3	1.3	-1.2	-1.4	-1.9	-1.5
463	Hs3st5	1.5	1.4	1	1.3	-2.9	-3	-3	-3
464	Hspb7	1.6	1.2	1.2	1.3	-1.2	-1.2	-1.6	-1.3
465	Htra4	1.4	1.3	1.3	1.3	-1.9	-2.3	-2	-2.1
466	Icam1	1.6	1.3	1.1	1.3	-1.5	-1.1	-1.8	-1.5
467	Ifih1	1.3	1.1	1.6	1.3	-1.4	-1.4	-2.1	-1.7
468	Itga6	1.1	1.6	1.1	1.3	-1.3	-1.2	-1.6	-1.4
469	Itga8	1.3	1.3	1.3	1.3	-1.8	-1.4	-1.2	-1.5
470	Kcne1l	1.4	1.2	1.3	1.3	-1.2	-1.3	-1.7	-1.4
471	Kcnma1	1.3	1.1	1.5	1.3	-1.8	-1.5	-1.7	-1.7
472	Kctd11	1.1	1.4	1.3	1.3	-1.3	-1.1	-1.6	-1.3
473	Lamb3	1.2	1.3	1.4	1.3	-1.4	-1.2	-1.9	-1.5
474	Lamc2	1.2	1.4	1.3	1.3	-1.5	-1.1	-1.9	-1.5
475	Lamc3	1.4	1.4	1.1	1.3	-1.6	-1.4	-1.6	-1.5
476	Lgals1	1.2	1.3	1.3	1.3	-1.3	-1.1	-1.5	-1.3
477	Lgals3	1.3	1.4	1.2	1.3	-1.8	-1.5	-1.8	-1.7
478	Lhfpl1	1.4	1.2	1.3	1.3	-1.6	-1.5	-2	-1.7
479	Lifr	1.3	1.2	1.4	1.3	-1.6	-1.4	-1.2	-1.4
480	Lsamp	1.1	1.5	1.3	1.3	-1.2	-1.6	-1	-1.3
481	Maff	1.2	1.3	1.3	1.3	-1.3	-1.3	-2.1	-1.6
482	Man2a1	1.2	1.5	1.3	1.3	-1.5	-1.4	-1.5	-1.4
483	Mcam	1.5	1.2	1.2	1.3	-1.4	-1.3	-2.5	-1.8
484	Meg3	1.4	1.3	1.1	1.3	-1.1	-1.3	-1.5	-1.3
485	Mfap3l	1.1	1	1.6	1.3	-1.3	-1.4	-1.1	-1.3
486	Mir22hg	1.4	1.3	1.4	1.3	-1.1	-1.4	-1.4	-1.3
487	Mirg	1	1.4	1.3	1.3	-1.4	-1.8	-1.5	-1.6
488	Msn	1.2	1.3	1.2	1.3	-1.5	-1.1	-1.3	-1.3
489	Mt1	1.3	1.3	1.4	1.3	-1.6	-1.5	-1.2	-1.4
490	Myadm	1.4	1.4	1.2	1.3	-1.4	-1.1	-1.4	-1.3
491	Ncf4	1.5	1.2	1.2	1.3	-1.4	-1.2	-1.5	-1.4
492	Nfkb2	1.5	1.4	1.1	1.3	-1.3	-1	-1.5	-1.3
493	Nuak1	1.4	1.2	1.2	1.3	-1.2	-1.1	-1.6	-1.3
494	Oas1f	1.4	1.3	1.4	1.3	-1.1	-1.2	-2	-1.4
495	Ovol1	1.1	1.3	1.7	1.3	-1.4	-1.4	-1.1	-1.3
496	Paqr5	1.1	1.3	1.4	1.3	-1.7	-1.7	-1.6	-1.7
497	Pcdh19	1.3	1.3	1.4	1.3	-1.7	-1.6	-1.4	-1.6
498	Pfkip	1.6	1.3	1	1.3	-2	-2	-3.3	-2.5
499	Phactr1	1.3	1.3	1.3	1.3	-1.6	-1.6	-1.6	-1.6
500	Tfcp2l1	1.3	1.3	1.4	1.3	-1.5	-1.4	-1.2	-1.4

Part 4 - RA signaling in ureter development

Rank	Gene symbol	BMS493 FC 1	BMS493 FC 2	BMS493 FC 3	BMS493 Avg FC	RA FC 1	RA FC 2	RA FC 3	RA Avg FC
501	Plac9a	1.7	1.1	1.1	1.3	-1.2	-1.4	-2.1	-1.6
502	Plau	1.3	1.3	1.2	1.3	-2.1	-2.4	-2.9	-2.5
503	Plcx2	1	1.3	1.5	1.3	-1.3	-1.4	-1.5	-1.4
504	Plcx3	1.2	1.3	1.3	1.3	-1.7	-2.6	-2.1	-2.1
505	Plp2	1.1	1.3	1.4	1.3	-1.3	-1.2	-1.3	-1.3
506	Postn	1.2	1.2	1.5	1.3	-1.7	-2.3	-2.1	-2
507	Ppap2c	1.2	1.3	1.3	1.3	-1.3	-1.3	-1.2	-1.3
508	Prkcdbp	1.3	1.4	1.2	1.3	-1.2	-1.2	-1.9	-1.4
509	Prss35	1.1	1	1.9	1.3	-1.1	-1.4	-1.4	-1.3
510	Ptger4	1.5	1.2	1.1	1.3	-1.4	-1.3	-1.5	-1.4
511	Rgs16	1.4	1.4	1.2	1.3	-1.2	-1.1	-2.1	-1.5
512	Rnd3	1.2	1.3	1.5	1.3	-2.1	-1.5	-1.5	-1.7
513	Rxfp1	1.2	1.3	1.3	1.3	-1.6	-1.3	-1.9	-1.6
514	Schip1	1.5	1.3	1.2	1.3	-1.2	-1.3	-2	-1.5
515	38231	1.4	1.3	1.1	1.3	-1.3	-1.4	-1.4	-1.3
516	Serpine2	1.3	1.3	1.2	1.3	-1.4	-1.5	-1.9	-1.6
517	Sertad1	1.4	1.2	1.3	1.3	-1.2	-1.2	-1.6	-1.3
518	Sgpp2	1.3	1.4	1.2	1.3	-1.5	-1.1	-1.2	-1.3
519	Sh3gl2	1.4	1.2	1.2	1.3	-1.8	-1.7	-1.4	-1.6
520	Sh3tc2	1.4	1.4	1.2	1.3	-1.5	-1.4	-1.6	-1.5
521	Slamf9	1.3	1.5	1.2	1.3	-1.4	-1.4	-2.2	-1.6
522	Slc16a14	1.3	1.3	1.4	1.3	-1.3	-1.8	-1.1	-1.4
523	Slc29a1	1.2	1.3	1.3	1.3	-1.4	-1.3	-1.3	-1.4
524	Slc41a2	1.4	1.3	1.2	1.3	-1.7	-1.5	-1.6	-1.6
525	Slc4a11	1.3	1.3	1.2	1.3	-1.2	-1.2	-1.7	-1.4
526	Slit3	1.5	1.3	1	1.3	-1.3	-1.1	-1.5	-1.3
527	Snai2	1.4	1.1	1.4	1.3	-1.2	-1.8	-1.2	-1.4
528	Heyl	1.3	1.5	1.2	1.3	-1.4	-1.2	-2.2	-1.6
529	Srpx	1.2	1.3	1.3	1.3	-1.3	-1.6	-1.7	-1.5
530	Stx11	1.2	1.3	1.3	1.3	-1.2	-1	-2.6	-1.6
531	Tagln	1.3	1.3	1.4	1.3	-1.7	-1.6	-2.7	-2
532	TC1598269	1.3	1.3	1.2	1.3	-1.5	-1.9	-1.6	-1.7
533	Tgfa	1.4	1.4	1	1.3	-1.6	-1.1	-1.1	-1.3
534	Timp1	1.3	1.4	1.2	1.3	-1.3	-1.2	-2.4	-1.6
535	Timp3	1.2	1.4	1.3	1.3	-1.7	-2	-2.1	-1.9
536	Tle4	1.3	1.3	1.3	1.3	-1.4	-1.2	-1.2	-1.3
537	Tmem173	1.2	1.3	1.3	1.3	-1.2	-1.1	-1.5	-1.3
538	Tmem213	1.4	1.5	1.1	1.3	-1.3	-1.3	-1.6	-1.4
539	Tph1	1.3	1.3	1.2	1.3	-1.7	-1.3	-1.8	-1.6
540	Tspan4	1.3	1.4	1.1	1.3	-1.4	-1.2	-1.6	-1.4
541	Vim	1.4	1	1.4	1.3	-1.3	-1.5	-1.5	-1.4
542	Vstm2l	1.3	1.6	1.1	1.3	-1.4	-1.5	-1.8	-1.6
543	Wisp1	1.4	1.3	1.2	1.3	-1.4	-1.3	-2.2	-1.6
544	Zfp608	1.3	1.3	1.4	1.3	-1.4	-1.4	-1.2	-1.3

Part 4 - RA signaling in ureter development

Supplemental Table 5: Transcripts identified by microarray analysis that were positively regulated by RA in the early ureter. Shown is a list of transcripts that were positively regulated by RA, i.e. downregulated after BMS493 treatment and upregulated after RA treatment of E12.5 ureter explants. Three groups were for each condition were compared to untreated controls and the resulting fold changes (FC) in expression are displayed. Intensity thresholds were >100 for the control; fold changes were larger than 1.2.

Rank	Gene symbol	BMS493 FC 1	BMS493 FC 2	BMS493 FC 3	BMS493 Avg FC	RA FC 1	RA FC 2	RA FC 3	RA Avg FC
1	Tgm5	-15.4	-16.3	-14.4	-15.4	1.6	1.9	2.1	1.9
2	Tnfsf13b	-10.1	-7.4	-11.1	-9.5	4.5	5.0	5.3	4.9
3	Dhrs3	-6.5	-7.4	-5.7	-6.5	2.7	2.8	3.6	3.0
4	Pnliprp1	-6.3	-5.7	-6.6	-6.2	1.9	2.7	3.1	2.6
5	Il33	-7.6	-5.6	-4.8	-6.0	3.7	2.8	3.6	3.4
6	Sst	-5.1	-4.7	-4.9	-4.9	5.1	5.2	5.1	5.1
7	Elf5	-5.1	-4.7	-4.6	-4.8	1.4	1.4	1.8	1.5
8	Ntsr1	-4.7	-3.4	-4.8	-4.3	2.5	3.1	4.4	3.3
9	Hic1	-4.5	-3.5	-4.3	-4.1	3.0	3.2	3.5	3.2
10	Colq	-4.1	-3.3	-4.9	-4.1	2.2	2.8	2.7	2.6
11	Ecm1	-3.7	-4.1	-4.0	-3.9	5.8	6.0	5.6	5.8
12	Angptl7	-3.5	-3.5	-3.4	-3.5	2.8	2.7	2.4	2.7
13	Ednrb	-4.0	-2.9	-3.5	-3.5	1.4	1.7	1.8	1.6
14	Shisa3	-3.4	-3.5	-3.2	-3.4	2.3	2.1	2.6	2.3
15	Tgm2	-3.0	-3.2	-3.6	-3.3	2.0	2.1	1.9	2.0
16	Slc38a5	-3.6	-2.5	-3.4	-3.2	1.8	1.7	2.1	1.9
17	Slitrk1	-3.7	-2.5	-2.5	-2.9	2.8	2.3	2.5	2.5
18	Akap12	-2.7	-2.7	-3.2	-2.9	1.7	2.2	2.0	2.0
19	Tmem62	-3.1	-2.9	-2.6	-2.9	2.0	2.0	2.2	2.1
20	Gna14	-3.0	-2.4	-3.1	-2.8	2.8	3.1	2.8	2.9
21	Kcnk2	-2.8	-2.7	-3.0	-2.8	2.1	2.5	3.5	2.7
22	Fut9	-3.1	-2.7	-2.6	-2.8	1.6	1.5	2.7	1.9
23	Rbm46	-2.6	-3.2	-2.4	-2.7	1.8	1.6	1.7	1.7
24	Spon2	-2.4	-2.8	-2.8	-2.7	2.0	2.0	1.8	1.9
25	Cntn1	-3.0	-2.8	-2.2	-2.7	1.9	1.6	3.0	2.2
26	Adamts14	-3.2	-2.3	-2.5	-2.6	3.9	4.0	4.2	4.1
27	Gdf10	-2.7	-2.2	-3.0	-2.6	1.4	1.5	1.6	1.5
28	Slitrk5	-3.1	-2.2	-2.5	-2.6	1.2	1.3	1.9	1.5
29	Flrt1	-3.0	-2.1	-2.6	-2.6	2.4	1.8	3.0	2.4
30	AI593442	-2.4	-2.2	-2.9	-2.5	1.5	2.3	2.4	2.1
31	Npy1r	-2.5	-2.4	-2.6	-2.5	1.5	1.4	1.5	1.4
32	AK141540	-2.6	-2.5	-2.4	-2.5	3.3	3.4	3.1	3.2
33	Rarb	-2.4	-2.8	-2.4	-2.5	1.8	1.8	2.0	1.9
34	A_55_P1960936	-2.6	-2.5	-2.4	-2.5	1.9	2.0	2.2	2.1
35	Hoxc4	-2.7	-2.4	-2.3	-2.5	3.0	3.2	4.6	3.6
36	Hs3st6	-3.2	-2.3	-1.9	-2.5	2.1	2.3	1.8	2.1
37	BB713741	-2.5	-2.6	-2.3	-2.5	1.7	1.9	2.2	1.9
38	AK046833	-2.8	-2.5	-2.0	-2.5	1.7	1.5	2.5	1.9
39	Cyp7b1	-2.7	-2.2	-2.4	-2.4	2.5	2.7	2.8	2.6
40	Sp5	-3.1	-2.2	-2.1	-2.4	1.5	1.6	2.1	1.8
41	Esrrg	-2.6	-2.2	-2.5	-2.4	1.8	1.8	2.2	2.0
42	Adh1	-2.7	-2.3	-2.1	-2.4	2.0	2.6	2.6	2.4
43	Mbd1	-2.5	-2.5	-2.2	-2.4	1.8	1.8	2.2	1.9
44	Crispld2	-2.7	-2.1	-2.3	-2.4	1.7	1.9	1.7	1.8
45	Hapln1	-2.3	-2.0	-2.7	-2.4	1.4	1.5	1.5	1.5
46	Wdr92	-2.6	-2.4	-2.1	-2.3	2.4	2.6	2.5	2.5
47	Gdf5	-2.0	-2.9	-2.1	-2.3	1.8	1.7	2.1	1.8
48	A_55_P1978866	-2.3	-2.5	-2.1	-2.3	1.7	1.6	2.1	1.8
49	Enpp1	-2.4	-2.0	-2.5	-2.3	1.5	1.7	1.3	1.5
50	Fam155a	-2.6	-2.2	-2.1	-2.3	1.7	1.7	1.8	1.8

Part 4 - RA signaling in ureter development

Rank	Gene symbol	BMS493 FC 1	BMS493 FC 2	BMS493 FC 3	BMS493 Avg FC	RA FC 1	RA FC 2	RA FC 3	RA Avg FC
51	Sprr1a	-2.1	-2.4	-2.3	-2.3	1.7	1.7	1.4	1.6
52	Vipr1	-2.4	-2.1	-2.3	-2.3	3.7	4.2	5.5	4.5
53	Fabp4	-1.9	-2.1	-2.7	-2.2	1.9	1.8	1.7	1.8
54	Nsg2	-2.2	-2.0	-2.4	-2.2	1.5	1.4	1.6	1.5
55	Fap	-2.2	-2.0	-2.4	-2.2	1.3	1.4	1.4	1.4
56	Cd83	-2.3	-2.1	-2.2	-2.2	1.8	1.9	2.0	1.9
57	Anxa9	-2.5	-2.2	-1.9	-2.2	1.5	1.5	1.4	1.5
58	AK035396	-2.4	-2.2	-1.9	-2.2	3.2	2.8	2.8	2.9
59	A_55_P1998811	-2.6	-2.3	-1.6	-2.2	1.6	1.7	2.0	1.7
60	Gfra1	-1.9	-1.9	-2.5	-2.1	1.7	2.1	2.1	2.0
61	3930401B19Rik	-2.4	-2.1	-1.9	-2.1	3.0	2.9	3.0	3.0
62	Sstr1	-2.4	-1.9	-2.0	-2.1	2.3	2.1	1.6	2.0
63	Tspan1	-1.8	-2.4	-2.2	-2.1	1.9	2.2	2.8	2.3
64	A_55_P2051596	-2.5	-2.1	-1.7	-2.1	1.4	1.5	1.8	1.6
65	Pdgfd	-2.2	-2.0	-2.0	-2.1	1.3	1.3	1.3	1.3
66	AK132033	-2.2	-2.1	-1.9	-2.1	3.0	2.9	3.0	2.9
67	Cd38	-2.1	-1.8	-2.3	-2.1	1.6	2.3	1.9	1.9
68	Ephb1	-2.9	-1.8	-1.4	-2.1	1.5	1.5	1.6	1.5
69	Gm4951	-2.3	-2.5	-1.4	-2.0	2.0	1.3	1.6	1.6
70	Synpr	-2.0	-2.0	-2.1	-2.0	2.1	1.5	1.7	1.8
71	Rbp1	-2.1	-1.8	-2.2	-2.0	1.6	1.6	1.9	1.7
72	BC057675	-2.4	-2.1	-1.6	-2.0	2.8	1.8	2.5	2.4
73	TC1616199	-2.4	-2.0	-1.7	-2.0	3.6	3.6	3.1	3.4
74	A_55_P2107785	-1.9	-1.9	-2.3	-2.0	1.5	1.7	1.4	1.5
75	ligp1	-2.2	-2.2	-1.5	-2.0	1.8	1.5	1.9	1.7
76	TC1703733	-2.1	-2.4	-1.3	-2.0	1.9	1.2	1.9	1.7
77	Mab211l1	-1.8	-1.8	-2.3	-1.9	1.8	1.6	1.5	1.6
78	5730446D14Rik	-1.9	-2.0	-2.0	-1.9	1.9	1.5	1.6	1.7
79	Adamts18	-2.1	-2.1	-1.6	-1.9	3.5	1.4	1.9	2.3
80	Insc	-2.0	-1.4	-2.3	-1.9	1.3	1.5	1.4	1.4
81	Hspa12a	-1.8	-2.1	-1.6	-1.9	2.4	2.0	3.8	2.7
82	Grik4	-1.9	-1.8	-1.9	-1.9	1.9	1.8	2.0	1.9
83	Anxa11	-2.2	-1.8	-1.7	-1.9	1.5	1.8	1.9	1.7
84	Lhfpl2	-2.0	-1.8	-1.8	-1.9	1.7	2.0	2.1	2.0
85	Enpp3	-1.9	-1.8	-1.9	-1.9	2.0	2.0	2.2	2.1
86	Syt6	-1.7	-1.5	-2.3	-1.8	1.4	2.1	1.9	1.8
87	Cdbl	-2.1	-1.5	-1.9	-1.8	1.6	1.5	1.5	1.5
88	Al427809	-2.0	-1.7	-1.8	-1.8	1.7	1.7	1.9	1.8
89	Stra6	-1.9	-1.5	-2.1	-1.8	2.3	2.6	3.2	2.7
90	Slc18a3	-1.6	-1.3	-2.6	-1.8	1.9	2.5	2.6	2.3
91	Ptprb	-2.0	-1.5	-1.9	-1.8	1.5	1.3	1.8	1.6
92	6030408B16Rik	-1.8	-1.9	-1.8	-1.8	1.7	1.6	1.4	1.6
93	Igf1	-1.8	-1.7	-2.0	-1.8	2.1	2.4	2.0	2.2
94	Cplx2	-1.8	-1.7	-2.0	-1.8	1.5	1.5	2.0	1.6
95	Stmn2	-1.8	-1.5	-2.1	-1.8	1.6	1.3	1.2	1.4
96	Lrrc3b	-2.3	-1.7	-1.3	-1.8	1.6	1.3	1.2	1.4
97	Oprl1	-1.8	-1.6	-1.9	-1.8	1.3	1.5	1.3	1.3
98	Al596198	-2.0	-1.8	-1.5	-1.7	2.1	1.8	2.3	2.1
99	Erc2	-2.0	-1.6	-1.6	-1.7	2.2	2.4	2.3	2.3
100	Hdhd3	-1.6	-1.9	-1.7	-1.7	1.8	1.6	1.5	1.6

Part 4 - RA signaling in ureter development

Rank	Gene symbol	BMS493 FC 1	BMS493 FC 2	BMS493 FC 3	BMS493 Avg FC	RA FC 1	RA FC 2	RA FC 3	RA Avg FC
101	Neurl3	-1.6	-1.6	-1.9	-1.7	1.3	1.6	1.4	1.4
102	Zfp958	-1.5	-2.3	-1.3	-1.7	1.6	1.5	2.4	1.8
103	Hoxc9	-1.9	-1.7	-1.5	-1.7	2.5	2.2	2.4	2.4
104	Adamts8	-1.9	-1.4	-1.8	-1.7	1.4	1.6	1.9	1.6
105	Scd1	-1.7	-1.5	-1.9	-1.7	1.4	1.9	1.3	1.5
106	Scnn1b	-1.8	-1.5	-1.8	-1.7	1.3	1.4	1.4	1.3
107	Hoxc6	-1.8	-1.5	-1.7	-1.7	1.3	1.7	1.9	1.6
108	A_55_P2007495	-1.7	-1.7	-1.6	-1.7	1.3	1.5	1.6	1.5
109	Plekhb1	-1.5	-1.6	-1.9	-1.7	1.5	1.5	1.3	1.4
110	Adra2a	-1.8	-1.3	-1.9	-1.7	1.3	1.7	1.9	1.6
111	Aifm2	-1.5	-1.8	-1.7	-1.7	1.3	1.4	1.4	1.4
112	2010300C02Rik	-1.6	-1.7	-1.7	-1.7	1.6	1.6	1.6	1.6
113	Smim3	-1.8	-1.7	-1.4	-1.6	1.8	1.4	1.3	1.5
114	A_55_P2114318	-1.7	-1.7	-1.6	-1.6	1.3	1.5	1.6	1.5
115	Ihh	-1.6	-1.9	-1.5	-1.6	2.0	2.1	2.5	2.2
116	A_55_P2090505	-1.8	-1.6	-1.5	-1.6	2.3	2.2	2.5	2.3
117	Oxnad1	-1.6	-1.7	-1.6	-1.6	1.5	1.4	1.4	1.4
118	Calca	-1.7	-1.4	-1.7	-1.6	1.6	1.5	1.3	1.5
119	Usp53	-1.7	-1.8	-1.4	-1.6	1.7	2.0	2.5	2.1
120	Asic4	-1.6	-1.5	-1.6	-1.6	1.8	1.8	2.4	2.0
121	Fam78b	-1.6	-1.4	-1.8	-1.6	1.3	1.4	1.8	1.5
122	Trim9	-1.7	-1.4	-1.6	-1.6	1.4	1.5	1.6	1.5
123	Fndc5	-1.6	-1.4	-1.8	-1.6	1.5	1.8	1.9	1.8
124	Agtppb1	-1.8	-1.6	-1.4	-1.6	1.4	1.4	1.4	1.4
125	Masp1	-1.8	-1.5	-1.5	-1.6	1.4	1.8	2.1	1.8
126	Ncoa3	-1.7	-1.3	-1.7	-1.6	1.2	1.5	1.3	1.3
127	Foxd1	-1.4	-1.8	-1.5	-1.6	1.6	1.3	1.9	1.6
128	Mrvi1	-1.5	-1.4	-1.8	-1.6	1.2	1.5	1.3	1.3
129	Gata2	-1.3	-1.5	-1.9	-1.6	1.3	1.8	1.9	1.7
130	Gstt3	-1.5	-1.7	-1.5	-1.6	1.3	1.5	1.4	1.4
131	Ano1	-1.5	-1.4	-1.7	-1.6	1.6	1.5	1.4	1.5
132	Coro2a	-1.4	-1.5	-1.7	-1.6	1.5	1.8	1.6	1.7
133	Foxf1	-1.5	-1.5	-1.7	-1.6	1.2	1.3	1.6	1.4
134	Eva1c	-1.5	-1.3	-1.8	-1.5	1.7	2.2	1.5	1.8
135	Pbx1	-1.7	-1.6	-1.3	-1.5	1.5	1.7	2.2	1.8
136	Hoxa3	-1.5	-1.5	-1.6	-1.5	1.7	1.6	2.4	1.9
137	Dzank1	-1.5	-1.4	-1.7	-1.5	1.4	1.3	1.5	1.4
138	Itpka	-1.4	-1.4	-1.8	-1.5	2.1	2.1	2.3	2.2
139	Arg1	-1.6	-1.7	-1.3	-1.5	1.4	1.5	1.2	1.4
140	Ubash3b	-1.9	-1.3	-1.4	-1.5	2.3	1.6	1.8	1.9
141	BB237529	-1.6	-1.7	-1.3	-1.5	1.3	1.3	1.4	1.3
142	Pparg	-1.7	-1.5	-1.3	-1.5	1.2	1.5	1.6	1.4
143	Trim24	-1.5	-1.6	-1.4	-1.5	1.2	1.2	1.5	1.3
144	Clec7a	-1.5	-1.4	-1.7	-1.5	1.5	1.8	2.6	2.0
145	Hoxc10	-1.4	-1.4	-1.8	-1.5	1.6	1.6	1.7	1.7
146	Pde2a	-1.4	-1.5	-1.6	-1.5	1.3	1.8	1.4	1.5
147	Cfl2	-1.6	-1.6	-1.4	-1.5	1.3	1.5	1.7	1.5
148	AK149472	-1.7	-1.6	-1.3	-1.5	2.2	1.7	2.1	2.0
149	Map3k5	-1.5	-1.4	-1.6	-1.5	1.3	1.3	1.3	1.3
150	Mpz1	-1.7	-1.4	-1.4	-1.5	1.6	1.6	1.6	1.6

Part 4 - RA signaling in ureter development

Rank	Gene symbol	BMS493 FC 1	BMS493 FC 2	BMS493 FC 3	BMS493 Avg FC	RA FC 1	RA FC 2	RA FC 3	RA Avg FC
151	Fmo5	-1.7	-1.5	-1.4	-1.5	1.6	1.7	2.1	1.8
152	Bace2	-1.4	-1.5	-1.6	-1.5	1.6	1.3	1.4	1.5
153	Gbp2	-1.4	-1.6	-1.5	-1.5	4.7	3.8	2.3	3.6
154	Tmem27	-1.6	-1.4	-1.5	-1.5	1.3	1.4	1.2	1.3
155	Efemp1	-1.6	-1.6	-1.3	-1.5	2.5	2.0	1.9	2.1
156	Plat	-1.3	-1.7	-1.5	-1.5	1.3	1.4	1.5	1.4
157	Ncoa4	-1.5	-1.6	-1.4	-1.5	1.5	1.6	2.0	1.7
158	Gm6557	-1.3	-1.5	-1.6	-1.5	1.4	1.7	1.6	1.5
159	Nrip1	-1.6	-1.5	-1.3	-1.5	1.3	1.6	1.9	1.6
160	Egfr	-1.4	-1.4	-1.6	-1.5	1.2	1.3	1.2	1.2
161	Clmn	-1.5	-1.3	-1.6	-1.5	1.7	1.8	2.0	1.8
162	Ephx2	-1.5	-1.6	-1.3	-1.5	1.9	1.8	2.4	2.0
163	Pitx1	-1.7	-1.3	-1.4	-1.5	1.5	1.9	2.0	1.8
164	Gpr116	-1.8	-1.2	-1.4	-1.5	1.3	1.5	1.6	1.4
165	Pou3f1	-1.4	-1.3	-1.6	-1.5	1.3	1.8	1.7	1.6
166	Tshz2	-1.3	-1.4	-1.6	-1.5	1.3	1.4	1.7	1.5
167	Spata33	-1.5	-1.4	-1.5	-1.5	1.6	1.3	1.4	1.4
168	Kbtbd11	-1.2	-1.4	-1.7	-1.5	1.5	1.8	1.5	1.6
169	1700017B05Rik	-1.4	-1.4	-1.6	-1.4	1.3	1.7	1.6	1.5
170	Add3	-1.4	-1.5	-1.5	-1.4	1.3	1.5	1.9	1.6
171	Rtn4rl1	-1.4	-1.2	-1.7	-1.4	1.2	1.6	1.6	1.5
172	Fam101a	-1.4	-1.5	-1.4	-1.4	1.6	1.2	1.4	1.4
173	Adam12	-1.4	-1.3	-1.6	-1.4	1.3	1.6	1.2	1.4
174	Larp6	-1.5	-1.3	-1.4	-1.4	1.4	1.5	1.3	1.4
175	S1pr3	-1.3	-1.4	-1.5	-1.4	1.3	1.6	1.6	1.5
176	St8sia2	-1.4	-1.3	-1.6	-1.4	1.4	1.8	1.8	1.7
177	Egfl6	-1.5	-1.3	-1.4	-1.4	1.4	1.7	1.9	1.6
178	Acsl1	-1.6	-1.4	-1.2	-1.4	1.5	1.4	1.5	1.5
179	Ptp4a3	-1.2	-1.4	-1.7	-1.4	1.4	1.7	1.3	1.5
180	Kcnj10	-1.8	-1.3	-1.2	-1.4	1.2	1.4	1.5	1.4
181	Clip4	-1.5	-1.4	-1.3	-1.4	1.8	1.3	1.4	1.5
182	Isoc1	-1.4	-1.3	-1.5	-1.4	1.3	1.4	1.3	1.4
183	Hoxa5	-1.6	-1.4	-1.2	-1.4	2.4	1.7	2.1	2.1
184	Rasl10b	-1.2	-1.3	-1.6	-1.4	1.3	1.5	1.5	1.4
185	Hey2	-1.4	-1.4	-1.5	-1.4	1.6	2.0	1.4	1.7
186	Cntnap2	-1.6	-1.3	-1.3	-1.4	1.3	1.3	1.4	1.3
187	Ccndbp1	-1.4	-1.4	-1.3	-1.4	1.4	1.3	1.4	1.3
188	Hoxa2	-1.4	-1.4	-1.4	-1.4	2.1	1.6	1.9	1.9
189	Sfxn1	-1.6	-1.3	-1.2	-1.4	1.6	1.2	1.5	1.4
190	Stard5	-1.3	-1.3	-1.6	-1.4	1.5	1.9	1.6	1.6
191	Rec8	-1.4	-1.4	-1.3	-1.4	1.2	1.6	1.4	1.4
192	Dna2	-1.4	-1.4	-1.4	-1.4	1.2	1.3	1.2	1.2
193	Abca1	-1.4	-1.5	-1.3	-1.4	1.4	1.3	2.0	1.6
194	Clhc1	-1.4	-1.5	-1.3	-1.4	1.8	1.6	1.4	1.6
195	Syndig1	-1.4	-1.4	-1.3	-1.4	1.3	1.6	1.8	1.6
196	Cdc25b	-1.3	-1.3	-1.6	-1.4	1.4	1.7	1.5	1.6
197	Bmp7	-1.6	-1.2	-1.3	-1.4	1.3	1.5	1.5	1.4
198	Ropn1l	-1.4	-1.4	-1.3	-1.4	1.3	1.3	1.4	1.3
199	Stac	-1.3	-1.5	-1.3	-1.4	1.2	1.2	1.4	1.3
200	Kank4	-1.3	-1.3	-1.4	-1.4	1.8	2.4	2.4	2.2

Part 4 - RA signaling in ureter development

Rank	Gene symbol	BMS493 FC 1	BMS493 FC 2	BMS493 FC 3	BMS493 Avg FC	RA FC 1	RA FC 2	RA FC 3	RA Avg FC
201	Tm7sf2	-1.4	-1.3	-1.3	-1.3	1.5	1.5	1.3	1.4
202	Celf2	-1.5	-1.2	-1.3	-1.3	1.3	1.3	1.2	1.3
203	Flrt3	-1.6	-1.3	-1.2	-1.3	1.4	1.3	1.5	1.4
204	Olfm1	-1.5	-1.3	-1.2	-1.3	3.1	3.4	2.9	3.2
205	Xkr5	-1.4	-1.2	-1.4	-1.3	1.3	1.8	1.4	1.5
206	Neto2	-1.4	-1.2	-1.4	-1.3	1.6	1.7	1.5	1.6
207	Hoxb2	-1.4	-1.3	-1.3	-1.3	1.7	1.8	1.8	1.8
208	Zfp937	-1.5	-1.2	-1.2	-1.3	1.4	1.3	1.6	1.4
209	Gse1	-1.3	-1.2	-1.4	-1.3	1.6	1.5	1.9	1.7
210	A_55_P2024391	-1.3	-1.4	-1.3	-1.3	1.4	1.3	1.2	1.3
211	Fblim1	-1.4	-1.3	-1.3	-1.3	1.4	1.3	1.7	1.5
212	Dcaf6	-1.3	-1.3	-1.4	-1.3	1.5	1.6	1.7	1.6
213	AK140216	-1.5	-1.2	-1.2	-1.3	1.6	1.8	2.1	1.9
214	Pbk	-1.3	-1.3	-1.3	-1.3	1.3	1.3	1.2	1.3
215	Rbpms	-1.3	-1.2	-1.3	-1.3	1.2	1.6	1.5	1.4
216	Fanca	-1.2	-1.3	-1.3	-1.3	1.3	1.2	1.4	1.3
217	Fry	-1.4	-1.3	-1.2	-1.3	1.5	1.8	1.7	1.7
218	Fads2	-1.3	-1.2	-1.4	-1.3	1.3	1.5	1.5	1.4
219	Gpa33	-1.4	-1.2	-1.2	-1.3	1.5	1.7	1.3	1.5
220	Qk	-1.3	-1.3	-1.2	-1.3	1.4	1.2	1.7	1.4
221	Gmnn	-1.3	-1.2	-1.2	-1.3	1.4	1.4	1.4	1.4
222	Uaca	-1.3	-1.3	-1.2	-1.3	1.3	1.4	1.5	1.4
223	Vps13d	-1.2	-1.2	-1.4	-1.3	1.4	1.5	1.8	1.6
224	Ptpru	-1.3	-1.3	-1.2	-1.3	1.4	1.4	1.6	1.4
225	Mex3b	-1.3	-1.2	-1.2	-1.3	1.7	1.2	1.5	1.5
226	Chd1l	-1.2	-1.2	-1.3	-1.3	1.3	1.2	1.2	1.2
227	Mreg	-1.2	-1.2	-1.3	-1.2	1.5	1.9	1.6	1.7
228	Nxnl2	-1.2	-1.3	-1.2	-1.2	2.2	2.1	2.2	2.1

Part 5 - A dominant mutation in *NR1P1* causes CAKUT

A dominant mutation in nuclear receptor interacting protein 1 causes urinary tract malformations via dysregulation of retinoic acid signaling

Asaf Vivante, Nina Mann, Hagith Yonath, Anna-Carina Weiss, Maike Getwan, Michael M. Kaminski, Tobias Bohnenpoll, Catherine Teyssier, Jing Chen, Shirlee Shril, Amelie T. van der Ven, Hadas Ityel, Johanna Magdalena Schmidt, Eugen Widmeier, Stuart B. Bauer, Simone Sanna-Cherchi, Ali G. Gharavi, Weining Lu, Daniella Magen, Rachel Shukrun, Richard P. Lifton, Velibor Tasic, Horia C. Stanescu, Vincent Cavallès, Robert Kleta, Yair Anikster, Benjamin Dekel, Andreas Kispert, Soeren S. Lienkamp, and Friedhelm Hildebrandt[§]

Due to the number of contributing authors, the affiliations are listed at the end of this article.

[§] Author for correspondence:

Email: Friedhelm.Hildebrandt@childrens.harvard.edu

Published in Journal of the American Society of Nephrology (J Am Soc Nephrol (2017), ePub ahead of print)

Reprinted with permission (see Appendix).

A Dominant Mutation in Nuclear Receptor Interacting Protein 1 Causes Urinary Tract Malformations via Dysregulation of Retinoic Acid Signaling

Asaf Vivante,^{*†} Nina Mann,^{*} Hagith Yonath,[‡] Anna-Carina Weiss,[§] Maïke Getwan,^{||} Michael M. Kaminski,^{||} Tobias Bohnenpoll,[§] Catherine Teyssier,[¶] Jing Chen,^{*} Shirlee Shril,^{*} Amelie T. van der Ven,^{*} Hadas Ityel,^{*} Johanna Magdalena Schmidt,^{*} Eugen Widmeier,^{*||} Stuart B. Bauer,^{**} Simone Sanna-Cherchi,^{††} Ali G. Gharavi,^{††} Weining Lu,^{‡‡} Daniella Magen,^{§§} Rachel Shukrun,^{|||} Richard P. Lifton,^{¶¶***} Velibor Tasic,^{†††} Horia C. Stanescu,^{†††} Vincent Cavallès,[¶] Robert Kleta,^{†††} Yair Anikster,^{|||} Benjamin Dekel,^{|||} Andreas Kispert,[§] Soeren S. Lienkamp,^{||§§§} and Friedhelm Hildebrandt^{*}

Due to the number of contributing authors, the affiliations are listed at the end of this article.

ABSTRACT

Congenital anomalies of the kidney and urinary tract (CAKUT) are the most common cause of CKD in the first three decades of life. However, for most patients with CAKUT, the causative mutation remains unknown. We identified a kindred with an autosomal dominant form of CAKUT. By whole-exome sequencing, we identified a heterozygous truncating mutation (c.279delG, p.Trp93fs*) of the nuclear receptor interacting protein 1 gene (*NRIP1*) in all seven affected members. *NRIP1* encodes a nuclear receptor transcriptional cofactor that directly interacts with the retinoic acid receptors (RARs) to modulate retinoic acid transcriptional activity. Unlike wild-type NRIP1, the altered NRIP1 protein did not translocate to the nucleus, did not interact with RAR α , and failed to inhibit retinoic acid-dependent transcriptional activity upon expression in HEK293 cells. Notably, we also showed that treatment with retinoic acid enhanced NRIP1 binding to RAR α . RNA *in situ* hybridization confirmed *Nrip1* expression in the developing urogenital system of the mouse. In explant cultures of embryonic kidney rudiments, retinoic acid stimulated *Nrip1* expression, whereas a pan-RAR antagonist strongly reduced it. Furthermore, mice heterozygous for a null allele of *Nrip1* showed a CAKUT-spectrum phenotype. Finally, expression and knockdown experiments in *Xenopus laevis* confirmed an evolutionarily conserved role for *NRIP1* in renal development. These data indicate that dominant *NRIP1* mutations can cause CAKUT by interference with retinoic acid transcriptional signaling, shedding light on the well documented association between abnormal vitamin A levels and renal malformations in humans, and suggest a possible gene-environment pathomechanism in this disease.

J Am Soc Nephrol 28: ●●●-●●●, 2017. doi: <https://doi.org/10.1681/ASN.2016060694>

Congenital anomalies of the kidney and urinary tract (CAKUT) constitute the most frequent cause of CKD in the first three decades of life, accounting for approximately 50% of all patients.^{1,2} CAKUT comprises a wide range of structural malformations that result from defects in the morphogenesis of the kidneys and/or the urinary tract.³⁻⁶ The pathologic basis of CAKUT lies in the disturbance of normal kidney development, primarily resulting from mutations

Received June 28, 2016. Accepted February 20, 2017.

A.V., N.M., and H.Y. contributed equally to this work.

Published online ahead of print. Publication date available at www.jasn.org.

Correspondence: Prof. Friedhelm Hildebrandt, Boston Children's Hospital, Division of Nephrology, 300 Longwood Avenue, HU319, Boston, MA 02115. Email: Friedhelm.Hildebrandt@childrens.harvard.edu

Copyright © 2017 by the American Society of Nephrology

in genes that direct this process. Most gene products that cause CAKUT in humans or mice if altered are transcription factors involved in protein-protein interactions that form large transcription complexes.^{7–13} These monogenic forms of CAKUT are often inherited in an autosomal dominant manner and exhibit the clinical features of incomplete penetrance and variable expressivity. Loose genotype/phenotype correlations, as well as extensive genetic locus heterogeneity, have rendered gene discovery in CAKUT very difficult. Although approximately 30 CAKUT genes have been identified,^{1,2,14–16} approximately 85% of patients with CAKUT do not have mutations in any known genes.^{17,18} Hence, the remaining challenge is to identify the missing components of the pathogenesis of CAKUT, in order to better understand how these proteins and transcription factor complexes exert their developmental and tissue-specific functions.

In addition to the regulatory roles of genetic factors for the proper development of the kidney and urinary tract, numerous studies also support the influence of environmental factors on normal and abnormal kidney development.^{4,19} This suggests that the pathogenesis of CAKUT can be multifactorial, likely due to a complex interplay between genes and the environment. The most prominent example of this is the effect of retinoic acid (RA), the active form of vitamin A, on the kidneys and urinary tract during development. During fetal life, nephrogenesis is influenced by RA levels, such that even modest fluctuations in maternal vitamin A levels in either direction can cause CAKUT in humans and rodents.^{20,21} In addition, elegant studies of murine kidney development by Mendelsohn *et al.* have shown that inactivation of genes in the RA pathway causes CAKUT in mice.^{22–24}

To gain further insight into the pathogenesis of CAKUT, we investigated a three-generation family with renal malformations by using whole-exome sequencing (WES). Here we identify a dominant mutation in the transcriptional cofactor *NRIP1* (*nuclear receptor interacting protein 1*) gene as causing human autosomal dominant CAKUT by interference with RA transcriptional signaling, thereby shedding light on the well documented association between RA and renal malformations.

RESULTS

Mutations in *NRIP1* Can Cause CAKUT

To identify a causative mutated gene for CAKUT, we investigated a three-generation Yemenite Jewish family with seven individuals who have CAKUT. Renal hypo/dysplasia was the predominant phenotype (six individuals), together with vesicoureteral reflux (VUR) (four individuals) and/or ectopia (two individuals) (Figure 1, A and B, Supplemental Figure 1, Table 1). The age at diagnosis ranged from the prenatal period to late adulthood (Table 1). Two of the seven affected individuals underwent unilateral nephrectomy for their malformations. None of the affected individuals had extrarenal malformations or syndromic features. The pedigree structure was compatible

with an autosomal dominant mode of inheritance with variable expressivity and incomplete penetrance (Figure 1A). Individual II:1 had a renal ultrasound showing bilateral small renal cysts (Supplemental Figure 1), which can be a common finding in his age group and is not necessarily related to the CAKUT phenotype in this family. Therefore, individual II:1 was not included in the initial WES analysis, which considered only affected family members.

Under the hypothesis that a mutation of an autosomal dominant gene causes CAKUT in this family, we selected six affected family members (individuals III:3, III:4, III:5, IV:7, IV:8, and IV:9) for WES. Given the pedigree structure (Figure 1A), the six affected individuals are expected to share about 3.125% of all alleles by descent, allowing a 32-fold reduction in the thousands of variants from the normal reference sequence that are expected to result from WES (Supplemental Table 1). We identified a novel heterozygous truncating mutation (c.279delG, p.Trp93fs*) in the gene encoding *NRIP1* (MIM 602490, RefSeq accession number NM_003489.3) (Figure 1, C and D, Table 1). Segregation analysis revealed that this mutation was shared by all seven available affected family members as well as by individual II:1, who, as expected from the pedigree structure, is an obligatory mutation carrier given that his brother (individual II:8) was found to have CAKUT on renal ultrasound and to harbor the *NRIP1* mutation (Figure 1A, Supplemental Figure 1, Table 1). In addition, the mutation was absent from seven unaffected family members, from all available databases of healthy controls including approximately 100,000 alleles in the ExAC database (Table 1), as well as from two in-house control cohorts of 200 individuals with nephronophthisis and 429 individuals with nephrotic syndrome. Finally, we showed by copy number variant (CNV) analysis that the affected index patient (IV:8) lacked any heterozygous deletions or duplications that have previously been associated with CAKUT, including the *HNF1B* locus and the DiGeorge/velocardiofacial syndrome locus.²⁵ Because Yemenite Jews are a genetically distinct Jewish sub-cluster,²⁶ we aimed to determine the frequency of the *NRIP1* mutation in 236 anonymized samples of ethnically matched Yemenite Jews whose disease status is unknown. The *NRIP1* c.279delG mutation was found in two individuals out of 236 screened (472 alleles) yielding a minor allele frequency (MAF) of 0.004. We next performed highly parallel exon sequencing of *NRIP1* in 155 sporadic cases and 253 familial cases of CAKUT (total of 724 affected individuals), but did not identify additional families with CAKUT and novel *NRIP1* variants.

The *NRIP1* Mutation Interferes with Nuclear Translocation, Transcriptional Repression, and *NRIP1* Interaction with Retinoic Acid Receptor α

NRIP1 is a nuclear receptor transcriptional cofactor.²⁷ Previous biochemical analyses showed that the murine *NRIP1* protein harbors two putative nuclear localization signals and four repression domains that mediate its transcriptional repression²⁷ (Figure 1C). In addition, *NRIP1* has been shown to directly interact with RA

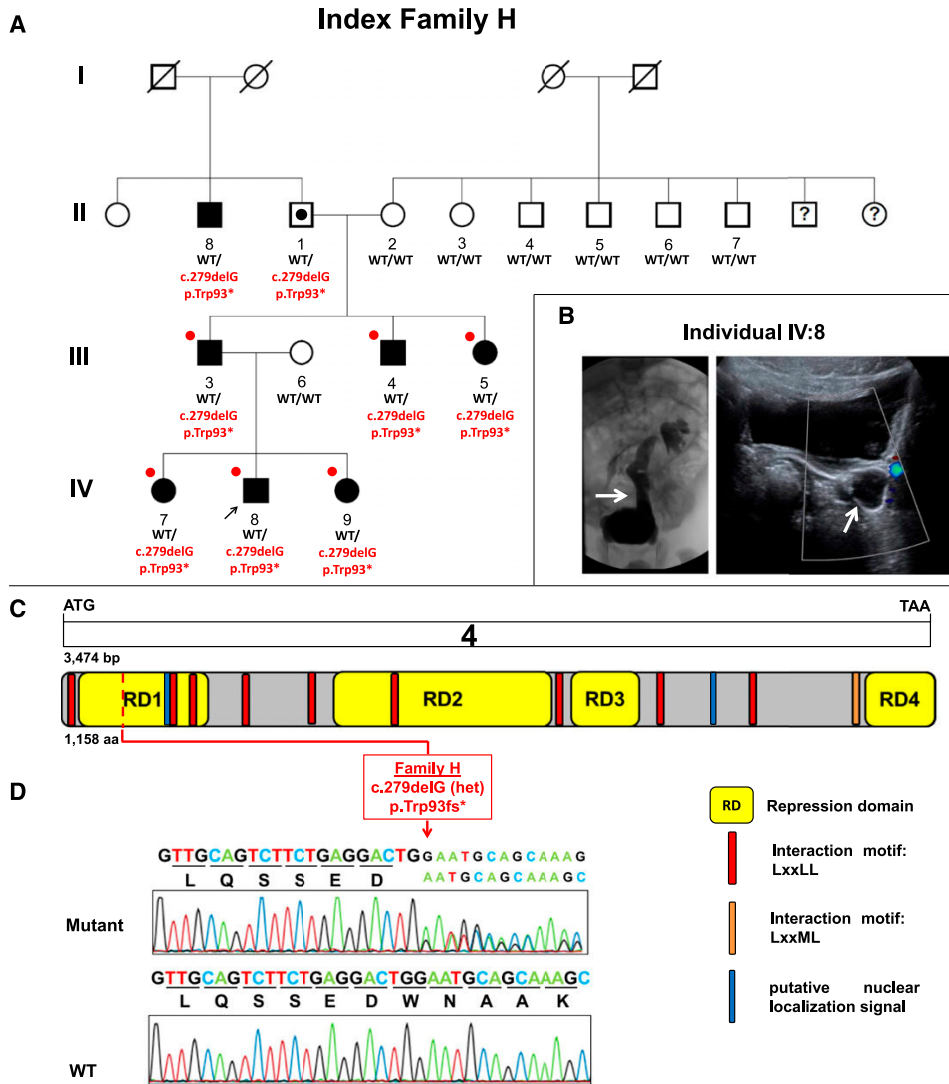


Figure 1. Identification of a heterozygous *NRIP1* truncating mutation in index family H with CAKUT. (A) Shows the pedigree of index family H. Squares represent males, circles females, black symbols affected persons, white symbols unaffected persons, and white symbol with black dot denotes an obligatory mutation carrier. White symbols with a black question mark indicate individuals with an unknown phenotype. Pedigree is compatible with an autosomal dominant mode of inheritance with incomplete penetrance and variable expressivity. Roman numerals denote generations. Individuals are numbered with Arabic numerals if DNA was tested in the study. The arrow points to the proband IV:8. WT denotes the wild-type allele. p.Trp93* indicates the mutation c.279 deletion of G in *NRIP1*, leading to a frame-shift mutation and introducing a premature stop codon. The mutation fully segregated heterozygously (WT/p.Trp93*) across all seven affected individuals examined and was absent from seven unaffected family members (WT/WT). Individual II:1 is an obligatory mutation carrier given the pedigree structure and segregation analysis. This patient was considered as having an inconclusive phenotype with only two renal cysts. Red circles indicate the persons selected for WES analysis. (B) Shows voiding cystourethrogram (left panel) and renal ultrasound (right panel) of the index individual IV:8, revealing severe grade five left VUR and hydronephrosis (white arrows, respectively). He presented during infancy after positive prenatal ultrasound screening. He is managed expectantly and has no extrarenal manifestations. (C) Shows exon structure of human *NRIP1* cDNA and domain structure of the *NRIP1* protein. *NRIP1* contains two putative nuclear localization signals (blue), four transcriptional repression domains (RD, yellow), and 10 interaction motifs LxxLL/LxxML (red and orange). Start codon (ATG) and stop codon (TAA) are indicated. (D) Shows chromatograms of the heterozygous mutation and WT sequence detected in *NRIP1* (in relation to exons and protein domains in [C]) in index family H [red] with CAKUT). The index family's heterozygous *NRIP1* mutation c.279delG leads to a frameshift and premature stop codon resulting in p.Trp93fs*.

receptors (RARs) and retinoid receptors (RXRs) to suppress their RA-mediated transcriptional activity.²⁸ The NRIP1 protein contains nine nuclear receptor interacting motifs (LxxLL) spread throughout the molecule (Figure 1C).²⁷ Interestingly, the binding of NRIP1 to RARs and RXRs was suggested to also require a slightly different sequence, an LxxML motif, located at the protein's C-terminus.²⁹

To determine how the c.279delG (p.Trp93fs*) mutation, which segregated with the CAKUT phenotype in the large family H, conveys NRIP1 loss of function, we evaluated NRIP1 for its known functional features. These include: (1) nuclear localization, (2) transcriptional repression, and (3) interaction with retinoic acid receptor α (RAR α). Transfection of expression constructs in HEK293 cells revealed that, whereas the wild-type NRIP1 protein translocated into the nucleus, the NRIP1-altered protein (p.Trp93fs*) remained localized in the cytoplasm (Figure 2, A and B). In target cells, RA, the active form of vitamin A, acts as a ligand for nuclear RARs and RXRs. The complex binds to a regulatory DNA segment, the RA response element (RARE), to control transcription of RA target genes.³⁰ Accordingly, we next determined whether the NRIP1 mutation affects RA-dependent transcriptional activity using NRIP1 expression plasmids and a reporter plasmid harboring an RARE. Although the wild-type NRIP1 expression construct acted as a transcriptional repressor, and completely suppressed RA-mediated transcriptional activity, the mutant construct (p.Trp93fs*) showed lack of transcriptional repressor activity (Figure 2C).

We previously showed that monogenic CAKUT can be secondary to a dominant-negative pathomechanism.¹⁴ To test this possibility, we cotransfected the NRIP1 wild-type construct with increasing amounts of mutant NRIP1, and subsequently performed luciferase reporter assays. This did not yield a dose-dependent lack of repression, suggesting that the loss of function caused by the mutation is not mediated *via* a dominant-negative mechanism (Supplemental Figure 2A). To further support this, we showed that wild-type and mutant NRIP1 proteins did not colocalize when cotransfected, suggesting that they do not dimerize (Supplemental Figure 2B). Furthermore, because proteins that hetero-dimerize are particularly prone, when altered, to exerting dominant-negative effects by sequestering functioning molecules into inactive dimers, we tested the interaction between the altered NRIP1 protein and RAR α . Notably, the altered NRIP1 protein still contains one intact interaction motif (Figure 1C), which may theoretically be sufficient to interact with the nuclear receptor ligand-binding domain of RAR α . We performed overexpression experiments of RAR α with either wild-type or altered NRIP1 protein. Interestingly, RAR α , when overexpressed with the wild-type NRIP1 protein, colocalized in a speckled nuclear pattern. When overexpressed with the altered NRIP1 protein (p.Trp93fs*), however, RAR α localized diffusely in the nucleus whereas the altered NRIP1 remained in the cytoplasm (Figure 2D). Furthermore, coimmunoprecipitation experiments showed that the NRIP1 mutation abrogates

NRIP1-RAR α interaction and that binding of NRIP1 to RAR α is enhanced by RA treatment (Figure 3, A and B). Taken together, these data argue against a dominant-negative pathomechanism and render a dominant mechanism of haploinsufficiency more likely.

NRIP1 mRNA Expression in the Nephric Duct and Ureteric Epithelium Depends on RA

Formation of the ureter and kidney begins with ureter budding, during which the epithelial tube sprouts from the base of the Wolffian ducts immediately above the urogenital sinus—an embryonic structure that eventually gives rise to the urinary bladder. Distally, the ureteric bud invades the renal metanephric mesenchyme and, after successive branching, gives rise to the renal collecting-duct system. The ureteric bud stalk differentiates into the ureter, and its proximal part is transposed to the primitive bladder *via* the common nephric duct. Elegant studies have shown that the common nephric duct undergoes apoptosis, thereby severing connections with the Wolffian duct as the ureter orifice is transposed to its final insertion site in the bladder ureter.²⁴ This crucial step is controlled by RA-induced signals, which govern ureter maturation and formation of proper connections between the bladder and ureter.²⁴

To further characterize the role of NRIP1 in RA signaling, we determined whether the mouse ortholog *Nrip1* is expressed in RA-dependent tissues in the development of the murine urogenital system. For this, we performed RNA *in situ* hybridization on whole-mount preparations of urogenital systems of E11.5–E18.5 mouse embryos and on sections of the urogenital system at the same stages (Figure 4A). Elevated levels of *Nrip1* transcripts were found in the nephric duct and ureter from E11.5 to E14.5, as well as in the collecting ducts at E14.5 (Figure 4A). Expression in the kidney and ureter was abolished at E18.5 (Supplemental Figure 3). To test whether *Nrip1* expression in the nephric duct and its derivatives depends on RA, we explanted E11.5 kidney rudiments and cultured them in the presence of 1 μ M RA or 1 μ M of the pan-RAR antagonist BMS493. Although BMS493 treatment strongly reduced *Nrip1* expression in the nephric duct and ureter epithelium, RA increased *Nrip1* expression in these tissues slightly (Figure 4B). Thus, *Nrip1* represents a novel RA-responsive gene in the genitourinary system.

Functional *In Vivo* Studies in *Xenopus laevis* Show a Major Role for NRIP1 during Renal Development Which Is Abolished with the Mutant NRIP1

Expression and knockdown experiments in *X. laevis* further confirmed a role for NRIP1 in renal development. Because unilateral injections allow a tissue-restricted knockdown and analysis of organ-specific phenotypes, we turned to the *Xenopus* model to analyze the developmental events in renal formation in further detail.³¹ *Nrip1* is expressed during *Xenopus* development at neurula and tadpole stages. Strong expression was detected in the condensing pronephric tubules and somites (Figure 5, A–C'). Neither overexpression of the wild type NRIP1 nor the altered protein significantly interfered

Table 1. Dominant *NRIP1* mutation detected in individuals with CAKUT^a

Family – Individual ^{a,b,c}	Presenting Symptoms or Diagnostic Test (at Age in yr)	Kidney Phenotype	Treatment	Serum Creatinine, mg/dl (at Age in yr)
H				
II:8	Renal US (69)	R small pelvic kidney with hydronephrosis	Conservative	0.93 (69)
III:3	Abdominal mass (newborn)	L MCDK; R VUR, dilated ureter, and dysplasia	L nephrectomy R nephrostomy	1.5 (35)
III:4	Abdominal pain (7)	L dysplastic kidney and VUR	L nephrectomy	0.75 (27)
III:5	Renal US and VCUG (3)	Bilateral grade 2 VUR	Conservative	0.64 (28)
IV:7	Renal US (2)	Small right kidney	Conservative	0.23 (5)
IV:8	Hydronephrosis on renal US (prenatal)	L VUR grade 5 and dysplasia; R VUR grade 2	Conservative	0.45 (8)
IV:9	Renal US (prenatal)	L ectopic dysplastic kidney	Conservative	0.23 (3)

Co-IP, coimmunoprecipitation; k.d., knock-down; US, ultrasound; R, right; L, left; MCDK, multicystic dysplastic kidney; VCUG, voiding cystourethrogram.

^aAll individuals were found to harbor a c.279delG mutation in *NRIP1*. The cDNA mutation is numbered according to human cDNA reference sequence NM_003489.3, isoform (*NRIP1*), where +1 corresponds to the A of ATG start translation.

^bThe c.279delG *NRIP1* mutation corresponds to the following alteration in the coding sequence: p.Trp93fs*. This mutation was absent from 200 control individuals with renal ciliopathies, 429 individuals with steroid-resistant nephrotic syndrome, from approximately 13,000 healthy control alleles of the EVS (<http://evs.gs.washington.edu/EVS/>), from 2577 control individuals of the “1000 genomes project” (<http://www.1000genomes.org/>), and from approximately 100,000 control chromosomes of the ExAC server (<http://exac.broadinstitute.org/>). In addition, *NRIP1* had an ExAC: pLI (probability of being loss-of-function intolerant) score of 0.99. The closer the pLI is to 1, the more loss-of-function-intolerant the gene appears to be. Genes with pLI \geq 0.9 are considered as an extremely loss-of-function-intolerant set of genes.

^cLoss of function of the *NRIP1* c.279delG allele was demonstrated in four assays: nuclear localization (Figures 2A and 2B), luciferase assay (Figure 2C), co-IP with RAR α (Figure 3A), or *Xenopus* knockdown and rescue experiments (Figure 5, D–K).

with pronephric development, again arguing against a dominant-negative effect of the mutant construct (Figure 5, E, F, and K). Knockdown with a translation-blocking *nrip1* MO inhibited renal development and resulted in distorted pronephric structures (Figure 5, H and K; $P < 0.001$). This could partially be rescued with the wild-type *NRIP1* mRNA (Figure 5, I and K; $P = 0.01$) but not with the mutant (*NRIP1* 279delG) mRNA (Figure 5, J and K; $P = 0.43$).

Further analysis of early pronephros markers after *nrip1* MO injection resulted in significantly reduced expression of transcription factors implicated in pronephros specification and patterning, such as *wt1*, *lhx1*, *tfap2b*, *sall1*, and *evi1* (Figure 6). No significant difference was observed for *gata3* or *pax8*. We conclude that *nrip1* is necessary for early specification events in pronephros formation in *Xenopus*. Taken together, these data support a role for *nrip1* during early tubular morphogenesis, and are consistent with the human CAKUT phenotype.

CAKUT Phenotype in *Nrip1*^{+/-} Mice

Previous work reported that mice homozygous for a null allele of *Nrip1* exhibit defective ovulation in females as well as reduced body weight and body fat content.³² The genitourinary system was not yet analyzed for defects. To uncover a possible involvement of *Nrip1* in the development of the murine urinary tract, we analyzed mice heterozygous for a null allele of *Nrip1* at E18.5 for phenotypic changes. In all three specimens analyzed we detected dysplastic kidneys with cystic dilations. One of the specimens exhibited severe hydroureter with hydronephrosis and ureterocele (Figure 7). Hence, heterozygous

loss of *Nrip1* results in a spectrum of CAKUT phenotypes in mice similar to the human situation.

DISCUSSION

We identified a truncating mutation of *NRIP1* as a novel autosomal dominant cause of human CAKUT. By studying *NRIP1* cellular localization, transcriptional activation, and protein-protein interaction, we demonstrate loss of function for a truncating *NRIP1* mutation (c.279delG; p.Trp93fs*) that segregated in a large CAKUT pedigree. We show that this mutation acts *via* haploinsufficiency rather than in a dominant-negative manner. By expression and knockdown experiments in *X. laevis*, as well as by analyzing the genitourinary system in mice with *Nrip1* heterozygous deletions, we generated additional data that suggest that dysregulation of *NRIP1*-dependent RA signaling during kidney and ureter morphogenesis causes CAKUT.

NRIP1, also known as receptor-interacting protein 140 (RIP140), is a transcriptional coregulator that plays an integral role in fine-tuning the activity of a large number of transcription factors during development.²⁷ *NRIP1* has been mainly implicated in transcriptional repression by interacting with different nuclear receptors, including the RARs.^{28,29,33,34} Nonetheless, the role of *NRIP1* during kidney and ureter development, as well as its relation to RA signaling, has remained unclear. In this study, our finding of a germline *NRIP1* mutation as a novel cause of human CAKUT

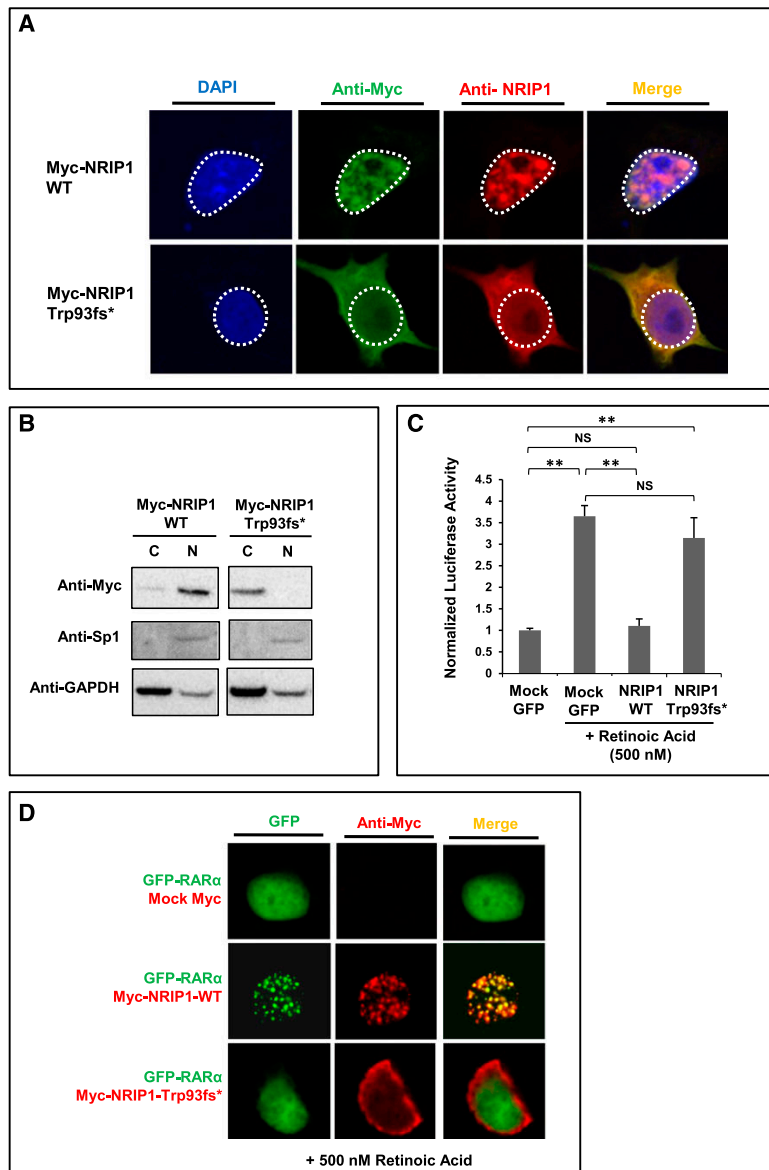


Figure 2. NRIP1 p.Trp93fs* fails to translocate to the nucleus, does not suppress RA-induced transcriptional activation, and fails to interact with RAR α . (A) Immunofluorescence staining of HEK293 cells transfected with Myc-tagged wild-type (WT) NRIP1 cDNA and Myc-tagged NRIP1 c.279delG cDNA. WT NRIP1 localizes to the nucleus, whereas the altered NRIP1 protein (p.Trp93fs*) predominantly localizes to the cytoplasm. (B) Western blot of cytoplasmic (C) and nuclear (N) extracts from transfected HEK293 cells shows localization of WT NRIP1 predominantly in the nucleus and of NRIP1 p.Trp93fs* in the cytoplasm. Sp1 and GAPDH were used as nuclear and cytoplasmic markers, respectively. (C) Luciferase assay of HEK293 cells transfected with Mock GFP, GFP-tagged WT NRIP1 cDNA, and GFP-tagged NRIP1 c.279delG mutant cDNA and subsequently treated with RA. WT NRIP1 suppresses RA-induced transcriptional activity, whereas the mutant form fails to do so. (D) Immunofluorescence staining of HEK293 cells cotransfected with GFP-tagged RAR α and either Mock Myc, Myc-tagged WT NRIP1, or Myc-tagged NRIP1 c.279delG. RAR α and WT NRIP1 colocalize in the nucleus (speckled pattern), whereas the

provides a link between the well documented association of vitamin A/RA and renal malformations.^{20,21,24}

RA is a signaling molecule that is crucial in the development of many organs.³⁵ In human^{21,36} and rodent^{20,37} embryos, both excess or deficiency (which was shown mainly in animal models) of RA can cause CAKUT. Classic mouse-model studies have highlighted the importance of RA signaling for proper ureter maturation and ureter-bladder connectivity.^{22–24} Perturbation of this process in mice can result in hypo/dysplastic kidneys as well as in backflow of urine to the ureters, clinically known as VUR. Interestingly, renal dysplasia and VUR were both the predominant phenotypes in the kindred we have studied (Figure 1, Supplemental Figure 1, Table 1). Furthermore, we detected a ureterocele in one *Nrip1*^{+/-} embryo, pointing to a role of NRIP1 in regulating RA signaling during ureter maturation. Our results indicate that NRIP1 inhibits RA-induced transcription. Because *Nrip1* is a target of RA signaling in the nephric duct and ureter, NRIP1 most likely serves as a feedback inhibitor for this pathway in ureter development. We postulate that loss of this feedback inhibition results in an excess of RA and RA signaling, leading to congenital renal and urinary tract malformations. A negative-feedback regulatory mechanism for NRIP1 is also supported by previous reports.³⁸

NRIP1 mutations have never been implicated before in human disease. Furthermore, early NRIP1 truncating mutations are absent from all available WES databases, supporting intolerance for this gene for loss of function (see ExAC: pLI score of 0.99 [*i.e.*, probability of being loss-of-function intolerant]). This is consistent with our finding that the early truncating NRIP1 mutation, which we identified, results in a pathomechanism of haploinsufficiency rather than a dominant-negative effect. The fact that we did not find a second CAKUT family with NRIP1 mutations supports the general notion that CAKUT is probably caused by a very large number of different

Trp93fs* altered protein remains in the cytoplasm and fails to produce a speckled nuclear pattern together with RAR α . ***P*<0.01.

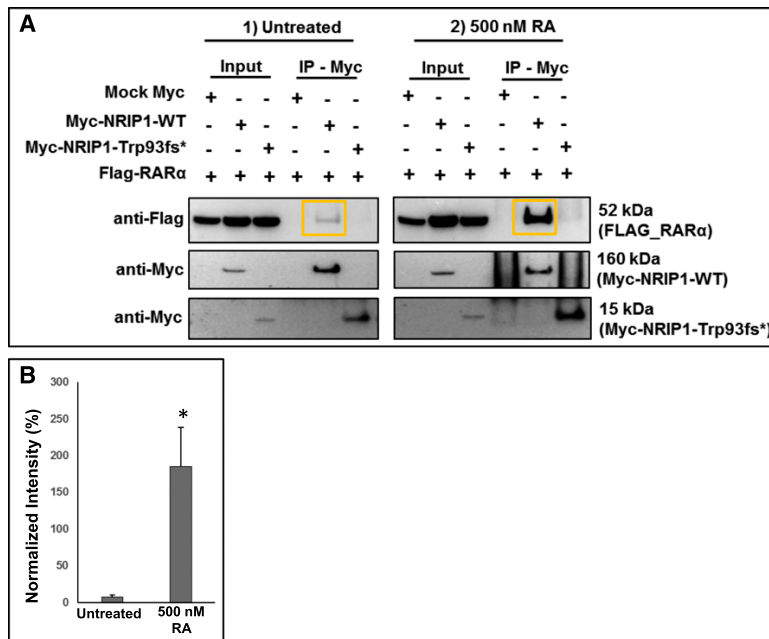


Figure 3. RA increases NRIP1 binding to RAR α *in vitro*. (A) Coimmunoprecipitation of protein lysates of wild type (WT) NRIP1 and RAR α overexpressed in HEK293 cells. Note that the Trp93fs* mutation abrogates binding to RAR α . Treatment with RA increases WT NRIP1 binding to RAR α (orange boxes). (B) Quantification of data shown in (A). RAR α coimmunoprecipitation band intensity was normalized to WT NRIP1 immunoprecipitation band intensity in the absence and presence of RA. * $P < 0.05$, average of three separate experiments.

and extremely rare disease-causing mutations in large numbers of different genes.^{1,17}

Our study provides several insights into the complex genetic basis of CAKUT.⁴ In addition to the genetic heterogeneity, low penetrance mutations, and variable expressivity already described in monogenic CAKUT, our results emphasize possible gene-environment interactions as an additional level of complexity in the pathogenesis of human CAKUT and provide insight into potential therapeutic targets.

The loss-of-function mutation we identified in the *NRIP1* gene may cause developmental renal abnormalities in humans and could indicate that *NRIP1* is an important player in the development of the kidneys and urinary tract. Any generalizations regarding its direct causal role, however, must await the description and characterization of mutations in additional patients.

CONCISE METHODS

Study Participants

After informed consent, we obtained clinical data, pedigree data, and blood samples from individuals with CAKUT from worldwide sources using a standardized questionnaire. Approval for human

subjects' research was obtained from the Institutional Review Boards of the University of Michigan, Boston Children's Hospital, Sheba Medical Center, and from other relevant local Ethics Review Boards. Informed consent was obtained from the individuals and/or parents, as appropriate. The diagnosis of CAKUT was made by (pediatric) nephrologists and/or urologists on the basis of relevant imaging.

WES

To identify a causative mutated gene for CAKUT, we investigated family members from a three-generation Yemenite Jewish family (Figure 1) with an autosomal dominant form of CAKUT characterized predominantly by lower urinary tract involvement, renal hypodysplasia, and/or ectopia (Table 1). DNA samples from six affected individuals (Figure 1) were subjected to WES using Agilent SureSelect human exome capture arrays (Life Technologies) with next-generation sequencing on an Illumina sequencing platform. Sequence reads were mapped against the human reference genome (NCBI build 37/hg19) using CLC Genomics Workbench (version 6.5.1) software (CLC bio). Mutation calling under an autosomal dominant model was performed by geneticists and cell biologists, who had knowledge regarding clinical phenotypes, pedigree structure, genetic mapping, and WES evaluation (Supplemental Table 1), and in line with proposed

guidelines.^{39,40} Sequence variants that remained after the WES evaluation process were examined for segregation.

WES Analysis

After WES, genetic variants were first filtered to retain only heterozygous, nonsynonymous variants that were shared between the six affected relatives of family H subjected to WES (Supplemental Table 1). Second, filtering was performed to retain only alleles with a MAF $< 0.1\%$, a widely accepted cutoff for autosomal dominant disorders.^{41,42} MAF was estimated using combined datasets incorporating all available data from the 1000 Genomes Project, the Exome Variant Server (EVS) project, dbSNP138, and the Exome Aggregation Consortium (ExAC). Third, observed sequence variants were analyzed using the UCSC Human Genome Bioinformatics Browser for the presence of paralogous genes, pseudogenes, or misalignments. Fourth, we scrutinized all variants with MAF $< 0.1\%$ within the sequence alignments of the CLC Genomic Workbench software program for poor sequence quality and for the presence of mismatches that indicate potential false alignments. Fifth, we employed web-based programs to assess variants for evolutionary conservation, to predict the effect of disease candidate variants on the encoded protein, and to predict whether these variants represented known disease-causing mutations. Finally, Sanger sequencing was performed to confirm the remaining variants in original DNA

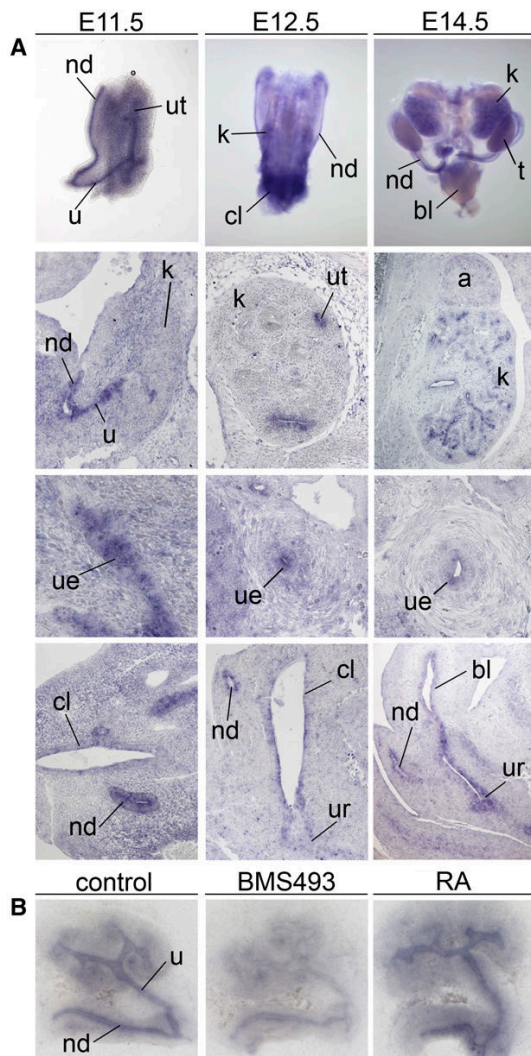


Figure 4. *Nrip1* is a target of RA in the nephric duct and ureter epithelium. (A) *In situ* hybridization analysis of expression of *Nrip1* in whole urogenital systems (first row), on coronal kidney sections (second row), on transverse ureter sections (third row), and on cloaca/bladder sections (fourth row) of wild-type embryos at E11.5, E12.5, and E14.5. *Nrip1* is expressed in the epithelium of the cloaca, the nephric duct, and the ureter from E11.5 to E14.5. a, adrenal gland; bl, bladder; cl, cloaca; k, kidney; nd, nephric duct; t, testis; u, ureter; ue, ureteric epithelium; ur, urethra; ut, ureteric tip. (B) *In situ* hybridization analysis of *Nrip1* expression in kidney rudiments dissected from E11.5 wild-type embryos and cultured for 24 hours in the presence of 1 μ M of BMS493 or 1 μ M RA. *Nrip1* mRNA expression in the nephric duct and the ureteric tree is downregulated after treatment with the pan-RAR antagonist BMS493, and upregulated after treatment with RA.

samples and to test for familial segregation of phenotype with genotype. Variants were also tested for absence from in-house control populations of 200 individuals with nephronophthisis

and 429 individuals with steroid-resistant nephrotic syndrome (Supplemental Table 1).

CNV Analysis

One individual from the index family (family H individual IV:8; Figure 1A, Table 1) was analyzed for copy number variations. CNV analysis was performed on a 180K genome-wide array, using array comparative genomic hybridization with approximately 180,000 oligonucleotides covering the whole genome at an average resolution of 30 kb, with denser coverage at disease loci. The array was designed by Baylor Medical Genetics Laboratories and manufactured by Agilent. The CNV calls were determined with generalized copy number variation algorithms. CNVs were mapped to the human reference genome hg19, and annotated with UCSC RefGene. Polymorphic variants were excluded on the basis of the database of genomic variants (<http://projects.tcag.ca/variation/>).

High-Throughput NRIP1 Mutation Analysis

Massively parallel sequencing of all *NRIP1* exons was performed in 155 sporadic cases and 253 familial cases of CAKUT (total of 724 affected individuals) from different pediatric nephrology centers worldwide using microfluidic PCR (Fluidigm) and next-generation sequencing (MiSeq; Illumina), as described previously.^{43,44} Variants were filtered against public variant databases (<http://evs.gs.washington.edu/EVS>) and only novel heterozygous variants were considered, confirmed by Sanger sequencing, and tested for segregation with the CAKUT phenotype.

cDNA Cloning

Full-length human *NRIP1* cDNA (cDNA clone MGC:9257 IMAGE:3918685) and *RAR α* cDNA (cDNA clone MGC:1651 IMAGE:3163891) were subcloned by PCR from full-length cDNA clones. Expression vectors were generated using LR Clonase (Thermo Fisher) according to the manufacturer's instructions. The following expression vectors were used in this study: pRK5-N-Myc, pcDNA6.2-N-GFP, and pDest69-FLAG. Mutagenesis was performed using the QuikChange II XL site-directed mutagenesis kit (Agilent Technologies) to generate a clone with the *NRIP1* mutation identified in family H.

Cell Culture, Transient Transfections, and RA Treatment

The experiments described were performed in HEK293 cells purchased from the American Type Culture Collection biologic resource center. For transient transfections, HEK293 cells were seeded at 60%–70% confluency in DMEM, supplemented with 10% fetal calf serum and 1% penicillin/streptomycin, and grown overnight. Transfections were carried out using Lipofectamine2000 (Thermo Fisher) and OptiMEM (Thermo Fisher) following the manufacturer's instructions. For experiments involving treatment with RA, HEK293 cells were treated with 500 nM RA 24 hours after transfection. Experiments were then carried out 24 hours after continuous treatment with RA.

NRIP1 Reporter Gene Assays

Reporter assays (Dual luciferase reporter assay system; Promega) were carried out using HEK293 cells seeded in 24-well dishes and transfected with constant amounts of reporter plasmids and 100 ng of

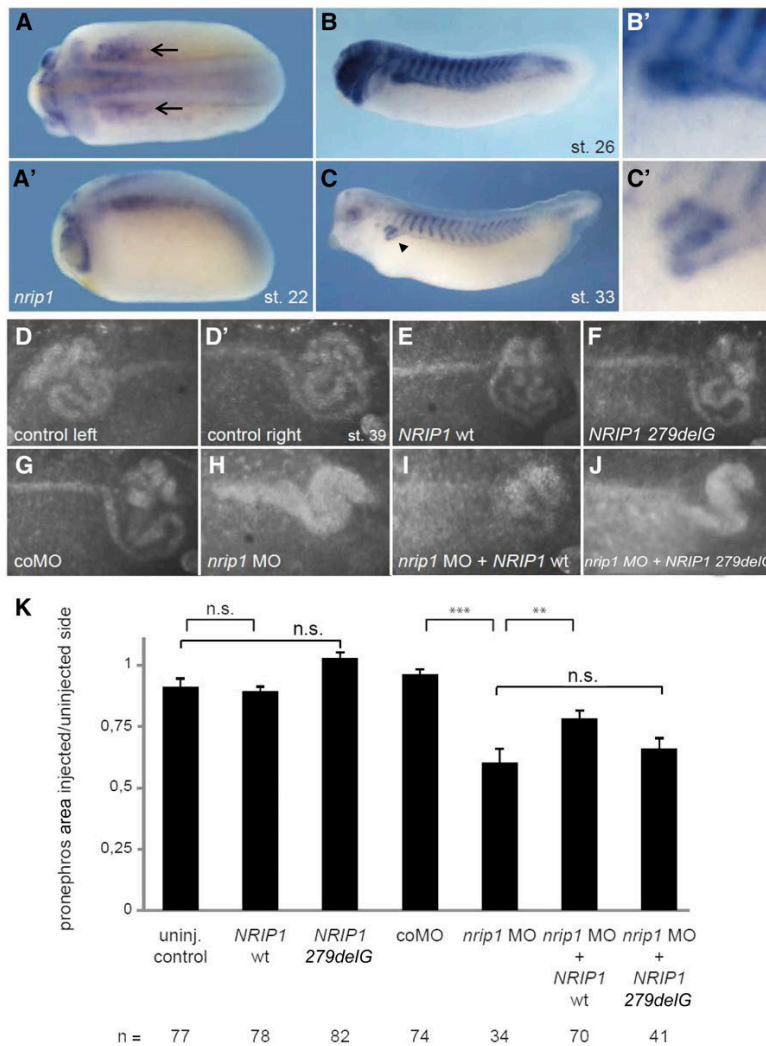


Figure 5. *Nrip1* deficiency affects pronephros development in *Xenopus*. (A–C) WM-ISH of *nrip1* expression in *X. laevis* shows its occurrence in the pronephros during development. Expression starts in the pronephric anlage at stage 22 (A, A') (black arrows) and is present in the tubules of stage 26 (B, B') and stage 33 tadpoles (C, C') (black arrow head). (D–K) Functional analysis of *nrip1* in *X. laevis*. Embryos were unilaterally injected with *nrip1* MO and/or *NRIP1*-encoding mRNA at the four-cell stage. Stage 39 tadpoles were stained with fluorescein-conjugated lectin to visualize the pronephros (D–J). The size of the pronephros was measured and the proportion between the injected (right) and uninjected (left) side calculated (K). The structure of the pronephros was not changed by microinjections of the *NRIP1* wt (E/K) mRNA or its truncated variant (*NRIP1* 279delG; [F]) compared with the controls (D'/K). Knockdown with a translation-blocking *nrip1* MO inhibited pronephros development (H/K; $P < 0.001$) and could be partially rescued with *NRIP1* wt (I/K; $P = 0.01$) but not with *NRIP1* G279 del (J/K; $P = 0.43$). Error bars represent SEM. ** $P < 0.01$, *** $P < 0.001$ (MWU-test). coMO, control morpholino oligonucleotide; del, deletion; MO, antisense morpholino oligonucleotide; st., stage according to Nieuwkoop and Faber⁵⁰; wt, wild-type.

pRL-TK Renilla luciferase for normalization. The total amount of expression plasmid was kept constant by adding empty *pcDNA6.2-N-GFP*. Per transfection, 500 ng of *pGL3-RARE* (RAREs) luciferase ([https://www.](https://www.addgene.org)

[addgene.org](https://www.addgene.org), plasmid, 13458; Addgene, Cambridge, MA) and 500 ng of *pcDNA6.2-N-GFP.NRIP1* expression plasmid were used. For competition experiments, the amount of *pcDNA6.2-N-GFP.NRIP1_WT* was held constant and increasing amounts of *pcDNA6.2-N-GFP.NRIP1_p.Trp93fs** were added. Firefly luciferase and Renilla luciferase activities were measured 24 hours after transfection. All transfections were performed in triplicate, and individual experiments were repeated at least three times. In addition, all experiments were repeated with a different RARE reporter plasmid (*RARE-tk-luciferase*, kind gift from Li-Na Wei). After normalization, the mean luciferase activities and standard deviations were plotted as “fold activation” when compared with the empty expression plasmid. *P* values were determined using the paired *t* test.

Immunofluorescence and Confocal Microscopy in Cell Lines

For immunostaining, HEK293 cells were seeded on fibronectin-coated coverslips in 6-well plates. After 16–24 hours, cells were transiently transfected using Lipofectamine2000 (Thermo Fisher) according to the manufacturer’s instructions. Experiments were performed 24–48 hours after transfection. Cells were fixed for 15 minutes using 4% paraformaldehyde and permeabilized for 15 minutes using 0.5% Triton X-100. After blocking with 10% donkey serum + BSA, cells were incubated with primary antibody overnight at 4°C. The following day, cells were incubated in secondary antibody for 60 minutes at room temperature, and subsequently stained for 5 minutes with 4',6-diamidino-2-phenylindole (DAPI) in PBS. Confocal imaging was performed using the Leica SP5 × system with an upright DM6000 microscope, and images were processed with the Leica AF software suite. Immunofluorescence experiments were repeated at least two times in independent experiments. The following antibodies were used for immunostaining: mouse anti-Myc (sc-40; Santa Cruz Biotechnology) and rabbit anti-NRIP1 (ab42125; Abcam), both diluted 1:100. Donkey anti-mouse secondary antibodies conjugated to Alexa Fluor 488 or 594 and donkey anti-rabbit secondary antibody conjugated to Alexa Fluor 594 were purchased from Thermo Fisher Scientific.

Coimmunoprecipitation Assays

Coimmunoprecipitation experiments were performed using protein lysates from transfected HEK293 cells. Cell lysates were precleared with Recombinant Protein G Sepharose beads (Thermo Fisher) at 4°C overnight in IP lysis buffer (Thermo Fisher) containing Halt Protease Inhibitor

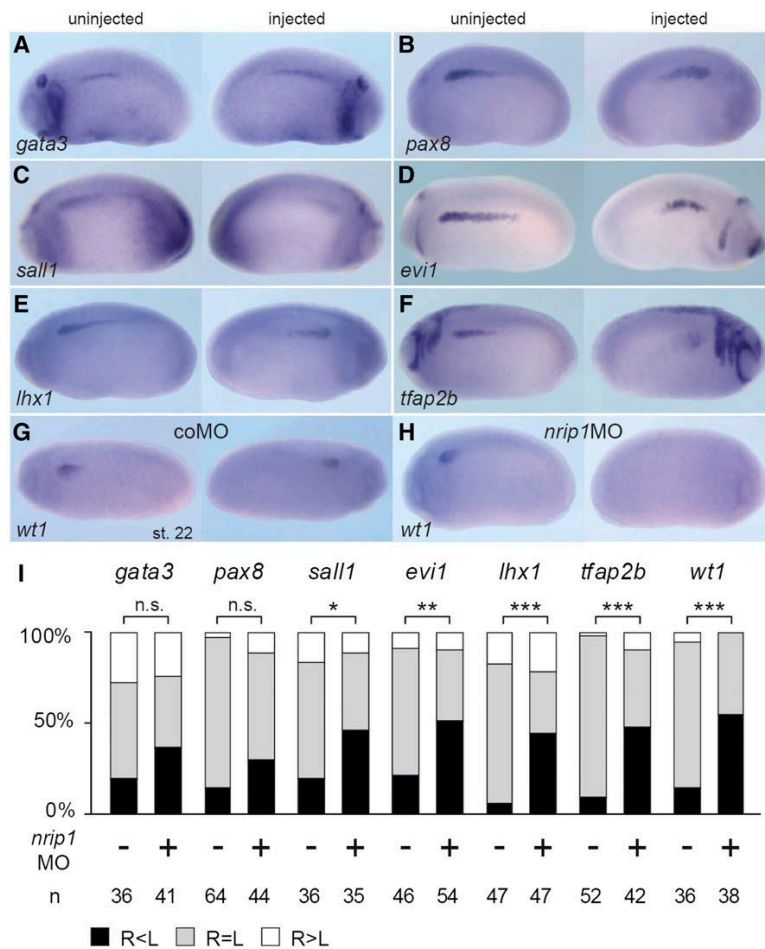


Figure 6. *Nrip1* deficiency affects early pronephros marker gene expression in *Xenopus* embryos. (A–H) Pronephros marker gene analysis of *Nrip1*-depleted embryos at stage 22. Embryos were injected with *nrip1* MO (+) or control MO (–) at the four-cell stage targeting their right sided pronephros. An *in situ* hybridization was performed for early pronephros markers (*gata3*, *pax8*, *sall1*, *emx1*, *evi1*, *lhx1*, *tfap2b*, and *wt1*) followed by the examination of their expression intensity on the injected (right) side compared with the un.injected side and quantified as shown in (I) (R, right side, injected; L, left side, un.injected). The expression of *gata3* was not affected ($P=0.16$ z-test). The expression of *pax8* ($P=0.09$) was slightly, but not significantly, reduced. Significant differences were observed for *sall1* (C; $P=0.035$ z-test), *evi1* (D; $P=0.004$), *lhx1*, *tfap2b*, and *wt1* (E–H; $P<0.001$). n, number of embryos analyzed. * $p<0.05$; ** $p<0.01$; *** $p<0.001$. coMO, control morpholino oligonucleotide; MO, antisense morpholino oligonucleotide; n.s., not significant.

Cocktail (Thermo Fisher) and EDTA (Thermo Fisher). Coimmunoprecipitation of Myc-tagged proteins was performed using Myc agarose beads (Sigma). The beads were washed four times with lysis buffer and proteins were eluted from the beads by incubating in loading buffer for 30 minutes at 30°C, shaking at 300 rpm. Samples were analyzed by western blot with anti-Myc (sc-40; Santa Cruz Biotechnology) and anti-FLAG (F3165; Sigma) antibodies at 1:1000 dilutions. Horseradish peroxidase-labeled secondary antibodies were purchased from Santa Cruz Biotechnology. Ten percent of the input was loaded as a

control. Experiments were repeated at least three times in independent experiments and quantification of band intensity was performed using ImageJ (<https://imagej.nih.gov/ij/>).

Organ Cultures

E11.5 kidney rudiments were dissected from the embryo, explanted on 0.4- μ m polyester membrane Transwell supports (Corning), and cultured at the air-liquid interface for 24 hours with DMEM/F12 (Gibco) supplemented with 10% FCS (Biocrom), 1 \times penicillin/streptomycin (Gibco), 1 \times pyruvate (Gibco), and 1 \times glutamax (Gibco). The pan-RA receptor antagonist BMS493 (Tocris) or RA (Tocris) was dissolved in DMSO and used at a final concentration of 1 μ M in the culture medium.

In Situ Hybridization Analysis

Whole-mount *in situ* hybridization (WM-ISH) was performed with a digoxigenin-labeled antisense riboprobe corresponding to position 3102–4030 of the *Nrip1* mRNA (NM_173440.2) following a standard procedure.⁴⁵ Stained specimens were cleared in 80% glycerol before documentation. *In situ* hybridization on 10- μ m paraffin sections was done essentially as described.⁴⁶ For each stage, at least three independent specimens were analyzed.

Xenopus Embryo Manipulations

Xenopus embryos were cultured and their stages determined as described before.⁴⁷ Microinjections were performed in the ventrolateral region of 4- and 8-cell stage *Xenopus* embryos targeting the pronephros anlagen. Five-hundred picograms of RNA and/or 10 ng MO in a volume of 10 nl were injected. A standard control MO was used as negative control. GFP-mRNA or RFP-mRNA were coinjected as lineage tracers and embryos showing fluorescence in the pronephros were sorted for further analysis.

Staining and Imaging of Xenopus Embryos

Xenopus embryos were fixed with MEMFA (0.1 mol/L Mops, 2 mmol/L EGTA, 1 mmol/L MgSO₄, 3.7% formaldehyde, pH 7.4) for 2 hours at room temperature. For WM-ISH, *nrip1* in *pBS II KS* (–) was linearized with *NotI*. The digoxigenin-labeled antisense probe was transcribed with SP6 (Roche) and bound probes detected with an alkaline phosphatase-conjugated secondary antibody (Roche). WM-ISH was performed as described before.⁴⁸ For immunofluorescence, embryos were fixed at stage 39 and their pronephros stained with fluorescein or Texas Red-labeled Lycopersicon esculentum

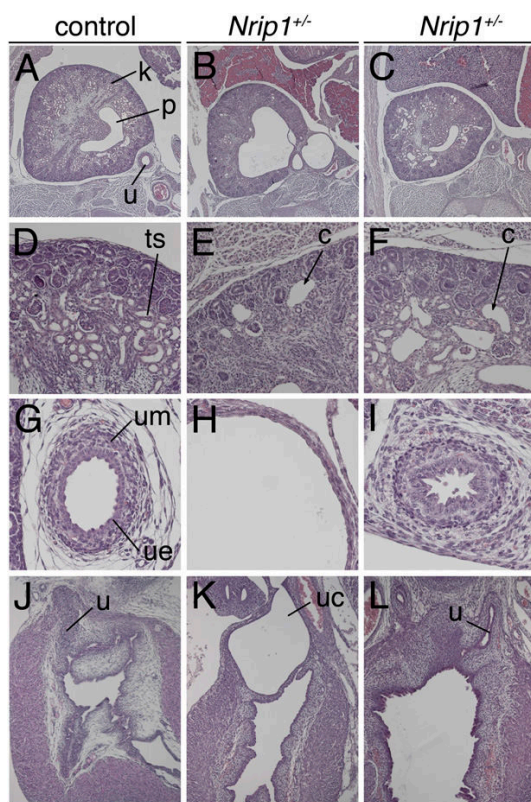


Figure 7. Mice heterozygous for an *Nrip1* null allele exhibit a spectrum of CAKUT phenotypes at E18.5. (A–L) Hematoxylin and eosin stainings of transverse sections of kidney and the ureter (A–C), kidney cortex (D–F), proximal ureter (G–I), and of sagittal sections of the embryonic bladder (J–L) from *Nrip1*^{+/-} E18.5 embryos. One of three *Nrip1*^{+/-} embryos analyzed exhibits a strong hydronephrosis, hydronephrosis, and ureterocele (middle panel). In two more specimens, kidneys are dysplastic and have microcystic dilations (right panel). In two more specimens, kidneys are dysplastic and have microcystic dilations (right panel). c, cysts; k, kidney; p, pelvis; ts, tubular structures of the kidney; u, ureter; uc, ureterocele; ue, ureteric epithelium; um, ureteric mesenchyme.

lectin (1:100 dilution; Vector Laboratories). Embryos were imaged with SteREO Discovery.V8 from Zeiss and Zen 2011 Blue Edition. The pronephros size was measured with ImageJ and the ratio of the injected and uninjected side calculated.⁴⁷ SigmaStat was used to show statistical significance with the Wilcoxon–Mann–Whitney test. Significances are quoted in the figure legend and above the bars with *** $P < 0.001$, ** $P < 0.01$, and * $P < 0.05$.

Xenopus Plasmids, MOs, and mRNA Synthesis

Full-length human *NRIP1* CDS was obtained from BIOCAT and subcloned into VF10⁴⁹ for overexpression in *Xenopus* after addition of a stop-codon. The deletion construct *NRIP1* 279delG was generated by site-directed mutagenesis (New England BioLabs). mRNAs for microinjections were synthesized by *in vitro* transcription of linearized plasmids using the mMessage Machine kit (Ambion, Kassel,

Germany). For WM-ISH full-length CDS of *X. laevis nrip1* (NM_001090238.1) was cloned with *MluI/NotI* restriction enzyme sites in *pBS II KS (-)*. The *nrip1* translation-blocking morpholino oligonucleotide (5'-AGCTCTCTCCATAAGTCATGTTCA-3') was designed by and ordered from GeneTools.

Analysis of *Nrip1*-Deficient Mice

Mice with a null allele of *Nrip1* (RIPKO mice) were generated in Professor MG Parker's laboratory (Imperial College London, London, UK).³² They were maintained at the ICRM under standard conditions, on a 12:12-hour light/dark schedule and fed a chow diet *ad libitum*, according to European Union guidelines for use of laboratory animals. In compliance with the French guidelines for experimental animal studies (agreement B34–172–27), heterozygous mice were mated to wild-type C57BL/6J mice. At E18.5, females were euthanized to obtain heterozygous *Nrip1* embryos which were fixed in 4% PFA and processed into methanol before paraffin-embedding and sectioning to 5 μ m. Hematoxylin and eosin staining was performed according to standard procedures. Three embryos of each genotype were used for each analysis.

Web Resources

<http://www.renalgenes.org>
 UCSC Genome Browser, <http://genome.ucsc.edu/cgi-bin/hgGateway>
 1000 Genomes Browser, <http://browser.1000genomes.org>
 Ensembl Genome Browser, <http://www.ensembl.org>
 Exome Variant Server, <http://evs.gs.washington.edu/EVS>
 Polyphen2, <http://genetics.bwh.harvard.edu/pph2/>
 Sorting Intolerant From Tolerant (SIFT), <http://sift.jcvi.org>
 Online Mendelian Inheritance in Man (OMIM), <http://www.omim.org/>
 ExAC Browser Beta, <http://exac.broadinstitute.org>
 Gudmap (GenitoUrinary Molecular Anatomy Project), <http://www.gudmap.org>
 Mutation Taster, <http://www.mutationtaster.org/>

ACKNOWLEDGMENTS

We are grateful to the family who contributed to this study. We thank Li-Na Wei for providing us with the RARE luciferase reporter.

This research was supported by grants from the National Institutes of Health to R.P.L. and to F.H. (DK088767), and from the March of Dimes to F.H. A.V. is a recipient of the Fulbright postdoctoral scholar award for 2013 and is also supported by grants from the Manton Center Fellowship Program, Boston Children's Hospital, Boston, Massachusetts, and the Mallinckrodt Research Fellowship Award. N.M. was supported by a Fred Lovejoy Resident Research and Education Award. A.T.v.d.V. is the recipient of a postdoctoral research fellowship from the German Research Foundation (DFG), VE916/1-1. R.P.L. is an Investigator of the Howard Hughes Medical Institute and is supported by a grant from the Yale Center for Mendelian Genomics, grant U54HG006504. Work in the laboratory of A.K. was supported by a grant from the German Research Council (DFG KI728/9-1). S.S.L. is supported by the Emmy Noether Programme (LI1817/2-1) and Project B07 of the collaborative research initiative (SFB 1140/KIDGEM) by the German

Research Foundation (DFG). E.W. is supported by the Leopoldina Fellowship Program, German National Academy of Sciences Leopoldina (LPDS 2015-07). E.H. is the William E. Harmon Professor of Pediatrics at Harvard Medical School.

DISCLOSURES

None.

REFERENCES

- Vivante A, Kohl S, Hwang DY, Dworschak GC, Hildebrandt F: Single-gene causes of congenital anomalies of the kidney and urinary tract (CAKUT) in humans. *Pediatr Nephrol* 29: 695–704, 2014
- Vivante A, Hildebrandt F: Exploring the genetic basis of early-onset chronic kidney disease. *Nat Rev Nephrol* 12: 133–146, 2016
- Dressler GR: Advances in early kidney specification, development and patterning. *Development* 136: 3863–3874, 2009
- Nicolaou N, Renkema KY, Bongers EM, Giles RH, Knoers NV: Genetic, environmental, and epigenetic factors involved in CAKUT. *Nat Rev Nephrol* 11: 720–731, 2015
- Caruana G, Bertram JF: Congenital anomalies of the kidney and urinary tract genetics in mice and men. *Nephrology (Carlton)* 20: 309–311, 2015
- Blake J, Rosenblum ND: Renal branching morphogenesis: Morphogenetic and signaling mechanisms. *Semin Cell Dev Biol* 36: 2–12, 2014
- Van Esch H, Groenen P, Nesbit MA, Schuffenhauer S, Lichtner P, Vanderlinden G, Harding B, Beetz R, Bilous RW, Holdaway I, Shaw NJ, Fryns JP, Van de Ven W, Thakker RV, Devriendt K: GATA3 haploinsufficiency causes human HDR syndrome. *Nature* 406: 419–422, 2000
- Clissold RL, Hamilton AJ, Hattersley AT, Ellard S, Bingham C: HNF1B-associated renal and extra-renal disease—an expanding clinical spectrum. *Nat Rev Nephrol* 11: 102–112, 2015
- Nie X, Sun J, Gordon RE, Cai CL, Xu PX: SIX1 acts synergistically with TBX18 in mediating ureteral smooth muscle formation. *Development* 137: 755–765, 2010
- Sharma R, Sanchez-Ferraz O, Bouchard M: Pax genes in renal development, disease and regeneration. *Semin Cell Dev Biol* 44: 97–106, 2015
- Ruf RG, Xu PX, Silviu D, Otto EA, Beekmann F, Muerb UT, Kumar S, Neuhaus TJ, Kemper MJ, Raymond RM Jr., Brophy PD, Berkman J, Gattas M, Hyland V, Ruf EM, Schwartz C, Chang EH, Smith RJ, Stratakis CA, Weil D, Petit C, Hildebrandt F: SIX1 mutations cause branchio-oto-renal syndrome by disruption of EYA1-SIX1-DNA complexes. *Proc Natl Acad Sci U S A* 101: 8090–8095, 2004
- Kohlhase J, Wischermann A, Reichenbach H, Froster U, Engel W: Mutations in the SALL1 putative transcription factor gene cause Townes-Brocks syndrome. *Nat Genet* 18: 81–83, 1998
- Paces-Fessy M, Fabre M, Lesaulnier C, Cereghini S: Hnf1b and Pax2 cooperate to control different pathways in kidney and ureter morphogenesis. *Hum Mol Genet* 21: 3143–3155, 2012
- Vivante A, Kleppa MJ, Schulz J, Kohl S, Sharma A, Chen J, Shril S, Hwang DY, Weiss AC, Kaminski MM, Shukrun R, Kemper MJ, Lehnhardt A, Beetz R, Sanna-Cherchi S, Verbitsky M, Gharavi AG, Stuart HM, Feather SA, Goodship JA, Goodship TH, Woolf AS, Westra SJ, Doody DP, Bauer SB, Lee RS, Adam RM, Lu W, Reutter HM, Kehinde EO, Mancini EJ, Lifton RP, Tasic V, Lienkamp SS, Jüppner H, Kispert A, Hildebrandt F: Mutations in TBX18 cause dominant urinary tract malformations via transcriptional dysregulation of ureter development. *Am J Hum Genet* 97: 291–301, 2015
- Vivante A, Mark-Danieli M, Davidovits M, Harari-Steinberg O, Omer D, Gnatek Y, Cleper R, Landau D, Kovalski Y, Weissman I, Eisenstein I, Soudack M, Wolf HR, Issler N, Lotan D, Anikster Y, Dekel B: Renal hypodysplasia associates with a WNT4 variant that causes aberrant canonical WNT signaling. *J Am Soc Nephrol* 24: 550–558, 2013
- Sanna-Cherchi S, Sampogna RV, Papeta N, Burgess KE, Nees SN, Perry BJ, Choi M, Bodria M, Liu Y, Weng PL, Lozanovski VJ, Verbitsky M, Lugani F, Sterken R, Paragas N, Caridi G, Carrea A, Dagnino M, Materna-Kiryluk A, Santamaria G, Murtas C, Ristoska-Bojkovska N, Izzi C, Kacak N, Bianco B, Giberti S, Gigante M, Piaggio G, Gesualdo L, Kosuljandic Vukic D, Vukojevic K, Saraga-Babic M, Saraga M, Gucev Z, Allegri L, Latos-Bielenska A, Casu D, State M, Scolari F, Ravazzolo R, Kiryluk K, Al-Awqati Q, D'Agati VD, Drummond IA, Tasic V, Lifton RP, Ghiggeri GM, Gharavi AG: Mutations in DSTYK and dominant urinary tract malformations. *N Engl J Med* 369: 621–629, 2013
- Nicolaou N, Pulit SL, Nijman IJ, Monroe GR, Feitz WF, Schreuder MF, van Eerde AM, de Jong TP, Giltay JC, van der Zwaag B, Havenith MR, Zwakenberg S, van der Zanden LF, Poelmans G, Cornelissen EA, Lilien MR, Franke B, Roeleveld N, van Rooij IA, Cuppen E, Bongers EM, Giles RH, Knoers NV, Renkema KY: Prioritization and burden analysis of rare variants in 208 candidate genes suggest they do not play a major role in CAKUT. *Kidney Int* 89: 476–486, 2016
- Hwang DY, Dworschak GC, Kohl S, Saisawat P, Vivante A, Hilger AC, Reutter HM, Soliman NA, Bogdanovic R, Kehinde EO, Tasic V, Hildebrandt F: Mutations in 12 known dominant disease-causing genes clarify many congenital anomalies of the kidney and urinary tract. *Kidney Int* 85: 1429–1433, 2014
- Groen In 't Woud S, Renkema KY, Schreuder MF, Wijers CH, van der Zanden LF, Knoers NV, Feitz WF, Bongers EM, Roeleveld N, van Rooij IA: Maternal risk factors involved in specific congenital anomalies of the kidney and urinary tract: A case-control study. *Birth Defects Res A Clin Mol Teratol* 106: 596–603, 2016
- Wilson JG, Warkany J: Malformations in the genito-urinary tract induced by maternal vitamin A deficiency in the rat. *Am J Anat* 83: 357–407, 1948
- Rothman KJ, Moore LL, Singer MR, Nguyen US, Mannino S, Milunsky A: Teratogenicity of high vitamin A intake. *N Engl J Med* 333: 1369–1373, 1995
- Batourina E, Gim S, Bello N, Shy M, Clagett-Dame M, Srinivas S, Costantini F, Mendelsohn C: Vitamin A controls epithelial/mesenchymal interactions through Ret expression. *Nat Genet* 27: 74–78, 2001
- Batourina E, Choi C, Paragas N, Bello N, Hensle T, Costantini FD, Schuchardt A, Bacallao RL, Mendelsohn CL: Distal ureter morphogenesis depends on epithelial cell remodeling mediated by vitamin A and Ret. *Nat Genet* 32: 109–115, 2002
- Batourina E, Tsai S, Lambert S, Sprengle P, Viana R, Dutta S, Hensle T, Wang F, Niederreither K, McMahon AP, Carroll TJ, Mendelsohn CL: Apoptosis induced by vitamin A signaling is crucial for connecting the ureters to the bladder. *Nat Genet* 37: 1082–1089, 2005
- Sanna-Cherchi S, Kiryluk K, Burgess KE, Bodria M, Sampson MG, Hadley D, Nees SN, Verbitsky M, Perry BJ, Sterken R, Lozanovski VJ, Materna-Kiryluk A, Barlassina C, Kini A, Corbani V, Carrea A, Somenzi D, Murtas C, Ristoska-Bojkovska N, Izzi C, Bianco B, Zaniew M, Fogelova H, Weng PL, Kacak N, Giberti S, Gigante M, Arapovic A, Drnasin K, Caridi G, Curioni S, Allegri F, Ammenti A, Ferretti S, Goj V, Bernardo L, Jobanputra V, Chung WK, Lifton RP, Sanders S, State M, Clark LN, Saraga M, Padmanabhan S, Dominiczak AF, Foroud T, Gesualdo L, Gucev Z, Allegri L, Latos-Bielenska A, Cusi D, Scolari F, Tasic V, Hakonarson H, Ghiggeri GM, Gharavi AG: Copy-number disorders are a common cause of congenital kidney malformations. *Am J Hum Genet* 91: 987–997, 2012
- Behar DM, Yunusbayev B, Metspalu M, Metspalu E, Rosset S, Parik J, Rootsi S, Chaubey G, Kutuev I, Yudkovsky G, Khusnutdinova EK, Balanovsky O, Semino O, Pereira L, Comas D, Gurwitz D, Bonne-Tamir B, Parfitt T, Hammer MF, Skorecki K, Villems R: The genome-wide structure of the Jewish people. *Nature* 466: 238–242, 2010
- Augereau P, Badia E, Carascossa S, Castet A, Fritsch S, Harmand PO, Jalaguier S, Cavallès V: The nuclear receptor transcriptional coregulator RIP140. *Nucl Recept Signal* 4: e024, 2006
- Farooqui M, Franco PJ, Thompson J, Kagechika H, Chandraratna RA, Banaszak L, Wei LN: Effects of retinoid ligands on RIP140: Molecular interaction with retinoid receptors and biological activity. *Biochemistry* 42: 971–979, 2003

29. Chen Y, Kerimo A, Khan S, Wei LN: Real-time analysis of molecular interaction of retinoid receptors and receptor-interacting protein 140 (RIP140). *Mol Endocrinol* 16: 2528–2537, 2002
30. Cunningham TJ, Duester G: Mechanisms of retinoic acid signalling and its roles in organ and limb development. *Nat Rev Mol Cell Biol* 16: 110–123, 2015
31. Lienkamp SS: Using *Xenopus* to study genetic kidney diseases. *Semin Cell Dev Biol* 51: 117–124, 2016
32. White R, Leonardsson G, Rosewell I, Ann Jacobs M, Milligan S, Parker M: The nuclear receptor co-repressor nrp1 (RIP140) is essential for female fertility. *Nat Med* 6: 1368–1374, 2000
33. Castet A, Boulahtouf A, Versini G, Bonnet S, Augereau P, Vignon F, Khochbin S, Jalaguier S, Cavallès V: Multiple domains of the receptor-interacting protein 140 contribute to transcription inhibition. *Nucleic Acids Res* 32: 1957–1966, 2004
34. Chen Y, Hu X, Wei LN: Molecular interaction of retinoic acid receptors with coregulators PCAF and RIP140. *Mol Cell Endocrinol* 226: 43–50, 2004
35. Duester G: Retinoic acid synthesis and signaling during early organogenesis. *Cell* 134: 921–931, 2008
36. Zomerdijk IM, Ruiter R, Houweling LM, Herings RM, Sturkenboom MC, Straus SM, Stricker BH: Isotretinoin exposure during pregnancy: A population-based study in The Netherlands. *BMJ Open* 4: e005602, 2014
37. Lee LM, Leung CY, Tang WW, Choi HL, Leung YC, McCaffery PJ, Wang CC, Woolf AS, Shum AS: A paradoxical teratogenic mechanism for retinoic acid. *Proc Natl Acad Sci USA* 109: 13668–13673, 2012
38. Kerley JS, Olsen SL, Freemantle SJ, Spinella MJ: Transcriptional activation of the nuclear receptor corepressor RIP140 by retinoic acid: A potential negative-feedback regulatory mechanism. *Biochem Biophys Res Commun* 285: 969–975, 2001
39. MacArthur DG, Manolio TA, Dimmock DP, Rehm HL, Shendure J, Abecasis GR, Adams DR, Altman RB, Antonarakis SE, Ashley EA, Barrett JC, Biesecker LG, Conrad DF, Cooper GM, Cox NJ, Daly MJ, Gerstein MB, Goldstein DB, Hirschhorn JN, Leal SM, Pennacchio LA, Stamatoyanopoulos JA, Sunyaev SR, Valle D, Voight BF, Winckler W, Gunter C: Guidelines for investigating causality of sequence variants in human disease. *Nature* 508: 469–476, 2014
40. Richards CS, Bale S, Bellissimo DB, Das S, Grody WW, Hegde MR, Lyon E, Ward BE: Molecular Subcommittee of the ACMG Laboratory Quality Assurance Committee: ACMG recommendations for standards for interpretation and reporting of sequence variations: Revisions 2007. *Genet Med* 10: 294–300, 2008
41. Bamshad MJ, Ng SB, Bigham AW, Tabor HK, Emond MJ, Nickerson DA, Shendure J: Exome sequencing as a tool for Mendelian disease gene discovery. *Nat Rev Genet* 12: 745–755, 2011
42. Lee H, Deignan JL, Dorrani N, Strom SP, Kantarci S, Quintero-Rivera F, Das K, Toy T, Harry B, Yourshaw M, Fox M, Fogel BL, Martinez-Agosto JA, Wong DA, Chang VY, Shieh PB, Palmer CG, Dipple KM, Grody WW, Vilain E, Nelson SF: Clinical exome sequencing for genetic identification of rare Mendelian disorders. *JAMA* 312: 1880–1887, 2014
43. Halbritter J, Diaz K, Chaki M, Porath JD, Tarrier B, Fu C, Innis JL, Allen SJ, Lyons RH, Stefanidis CJ, Omran H, Soliman NA, Otto EA: High-throughput mutation analysis in patients with a nephronophthisis-associated ciliopathy applying multiplexed barcoded array-based PCR amplification and next-generation sequencing. *J Med Genet* 49: 756–767, 2012
44. Halbritter J, Porath JD, Diaz KA, Braun DA, Kohl S, Chaki M, Allen SJ, Soliman NA, Hildebrandt F, Otto EA; GPN Study Group: Identification of 99 novel mutations in a worldwide cohort of 1,056 patients with a nephronophthisis-related ciliopathy. *Hum Genet* 132: 865–884, 2013
45. Wilkinson DG, Nieto MA: Detection of messenger RNA by in situ hybridization to tissue sections and whole mounts. *Methods Enzymol* 225: 361–373, 1993
46. Moorman AF, Houweling AC, de Boer PA, Christoffels VM: Sensitive nonradioactive detection of mRNA in tissue sections: Novel application of the whole-mount in situ hybridization protocol. *J Histochem Cytochem* 49:1–8, 2001.
47. Lienkamp S, Ganner A, Boehlke C, Schmidt T, Arnold SJ, Schäfer T, Romaker D, Schuler J, Hoff S, Powelske C, Eifler A, Krönig C, Bullerkotte A, Nitschke R, Kuehn EW, Kim E, Burkhardt H, Brox T, Ronneberger O, Gloy J, Walz G: Inversin relays Frizzled-8 signals to promote proximal nephros development. *Proc Natl Acad Sci USA* 107: 20388–20393, 2010
48. Sive HL, Grainger RM, Harland RM: Early Development of *Xenopus laevis*: A Laboratory Manual. Plainview, NY, Cold Spring Harbor Laboratory Press, 2000
49. Hoff S, Halbritter J, Epting D, Frank V, Nguyen TM, van Reeuwijk J, Boehlke C, Schell C, Yasunaga T, Helmstädter M, Mergen M, Filhol E, Boldt K, Horn N, Ueffing M, Otto EA, Eisenberger T, Elting MW, van Wijk JA, Bockenauer D, Sebire NJ, Rittig S, Vyberg M, Ring T, Pohl M, Pape L, Neuhaus TJ, Elshakhs NA, Koon SJ, Harris PC, Grahammer F, Huber TB, Kuehn EW, Kramer-Zucker A, Bolz HJ, Roepman R, Saunier S, Walz G, Hildebrandt F, Bergmann C, Lienkamp SS: ANKS6 is a central component of a nephronophthisis module linking NEK8 to INVS and NPHP3. *Nat Genet* 45: 951–956, 2013
50. Nieuwkoop J and Faber PD: *Normal Table of Xenopus laevis (Daudin)*. New York, Garland Publishing, 1994

This article contains supplemental material online at <http://jasn.asnjournals.org/lookup/suppl/doi:10.1681/ASN.2016060694/-/DCSupplemental>.

AFFILIATIONS

Departments of *Medicine and **Urology, Boston Children's Hospital, Harvard Medical School, Boston, Massachusetts; [†]Talpiot Medical Leadership Program, Sheba Medical Center, Tel-Hashomer, Israel; [‡]Department of Internal Medicine A and Genetics Institute, Sheba Medical Center and Sackler Faculty of Medicine Tel Aviv University, Tel Aviv, Israel; [§]Institut für Molekularbiologie, Medizinische Hochschule Hannover, Hannover, Germany; ^{||}Department of Medicine, Renal Division, University Medical Center, Faculty of Medicine, and ^{§§§}Center for Biological Signaling Studies (BIOSS), Albert Ludwig University, Freiburg, Germany; [¶]Institut de Recherche en Cancérologie de Montpellier (IRCM), Montpellier, France; Institut National de la Santé et de la Recherche Médicale (INSERM), Montpellier, France; Université Montpellier, Montpellier, France; Institut régional du Cancer de Montpellier, Montpellier, France; ^{††}Division of Nephrology, Columbia University, New York, New York; ^{‡‡}Renal Section, Department of Medicine, Boston University Medical Center, Boston, Massachusetts; ^{§§}Pediatric Nephrology Institute, Rambam Health Care Campus, and Technion-Israel Institute of Technology, Haifa, Israel; ^{|||}Department of Pediatrics, Edmond and Lily Safra Children's Hospital, Sheba Medical Center, Tel-Hashomer, Israel and Sackler Faculty of Medicine, Tel Aviv University, Tel Aviv, Israel; ^{¶¶}Department of Human Genetics, Yale University School of Medicine, New Haven, Connecticut; ^{***}Howard Hughes Medical Institute, Chevy Chase, Maryland; ^{†††}Department of Pediatric Nephrology, Medical Faculty Skopje, University Children's Hospital, Skopje, Macedonia; and ^{‡‡‡}Centre for Nephrology, University College London, London, United Kingdom

Concluding remarks

Specification and diversification of the ureteric lineages

The different components of the urinary system, the kidneys, the ureters, the urinary bladder and the urethra, arise in development from diverse mesenchymal and epithelial progenitor pools within the intermediate mesoderm. How these lineages are established and diversify in time and space, has been most intensively studied for the kidney. All renal cell types derive from common *Osr1*⁺ progenitors in the intermediate mesoderm. These progenitors segregate into the *Pax2*⁺ nephric duct lineage that gives rise to the ureteric epithelium and the collecting duct system, the *Six2*⁺ cap mesenchymal lineage that comprises all nephron progenitors and the *Foxd1*⁺ stromal lineage that contributes to interstitial cells of the kidney.^{15, 29, 48-50} The differentiated cell types of the ureter arise from uncommitted precursor cells in the distal ureteric bud and its surrounding mesenchyme, respectively. How the ureteric lineages are specified and how they segregate from the other renal lineages has remained poorly understood. Moreover, it is unclear how the distinct ureteric sub-lineages diversify to achieve tissue complexity.

Pulse labeling and lineage tracing of *Osr1* expressing intermediate mesoderm cells previously suggested that the ureteric mesenchymal lineage segregates early from that giving rise to nephrons.²⁹ Indeed, our comparative expression analysis indicated that *Tbx18* expression demarcates a mesenchymal cell population surrounding the ureteric bud stalk that is clearly separated from *Six2*⁺*Uncx*⁺ nephron progenitors. Genetic fate mapping and lineage tracing of *Tbx18*⁺ revealed that cells from this expression domain do not intermingle with the nephron lineage but give rise to the complete mesenchymal wall of the ureter, a subset of bladder smooth muscle cells and also contribute to interstitial cells of the kidney. These observations suggest that *Tbx18*⁺ cells are not yet specified towards a ureteric mesenchymal fate but represent a multipotent progenitor population. *Tbx18* expression at E10.5 is not yet confined to cells adjacent to the distal ureteric stalk but comprises a band of mesenchymal cells in between the nephric duct and the meta-nephric mesenchyme, suggesting that it encompassed stromal and bladder smooth muscle progenitors as well. Because *Tbx18* expression at E11.5 does not overlap with the stromal marker *Foxd1*, we propose that the lineage segregation is completed shortly before. From E12.5 on, *Tbx18* expression is restricted to the mesenchymal cells of the ureter. Our tissue recombination experiments indicated that signals from the ureteric epithelium are required to maintain *Tbx18* expression in the adjacent cell population and to impose a ureteric mesenchymal fate. *Tbx18* is

exclusively required in these cells to render them responsive for epithelial SHH and WNT signals. This suggests a function of *Tbx18* in the pre-patterning of the ureteric mesenchyme prior to the action of specifying signals from the ureteric epithelium.

Cells from the ureteric mesenchyme subsequently diversify into adventitial fibrocytes, smooth muscle and lamina propria cells. Adventitial fibrocytes are the first cell type to differentiate and express POSTN in the periphery of the ureteric mesenchyme at E13.5. They are succeeded by TAGLN⁺ACTA2⁺ smooth muscle cells which differentiate in a proximal to distal gradient starting from E15.5. By E16.5, subepithelial TAGLN⁻ACTA2⁻ lamina propria cells are established. While smooth muscle cells and lamina propria cells subsequently expand, adventitial fibrocytes decrease in number and are only present at low abundance in the mature ureter. The early differentiation of adventitial fibrocytes in the periphery of the ureteric mesenchyme, out of reach of inductive epithelial signals, may indicate that these cells represent the default fate of the ureteric mesenchyme. The expansion of adventitial fibrocytes at the expense of smooth muscle cells under WNT loss-of-function conditions suggest that WNT signals specify smooth muscle progenitors via a spatial inhibition of the adventitial program.²⁰ Our genetic lineage tracing experiments further supported this hypothesis and revealed that adventitial fibrocytes segregate early from WNT-responsive cells that preferentially contribute to the smooth muscle and lamina propria layers. It has been speculated that lamina propria cells arise from smooth muscle precursors by spatial inhibition of the smooth muscle gene program.²³ This thesis clearly defined their common origin from WNT-responsive progenitor cells in the inner compartment of the ureteric mesenchyme. Interestingly, lamina propria cells establish or maintain characteristics of the undifferentiated progenitors like the expression of components and target genes of the SHH, WNT and RA signaling pathways.^{20, 23} It is conceivable that lamina propria cells retain a progenitor character and are able to contribute to the smooth muscle layer in homeostasis or regeneration which should be addressed in future experiments. The mechanisms of mesenchymal specification, radial patterning and differentiation are likely to be conserved in the development of visceral smooth muscle organs of the urinary and gastrointestinal tract. A similar requirement for reciprocal epithelial-mesenchymal signaling has been reported in both systems.^{23, 51, 52}

The genetic fate mapping experiments in the urothelium confirmed the common origin of basal, intermediate and superficial cells from the *Pax2*⁺*Shh*⁺ ureteric bud lineage. The uncommitted ureteric bud cells start to stratify and differentiate into Δ NP63⁺UPK1B^[low] intermediate cells between E13.5 and E14.5. At E15.5, single luminal cells downregulate Δ NP63 expression and become Δ NP63⁻UPK1B^[high] superficial cells. At E16.5, the urothelium is stratified into three

Concluding remarks

layers and single cells in the basal layer start to co-express KRT5 and Δ NP63. These KRT5⁺ Δ NP63⁺UPK1B⁻ basal cells subsequently increase in number and constitute the main cell type of the mature urothelium. In the adult a single layer of binucleate superficial cells seal the urothelium and intermediate cells are maintained at low abundance. Our genetic tracing of the urothelial sub-lineages of the ureter and a recent report in the developing and regenerating urinary bladder⁴⁴ indicated that the sequence of differentiation and the nature of progenitor cells in the urothelium are fundamentally different compared to other stratified epithelia. While apical cell types arise in a sequential fashion from basal cells for example in the epidermis⁵³ or the bronchial epithelium⁵⁴, we clearly defined intermediate cells as urothelial progenitors that give rise to basal and superficial cells in development and homeostasis. However, a conflicting report described a subpopulation of KRT14⁺ basal cells as progenitors in the regenerating bladder urothelium.⁵⁵ KRT14 is expressed in a minor fraction of basal cells in the ureter only in adults, so it can be excluded that these cells constitute a progenitor population in development. Nevertheless, it remains to be solved whether basal cells can be reprogrammed to a progenitor status under injury conditions. Future studies should establish injury and regeneration models for the ureter to test the significance of the different cell populations in urothelial repair. In general, it has to be remarked that the set of urothelial differentiation markers is very limited. So far, no unique marker for intermediate cells is established and only a combination of several differentiation markers allows the labeling of the urothelial cell layers. Moreover, the presence of different subpopulations of basal cells indicates that large heterogeneity within the urothelial layers exists.^{25, 55} Cell type specific and single-cell transcriptome analyses should help to identify new differentiation markers and to elucidate the cellular heterogeneity within the urothelial populations.

Molecular control of growth and differentiation in the developing ureter

The importance of morphogenetic interactions of epithelial and mesenchymal tissues in the growth and differentiation of the ureters and the kidneys was discovered more than 50 years ago, but the molecular nature of these reciprocal signals has remained elusive for a long time.^{26, 27} Lately, the analysis of genetically modified mouse models revealed SHH and WNT signals from the ureteric epithelium to be involved in the growth and differentiation of the ureteric mesenchyme.^{20, 23, 30} Still it is unclear how these signaling activities are balanced to initiate the

ureteric differentiation programs in a precise temporal and spatial fashion. Moreover, it is unknown how the growth and differentiation of the mesenchymal and epithelial components of the ureter are coordinated between the two tissue compartments.

This thesis gave significant new insight into the molecular function of SHH signaling in the developing ureter. Genetic deletion of the SHH signal transducer smoothed (SMO) from the ureteric mesenchyme resulted in hypoplastic hydroureter formation at birth. Conditional SMO mutants failed to initiate the smooth muscle differentiation program and showed reduced proliferation and survival of ureteric mesenchymal cells. In a complementary approach, misexpression of a constitutive active form of SMO in the ureteric mesenchyme resulted in mesenchymal hyperplasia due to increased proliferation and cell survival but did not affect patterning or differentiation. As it was previously reported, ureteric smooth muscle differentiation also depends on epithelial WNT signals.²⁰ It seems plausible, that the initiation of the smooth muscle gene program requires the combinatorial activity of both SHH and WNT signaling and potentially other inductive signals. In contrast to previous studies^{23,30}, we also addressed the consequences of defective mesenchymal SHH signaling on urothelial growth and differentiation. Excitingly, proliferation was significantly reduced and the stratification and differentiation of the urothelium was not initiated. Our genetic approach specifically targeted SHH signaling only in the ureteric mesenchyme, suggesting that urothelial growth and differentiation are regulated by a paracrine relay signal downstream of mesenchymal SHH signaling. Pharmacological inhibition of SHH signaling and transcriptional profiling by microarray analysis revealed that expression of the forkhead transcription factor gene *Foxf1* was SHH dependent in the ureteric mesenchyme. The dependency of *Foxf1* on SHH signaling has previously been reported in the intestine, where *Foxf1* controls visceral smooth muscle differentiation as a direct target gene of the pathway.⁵⁶⁻⁵⁸ To address a potential function of *Foxf1* in the ureter, two transgenic alleles were generated that allowed a conditional misexpression of a dominant negative or wildtype version of *Foxf1* in the ureteric mesenchyme. While misexpression of the dominant negative allele recapitulated the growth and differentiation defects in the epithelial and mesenchymal compartments of the ureter that were observed under SHH loss-of-function conditions, re-expression of wildtype *Foxf1* rescued smooth muscle and urothelial differentiation when SHH signaling was inhibited. Further molecular analyses revealed that expression of *Bmp4* in the ureteric mesenchyme depends on both SHH signaling and FOXF1 function. Administration of exogenous BMP4 protein to ureter explant cultures with impaired SHH signaling or FOXF1 function was not able to rescue smooth muscle differentiation defects but partially restored tissue growth and completely rescued urothelial differentiation. Together these findings imply that epithelial SHH

Concluding remarks

is a crucial signal that couples the growth and differentiation of mesenchymal and epithelial tissues of the ureter via a FOXF1-BMP4 regulatory module. While this work clearly deciphered the epistatic relations of SHH signaling, FOXF1 and BMP4 in the developing ureter, some open questions remain. Our molecular analysis indicated SHH signaling alone is not sufficient to induce *Foxf1* expression. It is conceivable that *Foxf1* integrates multiple signaling inputs that culminate in the ureteric smooth muscle differentiation program and it remains to be tested whether a combinatorial activation of SHH and WNT signaling is sufficient to drive *Foxf1* expression and smooth muscle differentiation or if additional inductive signals are required. While BMP4 is a partial mediator of FOXF1 function in the ureter and an epistatic relation of the two factors has been implied in vasculogenesis⁵⁹ and development of the lateral plate mesoderm⁶⁰, it remains to be analyzed whether *Bmp4* is a direct target gene and which other factors are regulated by FOXF1. A genome wide analysis of DNA binding sites by chromatin immunoprecipitation combined with assays to detect the FOXF1 dependent transcriptome might help to unravel this open question in the future. Furthermore, our rescue experiments provided clear evidence that BMP signaling acts downstream of SHH and FOXF1 activity to induce urothelial differentiation. Although genetic ablation of *Bmp4* from the ureteric mesenchyme has been shown to impair superficial cell differentiation³⁹, the precise function of BMP4 signaling and its molecular mediators in the urothelium remain elusive.

While a gradual build-up and a combinatorial input of inductive signals seems to be a plausible explanation for the tight temporal and spatial sequence of ureteric differentiation, inhibitory or restrictive activities in the undifferentiated progenitors could represent an alternative scenario. We analyzed a potential function RA signaling in the ureter since it has been implicated in progenitor maintenance in other contexts. For example, RA is required to maintain skeletal muscle progenitors in an immature state and to control olfactory stem cell self-renewal and progenitor commitment.^{61, 62} A comprehensive expression analysis of components and target genes of RA signaling revealed pathway activity in the undifferentiated mesenchymal and epithelial progenitors of the ureter. Pharmacological inhibition of the early RA signaling activity resulted in an expansion of smooth muscle cells at the expense of lamina propria fibrocytes in the ureteric mesenchyme, and an increase of superficial cells at the expense of intermediate cells in the urothelium. In contrast, activation of the pathway expanded the mesenchymal lamina propria compartment and blocked basal cell differentiation in the urothelium. A precocious differentiation of the mesenchymal and epithelial cell types under RA loss-of-function conditions implied a critical requirement of the pathway in the maintenance of ureteric progenitors. The identification of the RA-responsive expression of WNT antagonist genes *Hic1* and *Shisa3*

in the ureteric mesenchyme suggested that a negative regulation of inductive signaling activities may represent a potential mechanism for the temporal-spatial control of smooth muscle differentiation which should be further tested. In the undifferentiated ureteric epithelium, expression of the E74 like ETS transcription factor gene *Elf5* was detected to be RA dependent. Interestingly, an enrichment of ELF5 motifs in the regulatory regions of urothelial differentiation genes has been reported.⁶³ While the paralogous gene *Elf3* is an activator of urothelial differentiation⁶⁴, misexpression of *Elf5* in the lung epithelium prevents terminal differentiation⁶⁵. It remains to be tested whether *Elf5* also negatively regulates urothelial differentiation.

This thesis and previous reports suggest that a combination of positive signaling inputs of the SHH^{23, 30}, WNT²⁰ and BMP³³⁻³⁵ pathway families and a negative input of RA are required to control the ureteric differentiation programs. If these factors are really sufficient to explain the strict temporal and spatial sequence of differentiation in the ureter remains to be solved. Further temporal characterization of signaling and transcription factor activities in the course of ureter development could provide us with additional factors that specifically act in the mesenchymal and epithelial progenitor populations and help to refine our current model of differentiation control.

Developmental basis of congenital ureter anomalies

Congenital anomalies of the kidney and urinary tract (CAKUT) are a leading cause of early-onset end-stage renal disease and are among the most common human birth defects.^{10, 11} Although more than 20 CAKUT-causing genes have been identified to date, the disease etiology as well as the underlying mutations have remained elusive for the majority of cases.¹³ Hydronephrosis and hydronephrosis represent frequent manifestations in CAKUT that are characterized by structural or functional defects of the ureteric tissues and their junctions to the renal pelvis and the urinary bladder. These anomalies arise from alterations of the morphogenesis or cellular differentiation programs during ureter development.^{12, 13} The novel insights into the cellular and molecular mechanisms of ureter development achieved in this thesis provide us with a better understanding of the disease etiology.

The proper investment of the ureter with a functional smooth muscle layer is a prerequisite for efficient urine drainage. Thus, defects in the differentiation of smooth muscle cells represent a potential cellular mechanism for hydronephrosis and hydronephrosis formation. Here, it was shown that a SHH-FOXF1-BMP4 regulatory axis is essential for the ureteric smooth muscle differentiation program. A complete or partial loss of components of this axis is not only associated

Concluding remarks

with urinary tract defects in the mouse, but heterozygous loss-of-function mutations in *BMP4* and *GLI3* genes have been identified in human patients with ureter and kidney defects.^{66, 67} Urinary tract anomalies may appear as isolated features but often encompass malformations in multiple organs.⁶⁸⁻⁷⁰ The requirement of SHH signaling in the development of numerous embryonic tissues renders components of this pathway as promising disease candidates. The VACTERL association represents a group of birth defects that include vertebral anomalies, anorectal malformations, cardiac anomalies, tracheoesophageal fistula, esophageal atresia, renal malformations, and limb defects. Mutations in the *FOXF1* gene or genomic imbalances around the *FOX* gene cluster have been associated with VACTERL phenotypes.⁷¹⁻⁷³ Moreover, disease-causing *FOXF1* mutations were identified in patients with component features of VACTERL that display alveolar capillary dysplasia and misalignment of the pulmonary veins (ACDMPV) but also develop hydroureter and hydronephrosis phenotypes.^{74, 75} Developmental expression of *Foxf1* in the mouse was detected in most VACTERL associated organs except the urinary system.^{72, 73} Given our finding that *Foxf1* is expressed and functionally required for ureteric smooth muscle differentiation, the renal manifestations of VACTERL and ACDMPV can now be explained.

The newly identified requirement of the SHH-FOXF1-BMP4 signaling axis for urothelial differentiation points to another potential cellular mechanism for hydroureter and hydronephrosis formation. An efficient sealing of the urothelium is required to protect the underlying mesenchyme from the hypertonic urine. Leakage of the urothelium could lead to damage of the ureteric smooth muscle layer and impede efficient urine transport. Interestingly, *Upk1b* deficiency disturbs urothelial plaque formation and results in progressive hydronephrosis in mice.⁷⁶ In contrast to functional or physical ureteric obstructions, urothelial defects should not necessarily result in a phenotype at birth but should display a delayed disease progression. If urothelial defects may also account for late-onset CAKUT in humans remains to be investigated.

A requirement for RA signaling has previously been described for multiple aspects of urogenital system development and is highlighted by urogenital defects that are caused by reduced or increased maternal Vitamin A levels in humans and rodents.^{77, 78} The insertion of the distal ureter into the bladder is a complex tissue remodeling process that requires RA signaling activity.¹⁷ The patency of the ureterovesical junction is a prerequisite for proper urine drainage and defects in the insertion of the ureters into the bladder can lead to physical obstruction or urine reflux. Defects in the RA-mediated maintenance of ureteric progenitors that was reported in this thesis could represent an additional disease mechanism. This work contributed to the functional char-

acterization of a heterozygous truncating mutation in the *Nrip1* gene in a kindred with autosomal dominant CAKUT. Biochemical analysis of NRIP1 revealed that the protein negatively regulates the RA-mediated transcriptional response via direct physical interaction with RA receptors. The finding that *Nrip1* expression in the nephric duct and ureteric bud depends on RA signaling suggests that the gene represents a negative feedback regulator and exemplifies the importance of a tight control of RA signaling activity in the developing urinary system. If the phenotypic manifestations of the *NRIP1* mutation in human CAKUT patients are caused by anomalies in the ureter-bladder connectivity or by RA-mediated differentiation defects remains to be investigated. Further analysis of *Nrip1* deficient mice should elucidate whether this gene really represents a negative feedback regulator and if ectopic RA signaling and associated differentiation defects like a loss of urothelial basal cells are detectable.

References

1. Velardo, JT: Histology of the Ureter. In: *The Ureter*, 2nd Ed., edited by Bergman, H, New York, Springer-Verlag, 1981.
2. Hicks, RM: The fine structure of the transitional epithelium of rat ureter. *J Cell Biol*, 26: 25-48, 1965.
3. Gosling, JA: The musculature of the upper urinary tract. *Acta Anat (Basel)*, 75: 408-422, 1970.
4. Santicioli, P, Maggi, CA: Effect of 18beta-glycyrrhetic acid on electromechanical coupling in the guinea-pig renal pelvis and ureter. *Br J Pharmacol*, 129: 163-169, 2000.
5. Gosling, JA: The innervation of the upper urinary tract. *J Anat*, 106: 51-61, 1970.
6. Boyarsky, S, Labay, P: Principles of Ureteral Physiology. In: *The Ureter*, 2nd Ed., edited by Bergman, H, New York, Springer-Verlag, 1981.
7. Gosling, JA, Dixon, JS: Morphologic evidence that the renal calyx and pelvis control ureteric activity in the rabbit. *Am J Anat*, 130: 393-408, 1971.
8. Lang, RJ, Takano, H, Davidson, ME, Suzuki, H, Klemm, MF: Characterization of the spontaneous electrical and contractile activity of smooth muscle cells in the rat upper urinary tract. *J Urol*, 166: 329-334, 2001.
9. Burdyga, T, Wray, S: Action potential refractory period in ureter smooth muscle is set by Ca sparks and BK channels. *Nature*, 436: 559-562, 2005.
10. Loane, M, Dolk, H, Kelly, A, Teljeur, C, Greenlees, R, Densem, J, Group, EW: Paper 4: EUROCAT statistical monitoring: identification and investigation of ten year trends of congenital anomalies in Europe. *Birth Defects Res A Clin Mol Teratol*, 91 Suppl 1: S31-43, 2011.
11. Renkema, KY, Winyard, PJ, Skovorodkin, IN, Levtchenko, E, Hindryckx, A, Jeanpierre, C, Weber, S, Salomon, R, Antignac, C, Vainio, S, Schedl, A, Schaefer, F, Knoers, NV, Bongers, EM, consortium, E: Novel perspectives for investigating congenital anomalies of the kidney and urinary tract (CAKUT). *Nephrol Dial Transplant*, 26: 3843-3851, 2011.
12. Schedl, A: Renal abnormalities and their developmental origin. *Nat Rev Genet*, 8: 791-802, 2007.
13. Vivante, A, Kohl, S, Hwang, DY, Dworschak, GC, Hildebrandt, F: Single-gene causes of congenital anomalies of the kidney and urinary tract (CAKUT) in humans. *Pediatr Nephrol*, 29: 695-704, 2014.
14. Airik, R, Kispert, A: Down the tube of obstructive nephropathies: the importance of tissue interactions during ureter development. *Kidney Int*, 72: 1459-1467, 2007.
15. Bouchard, M, Souabni, A, Mandler, M, Neubuser, A, Busslinger, M: Nephric lineage specification by Pax2 and Pax8. *Genes Dev*, 16: 2958-2970, 2002.

16. Chia, I, Grote, D, Marcotte, M, Batourina, E, Mendelsohn, C, Bouchard, M: Nephric duct insertion is a crucial step in urinary tract maturation that is regulated by a Gata3-Raldh2-Ret molecular network in mice. *Development*, 138: 2089-2097, 2011.
17. Batourina, E, Tsai, S, Lambert, S, Sprenkle, P, Viana, R, Dutta, S, Hensle, T, Wang, F, Niederreither, K, McMahon, AP, Carroll, TJ, Mendelsohn, CL: Apoptosis induced by vitamin A signaling is crucial for connecting the ureters to the bladder. *Nat Genet*, 37: 1082-1089, 2005.
18. Costantini, F, Shakya, R: GDNF/Ret signaling and the development of the kidney. *Bioessays*, 28: 117-127, 2006.
19. Lechner, MS, Dressler, GR: The molecular basis of embryonic kidney development. *Mech Dev*, 62: 105-120, 1997.
20. Trowe, MO, Airik, R, Weiss, AC, Farin, HF, Foik, AB, Bettenhausen, E, Schuster-Gossler, K, Taketo, MM, Kispert, A: Canonical Wnt signaling regulates smooth muscle precursor development in the mouse ureter. *Development*, 139: 3099-3108, 2012.
21. Airik, R, Bussen, M, Singh, MK, Petry, M, Kispert, A: Tbx18 regulates the development of the ureteral mesenchyme. *J Clin Invest*, 116: 663-674, 2006.
22. Weiss, RM, Guo, S, Shan, A, Shi, H, Romano, RA, Sinha, S, Cantley, LG, Guo, JK: Brg1 determines urothelial cell fate during ureter development. *J Am Soc Nephrol*, 24: 618-626, 2013.
23. Yu, J, Carroll, TJ, McMahon, AP: Sonic hedgehog regulates proliferation and differentiation of mesenchymal cells in the mouse metanephric kidney. *Development*, 129: 5301-5312, 2002.
24. Romih, R, Korosec, P, de Mello, W, Jr., Jezernik, K: Differentiation of epithelial cells in the urinary tract. *Cell Tissue Res*, 320: 259-268, 2005.
25. Tai, G, Ranjzad, P, Marriage, F, Rehman, S, Denley, H, Dixon, J, Mitchell, K, Day, PJ, Woolf, AS: Cytokeratin 15 marks basal epithelia in developing ureters and is upregulated in a subset of urothelial cell carcinomas. *PLoS One*, 8: e81167, 2013.
26. Grobstein, C: Inductive epitheliomesenchymal interaction in cultured organ rudiments of the mouse. *Science*, 118: 52-55, 1953.
27. Grobstein, C: Morphogenetic interaction between embryonic mouse tissues separated by a membrane filter. *Nature*, 172: 869-870, 1953.
28. Bush, KT, Vaughn, DA, Li, X, Rosenfeld, MG, Rose, DW, Mendoza, SA, Nigam, SK: Development and differentiation of the ureteric bud into the ureter in the absence of a kidney collecting system. *Dev Biol*, 298: 571-584, 2006.
29. Mugford, JW, Sipila, P, McMahon, JA, McMahon, AP: Osr1 expression demarcates a multi-potent population of intermediate mesoderm that undergoes progressive restriction to an Osr1-dependent nephron progenitor compartment within the mammalian kidney. *Dev Biol*, 324: 88-98, 2008.

References

30. Haraguchi, R, Matsumaru, D, Nakagata, N, Miyagawa, S, Suzuki, K, Kitazawa, S, Yamada, G: The hedgehog signal induced modulation of bone morphogenetic protein signaling: an essential signaling relay for urinary tract morphogenesis. *PLoS One*, 7: e42245, 2012.
31. Miyazaki, Y, Oshima, K, Fogo, A, Hogan, BL, Ichikawa, I: Bone morphogenetic protein 4 regulates the budding site and elongation of the mouse ureter. *J Clin Invest*, 105: 863-873, 2000.
32. Miyazaki, Y, Oshima, K, Fogo, A, Ichikawa, I: Evidence that bone morphogenetic protein 4 has multiple biological functions during kidney and urinary tract development. *Kidney Int*, 63: 835-844, 2003.
33. Wang, GJ, Brenner-Anantharam, A, Vaughan, ED, Herzlinger, D: Antagonism of BMP4 signaling disrupts smooth muscle investment of the ureter and ureteropelvic junction. *J Urol*, 181: 401-407, 2009.
34. Tripathi, P, Wang, Y, Casey, AM, Chen, F: Absence of canonical Smad signaling in ureteral and bladder mesenchyme causes ureteropelvic junction obstruction. *J Am Soc Nephrol*, 23: 618-628, 2012.
35. Yan, J, Zhang, L, Xu, J, Sultana, N, Hu, J, Cai, X, Li, J, Xu, PX, Cai, CL: Smad4 regulates ureteral smooth muscle cell differentiation during mouse embryogenesis. *PLoS One*, 9: e104503, 2014.
36. Caubit, X, Lye, CM, Martin, E, Core, N, Long, DA, Vola, C, Jenkins, D, Garratt, AN, Skaer, H, Woolf, AS, Fasano, L: Teashirt 3 is necessary for ureteral smooth muscle differentiation downstream of SHH and BMP4. *Development*, 135: 3301-3310, 2008.
37. Airik, R, Trowe, MO, Foik, A, Farin, HF, Petry, M, Schuster-Gossler, K, Schweizer, M, Scherer, G, Kist, R, Kispert, A: Hydroureteronephrosis due to loss of Sox9-regulated smooth muscle cell differentiation of the ureteric mesenchyme. *Hum Mol Genet*, 19: 4918-4929, 2010.
38. Martin, E, Caubit, X, Airik, R, Vola, C, Fatmi, A, Kispert, A, Fasano, L: TSHZ3 and SOX9 regulate the timing of smooth muscle cell differentiation in the ureter by reducing myocardin activity. *PLoS One*, 8: e63721, 2013.
39. Brenner-Anantharam, A, Cebrian, C, Guillaume, R, Hurtado, R, Sun, TT, Herzlinger, D: Tailbud-derived mesenchyme promotes urinary tract segmentation via BMP4 signaling. *Development*, 134: 1967-1975, 2007.
40. Bagai, S, Rubio, E, Cheng, JF, Sweet, R, Thomas, R, Fuchs, E, Grady, R, Mitchell, M, Bassuk, JA: Fibroblast growth factor-10 is a mitogen for urothelial cells. *J Biol Chem*, 277: 23828-23837, 2002.
41. Qiao, J, Bush, KT, Steer, DL, Stuart, RO, Sakurai, H, Wachsman, W, Nigam, SK: Multiple fibroblast growth factors support growth of the ureteric bud but have different effects on branching morphogenesis. *Mech Dev*, 109: 123-135, 2001.
42. Tash, JA, David, SG, Vaughan, EE, Herzlinger, DA: Fibroblast growth factor-7 regulates stratification of the bladder urothelium. *J Urol*, 166: 2536-2541, 2001.

43. Shin, K, Lee, J, Guo, N, Kim, J, Lim, A, Qu, L, Mysorekar, IU, Beachy, PA: Hedgehog/Wnt feedback supports regenerative proliferation of epithelial stem cells in bladder. *Nature*, 472: 110-114, 2011.
44. Gandhi, D, Molotkov, A, Batourina, E, Schneider, K, Dan, H, Reiley, M, Laufer, E, Metzger, D, Liang, F, Liao, Y, Sun, TT, Aronow, B, Rosen, R, Mauney, J, Adam, R, Rosselot, C, Van Batavia, J, McMahan, A, McMahan, J, Guo, JJ, Mendelsohn, C: Retinoid signaling in progenitors controls specification and regeneration of the urothelium. *Dev Cell*, 26: 469-482, 2013.
45. Varley, CL, Southgate, J: Effects of PPAR agonists on proliferation and differentiation in human urothelium. *Exp Toxicol Pathol*, 60: 435-441, 2008.
46. Varley, CL, Stahlschmidt, J, Lee, WC, Holder, J, Diggle, C, Selby, PJ, Trejdosiewicz, LK, Southgate, J: Role of PPARgamma and EGFR signalling in the urothelial terminal differentiation programme. *J Cell Sci*, 117: 2029-2036, 2004.
47. Mysorekar, IU, Isaacson-Schmid, M, Walker, JN, Mills, JC, Hultgren, SJ: Bone morphogenetic protein 4 signaling regulates epithelial renewal in the urinary tract in response to uropathogenic infection. *Cell Host Microbe*, 5: 463-475, 2009.
48. Kobayashi, A, Valerius, MT, Mugford, JW, Carroll, TJ, Self, M, Oliver, G, McMahon, AP: Six2 defines and regulates a multipotent self-renewing nephron progenitor population throughout mammalian kidney development. *Cell Stem Cell*, 3: 169-181, 2008.
49. Hatini, V, Huh, SO, Herzlinger, D, Soares, VC, Lai, E: Essential role of stromal mesenchyme in kidney morphogenesis revealed by targeted disruption of Winged Helix transcription factor BF-2. *Genes Dev*, 10: 1467-1478, 1996.
50. Levinson, RS, Batourina, E, Choi, C, Vorontchikhina, M, Kitajewski, J, Mendelsohn, CL: Foxd1-dependent signals control cellularity in the renal capsule, a structure required for normal renal development. *Development*, 132: 529-539, 2005.
51. Shiroyanagi, Y, Liu, B, Cao, M, Agras, K, Li, J, Hsieh, MH, Willingham, EJ, Baskin, LS: Urothelial sonic hedgehog signaling plays an important role in bladder smooth muscle formation. *Differentiation*, 75: 968-977, 2007.
52. Sukegawa, A, Narita, T, Kameda, T, Saitoh, K, Nohno, T, Iba, H, Yasugi, S, Fukuda, K: The concentric structure of the developing gut is regulated by Sonic hedgehog derived from endodermal epithelium. *Development*, 127: 1971-1980, 2000.
53. Blanpain, C, Fuchs, E: Epidermal stem cells of the skin. *Annu Rev Cell Dev Biol*, 22: 339-373, 2006.
54. Hong, KU, Reynolds, SD, Watkins, S, Fuchs, E, Stripp, BR: Basal cells are a multipotent progenitor capable of renewing the bronchial epithelium. *Am J Pathol*, 164: 577-588, 2004.
55. Papafotiou, G, Paraskevopoulou, V, Vasilaki, E, Kanaki, Z, Paschalidis, N, Klinakis, A: KRT14 marks a subpopulation of bladder basal cells with pivotal role in regeneration and tumorigenesis. *Nat Commun*, 7: 11914, 2016.

References

56. Ormestad, M, Astorga, J, Landgren, H, Wang, T, Johansson, BR, Miura, N, Carlsson, P: Foxf1 and Foxf2 control murine gut development by limiting mesenchymal Wnt signaling and promoting extracellular matrix production. *Development*, 133: 833-843, 2006.
57. Madison, BB, McKenna, LB, Dolson, D, Epstein, DJ, Kaestner, KH: FoxF1 and FoxL1 link hedgehog signaling and the control of epithelial proliferation in the developing stomach and intestine. *J Biol Chem*, 284: 5936-5944, 2009.
58. Hoggatt, AM, Kim, JR, Ustiyan, V, Ren, X, Kalin, TV, Kalinichenko, VV, Herring, BP: The transcription factor Foxf1 binds to serum response factor and myocardin to regulate gene transcription in visceral smooth muscle cells. *J Biol Chem*, 288: 28477-28487, 2013.
59. Astorga, J, Carlsson, P: Hedgehog induction of murine vasculogenesis is mediated by Foxf1 and Bmp4. *Development*, 134: 3753-3761, 2007.
60. Mahlapuu, M, Ormestad, M, Enerback, S, Carlsson, P: The forkhead transcription factor Foxf1 is required for differentiation of extra-embryonic and lateral plate mesoderm. *Development*, 128: 155-166, 2001.
61. El Haddad, M, Notarnicola, C, Evano, B, El Khatib, N, Blaquiere, M, Bonniou, A, Tajbakhsh, S, Hugon, G, Vernus, B, Mercier, J, Carnac, G: Retinoic acid maintains human skeletal muscle progenitor cells in an immature state. *Cell Mol Life Sci*, 74: 1923-1936, 2017.
62. Paschaki, M, Cammas, L, Muta, Y, Matsuoka, Y, Mak, SS, Rataj-Baniowska, M, Fraulob, V, Dolle, P, Ladher, RK: Retinoic acid regulates olfactory progenitor cell fate and differentiation. *Neural Dev*, 8: 13, 2013.
63. Fishwick, C, Higgins, J, Percival-Alwyn, L, Hustler, A, Pearson, J, Bastkowski, S, Moxon, S, Swarbreck, D, Greenman, CD, Southgate, J: Heterarchy of transcription factors driving basal and luminal cell phenotypes in human urothelium. *Cell Death Differ*, 2017.
64. Bock, M, Hinley, J, Schmitt, C, Wahlicht, T, Kramer, S, Southgate, J: Identification of ELF3 as an early transcriptional regulator of human urothelium. *Dev Biol*, 386: 321-330, 2014.
65. Metzger, DE, Stahlman, MT, Shannon, JM: Misexpression of ELF5 disrupts lung branching and inhibits epithelial differentiation. *Dev Biol*, 320: 149-160, 2008.
66. Kang, S, Graham, JM, Jr., Olney, AH, Biesecker, LG: GLI3 frameshift mutations cause autosomal dominant Pallister-Hall syndrome. *Nat Genet*, 15: 266-268, 1997.
67. Weber, S, Taylor, JC, Winyard, P, Baker, KF, Sullivan-Brown, J, Schild, R, Knuppel, T, Zurowska, AM, Caldas-Alfonso, A, Litwin, M, Emre, S, Ghiggeri, GM, Bakkaloglu, A, Mehls, O, Antignac, C, Network, E, Schaefer, F, Burdine, RD: SIX2 and BMP4 mutations associate with anomalous kidney development. *J Am Soc Nephrol*, 19: 891-903, 2008.
68. Sanyanusin, P, Schimmenti, LA, McNoe, LA, Ward, TA, Pierpont, ME, Sullivan, MJ, Dobyns, WB, Eccles, MR: Mutation of the PAX2 gene in a family with optic nerve colobomas, renal anomalies and vesicoureteral reflux. *Nat Genet*, 9: 358-364, 1995.

69. Abdelhak, S, Kalatzis, V, Heilig, R, Compain, S, Samson, D, Vincent, C, Weil, D, Cruaud, C, Sahly, I, Leibovici, M, Bitner-Glindzicz, M, Francis, M, Lacombe, D, Vigneron, J, Charachon, R, Boven, K, Bedbeder, P, Van Regemorter, N, Weissenbach, J, Petit, C: A human homologue of the *Drosophila* eyes absent gene underlies branchio-otorenal (BOR) syndrome and identifies a novel gene family. *Nat Genet*, 15: 157-164, 1997.
70. Lindner, TH, Njolstad, PR, Horikawa, Y, Bostad, L, Bell, GI, Sovik, O: A novel syndrome of diabetes mellitus, renal dysfunction and genital malformation associated with a partial deletion of the pseudo-POU domain of hepatocyte nuclear factor-1beta. *Hum Mol Genet*, 8: 2001-2008, 1999.
71. Agochukwu, NB, Pineda-Alvarez, DE, Keaton, AA, Warren-Mora, N, Raam, MS, Kamat, A, Chandrasekharappa, SC, Solomon, BD: Analysis of FOXF1 and the FOX gene cluster in patients with VACTERL association. *Eur J Med Genet*, 54: 323-328, 2011.
72. Hilger, AC, Halbritter, J, Pennimpede, T, van der Ven, A, Sarma, G, Braun, DA, Porath, JD, Kohl, S, Hwang, DY, Dworschak, GC, Hermann, BG, Pavlova, A, El-Maarri, O, Nothen, MM, Ludwig, M, Reutter, H, Hildebrandt, F: Targeted Resequencing of 29 Candidate Genes and Mouse Expression Studies Implicate ZIC3 and FOXF1 in Human VATER/VACTERL Association. *Hum Mutat*, 36: 1150-1154, 2015.
73. Reutter, H, Hilger, AC, Hildebrandt, F, Ludwig, M: Underlying genetic factors of the VATER/VACTERL association with special emphasis on the "Renal" phenotype. *Pediatr Nephrol*, 31: 2025-2033, 2016.
74. Sen, P, Yang, Y, Navarro, C, Silva, I, Szafranski, P, Kolodziejska, KE, Dharmadhikari, AV, Mostafa, H, Kozakewich, H, Kearney, D, Cahill, JB, Whitt, M, Bilic, M, Margraf, L, Charles, A, Goldblatt, J, Gibson, K, Lantz, PE, Garvin, AJ, Petty, J, Kiblawi, Z, Zuppan, C, McConkie-Rosell, A, McDonald, MT, Peterson-Carmichael, SL, Gaede, JT, Shivanna, B, Schady, D, Friedlich, PS, Hays, SR, Palafoll, IV, Siebers-Renelt, U, Bohring, A, Finn, LS, Siebert, JR, Galambos, C, Nguyen, L, Riley, M, Chassaing, N, Vigouroux, A, Rocha, G, Fernandes, S, Brumbaugh, J, Roberts, K, Ho-Ming, L, Lo, IF, Lam, S, Gerychova, R, Jezova, M, Valaskova, I, Fellmann, F, Afshar, K, Giannoni, E, Muhlethaler, V, Liang, J, Beckmann, JS, Liroy, J, Deshmukh, H, Srinivasan, L, Swarr, DT, Sloman, M, Shaw-Smith, C, van Loon, RL, Hagman, C, Sznajer, Y, Barrea, C, Galant, C, Detaille, T, Wambach, JA, Cole, FS, Hamvas, A, Prince, LS, Diderich, KE, Brooks, AS, Verdijk, RM, Ravindranathan, H, Sugo, E, Mowat, D, Baker, ML, Langston, C, Welty, S, Stankiewicz, P: Novel FOXF1 mutations in sporadic and familial cases of alveolar capillary dysplasia with misaligned pulmonary veins imply a role for its DNA binding domain. *Hum Mutat*, 34: 801-811, 2013.
75. Stankiewicz, P, Sen, P, Bhatt, SS, Storer, M, Xia, Z, Bejjani, BA, Ou, Z, Wiszniewska, J, Driscoll, DJ, Maisenbacher, MK, Bolivar, J, Bauer, M, Zackai, EH, McDonald-McGinn, D, Nowaczyk, MM, Murray, M, Hustead, V, Mascotti, K, Schultz, R, Hallam, L, McRae, D, Nicholson, AG, Newbury, R, Durham-O'Donnell, J, Knight, G, Kini, U, Shaikh, TH, Martin, V, Tyreman, M, Simonic, I, Willatt, L, Paterson, J, Mehta, S, Rajan, D, Fitzgerald, T, Gribble, S, Prigmore, E, Patel, A, Shaffer, LG, Carter, NP, Cheung, SW, Langston, C, Shaw-Smith, C: Genomic and genic deletions of the FOX gene cluster on 16q24.1 and inactivating mutations of FOXF1 cause alveolar capillary dysplasia and other malformations. *Am J Hum Genet*, 84: 780-791, 2009.

References

76. Carpenter, AR, Becknell, MB, Ching, CB, Cuaresma, EJ, Chen, X, Hains, DS, McHugh, KM: Uroplakin 1b is critical in urinary tract development and urothelial differentiation and homeostasis. *Kidney Int*, 89: 612-624, 2016.
77. Rothman, KJ, Moore, LL, Singer, MR, Nguyen, US, Mannino, S, Milunsky, A: Teratogenicity of high vitamin A intake. *N Engl J Med*, 333: 1369-1373, 1995.
78. Wilson, JG, Warkany, J: Malformations in the genito-urinary tract induced by maternal vitamin A deficiency in the rat. *Am J Anat*, 83: 357-407, 1948.

Appendix

The appendix contains license agreements for all copyright protected material used in this work.

**ELSEVIER LICENSE
TERMS AND CONDITIONS**

Mar 02, 2017

This Agreement between Tobias Bohnenpoll ("You") and Elsevier ("Elsevier") consists of your license details and the terms and conditions provided by Elsevier and Copyright Clearance Center.

License Number	4060731263102
License date	
Licensed Content Publisher	Elsevier
Licensed Content Publication	Developmental Biology
Licensed Content Title	Tbx18 expression demarcates multipotent precursor populations in the developing urogenital system but is exclusively required within the ureteric mesenchymal lineage to suppress a renal stromal fate
Licensed Content Author	Tobias Bohnenpoll,Eva Bettenhausen,Anna-Carina Weiss,Anna B. Foik,Mark-Oliver Trowe,Patrick Blank,Rannar Airik,Andreas Kispert
Licensed Content Date	1 August 2013
Licensed Content Volume	380
Licensed Content Issue	1
Licensed Content Pages	12
Start Page	25
End Page	36
Type of Use	reuse in a thesis/dissertation
Portion	full article
Format	print
Are you the author of this Elsevier article?	Yes
Will you be translating?	No
Order reference number	
Title of your thesis/dissertation	Lineage diversification and differentiation in mouse ureter development
Expected completion date	Jul 2017
Estimated size (number of pages)	100
Elsevier VAT number	GB 494 6272 12
Requestor Location	Tobias Bohnenpoll Forssmannweg 13 Hannover, other 30627

	Germany
	Attn:
Publisher Tax ID	GB 494 6272 12
Total	0.00 EUR

**American Society of Nephrology LICENSE
TERMS AND CONDITIONS**

Mar 02, 2017

This is a License Agreement between Tobias Bohnenpoll ("You") and American Society of Nephrology ("American Society of Nephrology") provided by Copyright Clearance Center ("CCC").

License Number	4060791396272
License date	Mar 02, 2017
Licensed content publisher	American Society of Nephrology
Licensed content title	Journal of the American Society of Nephrology
Licensed content date	Dec 31, 1969
Type of Use	Thesis/Dissertation
Requestor type	Author of requested content
Format	Print
Portion	chapter/article
Title or numeric reference of the portion(s)	Diversification of cell lineages in ureter development
Title of the article or chapter the portion is from	Diversification of cell lineages in ureter development
Editor of portion(s)	N/A
Author of portion(s)	Tobias Bohnenpoll et al.
Volume of serial or monograph.	N/A
Page range of the portion	
Publication date of portion	December 2016
Rights for	Main product
Duration of use	Current edition and up to 5 years
Creation of copies for the disabled	no
With minor editing privileges	no
For distribution to	Other territories and/or countries
Territory/Countries where you intend to distribute new product	Germany
In the following language(s)	Original language of publication
With incidental promotional use	no
The lifetime unit quantity of new product	Up to 499

Made available in the following markets	education
The requesting person/organization is:	Tobias Bohnenpoll
Order reference number	
Author/Editor	Tobias Bohnenpoll
The standard identifier of New Work	TB01
Title of New Work	Lineage diversification and differentiation in mouse ureter development
Publisher of New Work	Tobias Bohnenpoll
Expected publication date	Jul 2017
Estimated size (pages)	100
Total (may include CCC user fee)	0.00 USD

**American Society of Nephrology LICENSE
TERMS AND CONDITIONS**

Apr 07, 2017

This is a License Agreement between Tobias Bohnenpoll ("You") and American Society of Nephrology ("American Society of Nephrology") provided by Copyright Clearance Center ("CCC").

License Number	4083630952942
License date	Apr 07, 2017
Licensed content publisher	American Society of Nephrology
Licensed content title	Journal of the American Society of Nephrology
Licensed content date	Dec 31, 1969
Type of Use	Thesis/Dissertation
Requestor type	Author of requested content
Format	Print
Portion	chapter/article
Title or numeric reference of the portion(s)	A Dominant Mutation in Nuclear Receptor Interacting Protein 1 Causes Urinary Tract Malformations via Dysregulation of Retinoic Acid Signaling
Title of the article or chapter the portion is from	A Dominant Mutation in Nuclear Receptor Interacting Protein 1 Causes Urinary Tract Malformations via Dysregulation of Retinoic Acid Signaling
Editor of portion(s)	N/A
Author of portion(s)	Vivante et al.
Volume of serial or monograph.	N/A
Page range of the portion	
Publication date of portion	April 2017
Rights for	Main product
Duration of use	Current edition and up to 5 years
Creation of copies for the disabled	no
With minor editing privileges	no
For distribution to	Other territories and/or countries
Territory/Countries where you intend to distribute new product	Germany
In the following language(s)	Original language of publication
With incidental promotional use	no

The lifetime unit quantity of new product Up to 499

Made available in the following markets education

The requesting person/organization is: Tobias Bohnenpoll

Order reference number

Author/Editor Tobias Bohnenpoll

The standard identifier of New Work TB01

Title of New Work Lineage diversification and differentiation in mouse ureter development

Publisher of New Work Tobias Bohnenpoll

Expected publication date Jul 2017

Estimated size (pages) 100

Total (may include CCC user fee) 0.00 USD

Acknowledgements

First and foremost, I would like to thank my supervisor Prof. Dr. Andreas Kispert who aroused my interest in developmental biology already during my undergraduate studies. I am thankful for the numerous fascinating and challenging projects and the opportunity to participate in his excellent research group. I really appreciate the constant support and critical feedback he provided during the last years.

I would like to thank Prof. Dr. Achim Gossler for facilitating the IfM as a great research environment that allows students to start their work as independent scientists.

I would like to thank Prof. Dr. Hansjörg Küster for his kind acceptance to be chair of the examiners board and Dr. Roland Schmitt and Prof. Dr. Monika Hassel for their kind acceptance to be referees of my dissertation.

Thank you to all the past and present lab members for helpful discussions, support and fantastic team-work. In particular I would like to thank Dr. Mark-Oliver Trowe who introduced me to lab benchwork during my undergraduate studies. Special thanks to all my co-authors who intellectually and practically supported my research efforts and helped to get our work published.

Kindly acknowledged are Dr. Karin Schuster-Gossler for her help in the generation of genetically modified mice and Dr. Carsten Rudat and Dr. Marc-Jens Kleppa for their support with the ES cell work.

Finally, I want to say thank you to my family without whom this work would not have been successful and who always backed me up.

Curriculum vitae

Personal information

Name: Tobias Bohnenpoll
Date of birth: 10.06.1986
Place of birth: Hildesheim
Citizenship: German
Email: bohnepoll.tobias@mh-hannover.de; tobias.bohnepoll@gmail.com

School education

1992 – 1996 Grundschule, Sorsum
1996 – 2005 Gymnasium Marienschule, Hildesheim

Alternative civilian service

2005 – 2006 Diakonische Werke Himmelsthür

University studies

2006 – 2009 Undergraduate studies (B.Sc.) in Biology at the University of Hannover
B.Sc. thesis at the Institute for Molecular Biology, Hannover Medical School, under the supervision of Prof. Dr. rer. nat. Andreas Kispert, with the title:
“Funktionelle Analyse des kanonische Wnt Signalwegs in der Musterung und Differenzierung des periotischen Mesenchyms der Maus”

2009 – 2011 Graduate studies (M.Sc.) in Biomedicine at the Hannover Medical School
M.Sc. thesis at the Institute for Molecular Biology, Hannover Medical School, under supervision of Prof. Dr. rer. nat. Andreas Kispert, with the title:
“Semaphorine und Plexine in der Ureterentwicklung der Maus”

Practical experiences

2011 – 2017 Research assistant in the laboratory of Prof. Dr. rer. nat. Andreas Kispert at the Institute for Molecular Biology, Hannover Medical School.

List of publications

Vivante A, Mann N, Yonath H, Weiss AC, Getwan M, Kaminski MM, **Bohnenpoll T**, Teyssier C, Chen J, Shril S, van der Ven AT, Ityel H, Schmidt JM, Widmeier E, Bauer SB, Sanna-Cherchi S, Gharavi AG, Lu W, Magen D, Shukrun R, Lifton RP, Tasic V, Stanescu HC, Cavaillès V, Kleta R, Anikster Y, Dekel B, Kispert A, Lienkamp SS, Hildebrandt F. A dominant mutation in nuclear receptor interacting protein 1 causes urinary tract malformations via dysregulation of retinoic acid signaling. *Journal of the American Society of Nephrology* 2017, April

Bohnenpoll T, Feraric S, Nattkemper M, Weiss AC, Rudat C, Meuser M, Trowe MO, Kispert A. Diversification of cell lineages in ureter development. *Journal of the American Society of Nephrology* 2016, December

Häfner R, **Bohnenpoll T**, Rudat C, Schultheiss TM, Kispert A. Fgfr2 is required for the expansion of the early adrenocortical primordium. *Molecular and Cellular Endocrinology* 2015, September 413, 168-177

Weiss AC, Airik R, **Bohnenpoll T**, Greulich F, Foik A, Trowe MO, Rudat C, Costantini F, Adams RH, Kispert A. Nephric duct insertion requires EphA4/EphA7 signaling from the pericloacal mesenchyme. *Development* 2014, September 141(17), 3420-3430

Bohnenpoll T, Kispert A. Ureter growth and differentiation. *Seminars in Cell & Developmental Biology* 2014, December 36, 21-40

Bohnenpoll T, Trowe MO, Wojahn I, Taketo MM, Petry M, Kispert A. Canonical Wnt signaling regulates the proliferative expansion and differentiation of fibrocytes in the murine inner ear. *Developmental Biology* 2014, July 391(1), 54-65

Bohnenpoll T, Bettenhausen E, Weiss AC, Foik A, Trowe MO, Blank P, Airik R, Kispert A. *Tbx18* expression demarcates multipotent precursor populations in the developing urogenital system but is exclusively required within the ureteric mesenchymal lineage to suppress a renal stromal fate. *Developmental Biology* 2013, August 380(1), 25-36